



**UNIL** | Université de Lausanne

Unicentre

CH-1015 Lausanne

<http://serval.unil.ch>

---

*Year : 2013*

## LINKING MICROTUBULES TO THE ACTIVATION OF CDC42 IN FISSION YEAST

KOKKORIS Kyriakos

KOKKORIS Kyriakos, 2013, LINKING MICROTUBULES TO THE ACTIVATION OF CDC42 IN  
FISSION YEAST

Originally published at : Thesis, University of Lausanne

Posted at the University of Lausanne Open Archive.

<http://serval.unil.ch>

### **Droits d'auteur**

L'Université de Lausanne attire expressément l'attention des utilisateurs sur le fait que tous les documents publiés dans l'Archive SERVAL sont protégés par le droit d'auteur, conformément à la loi fédérale sur le droit d'auteur et les droits voisins (LDA). A ce titre, il est indispensable d'obtenir le consentement préalable de l'auteur et/ou de l'éditeur avant toute utilisation d'une oeuvre ou d'une partie d'une oeuvre ne relevant pas d'une utilisation à des fins personnelles au sens de la LDA (art. 19, al. 1 lettre a). A défaut, tout contrevenant s'expose aux sanctions prévues par cette loi. Nous déclinons toute responsabilité en la matière.

### **Copyright**

The University of Lausanne expressly draws the attention of users to the fact that all documents published in the SERVAL Archive are protected by copyright in accordance with federal law on copyright and similar rights (LDA). Accordingly it is indispensable to obtain prior consent from the author and/or publisher before any use of a work or part of a work for purposes other than personal use within the meaning of LDA (art. 19, para. 1 letter a). Failure to do so will expose offenders to the sanctions laid down by this law. We accept no liability in this respect.



Faculté de Biologie et Médecine

Département de Microbiologie Fondamentale

# LINKING MICROTUBULES TO THE ACTIVATION OF CDC42 IN FISSION YEAST

Thèse de doctorat

**PhD**

présenté à la

Faculté de Biologie et Médecine

de l' Université de Lausanne

par

**Kyriakos KOKKORIS**

Diplômé de l'Institut Technologique d'Athènes Grèce

**Jury**

Prof. Pierre Goloubinoff, président

Prof. Sophie Martin, directrice de thèse

Prof. Niko Geldner, expert

Prof. Viesturs Simanis, expert

Lausanne 2013

# Imprimatur

Vu le rapport présenté par le jury d'examen, composé de

<i>Président</i>	Monsieur Prof. Pierre <b>Goloubinoff</b>
<i>Directeur de thèse</i>	Madame Prof. Sophie <b>Martin</b>
<i>Experts</i>	Monsieur Prof. Viesturs <b>Simanis</b>
	Monsieur Prof. Nikko <b>Geldner</b>

le Conseil de Faculté autorise l'impression de la thèse de

**Monsieur Kyriakos Kokkoris**

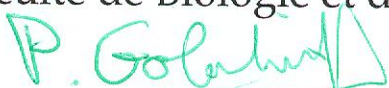
Master Université d'Uppsala, Suède

intitulée

**LINKING MICROTUBULES TO THE ACTIVATION  
OF CDC42 IN FISSION YEAST**

Lausanne, le 25 janvier 2013

pour Le Doyen  
de la Faculté de Biologie et de Médecine

  
Prof. Pierre Goloubinoff



***Dedicated to all previous and current members of  
Sophie Martin's Lab, Family, Friends and Lara!***



# Table of Contents

<b>Abbreviations</b> .....	7
<b>Scientific summary</b> .....	9
<b>Résumé scientifique</b> .....	11
<b>Public summary</b> .....	13
<b>Résumé public</b> .....	15
<b>Chapter 1</b> .....	17
<b>General introduction</b> .....	17
1.1. Cell polarity importance .....	17
1.2. Why fission yeast.....	20
1.3. Fission yeast cytoskeleton and growth .....	22
<b>Aim of research</b> .....	27
<b>Chapter 2</b> .....	29
<b>Analysis of Tea4 localization and function</b> .....	29
2.1. Introduction .....	29
2.2. Results.....	31
2.2.1. Tea4 and Tea1 transport and anchoring at cell tips .....	31
2.2.2. Phenotypic characterization of Tea4 SH3 domain .....	37
2.2.3. Tea4 <sup>SH3</sup> localization, transport and dynamics .....	40
2.2.4. Identification of Tea4 SH3 domain interactors <i>in vivo</i> .....	42
2.2.5. Role of novel Tea4-associated proteins.....	45
2.2.5.1. Ppk2 .....	45
2.2.5.2. Rga4 and Dis2 .....	46
2.2.6. Localization of Tea4-associated proteins .....	48
2.3. Conclusions and discussion.....	51
<b>Chapter 3</b> .....	55
<b>A phosphorylation cycle shapes gradients of the DYRK family kinase Pom1 at the plasma membrane. Cell 145, 1116-1128</b> .....	55
3.1. Summary.....	55
<b>Chapter 4</b> .....	79
<b>Tea4-mediated ectopic morphogenesis</b> .....	79
4.1. Introduction .....	79
4.2. Results.....	81
4.2.1. Ectopically targeted Tea4 induces growth .....	81
4.2.2. Localization of cell polarity regulators at ectopic growth site .....	85
4.2.3. Dis2 essentiality for bulge formation .....	87
4.2.4. Gef1 and Rga4 essentiality for bulge formation.....	90
4.2.5. Tea4-Dis2-Rga4 interplay.....	92
4.2.6. Rga4 analysis.....	93
4.2.7. Ectopically targeted Dis2 initiates growth in almost all cells and may negatively regulate Rga4 localization .....	98
4.2.8. Re-targeted cortical Rga4 inhibits ectopic growth .....	100
4.3. Conclusions and discussion.....	101

<b>General conclusions and discussion .....</b>	<b>105</b>
<b>Tea4 functions .....</b>	<b>105</b>
<b>Mass spectrometry results .....</b>	<b>105</b>
<b>Tea4 beyond fission yeast .....</b>	<b>106</b>
<b>Feedback loops .....</b>	<b>107</b>
<b>Rho GAPs importance .....</b>	<b>107</b>
<b>The role of phospholipids in polarized growth .....</b>	<b>108</b>
<b>Linking MTs with Cdc42 activation .....</b>	<b>108</b>
<b>Materials and methods .....</b>	<b>111</b>
<b>Yeast strains and genetic manipulations .....</b>	<b>111</b>
<u>Generation of plasmids .....</u>	<u>113</u>
<u>S. pombe strains used in this study .....</u>	<u>115</u>
<b>Microscopy and FRAP Analysis .....</b>	<b>121</b>
<b>TAP purification and immunoprecipitation .....</b>	<b>122</b>
<u>Mass spectrometry results .....</u>	<u>124</u>
<u>Predicted phosphorylated sites .....</u>	<u>136</u>
<b>References .....</b>	<b>137</b>
<b>Acknowledgments .....</b>	<b>147</b>
<b>Resume .....</b>	<b>149</b>
<b>List of Publications .....</b>	<b>151</b>

# Abbreviations

Cdc42	Cell division control protein 42
CRIB	Cdc42/Rac-interactive binding
Dis2	Defective in sister chromatid disjoining
DYRK	Dual-specificity tyrosine-phosphorylation regulated kinase
EMM	Edinburgh minimal medium
Gef1	Guanine exchange factor 1
GFP	Green fluorescent protein
GTP	Guanosine 5'-Triphosphate
LatA	LatrunculinA
M	Mitosis
MBC	Methyl benzimidazol-2-yl carbonate
MTs	Microtubules
NETO	New End Take Off
Pom1	Polarity misplaced 1
PP1	Type 1 protein phosphatase
Rga4	Rho Tapes activating protein 4
SH3 domain	SRC Homology 3 domain
TAP	Tandem affinity urification
Tea4	Tip elongation aberrant 4
YE5S	Yeast extract with supplements



# Scientific summary

Cell polarity is an essential property of most cell types and relies on a dynamic cytoskeleton of actin filaments and microtubules. In rod-shaped *S. pombe* cells microtubules are organized along the length of the cell and transport polarity factors to cell tips to regulate cell polarity. An important cell polarity factor is the protein Tea4, which is responsible for correct cell morphogenesis and bipolar growth. During my research I confirmed the known transport mechanism of Tea4 and I also showed alternative localization and anchoring mechanisms at the cell ends. Tea4 contains a conserved SH3 domain, the function of which was unknown and my results show that the SH3 domain of Tea4 is essential for Tea4 function *in vivo*. First, cells with *tea4*<sup>SH3</sup> mutations show aberrant cell shapes and monopolar growth patterns similar to *tea4*Δ and in addition SH3 domain is important for proper localization of multiple cell polarity proteins. Second, I showed that Tea4 associates with Type 1 Phosphatase Dis2 through both its SH3 domain and an RVxF motif. Tea4 also binds the DYRK kinase Pom1 through its SH3 domain. In addition Tea4 is proposed to promote the local dephosphorylation of Pom1 by Dis2 to induce the formation of a cortical gradient from cell ends essential for cell size homeostasis. Polarized growth is also controlled by cell tip-localized Cdc42. This Rho-family GTPase is activated by the Guanine Exchange Factors Gef1 and Scd1 and inactivated by the Rho GTPase Activating Protein Rga4. In this study, I investigated the mechanisms of how Tea4 promotes Cdc42 activation. My work suggests that Tea4 promotes the local exclusion of Rga4, which in turn allows the accumulation of active Cdc42, which may result in growth. Exclusion of Rga4 by Tea4 is likely to be mediated by Dis2-dependent dephosphorylation. These results suggest a molecular pathway that links the microtubule-associated factor Tea4 with Cdc42 to promote cell polarization and morphogenesis.

*Keywords: cell polarity, microtubule-associated proteins, Tea4, SH3 domain, Cdc42, Rho GTPase activating protein, Rga4, Type 1 phosphatase, Dis2, morphogenesis*



# Résumé scientifique

La polarité cellulaire est une propriété essentielle de la plupart des types cellulaires et s'appuie sur une dynamique des cytosquelettes d'actine et de microtubules. Dans les cellules en forme de bâtonnet de *S. pombe* les microtubules sont alignés selon l'axe longitudinal de la cellule et les facteurs de polarité transportés aux extrémités cellulaires afin de réguler la polarité cellulaire. Un facteur important de polarité cellulaire est la protéine Tea4, qui est responsable de la morphogénèse des cellules et leur croissance bipolaire. Au cours de mes recherches, j'ai confirmé les mécanismes connus de transport de Tea4 et j'ai aussi mis en évidence d'autres mécanismes de localisation et d'ancrage de Tea4 aux extrémités cellulaires. Tea4 contient un domaine SH3 conservé, dont la fonction était inconnue et mes résultats montrent que le domaine SH3 est essentiel pour la fonction de Tea4 *in vivo*. Tout d'abord, les cellules avec des mutations *tea4<sup>SH3</sup>* ont des formes aberrantes et leur croissance est monopolaire de manière similaire au mutant *tea4Δ*. De plus ce domaine SH3 est important pour la localisation correcte de plusieurs protéines de polarité cellulaire. Deuxièmement, j'ai montré que Tea4 s'associe avec la Phosphatase de Type-1 Dis2 par son domaine SH3 et un motif RVxF. Tea4 se lie également la kinase DYRK Pom1 par son domaine SH3. De plus, Tea4 pourrait favoriser la déphosphorylation locale de Pom1 par Dis2 afin d'induire la formation d'un gradient cortical de Pom1 essentiel pour l'homéostasie de la longueur des cellules. La croissance polarisée est également contrôlée par la protéine Cdc42 localisée aux extrémités cellulaires. Cette GTPase de la famille de Rho GTPase est activée par les facteurs échange de guanine Gef1 et Scd1 et inactivée par la protéine "Rho GTPase activating" Rga4. Dans cette étude, j'ai étudié les mécanismes d'activation de Cdc42 par Tea4. Mes résultats suggèrent que Tea4 favorise l'exclusion locale de Rga4, ce qui permet l'accumulation de Cdc42 active, nécessaire à la croissance. L'exclusion de Rga4 par Tea4 est vraisemblablement médiée par une déphosphorylation Dis2-dépendente. Ces résultats suggèrent une voie moléculaire qui lie le facteur associé aux microtubules Tea4 à Cdc42 pour promouvoir la polarisation cellulaire et la morphogénèse.

*Mots-clés: polarité cellulaire, protéines associées aux microtubules, Tea4, domaine SH3, Cdc42, Rho GTPase protéine activating, Rga4, Type 1 phosphatase, Dis2, morphogénèse*



## Public summary

Cell polarity is important for several essential biological functions such as generation of distinct cell fates during development and function of differentiated cells. Defective cell polarity has been related to uncontrolled cell division and subsequently to cancer initiation. Cell polarity depends on a functional cytoskeleton that consists of actin filaments and microtubules, which maintains cell shape, helps cellular motion, enables intracellular protein transport and plays a vital role in cell division. A component of cytoskeleton is microtubules that regulate cell polarization in diverse cell types. During my research, I worked with *Schizosaccharomyces pombe*, also named fission yeast, a powerful unicellular model organism that allows combination of genetic, biochemical and microscopic analysis for the proper study of cell polarity. Microtubule-associated protein Tea4 is transported to cell tips where it is thought to organize polarized growth. I showed that Tea4 and its evolutionarily conserved SH3 domain play an important role for maintenance of fission yeast cells shape and growth. Furthermore, Tea4 is responsible for the proper localization of multiple polarity proteins and acts as a mediator to control the local activity of an essential polarity regulator called Cdc42. Thus, my results provide a better understanding of the molecular mechanisms that regulate cell polarity.



# Résumé public

La polarité cellulaire est importante pour plusieurs fonctions biologiques essentielles telles que la différenciation cellulaires au cours du développement et de la fonction de cellules différenciées. Les défauts de la polarité cellulaire ont été liés à des divisions cellulaires incontrôlées et à l'initiation de tumeur. La polarité cellulaire dépend d'un cytosquelette fonctionnel, qui maintient la forme des cellules, aide à la migration cellulaire, permet le transport intracellulaire des protéines et joue un rôle essentiel dans la division cellulaire. Un composant du cytosquelette est constitué de microtubules qui régissent la polarisation cellulaire dans divers types cellulaires. Au cours de mes recherches, j'ai travaillé avec *Schizosaccharomyces pombe*, appelé également levure fissionnaire, un modèle unicellulaire puissant qui permet la combinaison de différentes d'approches expérimentales: génétiques, biochimiques et microscopiques pour l'étude de la polarité cellulaire. La protéine Tea4 associée aux microtubules est transportée aux extrémités cellulaires où elle organise la croissance polarisée. J'ai montré que Tea4 et son domaine conservé SH3 jouent un rôle important pour le maintien de la forme des cellules de levure et leur croissance. De plus, Tea4 est responsable de la localisation correcte de multiples facteurs de polarité et agit comme un médiateur pour contrôler l'activité locale d'un régulateur de polarité essentiel appelé Cdc42. Ainsi, mes résultats permettent de mieux comprendre les mécanismes moléculaires qui régulent la polarité cellulaire.



# Chapter 1

## General introduction

### 1.1. Cell polarity importance

Cell polarity is an essential biological property of almost all cell types and is defined as an asymmetrical distribution of proteins and functions. Cell polarity is found in single cell organisms such as budding yeast *Saccharomyces cerevisiae* and fission yeast *Schizosaccharomyces pombe*, multicellular invertebrates including the nematode *Caenorhabditis elegans* and the fruitfly *Drosophila*, and vertebrates such as mammals and birds. Even prokaryotic organisms such as bacteria and archaea are polarized. Cells can be of a large range of shapes and sizes, from meter long branching neurons in mammals to the micrometer long rod-shaped cells of *S. pombe*.

Cell polarity in these different cell types enables the cell to accomplish specialized functions. Stem cells give rise to non-identical daughter cells to achieve lineage-specific differentiation. This critical developmental process relies on accurate regulation of cell polarity to ensure asymmetric cell division (Knoblich, 2008). Neuronal polarity allows axons and dendrites to properly regulate signal transmission (Arimura and Kaibuchi, 2007). Polar localization of pin-formed proteins (PIN) establishes auxin efflux, an important signal for plant body development (Dhonukshe, 2009). Proper regulation of polarity is essential for tissue integrity by maintaining the apical-basal polarity of epithelial cells (Shin et al., 2006). The examples above clearly illustrate that understanding how cell polarity is regulated is of fundamental and universal biological importance.

Given the diversity and range of cell types present in nature it is remarkable that the mechanisms to generate and maintain polarity are highly similar. Indeed, many of the molecules responsible for regulating cell polarity are conserved across cell types and throughout metazoan species (Bryant and Mostov, 2008). One highly conserved mechanism of polarity establishment involves the localization of protein landmarks to specific areas at the cell membrane. The localization of these molecules requires cytoskeletal elements such as microtubules and actin to recruit the polarity regulators and to deliver vesicles to the cell matrix. I will mainly focus on the role of Rho GTPases, specifically that of Cdc42. Rho GTPases play an essential role in the regulation of cytoskeletal elements, vesicle transport and the localization of cytoplasmic proteins, all of which contribute to cell polarization (Jaffe

and Hall, 2005; Orlando and Guo, 2009). GTPases function as molecular switches that transit from a GDP-bound inactive state to a GTP-bound active state. Guanine Exchange Factors (GEF) and GTPase Activating Proteins (GAP) are the proteins involved in their activation and inactivation, respectively. The importance of Rho GTPases, especially Cdc42, in establishing polarized growth has been studied extensively in the budding yeast system (Chang et al., 1994; Miller and Johnson, 1994; Nobes and Hall, 1999; Pruyne et al., 2004a; Pruyne et al., 2004b). In budding yeast cells, Cdc42 controls actin assembly and is required for polarized localization of the exocyst (Lechler et al., 2001; Pruyne et al., 2004a; Zhang et al., 2001). It is believed that the exocyst provides information for the recruitment and tethering of secretory vesicles important for cell wall remodeling and growth (Heider and Munson, 2012; Pruyne et al., 2004b; Yu and Hughson, 2010)

Newborn budding yeast cells utilize polarity landmark proteins, which act as spatial and temporal cues to position correctly the emergence of the daughter bud. Wild type cells utilize the GTPase Rsr1 to provide the spatial information for bud emergence adjacent to the bud scar from the previous division (Chant and Herskowitz, 1991). This landmark protein transmits the information to recruit the Cdc42 module, which activates downstream effectors at the selected site of growth. Cdc42 will be part of a protein complex that will enhance symmetry breaking to allow for the emergence of a single bud. Even in absence of landmark protein Rsr1, Cdc42 can break symmetry and establish polarized growth. In *rsr1Δ* cells, Cdc42 concentrates at a random cortical site either in response to an extracellular cue or spontaneously and triggers symmetry breaking (Irazoqui et al., 2003). Studies with *rsr1Δ* budding yeast cells have established that two positive feedback mechanisms help breaking symmetry to allow for polarized growth (Fig. 1.1A and B) (Slaughter et al., 2009; Wedlich-Soldner et al., 2004). First, the Cdc42-based cortical complex recruits more cytoplasmic Cdc42 molecules resulting in an expanding Cdc42 cortical cluster (Goryachev and Pokhilko, 2008; Kozubowski et al., 2008). Cdc42 activates members of the formin family of actin nucleators, which build polarized arrays of actin cables that in turn serve as tracks for the transport of more Cdc42. The cooperation between Cdc42 and actin mutually enhance each other through positive feedback loops to achieve symmetry breaking (Slaughter et al., 2009; Wedlich-Soldner et al., 2003). The second positive feedback mechanism is believed to require the association of the scaffold Bem1, the Cdc42-GEF Cdc24 and a PAK kinase, which serves to drive Cdc42 into the GTP-bound active form (Goryachev and Pokhilko, 2008; Kozubowski et al., 2008). Importantly, recent work has discovered a role for negative feedback in symmetry breaking as well (Howell et al., 2012). Initially the positive feedback loops permit the amplification of new polarity clusters but the amplification of more than one cluster would require the competition between the clusters for “winning” the limited pool of

18

resources. Eventually the largest cluster would “win” explaining how budding yeast creates only one bud. This clustering is oscillatory when it is initially formed proposing also the presence of a negative feedback loop that scatters the polarity factors (Howell et al., 2012). Altogether this suggests that direct interactions between Rsr1 and Bem1, Cdc24, and Cdc42 (Kozminski et al., 2003; Park et al., 1997; Zheng et al., 1995) combined with the active Cdc42 and actin positive feedback loops and possibly a negative loop ensure polarized growth and correct bud site selection.

Since its original finding in *S. cerevisiae*, Cdc42 has been identified to regulate a variety of signaling pathways and cellular processes in many organisms from unicellular yeast to mammals (Adams et al., 1990; Johnson, 1999; Johnson and Pringle, 1990). Cdc42 acts upstream of numerous effectors controlling processes that include cell polarity, cytoskeletal rearrangements, migration, adhesion and membrane trafficking (Aznar and Lacal, 2001; Cerione, 2004; Stengel and Zheng, 2011). Studies in *Drosophila* showed that Cdc42 regulates the morphogenesis of axons and dendrites and maintains the polarization of epithelial cells (Eaton et al., 1996; Luo et al., 1994; Scott et al., 2003). In mice, Cdc42 also plays an important role for polarity maintenance in the neural system and in liver (Chen et al., 2006; van Hengel et al., 2008). In humans, overexpression of Cdc42 is strongly correlated with various cancer types and increased levels of Cdc42 associate with aging and mortality (Fritz et al., 2002; Fritz et al, 1999; Gomez Del Pulgar et al., 2008; Kamai et al., 2004; Kerber et al., 2009; Liu et al., 2009; Tucci et al., 2007). It is clear that Cdc42 misregulation affects a number of pathological conditions and understanding the exact control of Cdc42 is important for normal cell function.

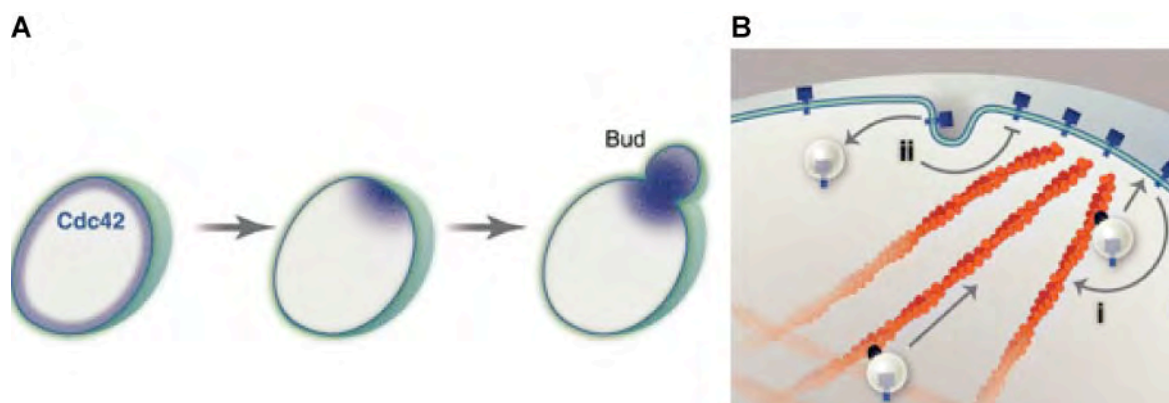


**Figure 1.1 Breaking symmetry and polarized growth in budding yeast (Mogilner et al., 2012).** (A) Initially symmetric cell has isotropic distribution of Cdc42 that becomes polarized leading to polarized growth. (B) Positive feedback loops help breaking cell symmetry to allow for polarized growth.

## 1.2. Why fission yeast

In Sophie Martin's lab, we have chosen to work with *Schizosaccharomyces pombe*, also called fission yeast, an ideal organism to study cell polarity. *S. pombe* is a species of ascomycetous fungi whose cells are rod-shaped and normally measure 3 to 4 micrometers in diameter and 7-14 micrometers in length. Historically, fission yeast was first isolated from African millet beer in 1893 by Lindner. Pombe means beer in Swahili language (Wixon, 2002). In the early 1950s in Scotland, Mitchison began to study the cell cycle of *S. pombe*. In parallel in Switzerland, Leupold studied fission yeast genetics and molecular technologies. Almost 2 decades later, Paul Nurse successfully combined Leupold's and Mitchison's approaches. Nurse together with Hunt and Hartwell discovered cell cycle regulators as the key molecules for controlling cell cycle transitions. They won for their findings the 2001 Nobel Prize in Physiology or Medicine. An additional landmark year of *S. pombe* history was 2002. An international collaboration of scientists led by the Sanger Institute published the sequence of fission yeast genome on 2002 (Wood et al., 2002). It was just the sixth model eukaryotic organism whose genome had been fully sequenced by that time. *S. pombe* genome is approximately 14.1 million base pairs, has 3 chromosomes and is estimated to contain 4,970 protein-coding genes and at least 450 non-coding RNA's (Wilhelm et al., 2008).

Fission yeast cells proliferate in a haploid state and maintain their cylindrical shape by growing exclusively at the cell tips and dividing by medial fission, which leads to the production of two daughter cells of equal sizes. After division, the newly born cells first grow in a monopolar manner at the cell end that existed before cell division (the old end). They then initiate bipolar growth in the G2 phase of the cell cycle by growing at the new end created by septation (remarkably *S. pombe* remains in G2 phase for an extended period). This process is called New End Take Off (Fig. 1.2), or NETO (Mitchison and Nurse, 1985). NETO provides a system of *de novo* initiation of growth. Regulation of "old" end growth followed by the "new" end growth requires cellular re-arrangements controlled by polarity factors. This polarity machinery has to tightly control polarized growth to ensure shape maintenance.

The prerequisite of rod-shaped fission yeast cell morphogenesis is the establishment of cell polarity, thus understanding how cells initiate and maintain polarized growth is of fundamental importance. Fission yeast provides an ideal organism to study polarity not only because of NETO but also due to the uniqueness of its polarity regulation. Even though several studies have been done with *S. cerevisiae*, another yeast model organism, which has provided key aspects of understanding polarized growth, there are some major advantages

working with fission yeast compared to budding yeast. Budding yeast buds are formed in specific regions of the cell distinct from the position of previous bud sites and specifically the new bud forms next to the previous bud in haploid cells. The actin cytoskeleton is required for bud growth but microtubules are not required. Although microtubules are necessary for the correct position of the nucleus and the mitotic spindle, in the absence of microtubules buds are still formed at the correct position (Jacobs et al., 1988; Huffaker et al., 1988). In contrast to budding yeast, microtubules have a major role in polarized growth and cell morphogenesis in fission yeast. *S. pombe* morphogenesis relies on functional microtubules and microtubules ensure that elongation of the cell occurs along the long axis of the cell by maintaining the symmetrical accumulation of polarity factors at the cell ends where growth occurs (for more details see Chapter 1.3). Although the exact processes that generate and maintain polarized growth still remain unclear, the study of cell polarity in fission yeast provides an excellent insight into the microtubule role to control cell polarization. Studies in both fission and budding yeast provide complementary evidence to strengthen a solid model of how polarized growth is regulated that could apply not only in fungal systems but also in metazoans.

Fission yeast has also other advantages to work with. *S. pombe* simple rod shape is reproducible and cells can be easily grown and manipulated time-wise in laboratory conditions since each cell cycle requires approximately 2.5-3 hours in rich medium. In addition, fission yeast's non-pathogenic nature makes it a safe organism to work with. Importantly, the ease of molecular, genetic and biochemical manipulations coupled with powerful live-cell imaging techniques makes *S.pombe* a great tool in cell polarity research.

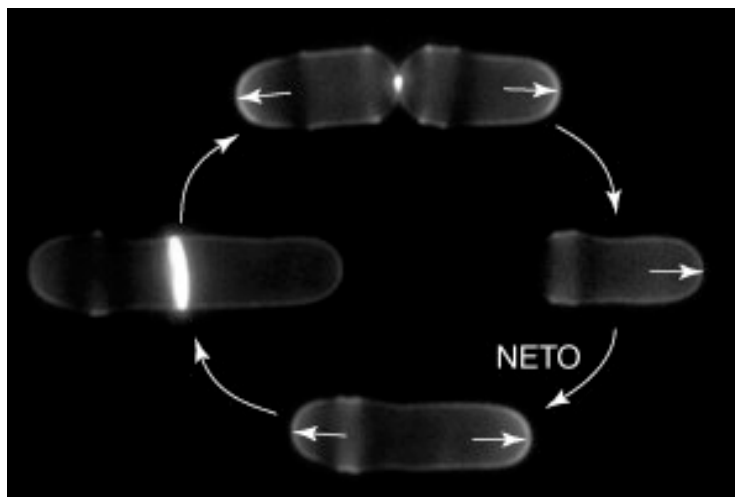


**Figure 1.2. New End Take Off in Fission Yeast (Martin, 2009).** Cells were stained with calcofluor to mark newly formed cell walls. Large arrows show cell cycle progression (clock-wise from top) and small arrows indicate polarized growth.

### 1.3. Fission yeast cytoskeleton and growth

Polarity regulators and landmark proteins provide the signal where growth will occur. The cytoskeleton serves as the transport mechanism of vesicles that need to be deposited at the plasma membrane and, in mammals, the cytoskeleton also provides the forces for growth to occur. In contrast, in walled cells like plants, algae and yeast the force for growth depends on turgor pressure, but not directly on the cytoskeleton (Boudaoud, 2003; Dumais et al., 2006). Turgor pressure pushes the plasma membrane against the cell wall and this pressure is caused by the osmotic difference between the extracellular environment having low solute concentration and the cell cytoplasm that has a higher solute concentration. Cells rely on turgidity to maintain their rigidity and shape. To grow in a polarized manner, the cell has to deliver vesicles to the cell membrane and deposit new cell wall materials at specific locations. In fission yeast, the rod shape of the cells is organized and maintained by interactions between the cytoskeleton that consists of actin and microtubules and the cell membrane, which lead to the polarized delivery of cell wall components at cell tips (Martin and Chang, 2005). The cytoskeleton regulates cell polarity and cell shape and in turn cell shape also directs the organization of the cytoskeleton in a feedback loop (Minc et al., 2009; Terenna et al., 2008).

In fission yeast, actin forms three different structures: the cytokinetic actin ring (CAR), actin patches and actin cables. During cytokinesis, actin bundles are present at the cell middle in a meshed-like structure and actin-driven forces compact these bundles into a tight ring, forming the CAR in the equatorial cortex followed by cell division in two equal daughter cells (Arai and Mabuchi, 2002; Lee et al., 2012; Vavylonis et al., 2008). It is proposed that the forces for cytokinesis are mainly produced by the assembly of cell wall proteins due to high internal turgor pressure and the contractile ring is not the primary force generator for ingression (Proctor et al., 2012). Actin patches and cables localize to sites of polarized cell growth and cytokinesis (Gachet and Hyams, 2005). Actin patches assemble at sites of endocytosis and they are responsible for the uptake of extracellular material and the recycling of lipids and surface proteins (Arellano et al., 1997; Gachet and Hyams, 2005; Kovar et al., 2011). Actin cables polarize exocytosis by serving as tracks for myosin-driven delivery of secretory vesicles to cell tips (Feierbach and Chang, 2001). Specifically, Myo52 is the only fission yeast myosin V motor protein that transports vesicles to the cell ends, resulting in cell wall remodeling and polarized growth (Cortes et al., 2005; Feierbach and Chang, 2001; Motegi et al., 2001; Win et al., 2001). The assembly of actin cables to mediate this process depends on formins, a family of highly conserved eukaryotic proteins implicated in actin nucleation (Prune et al., 2002; Sagot et al., 2002). Polarized exocytosis also involves

the fusion of intracellular secretory vesicles with the plasma membrane and the release of material out of the cell. This depends on the function of a multi-component complex, the exocyst, which tethers incoming vesicles at the plasma membrane for fusion (He and Guo, 2009; TerBush et al., 1996). Interestingly actin cable mediated transport and the exocyst form two redundant morphogenesis pathways, although disruption of both systems results in isotropic growth (Bendezu and Martin, 2011; Nakano et al., 2011; Snaith et al., 2011).

Fission yeast encodes three formins. Cdc12 plays a role for cytokinesis and Fus1 is important for mating (Chang et al., 1997; Petersen et al., 1995). For3 is the only formin playing a major role for polarized growth by nucleating actin cables at the cell tips (Feierbach and Chang, 2001; Nakano et al., 2002). For3 is regulated by an autoinhibitory mechanism that involves an interaction of the N-terminus Dia Inhibitory Domain (DID) with the C-terminus Dia Autoregulatory Domain (DAD), a system also observed in other formins (Goode and Eck, 2007). The proper localization of For3 depends on relief of this autoinhibition and the proteins regulating this process are the actin-interacting protein Bud6, the Boi family protein Pob1 and Cdc42 (Martin et al., 2007; Rincon et al., 2009). Pob1 plays a role for cell elongation and separation and in addition binds the For3 N-terminus and facilitates the Cdc42-mediated relief of For3 autoinhibition. Bud6 binding at the C terminus of For3 plays a role for For3 cell tip anchoring and activation. Cdc42 acts upstream of Pob1 and For3 and is the main regulator for actin cable assembly and For3 regulation (Martin et al., 2007; Rincon et al., 2009). Cdc42 regulation depends on two GEFs called Gef1 and Scd1, the scaffold protein Scd2 and only one known GAP named Rga4 (Chang et al., 1994; Das et al., 2007; Garcia et al., 2006; Tatebe et al., 2008). Scd2, the homologue of budding yeast protein Bem1, is necessary for the localization of Scd1 and is believed to serve as a scaffold protein mediating the interaction between Scd1 and Cdc42 (Endo et al., 2003; Wheatley and Rittinger, 2005). Rga4 is an evolutionary conserved GAP protein that functionally interacts with For3 and deletion of Rga4 effects cell diameter and polarized growth in fission yeast (Das et al., 2007; Tatebe et al., 2008). In conclusion, Cdc42 is likely to be the most upstream polarizing cue for polarizing actin (Feierbach and Chang, 2001; Martin et al., 2007; Nakano et al., 2002; Rincon et al., 2009).

The cytoskeleton also consists of microtubules that align along the long axis of the cells and have a more instructive role for defining sites of polarized growth compared to the role of actin for growth per se. In fission yeast, the spindle pole body (SPB) is functionally equivalent to the centrosome and it functions as a microtubule-organizing center (MTOC) where microtubules begin to assembly (Sawin and Tran, 2006; Snyder, 1994). Nuclear division arrest genes *nda2* and *nda3* regulate the organization of microtubules and specifically *nda2*

controls proper nuclear placement and correctly situated spindle pole bodies, while *nda3* maintains the rod shape of fission yeast cells (Toda et al., 1983; Umesono et al., 1983). During interphase, the microtubule cytoskeleton consists of three to six microtubule bundles arranged along the long axis of the cell. Within each bundle, a pair of microtubules is organized in an anti-parallel manner where their minus ends overlap in the center of the cell and their plus ends extend toward opposite cell ends (Drummond and Cross, 2000; Hoog et al., 2007; Sagolla et al., 2003; Tran et al., 2001). The plus ends show cycles of growth towards cell tips, dwelling upon cell end contact and disassembly (Drummond and Cross, 2000; Tran et al., 2001). Manipulating fission yeast shape physically with microfluidic chambers re-aligns the MTs leading to accumulation of polarity factors ectopically and resulting in local growth (Minc et al., 2009; Terenna et al., 2008). These evidence show that microtubules provide the spatial information for polarity to occur and even if MTs are not essential for cell polarity they play a key role in cell morphogenesis by targeting polarity factors involved in cell growth at the cell cortex.

Under physiological conditions, polarized growth in fission yeast is a complex process that involves the interplay of many polarity proteins and this protein complex is called the polarisome. The polarisome is formed at the cell tips and it functions in actin regulation and additional aspects of polarized cell growth, such as exocytosis (Feierbach et al., 2004). I would like to describe in more details this network of multiple polarity factors that is believed to instruct polarization in fission yeast. Tea2 is a kinesin motor protein, important for establishing and maintaining polarized growth along the long axis of the cell (Bieling et al., 2007; Browning et al., 2003; Browning et al., 2000; Wu et al., 2006). A cargo of Tea2 is Tip1, a CLIP-170 +TIP protein that stabilizes and targets the growing tips of MTs along the long axis of the cell and is associated with Tea1 (Martin et al., 2005). Tea1 is a major regulator of cell polarity transported on the plus ends of elongating microtubules and deposited at the cortex where it is anchored by the prenylated membrane protein Mod5 (Fig. 1.3) (Behrens and Nurse, 2002; Brunner and Nurse, 2000; Feierbach et al., 2004; Mata and Nurse, 1997; Snaith and Sawin, 2003). One Tea1-binding partner is the protein Tea4, which co-localizes with Tea1 at microtubule plus ends and cell tips, and whose localization is dependent on Tea1 and Mod5 (Fig. 1.3) (Martin et al., 2005; Tatebe et al., 2005). Deletion of *tea4* leads to bent or T-shaped cells and the cells fail to switch to a bipolar mode of growth (Martin et al., 2005), a similar phenotype previously described for *tea1* deleted cells (Snell and Nurse, 1994). Tea4 is proposed to link Tea1 with For3 at the new cell end for NETO establishment (Fig. 1.3) (Martin and Chang, 2005; Martin et al., 2005). Tea4 like Tea1 is important for correct cell morphogenesis and bipolar growth during normal cell cycle. My main focus is to understand how exactly Tea4 establishes cell polarity and actin assembly resulting in bipolar

growth. Interestingly, Tea4 contains an Src homology 3 (SH3) domain located at its N terminus. The SH3 domain is a highly conserved sequence that it is believed to play important role for various biological functions. Thus **in Chapter 2**, I will try to analyze Tea4 delivery and anchoring to the cell tips and investigate the importance of its SH3 domain.

Tea1 and Tea4 are required for the localization of a third key factor: Pom1. Pom1 belongs to an evolutionarily conserved serine/threonine kinase family, DYRK (Dual-specificity tyrosine-phosphorylation-Regulated protein Kinase (Becker et al., 1998). Pom1 along with Tea1 and Tea4 is required for bipolar growth and provides an inhibitory mechanism to prevent division-septum assembly at the cell ends (Huang et al., 2007). In addition, in the course of my work, an additional role of Pom1 was discovered: Pom1 forms gradients that emanate from the cell ends and provide a measure of cell length for mitotic entry (Martin and Berthelot-Grosjean, 2009; Moseley et al., 2009). Tea1 and Tea4 recruit Pom1 to the cell ends yet Pom1 is not required for their localization (Bahler and Nurse, 2001; Bahler and Pringle, 1998; Tatebe et al., 2005). Shortly before the start of my work, Tea4 was also shown to associate with the Type 1 Phosphatase Dis2 (Alvarez-Tabares et al., 2007). **In Chapter 3**, I will describe published data (Hachet et al., 2011) where I also contributed to show how Tea4 associates with the Phosphatase Type 1 Dis2 and the DYRK kinase Pom1 to form the cortical Pom1 gradients that regulate mitotic entry.

Pom1 physically interacts with the Cdc42 GAP Rga4, which normally localizes at the cell sides and it has been shown that when *tea4*, *tea1*, or *pom1* is deleted Rga4 also accumulates at the non-growing end (Tatebe et al., 2008). Interestingly, when *pom1* is deleted, cells share similar monopolar growth pattern (Bahler and Pringle, 1998) with *tea1Δ* and *tea4Δ* cells. It is suggested that in *tea4*, *tea1*, or *pom1Δ* mutants, Rga4 localization at the cell tips does not allow Cdc42 activation resulting in NETO failure and monopolar growth, even though presence of active Cdc42 at both cell tips it is not sufficient to rescue the monopolar growth of *pom1Δ rga4Δ* double mutant (Tatebe et al., 2008). This protein network may form microtubule-dependent cell end landmarks that link to Cdc42 GTPase activity. Thus **in Chapter 4**, I will investigate the mechanisms of how Tea4 may link microtubules with Cdc42 activation.

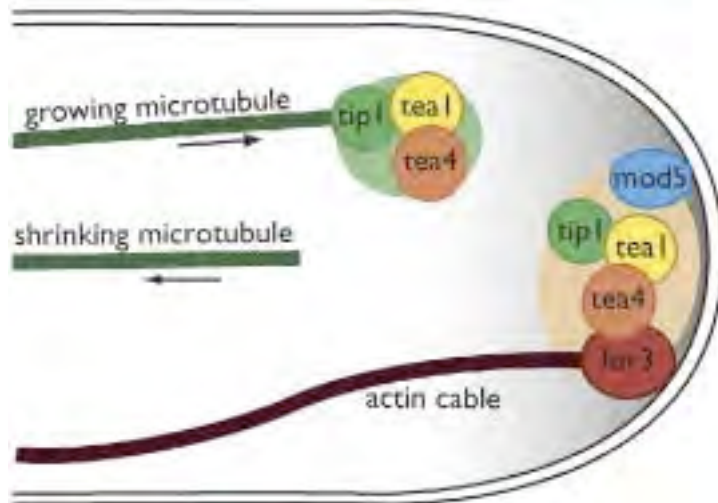


**Figure 1.3. Microtubules and polarity factors (Martin et al., 2005).** MTs transport polarity regulators Tea1 and Tea4 to cell ends where they are anchored by prenylated protein Mod5. Then, a protein complex of Tea1, Tea4 and the actin nucleator For3 is formed to establish cell polarity.

# Aim of research

The puzzle of cell polarity regulation still remains unsolved. Many interesting questions are raised that I will try to answer during my research. In **Chapter 2**, I describe unexpected findings on the localization of Tea1 and Tea4, in which I show that both proteins reside and recycle at cell tips even in absence of microtubule-based transport. In addition, Tea4 has an SH3 domain whose function remains unknown. By generating a non-functional Tea4 SH3 domain and investigating its phenotype, I investigate the importance of this domain for Tea4 function *in vivo* and describe a biochemical strategy to identify novel Tea4 interactors that may associate with its SH3 domain to control polarized growth.

In **Chapter 3**, I will present my contribution to published data (Hachet et al., 2011) proposing a model in which Tea4 bridges DYRK kinase Pom1 with Dis2 to promote Pom1 cortical anchoring essential for cell size homeostasis. Furthermore in **Chapter 4**, I will try to dissect the minimal genetic requirements for cell polarity and growth. I show that ectopically localized Tea4 promotes local growth. I use this assay to investigate the role of Tea4 for ectopic growth initiation and to understand how Tea4 may link microtubules with actin.



## Chapter 2

# Analysis of Tea4 localization and function

### 2.1. Introduction

As described in Chapter 1, *S. pombe* cells grow along the long axis and microtubules (MTs) are organized along this axis of the cell and transport polarity factors to cell ends to mark the cell ends for growth. One major regulator of cell polarity delivered by microtubules to the cell tips is the tip elongation aberrant 1 (Tea1) protein (Verde et al., 1995). Tea1 is transported on the plus ends of elongating microtubules and deposited at the cortex before microtubules shrink back (Behrens and Nurse, 2002; Brunner and Nurse, 2000; Feierbach et al., 2004; Mata and Nurse, 1997; Snaith and Sawin, 2003). A prenylated membrane protein, called Mod5 is important for anchoring Tea1 at the cell tips (Snaith and Sawin, 2003). Mod5 association with Tea1 also enhances Tea1 incorporation to form a stable self-focusing landmark at the cell ends. This Tea1-Mod5 cluster network adds robustness in polarized growth (Bicho et al., 2010). Functional Tea1 is necessary for cell growth in a straight line. When *tea1* is deleted, cells exhibit morphology defects and become bent or branched. Tea1 acts as a cell end marker and plays important roles for the organization of microtubules and the retention of polarity factors at the cell tips (Behrens and Nurse, 2002; Mata and Nurse, 1997).

Tea4 is an additional microtubule-associated protein and was first identified by using Tandem Mass Spectrometry as a Tea1-associated factor (Martin et al., 2005). Tea4 co-localizes with Tea1 at microtubule plus ends and cell tips, and its localization is dependent on Tea1 and Mod5 (Martin et al., 2005). Tea4 is thought to organize a molecular network between MTs, actin and polarity factors at the cell tip for the regulation of polarized growth. Tea4 binds *in vivo* both the polarity regulator Tea1 and the actin nucleator For3. Tea4 C-terminus interacts with Tea1 but no specific domain of Tea4 has been yet identified for For3 binding (Martin et al., 2005). Tea4 is proposed to link Tea1 with For3 at the new cell end for NETO establishment (Martin and Chang, 2005; Martin et al., 2005). Under stress conditions, Tea4 also contributes to cell polarity maintenance together with the mitogen-activated protein kinase (MAPK) signaling cascade (Tatebe et al., 2005). Deletion of *tea4* leads to bent or T-shaped cells and the cells fail to switch to a bipolar mode of growth (Martin et al., 2005), a similar phenotype previously described for *tea1* deleted cells. In conclusion, Tea4 plays an essential role for actin assembly at new cell ends and for cell polarity establishment.

Tea4 contains an Src homology 3 (SH3) domain located at its N terminus. The SH3 domain is a conserved sequence of approximately 60 amino acids involved in many different signaling pathways and it has a characteristic fold made of five or six  $\beta$  strands positioned as two anti-parallel  $\beta$  sheets (Mayer, 2001; Mayer and Baltimore, 1993; Musacchio et al., 1992; Pawson and Schlessingert, 1993). SH3 domains are identified in the non-catalytic part of several cytoplasmic proteins and are important for the creation of specific protein complexes usually through binding to proline-rich peptides (Mayer, 2001; Pawson and Scott, 1997). Interestingly, Tea4 SH3 domain is not required for either Tea1 or For3 binding (Martin et al., 2005).

All the above raise interesting questions that I will try to address in this chapter. I will describe unexpected findings on the localization of Tea1 and Tea4, in which I show that both proteins reside and recycle at cell tips even in absence of microtubule-based transport. In addition, Tea4 has an SH3 domain whose function remains unknown. By generating a non-functional Tea4 SH3 domain and investigating its phenotype, I investigate the importance of this domain for Tea4 function *in vivo* and describe a biochemical strategy to identify novel Tea4 interactors that may associate with its SH3 domain to control polarized growth.

## 2.2. Results

### 2.2.1. Tea4 and Tea1 transport and anchoring at cell tips

Tea4 is a microtubule-associated protein that associates with microtubule plus ends and then it is transported to the cell ends. At cell tips Tea4 is considered to maintain cell shape and bipolar growth. To confirm that Tea4 is deposited at cell ends by microtubules, I co-imaged Tea4-GFP with microtubules, labeled with Atb2-mCherry (alpha-2-tubulin subunit) that marks microtubules (Tatebe et al., 2001), in time-lapse experiments (Fig. 2.1A). Tea4 associates with microtubule plus ends moving towards the cell end and then accumulates there (Fig. 2.1A). To further study Tea4 dynamics I analyzed kymographs of Tea4-GFP. Kymographs provide a graphical representation of the spatial position of a point of interest (Tea4-GFP) over time. Tea4-GFP kymographs were constructed with the "Make Montage" tool of the ImageJ software. Tea4-GFP movies were a single medial section taken with inverted spinning disk microscope (see materials and methods). Tea4 kymograph analysis showed Tea4 movement towards the cell tip at a rate of  $2.9 \pm 0.3 \mu\text{m}/\text{minute}$  ( $n=10$ ) (Fig. 2.1B) similar to microtubule growth rate ( $3 \mu\text{m}/\text{minute}$ ) (Drummond and Cross, 2000). These measurements show the lack of retrograde movements with depolymerizing microtubules, and therefore the fact that Tea4 is deposited at cell ends. However, I also noticed a small fraction of retrograde movement (3% of the number of directed Tea4 movement) of Tea4 towards the cell middle (Fig. 2.1C) at a rate of  $4.4 \pm 0.4 \mu\text{m}/\text{minute}$  ( $n=5$ ), similar to microtubule shrinkage rate ( $4.5 \mu\text{m}/\text{minute}$ ) (Drummond and Cross, 2000). This kind of movement suggests that Tea4 deposition at the cell end is not 100% efficient and it could be explained by Tea4 attachment at microtubule plus ends during their shrinkage. Overall, these results verify that Tea4 is transported by growing microtubules and then is anchored at cell ends.

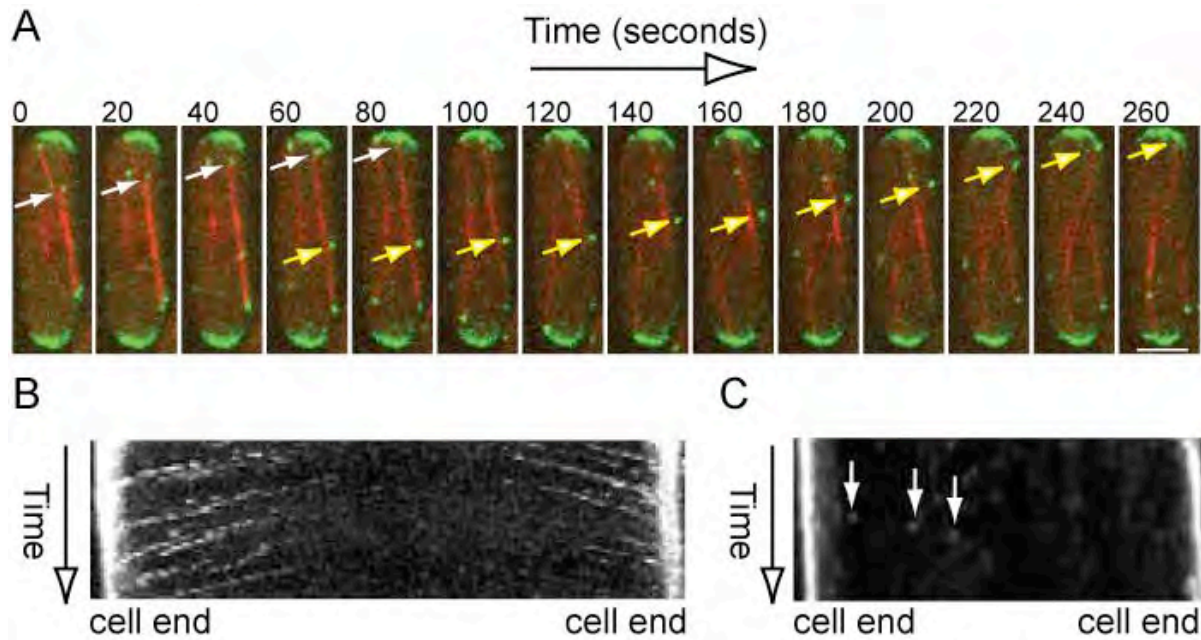


**Figure 2.1. Microtubule-dependent Tea4 transport towards the cell ends.** (A) Visualization of microtubules through tagging of tubulin alpha-2 (*atb2*) with RFP (red) and visualization of Tea4 through tagging with GFP (green) shows Tea4 association with MT plus ends and its delivery at the cell tip (white and yellow arrows). Scale bar 3 $\mu$ m. (B) Kymograph of Tea4 shows its movement towards the cell tips with a rate of 2.9 $\pm$ 0.3 $\mu$ m/minute (n=10) followed by its accumulation at both cell ends. (C) Tea4 movement (3% of the number of directed Tea4 movement) towards the cell middle (white arrows) occurs at a rate of 4.4 $\pm$ 0.4 $\mu$ m/minute.

To test the importance of microtubule transport, I decided to observe Tea4 localization upon disruption of microtubules by using methyl benzimidazol-2-yl carbamate (MBC), a microtubule inhibitor. Unexpectedly, Tea4 was still detected at the cell ends after disruption of microtubules with 25 $\mu$ M MBC for 15 minutes indicating redundant mechanisms of Tea4 transport and/or its strong anchoring at cell tips (Fig. 2.2C). Surprisingly, prolonged MTs disruption with 25 $\mu$ M MBC for one hour resulted in monopolar growth patterns (52 $\pm$ 6%) and Tea4 accumulated preferentially at the growing end of these monopolar cells (Fig. 2.2A). The 48% of the cells was still growing in a bipolar manner and Tea4 was accumulated at both cell tips. Since actin cables also serve as tracks for transport to the cell ends, I checked whether disruption of actin affected Tea4 cell tip localization. Disruption of all actin structures with 200 $\mu$ M Latrunculin A (LatA), an actin inhibitor, had no significant effect on the localization of Tea4 (Fig. 2.2B). Since Tea1 has similar localization pattern as Tea4, I conducted similar experiments using Tea1-GFP. Tea1 also remained localized at the cell ends when microtubules were disrupted (Fig. 2.2C) and also exhibited accumulation at the growing end after 1hour treatment with MBC, similar as Tea4. In addition, the finding of Tea1 and Tea4 presence at the cell end when microtubules are disrupted suggests the existence of an

alternative transport mechanism and/or reflects the high stability of tip localization for both proteins.

I further investigated Tea4 localization mechanisms at the cell tips with Fluorescence Recovery After Photobleaching (FRAP) experiments. In FRAP experiments a region of interest is photobleached and then two critical values are extracted; the percentage of fluorescence recovery at steady state, called mobile fraction, and the speed of recovery after photobleaching. The speed of recovery is estimated from the time it takes for the curve to reach 50% of the plateau of fluorescence intensity level and is called half-time ( $T_{1/2}$ ). FRAP experiments after photobleaching the cell tip reveal a Tea4-GFP mobile fraction of 50% and a  $T_{1/2}$  of approximately 60 seconds (Fig. 2.2C). When microtubules are disrupted with MBC for 15 minutes before photobleaching there is a higher and faster recovery of Tea4-GFP (mobile fraction of 80% and  $T_{1/2}$  of 20 seconds) compared to FRAP values with functional microtubules (mobile fraction of 50% and  $T_{1/2}$  of 60 seconds) suggesting that presence of microtubules anchors Tea4 more stably at the cell tip and makes it less dynamic (Fig. 2.2C). Similar FRAP experiments for Tea1-GFP exhibited the same mobile fraction and  $T_{1/2}$  as Tea4-GFP (Fig. 2.2C). Tea1 and Tea4 seem to share almost identical dynamics and FRAP experiments show that microtubules are not essential for their recovery at cell ends.

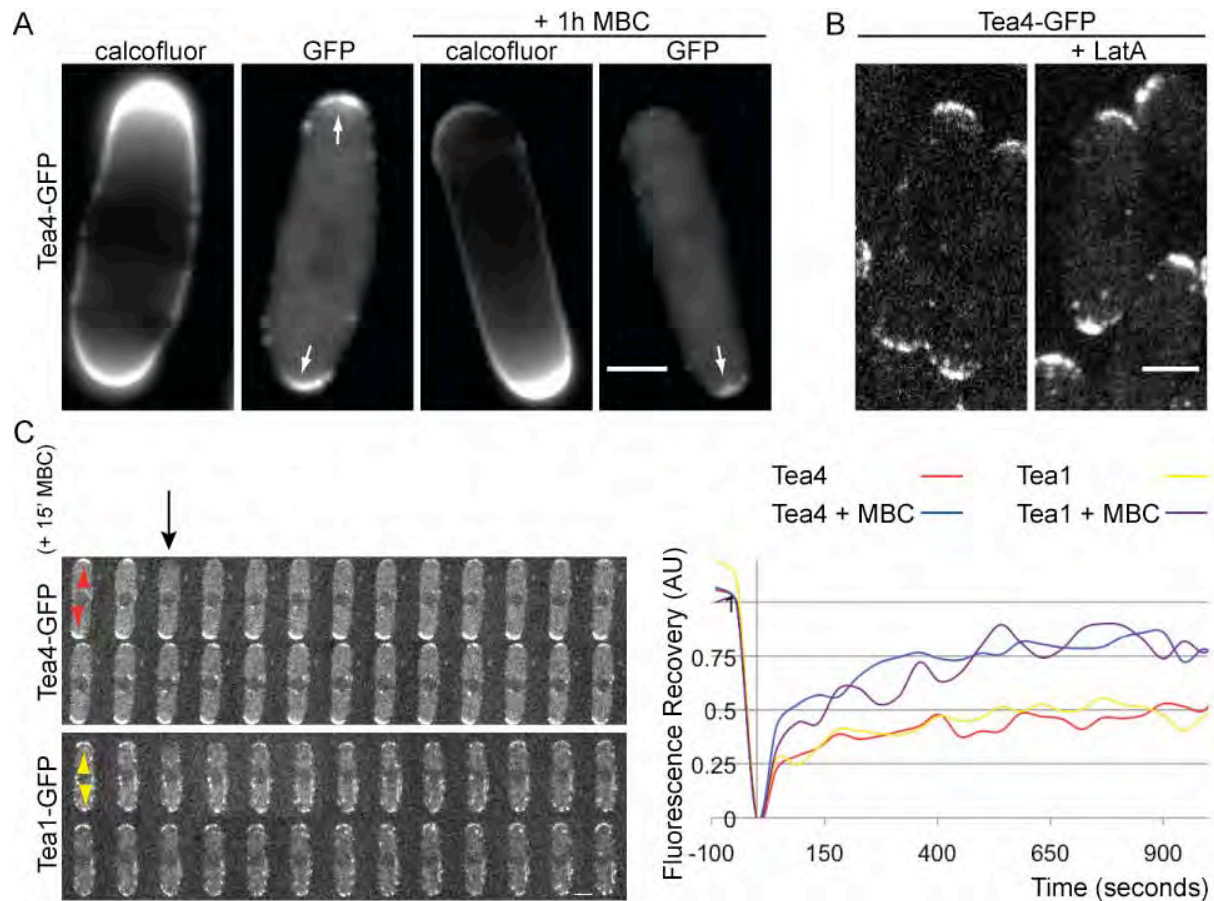


**Figure 2.2. Redundant transport mechanisms of Tea1 and Tea4 localization to the cell tip.** (A) Cells grow in a bipolar manner and Tea4 localizes at both growing tips (white arrows). After 1 hour of 25 $\mu$ M MBC treatment, Tea4 accumulates at one cell end (preferentially the growing end, white arrow). Staining with 10 $\mu$ g/ml calcofluor labels newly formed cell wall indicating growth. Scale bar 3 $\mu$ m. (B) Disruption of all actin structures with 200 $\mu$ M Latrunculin A (LatA) has no significant effect in Tea4 localization at cell ends. Scale bar 3 $\mu$ m. (C) Tea4 and Tea1 still localize at the cell ends even after disruption of MTs with 25 $\mu$ M MBC for 15 minutes (red and yellow arrows, respectively). Images were taken at 45" intervals. The arrow indicates the time of photobleaching. FRAP experiment graph of Tea4-GFP and Tea1-GFP shows the same mobile fraction of 50% and  $T_{1/2}$  of approximately 60 seconds (red and yellow lines, respectively). When microtubules are disrupted with 25 $\mu$ M MBC for 15 minutes there is a higher and faster recovery (mobile fraction of 80% and  $T_{1/2}$  of 20 seconds) of Tea4-GFP and Tea1-GFP (blue and purple lines, respectively). All FRAP graphs for Tea1-GFP and Tea4-GFP represent an average of at least five different photobleached cells. Scale bar 3 $\mu$ m.

The known anchoring factor of Tea1 and Tea4 at the cell ends is the prenylated protein Mod5 (Snaith and Sawin, 2003). Surprisingly, I found that Tea1 and Tea4 are still present at the cell tips in *mod5Δ* cells, albeit at lower levels, and FRAP experiments showed that the mobile fraction of Tea4 is 60% and the  $T_{1/2}$  is approximately 50 seconds (Fig. 2.3) similar to wild type Tea4-GFP cells. Furthermore, Tea4 was still localized at the non-growing end even when microtubules were disrupted with MBC for 15 minutes in *mod5Δ* background, although its localization was severely compromised. FRAP experiments in *mod5Δ* cells treated with MBC showed that the mobile fraction of Tea4 is 80% and the  $T_{1/2}$  is approximately 15 seconds (Fig. 2.3). Thus, in absence of microtubules in *mod5Δ* cells, Tea4 is less stable and more dynamic at the cell ends. Furthermore, Tea1 dynamics are similar to Tea4 dynamics suggesting that these two microtubule-associated proteins behave in a similar way. Collectively, these results confirm that microtubules and Mod5 both contribute to Tea1 and Tea4 localization at the cell ends. They also reveal that additional mechanism(s) exist to localize these proteins at the cell tips.

An additional microtubule-associated protein that could possibly play an important role for Tea4 transport and/or anchoring at the cell tips is the kinesin motor protein Tea2. Since Tea2 is a kinesin, it could possibly transport Tea4 at the cell tips as its cargo. Tea2 is important for tip localization of Tea1 and when *tea2* gene is deleted Tea1 is unable to localize at the cell ends and accumulates along the short interphase MTs (Browning et al., 2000). I deleted *tea2* gene and I checked whether Tea4 is still present at the cell tips. Interestingly, Tea4 accumulates at one cell end in *tea2Δ* cells (Fig. 2.3). To check the dynamics of Tea4 in *tea2Δ* cells I performed FRAP experiments that showed Tea4 mobile fraction of 80% and a  $T_{1/2}$  of approximately 20 seconds (Fig. 2.3), similar to the values observed in wild type cells after MBC treatment. These results suggest that Tea4 behaves the same way either when cells have disrupted MTs or a dysfunctional Tea2 kinesin motor. In conclusion, Tea2 is another important factor for Tea4 localization albeit there are still undefined factor(s) that contribute to Tea4 transport and anchorage at the cell end. Further investigation with localization patterns and FRAP experiments in double mutant *mod5Δ* and *tea2Δ* and with or without MBC could give evidence whether these factors have redundant properties for transporting and anchoring Tea4 at the cell tips. Mass spectrometry analysis of Tea4 in cells with either *mod5* and/or *tea2* deleted could also reveal novel partners that could associate with Tea4 and may play a role for its localization.

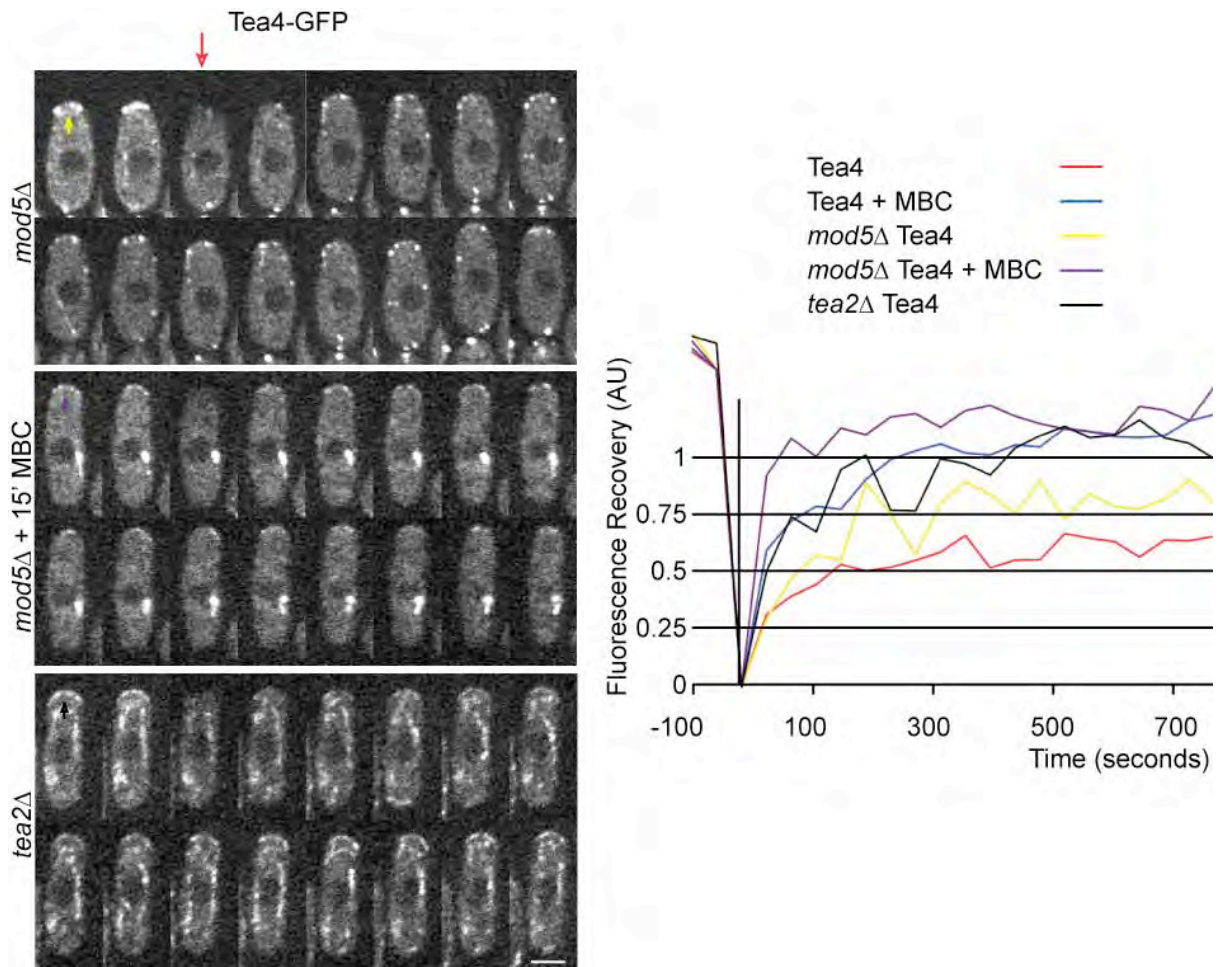


**Figure 2.3. Redundant mechanisms of Tea4 localization at the cell tip.** Tea4 still localizes at the cell end when either *mod5* or *tea2* is deleted (yellow and black arrow, respectively). Tea4 accumulates at one cell end even after disruption of microtubules with 25 $\mu$ M MBC for 15 minutes in *mod5 $\Delta$  cells (blue arrow). Images taken with 45'' intervals and the red arrow indicate the time of photobleaching. FRAP experiment graph shows that when MTs are disrupted Tea4-GFP seems to share the same values with *tea2 $\Delta$  cells (blue and black line, respectively). When only *mod5* is deleted it seems that Tea4 has less and slower recovery compared to *mod5 $\Delta$  cells with disrupted MTs (yellow and purple lines, respectively,  $p$ -value= $10^{-4}$ ). Tea4-GFP shows similar mobile fraction but higher  $T_{1/2}$  in *mod5 $\Delta$  cells treated with MBC compared to cells only treated with MBC (purple and blue lines, respectively). All FRAP graphs for Tea4-GFP represent an average of at least five independent experiments. Scale bar 3 $\mu$ m.****

## 2.2.2. Phenotypic characterization of Tea4 SH3 domain

At the beginning of my work, the role of Tea4 SH3 domain was unknown. Sequence alignment of SH3 domains from different species identified two conserved residues found at 155-156 amino acid positions in Tea4 sequence (Fig. 2.4A). These two tryptophans (WW) 155-156 are predicted to be important for ligand binding (Fig. 2.4A). Sophie Martin mutated the two tryptophans to alanines and I characterized this mutant (Fig. 2.4B). From now on, I will refer to the Tea4 SH3 WW155-156AA mutant as Tea4<sup>SH3</sup>. *tea4* gene was replaced by *tea4*<sup>SH3</sup> and *tea4*<sup>SH3</sup> was expressed under control of the endogenous promoter. I then compared the expression levels of Tea4 and Tea4<sup>SH3</sup> in wild type and *tea4*<sup>SH3</sup> mutant cells, respectively. As shown in Fig. 2.4C both proteins are expressed at similar levels.

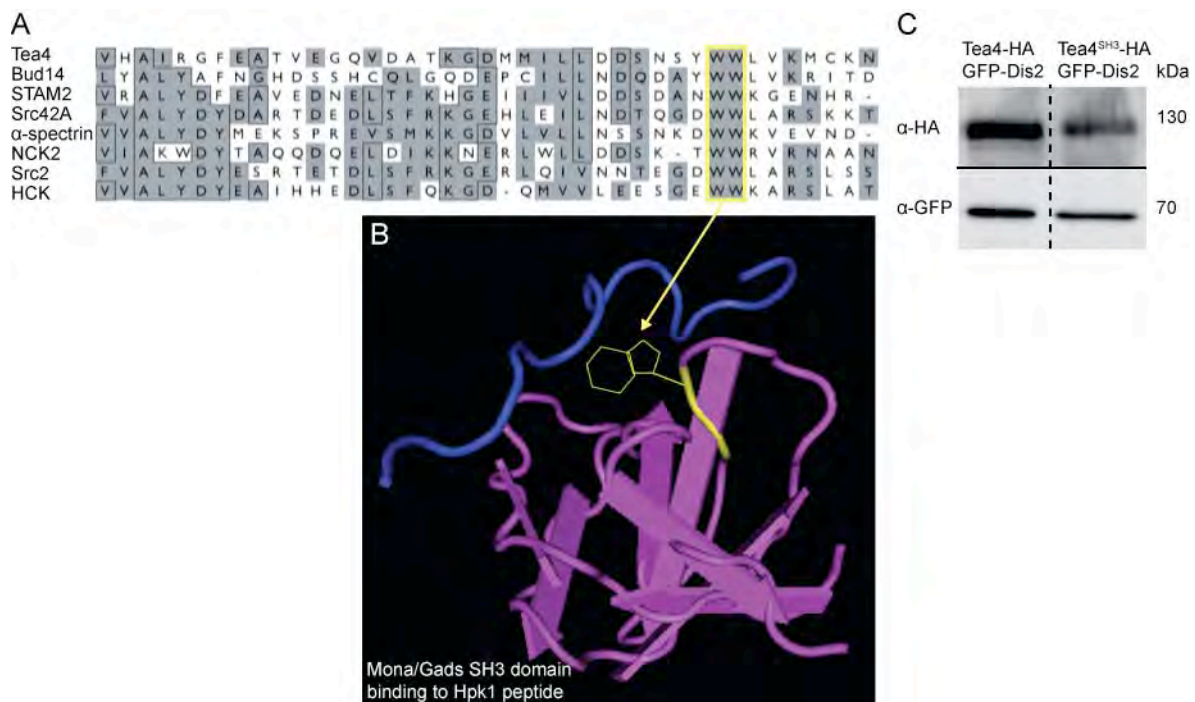


**Figure 2.4. Characterization of the SH3 domain.** (A) Alignment of SH3 domains of different proteins from various organisms. Conserved tryptophan residues indicated in the yellow box are predicted to bind the ligand. Mutation of these tryptophans (WW) generated the *tea4*<sup>SH3</sup> mutant allele (B) β barrel structure arranged as anti-parallel β sheets of the SH3 domain of mouse adaptor protein Mona/gads. Tryptophan residues in yellow mediate the binding with the hematopoietic progenitor kinase 1 Hpk1 peptide. The corresponding mutated residues are indicated in yellow. (C) Tea4-HA and Tea4<sup>SH3</sup>-HA have similar expression levels. GFP-Dis2 protein was used as a loading control.

To characterize the role of the Tea4 SH3 domain I first compared the phenotype of *tea4*<sup>SH3</sup> mutant cells with wild type and *tea4*Δ cells. In contrast to wild type, *tea4*<sup>SH3</sup> cells exhibit morphology defects (bent or T-shaped) and monopolar cell growth (Fig. 2.5A and B) similar to complete deletion of *tea4*. *tea4*<sup>SH3</sup> cells were stained with calcofluor, a chemical that marks the newly formed cell wall, and 53 +/- 4% (n=100) of septated cells exhibited previous growth only at one cell end. I measured cells exhibiting monopolar growth in septated cells because I wanted to check cell growth at the same cell cycle phase. In complete deletion of *tea4* 90 +/- 3% (n=100) of the cells grow in a monopolar manner (Fig. 2.5A). Monopolar growth pattern exhibited in *tea4*<sup>SH3</sup> cells was further supported by AlexaFluor 488-phalloidin staining, a chemical that labels actin structures. Actin filaments and patches were observed at both cell ends in wild type cells but only at one end in *Tea4*<sup>SH3</sup> cells (55 +/-6%, n=50) (Fig. 2.5C) indicating that point mutations in the Tea4 SH3 domain prevent bipolar growth.

I further analyzed the *tea4*<sup>SH3</sup> morphological defects by performing re-feeding experiments wherein cells were overgrown for 48 hours and then diluted 1:20 in fresh yeast extract (YE5S) medium for 3 hours. In the re-feeding experiments, cells become rounded after consuming all nutrients and stop growing. Then rich medium is added and cells need to re-establish growth de novo. These re-feeding experiments showed that almost all *tea4*<sup>SH3</sup> and *tea4*Δ cells form branches at the cell middle (92 +/-3% and 95+/-4%, respectively, n=100), (Fig. 2.5A). *tea4*Δ cells also display to some extent off-center septum (Martin et al., 2005) so I investigated whether *tea4*<sup>SH3</sup> mutant shares the same abnormality. I measured the septum position by taking the ratio between two values: the distance between the septum and the cell end furthest away and the total cell length. *tea4*<sup>SH3</sup> mutant cells exhibit septum misplacement equal to  $0.56 \pm 0.02$  compared to  $0.52 \pm 0.01$  for wild type cells (Fig. 2.5A). *tea4*Δ cells also have off-center septum equal to  $0.56 \pm 0.02$  (Fig. 2.5A). In conclusion, monopolar growth, aberrant cell shape and septum misplacement in *tea4*<sup>SH3</sup> cells suggest that an intact SH3 domain is required for Tea4 function *in vivo*. Although it seems that many Tea4 properties *in vivo* depend on its functional SH3 domain, the defects observed when the Tea4 SH3 domain is mutated are less severe compared to the complete deletion of *tea4* suggesting *tea4*<sup>SH3</sup> is likely to be a hypomorphic allele compared to the *tea4* null mutant.

A	Long half ratio septum-cell ( $\mu\text{m}$ )	Monopolar growth in septated cells, n=100, (%)	Aberrant cell shape (T-shape) in re-feeding experiments, n=100, (%)
wild type	0.52 $\pm$ 0.01	11 $\pm$ 8	0
<i>tea4<sup>SH3</sup></i>	0.56 $\pm$ 0.02	53 $\pm$ 4	92 $\pm$ 3
<i>tea4<math>\Delta</math></i>	0.57 $\pm$ 0.01	90 $\pm$ 3	95 $\pm$ 4

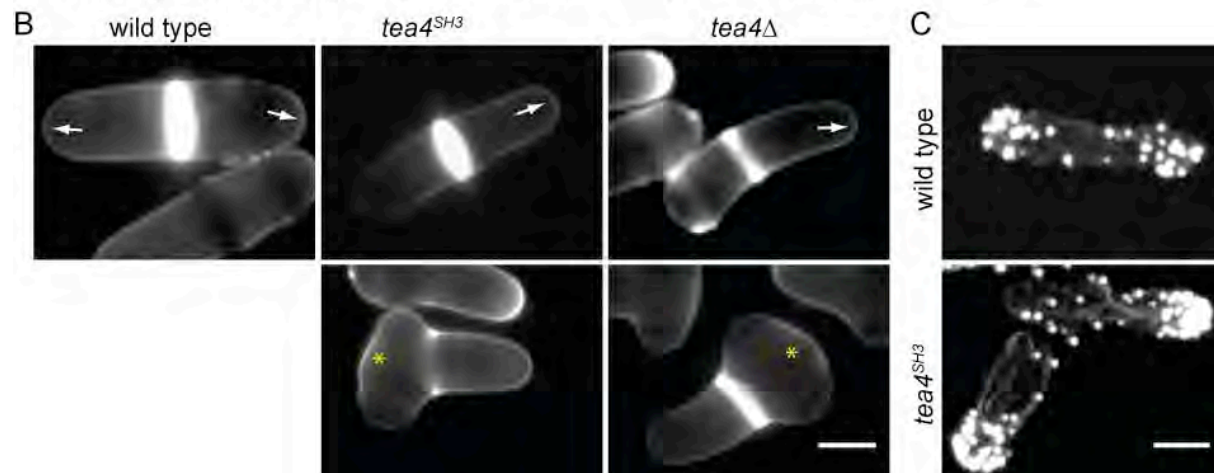


**Figure 2.5. Phenotypic analysis of Tea4<sup>SH3</sup>.** (A) *tea4<sup>SH3</sup>* cells exhibit septum misplacement, monopolar growth and morphology defects similar to *tea4 $\Delta$*  cells. (B) Staining with 10 $\mu\text{g/ml}$  calcofluor shows that wild type cells grow at both cell ends in contrast to *tea4<sup>SH3</sup>* and *tea4 $\Delta$*  cells, which grow in a monopolar manner (arrows). Asterisks indicate cells with morphology defects when either the Tea4 SH3 domain is mutated or *tea4* is deleted. Scale bar 3 $\mu\text{m}$ . (C) Cells stained with AlexaFluor 488-phalloidin to visualize actin organization. Actin cables and patches localize at both cell tips in wild type cells but only at one cell tip in *tea4<sup>SH3</sup>* mutant (55  $\pm$  6%, n=50). Scale bar 3 $\mu\text{m}$ .

### 2.2.3. Tea4<sup>SH3</sup> localization, transport and dynamics

Tea4 normally localizes at microtubule plus ends and then is transferred and anchored at the cell tips by the prenylated protein Mod5. I investigated the localization of Tea4<sup>SH3</sup> tagged with GFP. Tea4<sup>SH3</sup> associated with microtubule plus-ends similar to Tea4-GFP but its cell tip localization changed: Tea4<sup>SH3</sup> accumulated only at one cell end (Fig. 2.6A). To identify at which end Tea4<sup>SH3</sup> was localized, I imaged cells stained with calcofluor. Tea4<sup>SH3</sup> cell tip localization correlates with the non-growing cell end (Fig. 2.6C). Thus Tea4 SH3 domain may regulate Tea4 cell tip localization.

Asymmetric accumulation of Tea4<sup>SH3</sup> suggests either a defect in its transport to the growing cell end and/or a defect in its anchoring at the cell end. I thus analyzed the delivery of Tea4<sup>SH3</sup> by microtubules towards the cell ends with kymographs (Fig. 2.6B). Even though Tea4<sup>SH3</sup> is delivered at both cell ends, it is anchored preferentially at the non-growing cell end. Comparison of Tea4<sup>SH3</sup> kymographs with wild type Tea4 kymographs showed that both proteins share the same dynamic properties (movement towards the cell tip with a rate of 2.8+/-0.3µm/minute and 2.9+/-0.3µm/minute, respectively). Despite the different localization of Tea4 and Tea4<sup>SH3</sup>, it seems that they are both transported to the cell ends in the same way. I further investigated the mechanisms of Tea4<sup>SH3</sup> localization at cell tips by FRAP experiments, similar to those described in section 2.2.1. I found that the mobile fraction and T<sub>1/2</sub> of Tea4<sup>SH3</sup> are similar to those of wild type Tea4 (50% and approximately 60 seconds, respectively) (Fig. 2.6D). Tea4 and Tea4<sup>SH3</sup> molecules seem to share the same dynamics although their localization is different. The above results suggest that Tea4 SH3 mutated domain does not affect significantly the association of Tea4 with microtubules plus ends and its stability at the cell tips but an intact SH3 domain mediates Tea4 anchoring at the second cell end. The localization of Tea4<sup>SH3</sup> only at the non-growing cell end is reminiscent of that of Tea1 in *tea4Δ* cells (Martin et al., 2005; Tatebe et al., 2005) supporting the idea that *tea4<sup>SH3</sup>* mutant is non-functional regarding the cell tip localization phenotype.

As described in section 2.2.1, there are microtubules and Mod5-independent mechanisms for Tea4 localization at the cell tips. I investigated what would happen to Tea4<sup>SH3</sup> localization in absence of microtubules and/or when *mod5* is deleted. Here again, Tea4<sup>SH3</sup> behaved like wild type Tea4, localizing at one cell tip when *mod5* is deleted, even after addition of MBC (Fig. 2.6C). When microtubules are disrupted with MBC for 15 minutes before photobleaching there is a higher and faster recovery of Tea4<sup>SH3</sup>-GFP compared to FRAP values with functional microtubules suggesting that presence of microtubules anchors Tea4<sup>SH3</sup> more stably at the cell tip and makes it less dynamic, similar to wild type Tea4 (Fig. 2.6D). I also observed that Tea4<sup>SH3</sup> cells exhibit more severe morphology defects when

microtubules are disrupted for 1 hour (Fig. 2.6C). It is not yet studied whether MT disruption leads to more aberrant cell shape in complete deletion of *tea4*. In addition,  $Tea4^{SH3}$  switches its monopolar accumulation from the non-growing cell end towards the growing end when cells are treated with MBC for 1 hour (Fig. 2.6C). As shown previously in Fig. 2.2C *Tea4*-GFP showed the same localization pattern after treatment with MBC. Enhancement of the phenotype by MT disruption could be due to the fact that  $Tea4^{SH3}$  behaves as a hypomorphic allele since it seems that *Tea4* and  $Tea4^{SH3}$  share the same dynamics but their cell tip localization is different.

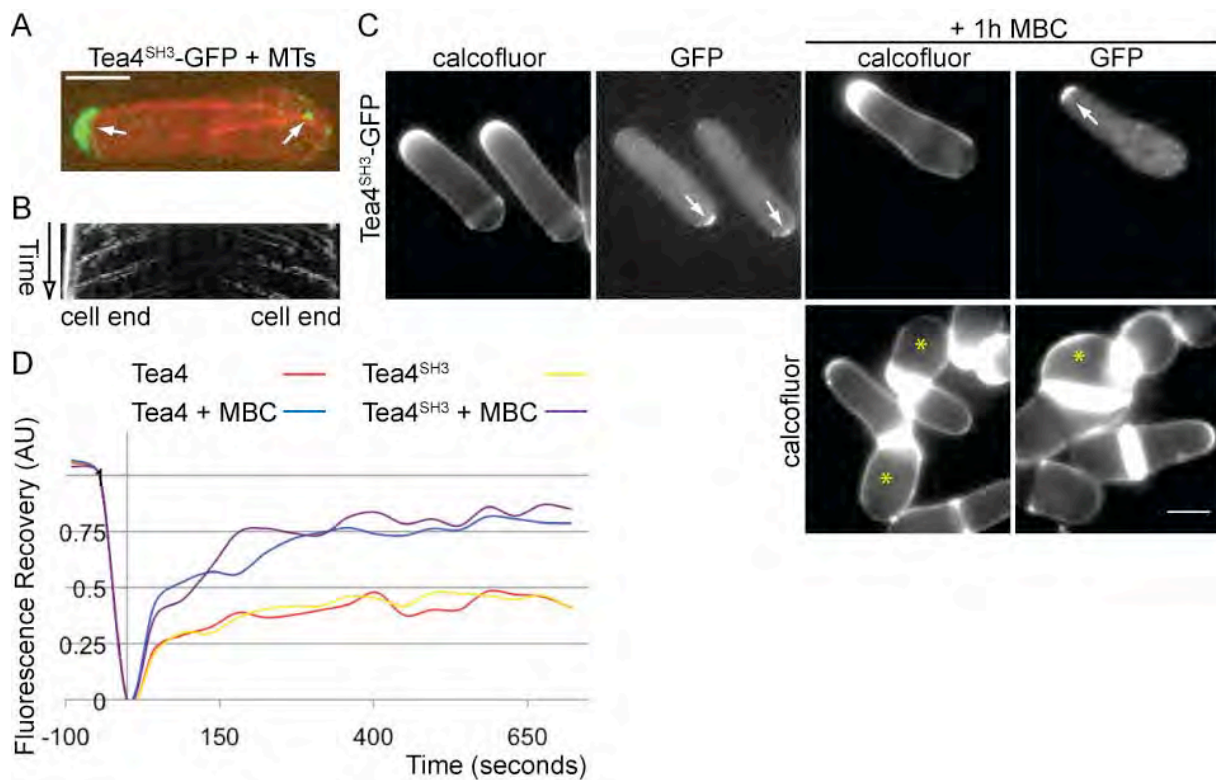


**Figure 2.6.  $Tea4^{SH3}$  transport and localization.** (A)  $Tea4^{SH3}$  associates with MT plus ends and it is delivered at the cell ends but it is only anchored at one tip. Scale bar  $3\mu\text{m}$ . (B) Kymograph of  $Tea4^{SH3}$  shows its movement towards the cell tips and its accumulation at only one cell end. (C) Staining with  $10\mu\text{g/ml}$  calcofluor shows that  $Tea4^{SH3}$  localizes preferentially at the non-growing cell end (arrows). After disruption of microtubules with  $25\mu\text{M}$  MBC for 1 hour,  $Tea4^{SH3}$  is still present at one cell end but this time  $Tea4^{SH3}$  accumulates preferentially at the growing end (arrow). Asterisks indicate *tea4<sup>SH3</sup>* cells that exhibit more severe morphology defects when MTs are disrupted. Scale bar  $5\mu\text{m}$ . (D) FRAP experiment graph of *Tea4*-GFP and  $Tea4^{SH3}$ -GFP shows almost identical mobile fraction of 50% and  $T_{1/2}$  of approximately 60 seconds (red and yellow lines, respectively). When microtubules are disrupted with  $25\mu\text{M}$  MBC for 15 minutes there is similar higher and faster recovery for both *Tea4*-GFP and  $Tea4^{SH3}$ -GFP (blue and purple lines, respectively). All FRAP graphs for *Tea4*-GFP and  $Tea4^{SH3}$ -GFP are an average of at least five independent experiments.

#### 2.2.4. Identification of Tea4 SH3 domain interactors *in vivo*

To better understand how the SH3 domain contributes to proper function and localization of Tea4, I considered whether the SH3 domain is important for interaction with other undefined proteins. To address this question, I purified Tea4 and Tea4<sup>SH3</sup> using Tandem Affinity Purification (TAP) method (Fig. 2.7A) (Gould et al., 2004). TAP is a technique that allows purification of complexes in two steps under native conditions and requires fusion of the TAP tag to the protein of interest. The protein of interest with the TAP tag binds to beads coupled with IgG. Then, the TAP tag is cleaved by protease and a second affinity purification step follows (Fig. 2.7A) Afterward, potential binding partners can be identified by mass spectrometry. I did not perform the second purification step since it did not improve the purification of my samples (Fig. 2.7B).

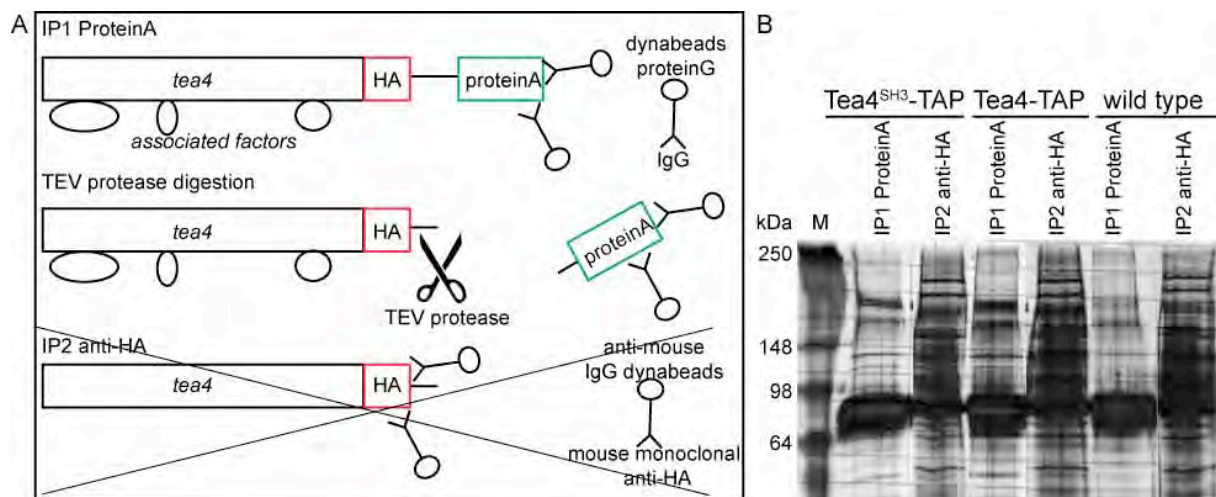


**Figure 2.7. TAP analysis.** (A) During Tandem Affinity Purification (TAP) method antibody (mouse IgG) is coupled to magnetic beads (dynabeads proteinG) followed by immunoprecipitation of proteinA (IP1). Addition of TEV protease cleaves the proteinA and isolates Tea4 with its associated partners. (B) The second purification step of anti-HA immunoprecipitation (IP2) was not performed since it did not result in better-purified samples.

I first purified wild type Tea4-TAP and Tea4<sup>SH3</sup>-TAP in cells that were grown in YE5S rich medium (Fig. 2.8A). After purification, mass spectrometry analysis was performed by the proteomic facility at the University of Lausanne. Mass spectrometry results (Fig. 2.8B) identified as expected Tea1 and Tea3, a cell end marker required for efficient NETO (Arellano et al., 2002), to be interacting partners with Tea4 and Tea4<sup>SH3</sup>. Both Tea4 and Tea4<sup>SH3</sup> also seemed to associate with protein subunits of the molecular chaperone T-complex and the proteasome. The role of Tea4 in these complexes is undefined but a primary idea would be either it has a regulatory task or it has a function to stabilize their conformation. Interestingly, Tea4 also associated with the only two Type 1 Phosphatases (Dis2 and Sds21) found in fission yeast, as described previously (Alvarez-Tabares et al., 2007). These two phosphatases are redundant, as deletion of both of them is lethal for the cell; cells enter mitosis but they are deficient for the disjunction of sister chromatids (Ohkura et al., 1989). Excitingly, these two phosphatases were not recovered in the Tea4<sup>SH3</sup> purification, suggesting that a mutated SH3 domain abolishes the association of Tea4 with these two phosphatases.

I repeated the TAP for Tea4 and Tea4<sup>SH3</sup> to confirm the previous mass spectrometry results but this time cells were grown in minimal medium (EMM) supplemented with the required amino acids (ALU) (Fig. 2.8A). These conditions provide a more controlled growth medium. Mass spectrometry analysis reproduced the results obtained in the first TAP (Fig. 2.8B). Tea4 and Tea4<sup>SH3</sup> still associate with polarity factors Tea1, Tea3 and protein subunits of T-complex and proteasome. Dis2 and Sds21 peptides were again associated only with Tea4. In addition, I identified the Rho GTPase-activating protein Rga4 in the Tea4<sup>SH3</sup> purification. Rga4 is a GAP for Cdc42 (Tatebe et al., 2008), an evolutionary conserved GTPase that contributes to polarized growth and actin organization. Additionally, two more proteins were found in the mass spectrometry results, the kinase Ppk2 and the Sjogren syndrome protein homologue (SPBC3B8.08). In conclusion, mass spectrometry results from both TAPs identified novel proteins that associate with Tea4 and its SH3 domain and importantly point mutations on the SH3 domain abolish the association with Dis2 and Sds21.

Both mass spectrometry results identified known Tea4-associated factors such as Tea1 and novel Tea4 partners such as Ppk2. It has been shown that Tea4 also binds For3 and Pom1 (Hachet et al., 2011; Martin et al., 2005). An interesting remark is that neither For3 nor Pom1 were identified in mass spectrometry results suggesting that Tea4 may interact transiently with both For3 and Pom1. In addition, the TAP conditions could be harsh resulting in the abolishment of their association. The purified samples stayed several hours at 4<sup>0</sup>C before proceeding to mass spectrometry analysis. Improved tandem affinity purification protocol with

less stringent conditions with washing steps of lower concentrations than the ones used (7 times washing with 150mM NaCl) and direct mass spectrometry analysis could potentially identify For3, Pom1 and/or other proteins that associate weakly with Tea4.

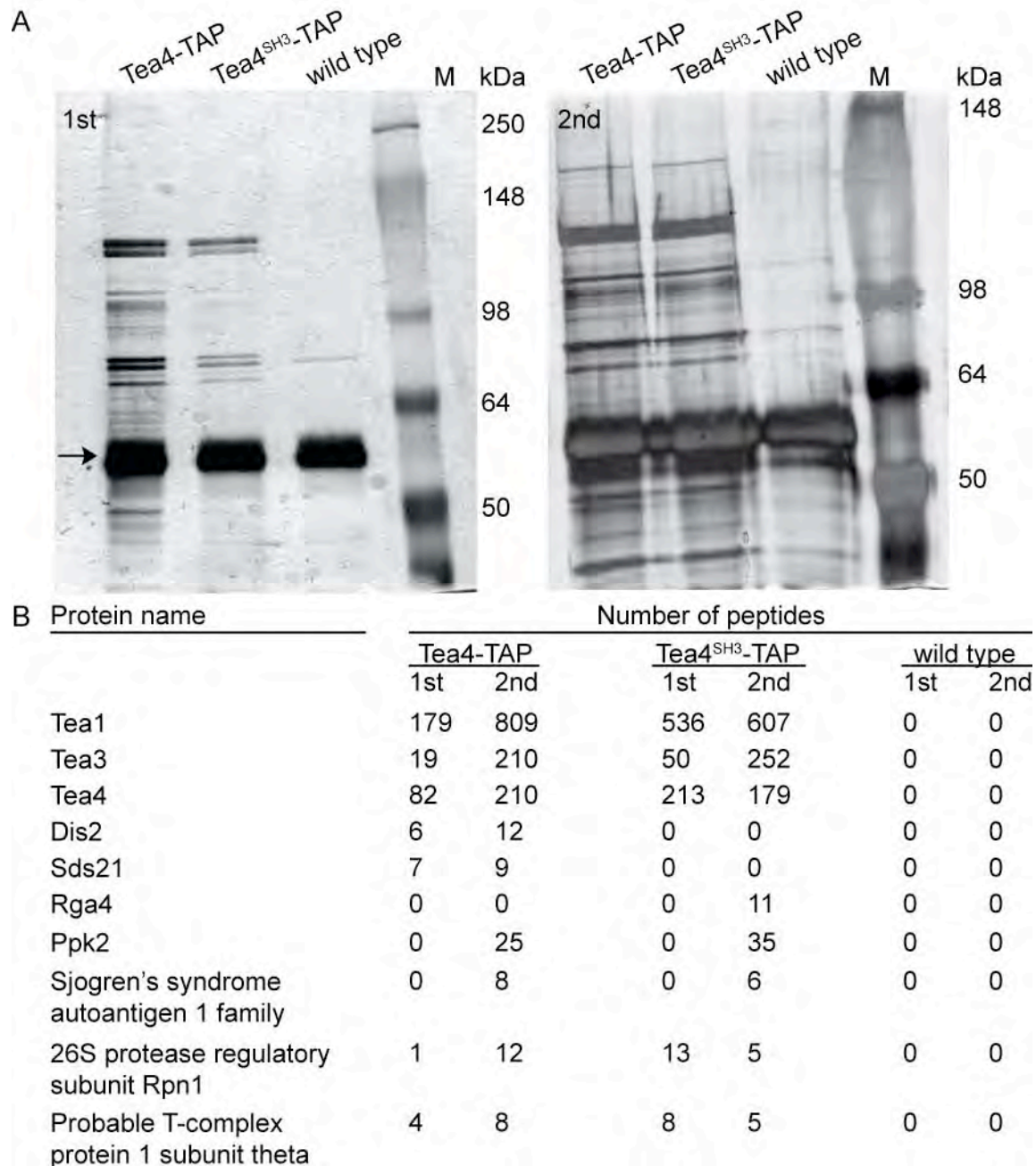


**Figure 2.8. TAP analysis.** (A) Purified samples after cleavage with protease were separated by SDS-PAGE and stained with silver nitrate solution. Black arrow indicates IgG. Cells were grown at 30°C in Yeast Extract medium (YE5S) in 1<sup>st</sup> round of mass spectrometry (left) and in EMM medium containing the required supplements (EMM) in 2<sup>nd</sup> round of mass spectrometry (right). (B) Number of peptides identified in 1<sup>st</sup> and 2<sup>nd</sup> round of mass spectrometry in YE5S and EMM, respectively.

## 2.2.5. Role of novel Tea4-associated proteins

### 2.2.5.1. Ppk2

Mass spectrometry results demonstrated that Tea4 associates with Ppk2, thus I investigated the role of Ppk2 kinase. The kinase domain of Ppk2 is predicted to be catalytically inactive. The function of this pseudokinase remains unknown therefore I first tried to check its localization. I tagged the C-terminus of *ppk2* with GFP and I observed that Ppk2 mostly localizes at the cell ends (Fig. 2.9A). I also observed Ppk2 to localize as cytosolic dots but it seems not to be associated with microtubule plus ends. However more detailed investigation of Ppk2 with time-lapse experiments and co-localization with microtubules could clarify its cytosolic localization. I then deleted *ppk2* gene and I observed its phenotype. *ppk2Δ* cells exhibit monopolar cell growth (51 +/-3%, n=100), which becomes more severe in re-feeding experiments (88 +/-3%, n=100) (Fig. 2.9B). However, there were neither aberrant cell shapes nor septum misplacement (data not shown) in re-feeding experiments. Ppk2 could potentially play a significant role for cell polarity control and I will further comment on Ppk2 in the general discussion part.

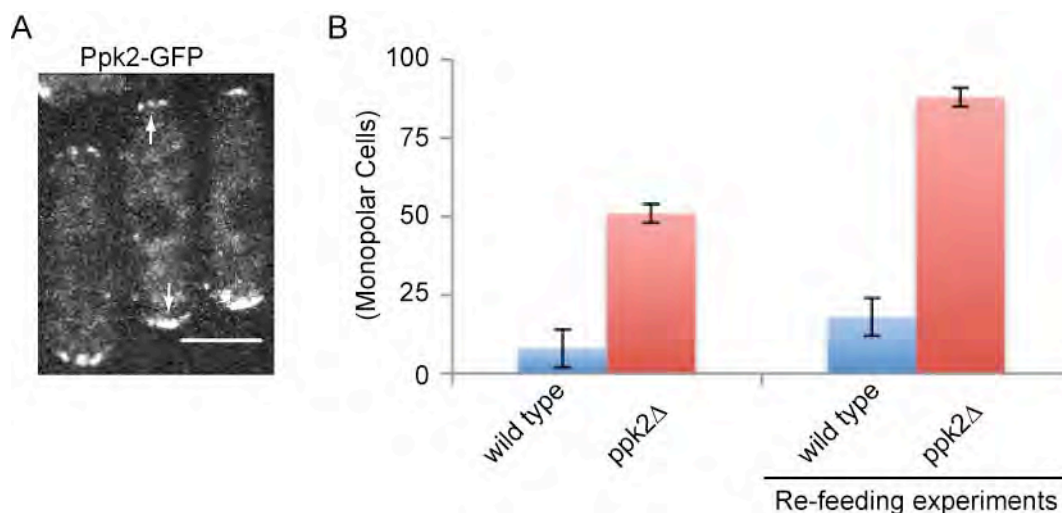


**Figure 2.9. Ppk2 localization and phenotype.** (A) Ppk2-GFP localizes at both cell tips (arrows). Scale bar 5 $\mu$ m. (B) Almost half of the cells grow in a monopolar manner when *ppk2* is deleted compared to wild type cells. In re-feeding experiments almost all cells grow only at one cell end.

### 2.2.5.2. Rga4 and Dis2

Mass spectrometry results identified Rga4 to be associated with Tea4<sup>SH3</sup>. To further investigate the role of Rga4, I observed its phenotypic and localization properties. Tatebe et al. in 2008 have shown that Rga4 normally localizes at the cell sides and is excluded from cell ends. It aberrantly localizes at the non-growing cell end in *tea4Δ* background. My study supports that Rga4 is also present at the non-growing tip when the SH3 domain is mutated and functional Tea4 SH3 domain negatively regulates Rga4 to localize at the cell tips (Figure 2.10B) so the cell can grow normally at both ends. *rga4Δ* cells exhibit monopolar cell growth (53+/-3%, n=100) when cells are grown in exponential phase similar to *tea4<sup>SH3</sup>* (Figure 2.10A). I also constructed an *rga4Δ tea4<sup>SH3</sup>* double mutant strain and cells showed an increase in monopolar growth (68+/-4%, n=100). This epistatic experiment suggests that deletion of both genes has additive effects regarding the monopolar growth of the cells. Interestingly, *rga4Δ* cells do not show morphology defects (bent or T-shapes) similar to the *tea4<sup>SH3</sup>* mutant. In fact, phenotypic analysis of *tea4<sup>SH3</sup> rga4Δ* double mutant in re-feeding experiments showed 12+/-2% (n=100) T-shaped cells compared to (90 +/-3%, n=100) T-shaped cells observed in *tea4<sup>SH3</sup>* single mutant (Figure 2.10A). Thus, deletion of *rga4* rescues in part the *tea4<sup>SH3</sup>* morphology defects suggesting that Rga4 presence is important for the ectopic growth observed at the cell side.

Additional proteins identified through mass spectrometry to associate with Tea4 were the redundant Type 1 Phosphatases Dis2 and Sds21. Interestingly, no peptides were found for these phosphatases in the *tea4<sup>SH3</sup>* mutant cells. Normally, Dis2 localizes at nuclei, at the cell tips and is likely associated with endocytic vesicles (Alvarez-Tabares et al., 2007). In wild type cells Sds21 localizes at the nucleolus. In *dis2Δ* cells, Sds21 localizes like Dis2. It has been also shown that in *tea4Δ* cells Dis2 is no longer localized at the cell ends (Alvarez-Tabares et al., 2007). I investigated whether Dis2 is delocalized when the Tea4 SH3 domain is mutated. Dis2 is no longer present at the cell ends in the SH3 mutant background (Figure 2.10B). As expected, deletion of *dis2* did not have any defect in cell growth and shape since Sds21 restores the loss of functions of *dis2Δ* cells (data not shown).

Since Dis2 is a Type 1 Phosphatase I checked whether Tea4 could be a substrate for dephosphorylation by Dis2. The Protein Analysis Facility (PAF) of CIG analyzed the samples of the 2<sup>nd</sup> TAP and tried to identify possible differences in phosphorylation between wild type and Tea4<sup>SH3</sup> peptides. Interestingly, phosphorylation analysis by shotgun approach and Mascot software identified a Tea4 peptide that contained 3 serines and 1 tyrosine (SSYS425-428) and was only phosphorylated in *tea4<sup>SH3</sup>* (Figure 2.10C) (also see predicted

phosphorylated sites in materials and methods). According to the analysis, the most likely phosphorylated residue is the S426 but it is also possible that one of the other residues is the real phosphorylation site. If dephosphorylation of one of these four residues by Dis2 occurs in wild type cells then the phenotype of *tea4<sup>SH3</sup>* mutant could be caused by constitutive phosphorylation of this amino acid (Dis2 is no longer associated with Tea4 when the SH3 domain is mutated). I substituted the SSYS425-428 to alanines (A), since alanines cannot be phosphorylated, in *tea4<sup>SH3</sup>* mutant cells (*tea4<sup>SH3</sup> AAAA425-428*). The expected result would be a partial or complete rescue of the mutant phenotype in the *tea4<sup>SH3</sup> AAAA425-428* cells. However, no changes were observed either to the phenotype or to the localization pattern in *tea4<sup>SH3</sup> AAAA425-428* (data not shown).

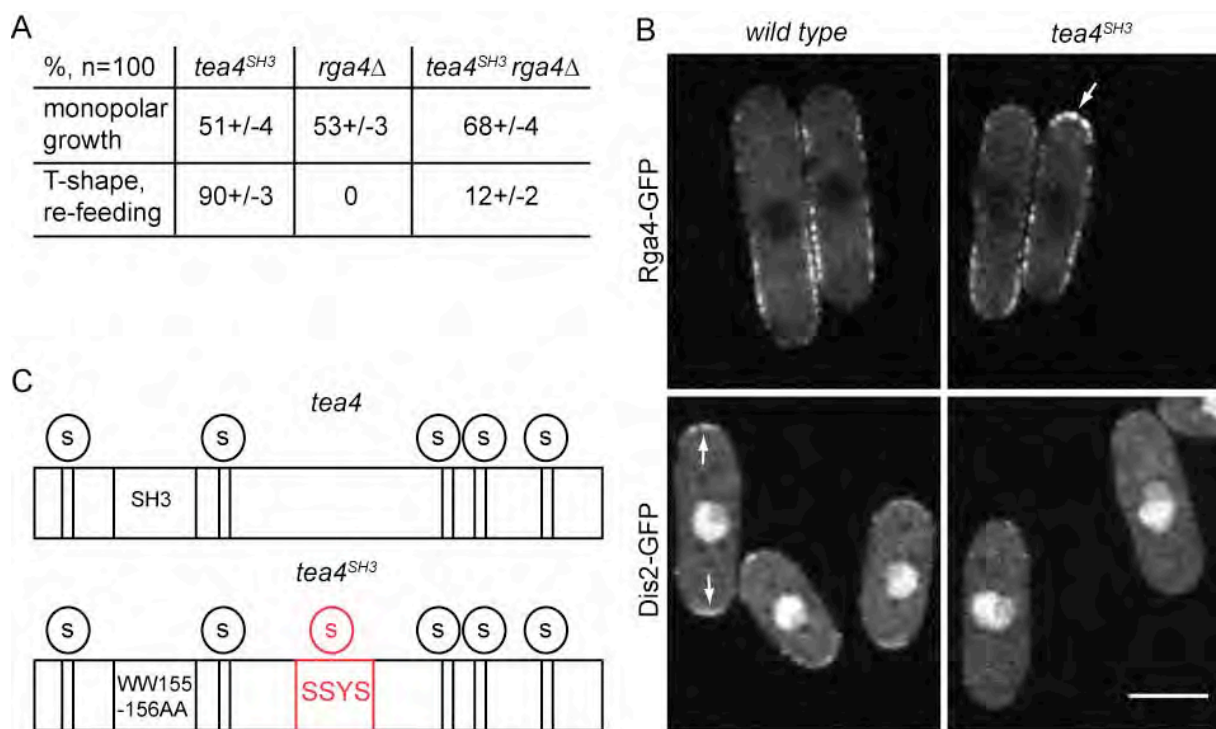


**Figure 2.10. Rga4 phenotype and localization. Dis2 localization and identification of Tea4 phosphorylated residues.** (A) Double mutant *tea4<sup>SH3</sup> rga4Δ* shows an increase in cells growing in a monopolar manner but rescues the T-shape phenotype observed in *tea4<sup>SH3</sup>* mutant. (B) Rga4 normally localizes at the cell sides and is excluded from the cell tips but in *tea4<sup>SH3</sup>* mutant is also present at the non-growing cell end (white arrow). Dis2 normally localizes at the cell ends (white arrows) but in *tea4<sup>SH3</sup>* mutant is no longer present at the cell tips. Scale bar 5μm. (C) Schematic structure of Tea4 and Tea4<sup>SH3</sup>. Phosphorylated residues only found in the mutant are highlighted in red.

### 2.2.6. Localization of Tea4-associated proteins

At this point of my research, I investigated whether the Tea4 SH3 domain is important for the localization of known polarity proteins. As shown in Chapter 3, DYRK kinase Pom1 was no longer anchored at the cortex and became completely cytosolic when the Tea4 SH3 domain was mutated (See Fig. 5C in Chapter 3) similar to *tea4* $\Delta$ . These results, combined with the disruption of Dis2 localization in *tea4*<sup>SH3</sup> mutant background shown above, were published in Hachet et al., 2011 (see Fig. 6D in Chapter 3). This paper of which I am a co-author proposes that Tea4 through Dis2 locally dephosphorylates Pom1 leading to its cortical localization.

I then imaged Tea1-GFP localization in *tea4*<sup>SH3</sup> cells. Tea1 localizes asymmetrically at the cell ends when the Tea4 SH3 domain is mutated (Fig. 2.11). Parallel imaging of Tea1-GFP with calcofluor staining showed that Tea1 accumulates at the non-growing cell end in *tea4*<sup>SH3</sup> cells (Fig. 2.11) as in *tea4* $\Delta$  (Martin et al., 2005). Remarkably, I found that polarity factors (Mod5, Tip1, Tea2 and Tea3, data not shown) were also localized at the non-growing cell end when the Tea4 SH3 domain is mutated. These results suggest that Tea4 through a functional SH3 domain seems to be responsible for the localization of these proteins at the growing cell end.

I checked the localization of the formin For3 and interestingly it was localized at the growing cell end in *tea4*<sup>SH3</sup> cells (Fig. 2.11) as in *tea4* $\Delta$  (Martin et al., 2005). Tea4 is thought to bring together Tea1 and For3 for NETO establishment. Although the SH3 domain is not important for Tea4 binding with Tea1 or For3, the Tea1-Tea4-For3 complex could fail to be formed in *tea4*<sup>SH3</sup> cells explaining why For3 accumulates only at the growing end. Furthermore, Bud6 and active Cdc42 (visualized by CRIB (Cdc42/Rac interactive binding)-GFP), two For3 regulators (Martin et al., 2007; Miller and Johnson, 1994; Tatebe et al., 2008), were also accumulated at the growing end when the SH3 domain was mutated (Fig. 2.11). These results suggest that cells expressing mutated Tea4 SH3 domain cannot assemble actin at the second cell end, thus failing to initiate bipolar growth.

To sum up, cell tip localization of various cell polarity factors depends on the SH3 domain of Tea4. Dis2 is no longer associated with the cell tips and Pom1 is cytosolic in *tea4*<sup>SH3</sup> mutant background but Rga4 is present at one cell end (non-growing). Furthermore, Tea1 and other microtubule-associated factors such as Tea2 and Tip1 accumulate preferentially at the non-growing end. It seems that these proteins are unable to be anchored at the growing end. In contrary, For3 and other actin-associated factors such as active Cdc42 and Bud6

accumulate preferentially at the growing end. These localization patterns are the same as in *tea4*Δ cells suggesting that *tea4*<sup>SH3</sup> allele shows loss of function phenotypes.

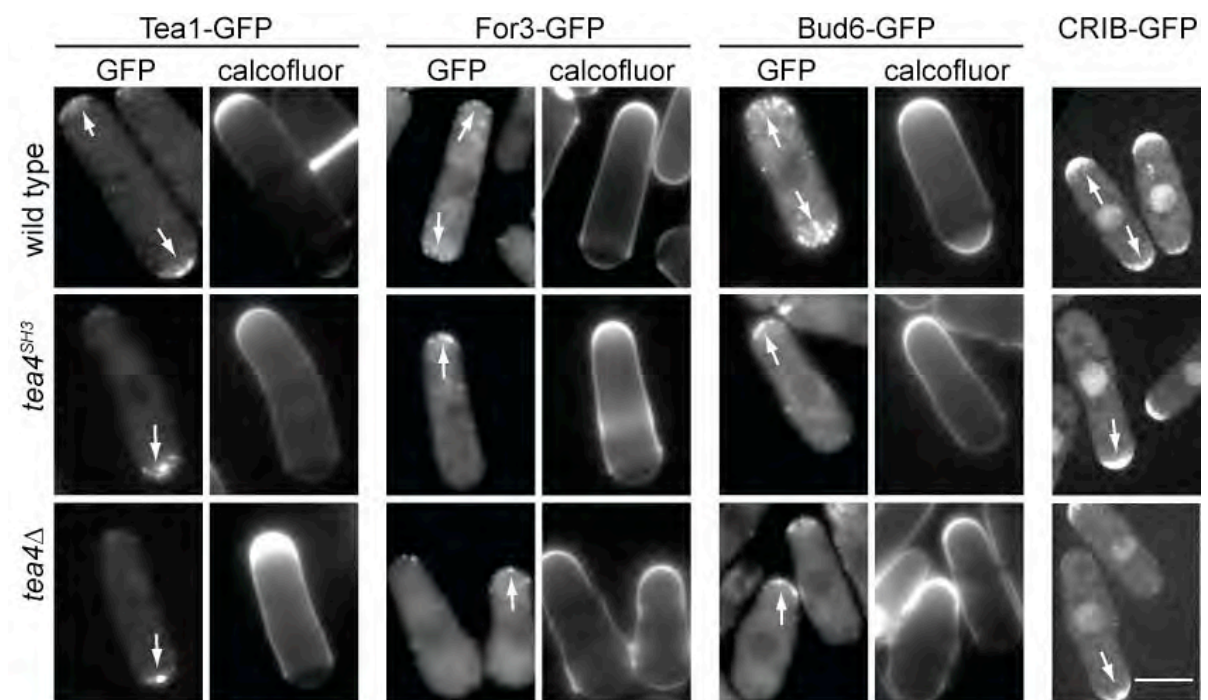


**Figure 2.11. Accumulation of multiple polarity proteins at only one cell end in *tea4*<sup>SH3</sup>.** Staining with 10μg/ml calcofluor shows microtubule-associated protein Tea1 to accumulate at the non-growing cell end and the actin-associated proteins For3 and Bud6 to accumulate at the growing end in *tea4*<sup>SH3</sup> cells similar to *tea4*Δ (arrows). CRIB-GFP also localizes at one cell tip (growing tip, calcofluor images are not shown). Scale bar 5μm.



## 2.3. Conclusions and discussion

The results presented in this chapter have shown that a functional Tea4 SH3 domain is necessary for the proper localization of various proteins. *tea4<sup>SH3</sup>* mutant cells share similar delocalization patterns of multiple polarity factors and morphologic abnormalities as *tea4Δ* cells. However, as the monopolar phenotype is more penetrant for *tea4Δ*, *tea4<sup>SH3</sup>* is likely a hypomorphic allele of *tea4*. The SH3 domain thus plays an important role for Tea4 functions, but other Tea4 regions also contribute to Tea4 role for control of polarized growth. For instance, the Tea4 RVxF motif downstream of its SH3 domain is also important for Type 1 Phosphatase Dis2 binding and its localization at the cell tips (Alvarez-Tabares et al., 2007; Hachet et al., 2011). Although the RVxF mutation specifically blocks Dis2 binding, which is already disrupted by SH3 mutations, mutating both SH3 domain and RVxF motif could show whether the RVxF plays additional role for Tea4 functions in addition to binding Dis2. Other Tea4 regions, especially at the C-terminus, are also implicated in Tea1 and For3 binding (Martin et al., 2005), which could also play a role in Tea4 function.

Microtubule-associated proteins Tea1 and Tea4 accumulate at the non-growing end in *tea4<sup>SH3</sup>* cells, similar to what was observed in *tea4Δ* cells (Martin et al., 2005). How does this asymmetry come about? It is possible that monopolar accumulation at the non-growing tip could be due to the absence of endocytosis at this tip. Bipolar growing wild type cells should have similar turnover of Tea1 and Tea4 at the cell tips (Fig. 2.12A). In contrast, *tea4<sup>SH3</sup>* monopolar cells accumulate actin patches only at the growing tip indicating limited endocytosis events at the non-growing end. Defects in endocytosis could prevent recycling of polarity factors from the non-growing tip leading to their accumulation. More studies with proteins involved in regulation of cortical actin patch distribution such as Arp2 would be of major interest (Morrell et al., 1999). Investigating Arp2 mutant to see whether cells grow in monopolar manner and whether Tea4 accumulates at one cell tip could support the hypothesis that defective endocytosis may result in Tea4 asymmetric localization. In addition, it has also been proposed that Tea1 forms clusters with Mod5 and through positive feedback loops this Tea1-Mod5 complex establishes polarized growth (Bicho et al., 2010) (Fig. 2.12A). Positive feedback loops between Mod5 and Tea1/ Tea4 may retain Tea1 and Tea4 at the cell ends in wild type cells but in *tea4<sup>SH3</sup>* cells Mod5 is preferentially accumulated at the non-growing end suggesting Tea1 and Tea4 anchoring at the growing end may become transient and not enhanced by positive feedback loops due to Mod5 absence resulting in Tea1 and Tea4 tip dissociation.

Interestingly, after 1 hour addition of MBC, Tea1 and Tea4 switch their localization from the non-growing to the growing cell end, even in *mod5Δ* cells (Fig. 2.12B). This observation is intriguing. Defective endocytosis may explain the Tea1 and Tea4 monopolar accumulation but cannot explain how they become enriched at the growing end after 1 hour MT disruption. According to FRAP values, absence of microtubules results in more dynamic and less stable Tea1 and Tea4 tip localization. Tea1 and Tea4 could abolish the non-growing cell end localization and randomly move through diffusion and then be “trapped” at the growing cell tip (Fig. 2.12A and B). These results indicate that Mod5-independent mechanisms exist to anchor Tea1 and Tea4 at the growing end and also suggests that microtubule-independent localization mechanisms exist, which allow the cell end switch of Tea4<sup>SH3</sup>. Tea3 has been shown to be responsible for Tea1 anchoring to the growing cell end after disruption of MTs (Snaith et al., 2005) suggesting it may be an important factor for both Tea1 and Tea4 anchoring at the growing end (Fig. 2.12B). Tea4-binding factor, the actin nucleator For3 could also be a potential candidate for Tea4 anchoring at or transport to the growing tip (Fig. 2.12B). For3 localizes only at the growing end in cells having non-functional Tea4. Since actin cables serve as tracks for myosin-mediated cargo transport, Tea4 could associate with actin cables and be transported towards the growing end (Fig. 2.12B). It has been shown that a Tea2 kinesin chimeric motor protein can transport myosin V cargos along microtubules (Lo Presti and Martin, 2011). In my study, the opposite may apply: In this scenario, actin cables and specifically myosins may serve as back-up transport for microtubule-associated factors. Checking Tea1 and Tea4 localization in double mutant *for3Δmod5Δ* in absence of microtubules could clarify whether presence of Tea1 and Tea4 at the growing cell end is actin-mediated when *mod5* is deleted and microtubules are disrupted. Fission yeast cells may have redundant robust polarization strategies enough to utilize both cytoskeleton mechanisms to target polarity factors towards the cell end. Possible interactions between microtubule-associated proteins and actin could establish and maintain fission yeast polarized growth similar to other mammalian systems (Rodriguez et al., 2003).

I showed that Tea4 and multiple polarity proteins have asymmetric localization patterns and grow in a monopolar manner when the SH3 domain is mutated similar to *tea4Δ*. What comes first? Does monopolar growth lead to asymmetric localization of polarity factors or does asymmetric accumulation of polarity factors only at one cell end lead to monopolar growth? Understanding whether local accumulation of Tea1 and Tea4 establishes growth or growth enforces them to be locally accumulated still remains of major importance. In fission yeast, symmetric Cdc42 at the cell ends is proposed to lead to polarized growth at the cell tips (Das et al., 2009). Although localization of Cdc42 at both tips in *pom1Δ rga4Δ* monopolar mutant cells does not rescue result in bipolar growth (Tatebe et al, 2008) indicating that Cdc42

cannot act as a sole protein to initiate growth, it is also proposed that specific Cdc42 amounts at the cell end enable pre-NETO cells to initiate bipolar growth (Das et al., 2012b). Furthermore manipulating fission yeast shape physically with microfluidic chambers leads to accumulation of polarity factors ectopically resulting in local growth (Minc et al., 2009; Terenna et al., 2008). In addition, spheroplasts seem to first locally accumulate polarity factors and then resume polarized growth independent of their initial round cell shape (Kelly and Nurse, 2011a). Even if the geometry of budding yeast cells is different compared to fission yeast, growth in *S. cerevisiae* occurs in a similar way. Based on the model proposed for polarized growth in budding yeast, Cdc42 is the major highly conserved protein landmark to break symmetry and define the site of bud emergence in pre-budded rounded cells (Butty et al., 2002; Johnson, 1999; Johnson et al., 2011; Park and Bi, 2007). Altogether this suggests that *tea4*<sup>SH3</sup> similar to *tea4*Δ localize active Cdc42 asymmetrically that may lead to monopolar growth. It seems that cell tip accumulation of polarity factors such as For3 and especially active Cdc42, first defines the growth zone followed by growth.

Showing that Cdc42 may result in local growth still does not explain clearly what comes first regarding Tea1 and Tea4 asymmetric accumulation and monopolar growth. As previously mentioned, localization of Cdc42 at both tips in *pom1*Δ *rga4*Δ double mutant cells does not rescue their monopolar growth (Tatebe et al., 2008). In this monopolar mutant it is most likely that Tea1 and Tea4 still localize asymmetrically. Interestingly, the formation of a Tea1-For3 complex at the new cell end is sufficient to initiate bipolar growth in *tea4*Δ monopolar cells (Martin et al., 2005). This result suggests that bipolar distribution of actin in *tea4*Δ mutant cells rescue their monopolar growth pattern proposing that growth might follow symmetry. Generating a Tea1-Arp2 chimera that could recruit actin patches also at the non-growing cell end in *tea4*Δ monopolar cells could result in bipolar endocytosis and eventually growth, supporting the hypothesis that growth may come after symmetry. In addition, detailed time-lapse microscopy of polarity factors localization in cells in re-feeding experiments whereas cells stopped growing and then need to re-establish growth *de novo* could give more clear answers of what comes first: the symmetry or the growth.



## **Chapter 3**

# **A phosphorylation cycle shapes gradients of the DYRK family kinase Pom1 at the plasma membrane. *Cell* 145, 1116-1128.**

### **3.1. Summary**

In many biological functions, concentration gradients play a crucial role and specifically in rod-shaped fission yeast cells, DYRK family kinase Pom1 forms gradients that emanate from the cell tips regulating cell cycle progression. This paper tries to answer three key questions regarding Pom1 gradient formation: how Pom1 associates with the cell cortex, how this association is modulated by kinase activity and how Tea4 mediates Pom1 recruitment to cell tips. First, microtubule-associated protein Tea4 is necessary and sufficient to recruit Pom1 to the cell cortex. Pom1 then moves laterally at the plasma membrane, which it binds through a basic region exhibiting direct lipid interaction. Then, Pom1 autophosphorylates in this region to lower lipid affinity and promotes membrane release. Tea4 triggers Pom1 plasma membrane association by promoting its dephosphorylation through the Type 1 Phosphatase Dis2. My contribution in this paper was first to show that Pom1 becomes cytosolic in *tea4<sup>SH3</sup>* mutant cells (Fig. 5C). Second, I performed the experiments in Figure 6C and 6D showing the interaction of Tea4 with Dis2. Tea4-HA was coimmunoprecipitated with GFP-Dis2 in wild-type cells (Figure 6C) and this interaction was dependent on the Tea4 RVxF motif, as previously described (Alvarez-Tabares et al., 2007). In addition, I also found that the integrity of the Tea4 SH3 domain was essential for this interaction. Indeed, both Tea4<sup>RVxF</sup> and Tea4<sup>SH3</sup> failed to coimmunoprecipitate with GFP-Dis2 (Figure 6C). Accordingly, Dis2 was delocalized from the cell tips in *tea4Δ*, *tea4<sup>RVxF</sup>*, and *tea4<sup>SH3</sup>* mutants, but not in *pom1Δ* backgrounds (Figure 6D). These results, together with other lines of evidence presented in the manuscript, led to the hypothesis that efficient localization of Pom1 to the cell tip cortex requires both binding to Tea4 and interaction between Tea4 and the phosphatase Dis2, indicating that Tea4 bridges Pom1 with Dis2 to promote the dephosphorylation of Pom1 at cell tips. In conclusion, Tea4 mediates the cell tip dephosphorylation of Pom1 through Dis2 resulting in Pom1 binding to the cell membrane and followed by Pom1 lateral diffusion and autophosphorylation leading to Pom1 gradients formation.



# A Phosphorylation Cycle Shapes Gradients of the DYRK Family Kinase Pom1 at the Plasma Membrane

Olivier Hachet,<sup>1</sup> Martine Berthelot-Grosjean,<sup>1,2</sup> Kyriakos Kokkoris,<sup>1</sup> Vincent Vincenzetti,<sup>1</sup> Josselin Moosbrugger,<sup>1</sup> and Sophie G. Martin<sup>1,\*</sup>

<sup>1</sup>Department of Fundamental Microbiology, Faculty of Biology and Medicine, University of Lausanne, CH-1015 Lausanne, Switzerland

<sup>2</sup>Present address: Centre des Sciences du Goût et de l'Alimentation, UMR-6265 CNRS, UMR-1324 INRA, Université de Bourgogne, Agrosup Dijon, 21000 Dijon, France

\*Correspondence: [sophie.martin@unil.ch](mailto:sophie.martin@unil.ch)

DOI 10.1016/j.cell.2011.05.014

## SUMMARY

Concentration gradients regulate many cell biological and developmental processes. In rod-shaped fission yeast cells, polar cortical gradients of the DYRK family kinase Pom1 couple cell length with mitotic commitment by inhibiting a mitotic inducer positioned at midcell. However, how Pom1 gradients are established is unknown. Here, we show that Tea4, which is normally deposited at cell tips by microtubules, is both necessary and, upon ectopic cortical localization, sufficient to recruit Pom1 to the cell cortex. Pom1 then moves laterally at the plasma membrane, which it binds through a basic region exhibiting direct lipid interaction. Pom1 autophosphorylates in this region to lower lipid affinity and promote membrane release. Tea4 triggers Pom1 plasma membrane association by promoting its dephosphorylation through the protein phosphatase 1 Dis2. We propose that local dephosphorylation induces Pom1 membrane association and nucleates a gradient shaped by the opposing actions of lateral diffusion and autophosphorylation-dependent membrane detachment.

## INTRODUCTION

Concentration gradients regulate various cell biological and developmental processes, ranging from mitotic spindle organization to body patterning. Biological gradients are best understood during development, when morphogen gradients translate cell position into distinct cell fate, depending on local morphogen concentration. Gradients also occur at much smaller scales within cells, where they impart spatial cellular order. For instance, gradients of Ran-GTP and phospho-stathmin regulate mitotic spindle formation around chromatin, Aurora B gradients control cytokinesis, and gradients of MinD, MipZ, and Pom1 provide spatial control on cell division in various prokaryotes and eukaryotes (Fuller, 2010; Lutkenhaus, 2007). A defining feature of gradients is their potential to communicate information

over long distances, for which gradient shape should be carefully monitored. Thus, understanding the molecular mechanisms underlying gradient formation is crucial. Here, we have dissected the mechanisms of gradient formation of the DYRK family kinase Pom1 in fission yeast.

*Schizosaccharomyces pombe* cells are rod-shaped, grow by cell tip extension, and divide by medial fission. Spatial order is conferred by a system of antiparallel microtubules aligned along the length of the cell and nucleated from nuclear-associated organizing centers. Microtubules serve to position the nucleus to the geometric middle of the cell and transport a pair of landmark proteins, Tea1 and Tea4, to cell ends (Chang and Martin, 2009; Martin et al., 2005; Mata and Nurse, 1997; Tatebe et al., 2005). In turn, these landmarks recruit Pom1 to cell ends, from where this protein forms concentration gradients (Bähler and Pringle, 1998; Padte et al., 2006; Tatebe et al., 2005). These three proteins regulate cell morphology and bipolar growth, in part by allowing Cdc42 activation and recruiting actin nucleation factors to cell tips (Martin et al., 2005; Tatebe et al., 2008). Tea4 also directly associates with and recruits the protein phosphatase 1 (PP1) Dis2 to cell tips (Alvarez-Tabarés et al., 2007). Dis2 is one of only two PP1 catalytic subunits in *S. pombe* and is recruited to many cellular locations by specific regulatory factors. Tea1, Tea4, and Pom1 also impart negative signal to prevent cell division at cell tips (Almonacid et al., 2009; Celton-Morizur et al., 2006; Huang et al., 2007; Padte et al., 2006). Together with positive signals conferred by the nucleus through the protein Mid1 (Almonacid et al., 2009), negative signals from cell tips define the position of cell division at midcell.

In addition to Pom1's roles in bipolar growth, cell morphogenesis, and septum positioning, we and others recently discovered that this kinase functions as a dose-dependent inhibitor of entry into mitosis (Martin and Berthelot-Grosjean, 2009; Moseley et al., 2009). Pom1 negatively regulates an activator of mitotic entry, the protein kinase Cdr2. While Pom1 forms polar gradients, Cdr2 localizes to a cortical band placed at the cell equator (Morrell et al., 2004). The observation that Pom1 concentration at midcell is higher in short than long cells suggested a model where Pom1 inhibits Cdr2 until the cell has reached a sufficient length. Accordingly, experiments in which Pom1 was ectopically localized at the cell equator led to a delay of mitosis and the formation of elongated

cells. Thus, Pom1 gradients form a cell length-monitoring system for coordinating mitotic commitment with cell growth.

Pom1 is part of the DYRK (*d*ual-specificity tyrosine-regulated kinase) family of kinases conserved in eukaryotes. These kinases self-catalyze the phosphorylation of tyrosines in their activation loop in an autophosphorylation reaction that occurs on a DYRK translational intermediate (Lochhead et al., 2005). Mature DYRKs do not phosphorylate tyrosines but can phosphorylate substrates on serines and threonines. In vitro work on mammalian DYRK1a, DYRK2, and DYRK3 has shown that phosphorylation occurs preferentially within the consensus  $RX_{(1-3)}[ST][PVL]$  (Campbell and Proud, 2002; Himpel et al., 2000), although several DYRK substrates show considerable variation relative to this consensus (Aranda et al., 2011). Although the specific substrates of each DYRK diverge widely and are still poorly defined, a common function of this family may be coordination of cell cycle, cell growth, and differentiation (Aranda et al., 2011).

To understand how the Pom1 length-sensing device works for cell size homeostasis, we asked how Pom1 gradients are established. Our experiments were guided by two previously known pieces of information: first, Tea1 and Tea4 are essential for the localization of Pom1 to cell tips (Bähler and Pringle, 1998; Celton-Morizur et al., 2006; Padte et al., 2006; Tatebe et al., 2005); and second, Pom1 distribution depends on its activity because a kinase-dead version of Pom1 localizes indiscriminately around the entire cell periphery (Bähler and Nurse, 2001). We demonstrate a simple mechanism underlying the formation of cortical concentration gradients of Pom1, which are nucleated by local Tea4-mediated dephosphorylation and shaped by lateral movement and autocatalytic activity.

## RESULTS

### Tea4 Is Necessary and Sufficient to Nucleate Pom1 Gradients at the Cell Cortex

Pom1-GFP gradients have previously been measured in projections of the entire cell volume including both cytoplasmic and cortical compartments onto a single line. Confocal sectioning suggests that these gradients are primarily cortical (Figure 1A and Figure S1A available online). This can be illustrated by measuring the fluorescence along lines drawn at the cell cortex or across the length of the cell. Whereas the latter shows a uniform low concentration of Pom1 in the cytoplasm, the fluorescence profile along the cell cortex reveals gradients of Pom1 with highest concentration at cell tips. We note that these gradients are not completely smooth but that clusters of higher intensity are visible at the cortex.

We envisaged a simple model where Pom1 concentration gradients are established by protein transport/trapping and lateral movement. The microtubule-associated polarity landmarks Tea1 and Tea4 are required for Pom1 localization (Bähler and Pringle, 1998; Celton-Morizur et al., 2006; Padte et al., 2006; Tatebe et al., 2005). In a limited screen through polarity mutants, we found that *tea1*Δ and *tea4*Δ were the only mutants to robustly affect Pom1-GFP localization (Figures S1B and S1C). Pom1 failed to localize to the cell cortex in *tea4*Δ cells, except for weak residual localization at the division site, and instead appeared cytoplasmic. In *tea1*Δ cells in contrast, in which

Tea4 fails to localize to cell ends (Martin et al., 2005; Tatebe et al., 2005), weak cortical localization of Pom1 was observed (Padte et al., 2006) (Figure S1B). Thus, we focused our attention on Tea4. Measurement of Tea4-GFP and Pom1-GFP distributions at cell tips showed that these are distinct: Pom1 exhibits a wider cortical localization than Tea4 (Figure 1B, far right). Similarly, Tea4-GFP and Pom1-tdTomato imaged in double-tagged strains do not precisely overlap: whereas Tea4 is restricted to the tips of the cells, Pom1 spreads further along cell sides (Figure 1B). Importantly, Pom1-tdTomato exhibits the same localization pattern as Pom1-GFP (Figure 1B, far right panel), indicating that different fluorophores do not influence the observed patterns of Pom1 localization. This differential distribution suggests that Tea4 may recruit Pom1 to cell tips from where Pom1 moves in the plane of the membrane.

To visualize Pom1 lateral movement, we photobleached Pom1-GFP at half-cell tips (Figure 1C). Recovery of signal occurred faster at the edges of the bleached region, indicating movement from the adjacent fluorescent half. Fluorescence recovery after photobleaching (FRAP) experiments on inactive Pom1<sup>KD</sup>-GFP, which localizes around the entire cell cortex (Bähler and Nurse, 2001), confirmed this behavior. Here, we photobleached the entire midsection of the cell (Figure 1D). Again, we detected nonuniform recovery of fluorescence suggestive of movement from the adjacent nonbleached zone. Thus, Pom1 moves laterally at the plasma membrane.

These results suggest that recruitment of Pom1 by Tea4 at cell tips and lateral movement are key elements for the formation of Pom1 gradients. To test whether these are sufficient to generate Pom1 gradients, we ectopically localized Tea4 by generating a fusion between the spindle pole body (SPB) component Ppc89, GFP, and Tea4 and expressing it in *tea4*Δ *pom1*-tdTomato cells. Ppc89-GFP-Tea4 mimicked the localization patterns of both Ppc89 and Tea4 to the SPB and cell ends, respectively. This fusion also unexpectedly formed ectopic foci along cell sides. Pom1-tdTomato was recruited to cell ends and to these ectopic lateral foci, but not to the SPB (Figure 1E). Measurement of the distribution of these proteins suggested that, whereas the Ppc89-GFP-Tea4 fusion formed tight dots, Pom1-tdTomato spread further along the plane of the membrane (Figure 1F, a), indicating the formation of local cortical Pom1 gradient. In contrast, control measurements perpendicular to the plane of the membrane showed nearly identical distribution of Tea4 and Pom1 along this axis (Figure 1F, b). Thus, Tea4 is not only necessary but also sufficient to nucleate the formation of a Pom1 gradient anywhere along the cell cortex.

Below, we dissect three key elements in the formation of Pom1 gradients: how Pom1 associates with the cell cortex; how this association is modulated by kinase activity; and finally, how Tea4 mediates Pom1 recruitment to cell tips.

### Pom1 Binds Lipids

To map the region of Pom1 required for cortex localization, we generated a series of GFP-tagged truncations of Pom1 on plasmids and observed their localization in *pom1*Δ cells (Figures 2A–2C). Truncation of the first 305 amino acids had no apparent effect on Pom1 localization. Pom1 lacking the first 419 residues still localized to the cortex, albeit less efficiently. In contrast,

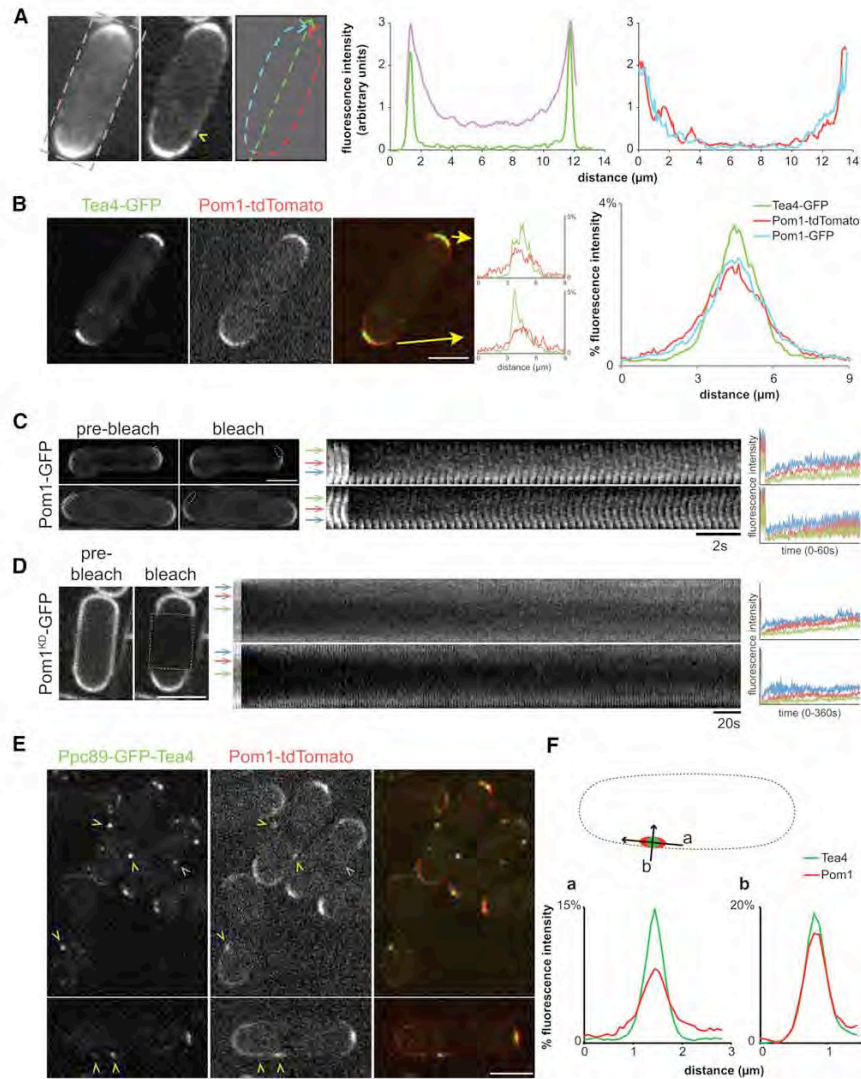


**Figure 1. Tea4 Is Sufficient to Nucleate a Cortical Pom1 Gradient**

(A) Sum projection (left) and single medial confocal section (right) of Pom1-GFP. The purple line represents the total cellular measure of Pom1-GFP fluorescence intensity projected onto a single line. Green, red, and blue lines represent measures on the medial confocal section, as shown. The yellow arrowhead labels a Pom1-GFP cluster at the cell cortex.

(B) Localization of Tea4-GFP and Pom1-tdTomato in the same cell. The profile of fluorescence intensity along the periphery of both cell ends is shown on the right. The far-right graph shows an average over 16 such measurements, as well as measurements of Pom1-GFP distribution as shown in (A). To compare fluorescence distribution, the integrated fluorescence intensity for each curve was normalized to one, and percentage of this total is shown on the graphs.

(C and D) Kymographs of FRAP at the lateral cortex of Pom1-GFP and Pom1<sup>KD</sup>-GFP expressed from plasmids. The cells on the left show the prebleach and bleach time points. Boxes represent the regions used in the kymographs and the bleach zone, respectively. Graphs show the fluorescence profile along lines drawn on the kymographs at the levels of the colored arrows. Note that recovery occurs preferentially from the edges of the bleached region.

(E) Ppc89-GFP-Tea4 recruits Pom1-tdTomato to the lateral cortex, but not the nuclear membrane. Yellow arrowheads denote lateral localization of Ppc89-GFP-Tea4 and Pom1-tdTomato. Blue arrowhead shows SPB localization of Ppc89-GFP-Tea4 and absence of Pom1-tdTomato. Scale bars, 5 μm.

(F) Distribution of Ppc89-GFP-Tea4 and Pom1-tdTomato along (a) and perpendicular to (b) the lateral plasma membrane. Average of 30 measurements is shown. Curves were normalized as in (B).

See also Figure S1.

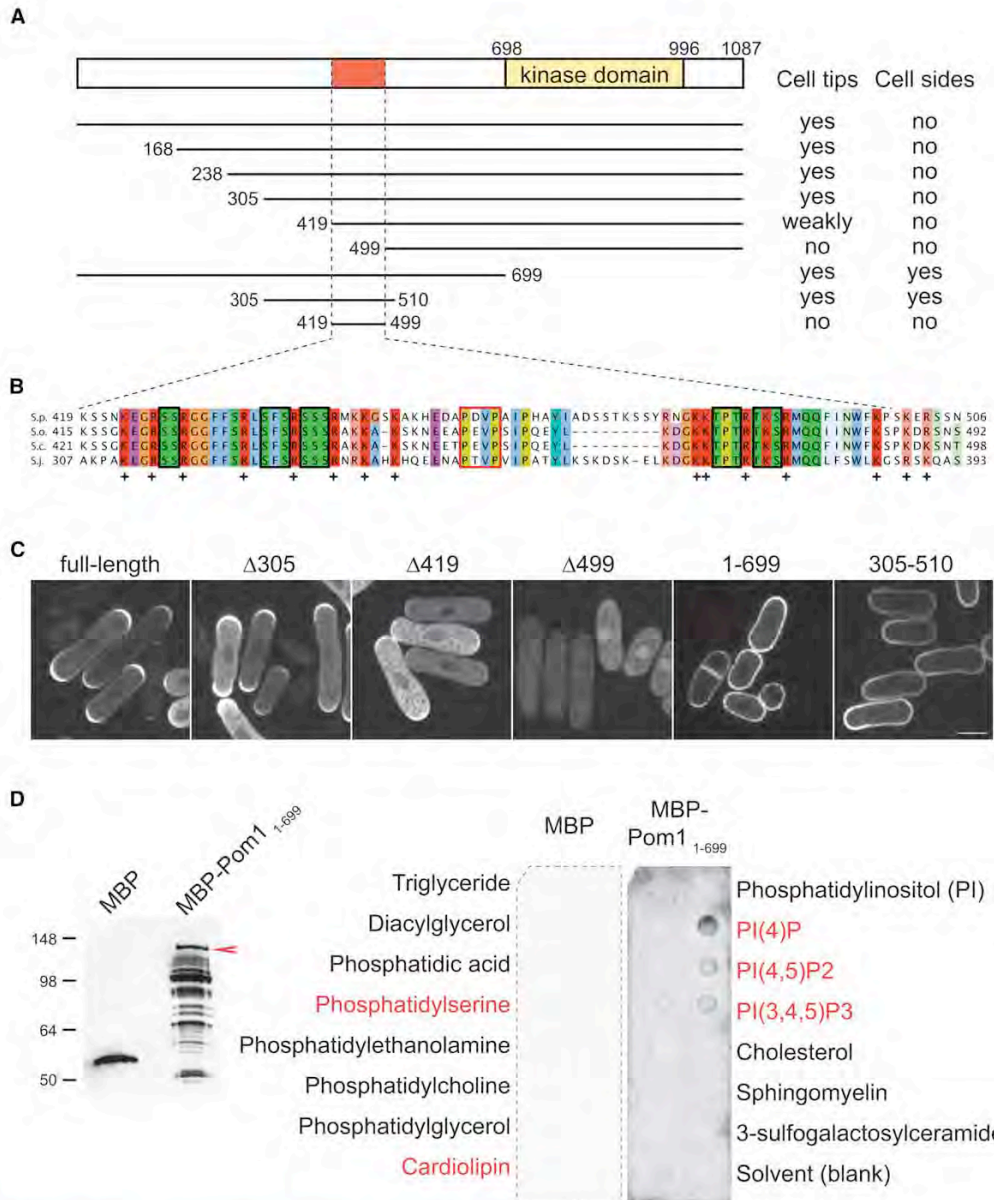


**Figure 2. A Positively Charged Region of Pom1 Mediates Lipid Binding**

(A) Schematic representation of Pom1 and truncation fragments. These were tagged with GFP, expressed from plasmids in *pom1*  $\Delta$  cells and imaged. Description of their localization is detailed on the right.

(B) Alignment of the region necessary for cortical binding between Pom1 orthologs in four *Schizosaccharomyces* species: *S.p.*, *pombe*; *S.o.*, *octosporus*; *S.c.*, *cryophobus*; and *S.j.*, *japonicus*. Conserved basic residues are highlighted in red and by plus (+) signs. Black squares box serine/threonine residues mutated to alanine in the Pom1<sup>6A</sup> allele. The red square boxes proline residues mutated to alanine in the Pom1<sup>SPXXP</sup> allele.

(C) Localization of selected constructs as described in (A). Scale bar, 5  $\mu$ m.

(D) Protein-lipid overlay assay with MBP and MBP-Pom1<sub>1-699</sub>. Loading control is shown as anti-MBP western blot on the left. Full-length MBP-Pom1<sub>1-699</sub> fragment is labeled by red arrowhead. Lower bands likely represent breakdown products. Lipids spotted on each side of both membranes are indicated on the left and right, respectively. Lipids to which MBP-Pom1<sub>1-699</sub> shows significant association are shown in red. Both blots were treated in parallel using identical conditions throughout.

See also Figure S2.

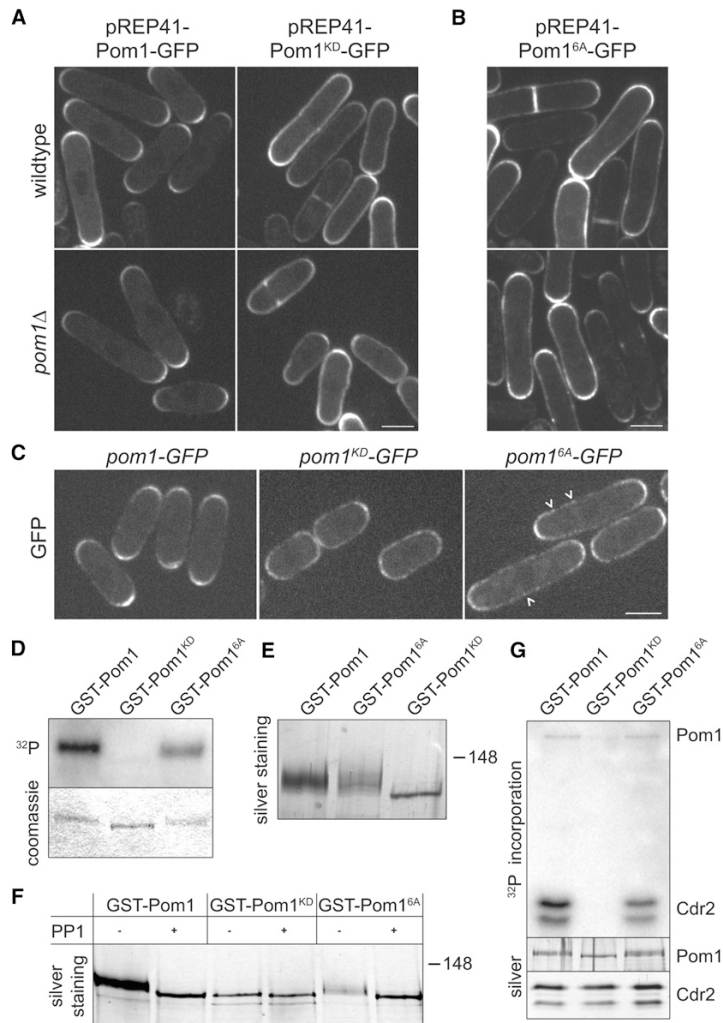


**Figure 3. Autophosphorylation of Pom1 Restricts Its Cortical Localization to Cell Tips**

(A) Localization of Pom1-GFP and inactive Pom1<sup>KD</sup>-GFP expressed from plasmids in wild-type and *pom1Δ* strains. (B) Localization of nonphosphorylatable Pom1<sup>6A</sup>-GFP expressed from plasmids in wild-type and *pom1Δ* strains. (C) Localization of Pom1-GFP, Pom1<sup>KD</sup>-GFP, and Pom1<sup>6A</sup>-GFP integrated as sole copy at the endogenous *pom1* locus. Arrowheads label a few Pom1<sup>6A</sup>-GFP clusters at the cell cortex. Scale bars, 5 μm. (D) In vitro kinase assay on recombinant GST-Pom1, GST-Pom1<sup>KD</sup>, and GST-Pom1<sup>6A</sup>. Top panel shows phosphorimager detection of <sup>32</sup>P incorporation; bottom panel shows Coomassie-stained gel. (E) Side-by-side comparison of the migration patterns of GST-Pom1, GST-Pom1<sup>6A</sup>, and GST-Pom1<sup>KD</sup>. (F) Migration pattern of recombinant GST-Pom1, GST-Pom1<sup>KD</sup>, and GST-Pom1<sup>6A</sup> with or without PP1 treatment. Silver-stained gel is shown. (G) In vitro kinase assay of recombinant GST-Pom1, GST-Pom1<sup>KD</sup>, and GST-Pom1<sup>6A</sup> with 6His-Cdr2<sub>423-532</sub> as substrate. Top panel shows phosphorimager detection of <sup>32</sup>P incorporation; bottom panels show silver-stained gels. See also Figure S3.

(Figure 2D). Phosphatidylserine and phosphatidylinositol phosphates are components of the plasma membrane. Cardiolipin is mostly found in the inner mitochondrial membrane, and so it is unclear whether this interaction exists in vivo. We also note that, probably due to its high global positive charge (+15.5 for MBP-Pom1<sub>1-699</sub>, +25 for Pom1<sub>1-699</sub> at pH 7), MBP-Pom1<sub>1-699</sub> bound the nitrocellulose membrane, resulting in significant background. Together, these experiments suggest that Pom1 directly associates with lipids at the plasma membrane through its basic region.

**Pom1 Autophosphorylates to Restrict Its Localization to Cell Tips**

Investigation of a kinase-dead allele of *pom1* (*pom1-2*; here labeled *pom1<sup>KD</sup>*) has previously shown that Pom1 kinase activity modulates its localization: in contrast to Pom1-GFP localization to cell tips, Pom1<sup>KD</sup>-GFP expressed as sole copy from the endogenous promoter localizes indiscriminately around the entire cell cortex (Bähler and Nurse, 2001) (see also Figure 3C). We confirmed this observation by expressing Pom1<sup>KD</sup>-GFP from plasmids in *pom1Δ* cells. Importantly, when expressed in wild-type cells, Pom1<sup>KD</sup>-GFP was also mislocalized around the entire cortex, indicating that the endogenous wild-type Pom1 activity, though competent for regulating cell morphogenesis and size, was not able to restore correct localization to the inactive kinase (Figure 3A). Similarly, expression of wild-type untagged Pom1 from plasmids in *pom1<sup>KD</sup>-GFP* cells was unable to restore the localization of endogenous Pom1<sup>KD</sup>-GFP to cell tips (data not shown). These data suggest that Pom1 autophosphorylates to restrict its localization to cell tips.

deleting the first 499 residues prevented cortex localization, defining amino acids 419–499 as essential for cortical localization. Pom1 fragments containing this region but lacking the kinase domain (i.e., Pom1<sub>1-699</sub> and Pom1<sub>305-510</sub>) localized efficiently to the cell cortex but were not restricted to cell ends (see below). However, we note that the fragment 419–499 was not sufficient for cortical localization. Sequence alignment showed that this region was well conserved between Pom1 and orthologs in other *Schizosaccharomyces* species (Figure S2 and Figure 2B).

This region is rich in arginine and lysine residues (19 out of 81 residues) and, thus, highly positively charged, suggesting that it may bind negatively charged lipids directly through electrostatic interactions. Indeed, recombinant Pom1 N-terminus (MBP-Pom1<sub>1-699</sub>) was able to bind directly to several, but not all, negatively charged lipids, namely phosphatidylserine, phosphatidylinositol phosphates, and cardiolipin in a protein-lipid overlay assay

Work on mammalian DYRKs has defined a loose phosphorylation consensus site  $RX_{(1-3)}[ST][PVL]$  (Campbell and Proud, 2002; Himpel et al., 2000). We hypothesized that Pom1 phosphorylates similar sites and looked for conserved candidate autophosphorylation sites in the Pom1 sequence using the degenerate simplified  $[RK]X_{(1-3)}[ST]$  motif. This identified 15 candidate sites. We focused on those located outside the kinase domain and in well-conserved regions of the proteins and mutated up to six to alanine to generate Pom1<sup>1A</sup>–Pom1<sup>6A</sup>. (Note that one site can include one to three serines or threonines that we mutated simultaneously.) Five of these sites were in the region mediating lipid binding defined above (Figure S2 and Figure 2B). Expression of Pom1<sup>1A</sup>-GFP to Pom1<sup>6A</sup>-GFP on plasmids in *pom1Δ* cells showed a progressive spreading of the kinase along the cortex of the cells (Figure S3). Pom1<sup>6A</sup>-GFP recapitulated the largely homogeneous cortical localization observed for Pom1<sup>KD</sup>-GFP in either wild-type or *pom1Δ* cells (Figure 3B). We note that strong overexpression of Pom1<sup>6A</sup>-GFP produces morphological abnormalities, a phenotype also observed upon overexpression of wild-type but not the kinase-dead allele (Bähler and Nurse, 2001) (Figure S3). This suggests that Pom1<sup>6A</sup> is an active kinase. We tested more stringently the localization of the *pom1*<sup>6A</sup> allele by integrating it at the endogenous locus as sole copy of *pom1*. Pom1<sup>6A</sup>-GFP expressed under endogenous promoter also localized around the entire cortex, displaying numerous clusters of Pom1 scattered around the cell periphery, similar to inactive Pom1<sup>KD</sup> (Figure 3C). This localization is consistent with the idea that these six sites represent targets of autophosphorylation.

To confirm biochemically that Pom1 autophosphorylates, we purified recombinant full-length Pom1 and Pom1<sup>KD</sup> and performed *in vitro* kinase assays (Figure 3D). A significant amount of <sup>32</sup>P was incorporated by wild-type, but not kinase-dead Pom1. We also noticed that Pom1 migrated more slowly than Pom1<sup>KD</sup> on SDS-PAGE (Figure 3E). Treatment of Pom1 with commercial PP1 abolished this slow migration but did not change the Pom1<sup>KD</sup> migration pattern, indicating that recombinant Pom1 is autophosphorylated in the bacterial cell (Figure 3F). Similar assays with Pom1<sup>6A</sup> showed an intermediate behavior, where Pom1<sup>6A</sup> incorporated less <sup>32</sup>P and migrated at levels intermediate between wild-type and kinase-dead Pom1 (Figures 3D–3F). This shows that Pom1<sup>6A</sup> is active and that the mutated sites likely represent some but not all autophosphorylation sites. Pom1<sup>6A</sup> was also active in kinase assays with Cdr2 fragment as substrate, indicating that it remains competent in phosphorylating a known exogenous substrate (Figure 3G) (Martin and Berthelot-Grosjean, 2009). We subsequently identified all autophosphorylation sites on recombinant wild-type Pom1 by mass spectrometry. This analysis identified a total of 41 autophosphorylation sites and confirmed that 2 of the 6 mutated sites were indeed autophosphorylated (Figure S2). This analysis unfortunately did not inform about the phosphorylation status of the four other sites, which were not covered by any peptide identified by mass spectrometry, despite extensive effort and sequence coverage of over 95% (see *Extended Experimental Procedures* and Figure S2). In summary, Pom1 is heavily autophosphorylated, and partly unphosphorylated Pom1<sup>6A</sup> is not restricted to the cell tip cortex and disrupts Pom1 gradients.

### Pom1 Autophosphorylation Weakens Membrane Binding

To explore the dynamics of Pom1 autophosphorylation, we made use of the *pom1-as1* allele, which encodes an ATP analog-sensitive Pom1 form that can be inhibited by addition of the chemical inhibitor 1NM-PP1 (Padte et al., 2006). Under normal growth conditions, Pom1-*as1*-tdTomato localizes correctly to the cell tip cortex. However, within 1–2 min of 1NM-PP1 addition, Pom1-*as1*-tdTomato was delocalized around the entire cell periphery (Figure 4A). This fast delocalization suggests that inactivated Pom1-*as1* is rapidly dephosphorylated. An alternative possibility is that phospho-Pom1 may be rapidly degraded and resynthesized. However, we found that inhibition of protein translation with cycloheximide or disruption of protein degradation in proteasome mutants did not significantly affect the levels and distribution of Pom1 even after several hours (Figure S4), suggesting that Pom1 protein is stable over a significantly longer time. Thus, kinase activity is continuously required to antagonize dephosphorylation and prevent Pom1 localization along the lateral cortex.

Using FRAP experiments, we determined the turnover of Pom1 at the cell cortex (Figures 4B and 4C). We photobleached one entire cell tip to measure the exchange between cortical and cytoplasmic Pom1-GFP. Wild-type Pom1-GFP recovered with an estimated half-time of about 60 s. Inactive Pom1<sup>KD</sup>-GFP and nonphosphorylatable Pom1<sup>6A</sup>-GFP also recovered but with significantly slower half-time of over 120 s. Reduced exchange of these alleles suggest that unphosphorylated Pom1 alleles are more stable at the membrane and may also reflect their lower abundance in the cytoplasm. In agreement with these results, recombinant full-length Pom1, which autophosphorylates in bacteria, bound phospholipids *in vitro* with significantly higher affinity after dephosphorylation (Figure 4D). Dephosphorylated Pom1 also bound the nitrocellulose membrane, resulting in high background signal, similar to MBP-Pom1<sub>1-699</sub> tested above. Again, this may be due to the high global positive charge of Pom1 (+22.5 for MBP-Pom1, +32 for Pom1 at pH 7), which is likely abolished upon autophosphorylation at over 40 potential sites. We also note a slight change in the lipid specificity of Pom1: autophosphorylated Pom1 bound phosphatidic acid, a rare phospholipid in *S. pombe* (Koukou et al., 1990), whereas this phospholipid was not bound by the dephosphorylated form of Pom1. In summary our results suggest that Pom1 binds the plasma membrane directly when nonphosphorylated and that autophosphorylation weakens this interaction.

### Pom1 Binds Tea4

We showed above that Tea4 is both necessary and sufficient to nucleate Pom1 gradient formation. Tea4 is an SH3 domain-containing protein. Direct interactions have been described with Tea1, the formin For3, the PP1 Dis2, and the MAPKKK Win1, none of which involves the SH3 domain (Alvarez-Tabarés et al., 2007; Martin et al., 2005; Tatebe et al., 2005). In two-hybrid assays we found that Tea4 binds Pom1 through its SH3 domain because complete deletion or point mutation in the ligand-binding interface of the SH3 domain abolished this interaction (Figure 5A). This interaction occurs *in vivo*, as Tea4-HA was coimmunoprecipitated with Pom1-GFP (Figure 5B). Again, point

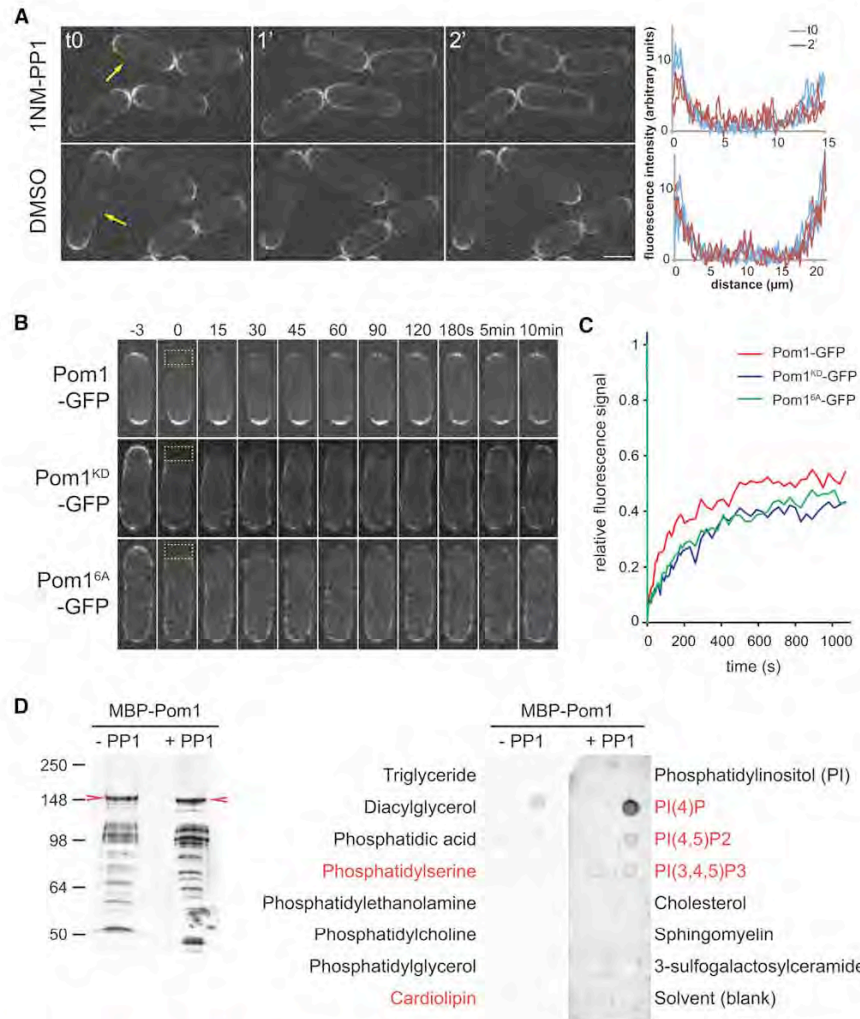


**Figure 4. Pom1 Activity Modulates Membrane Attachment**

(A) Localization of Pom1-as1-TdTomato before and after 1–2 min treatment with 20  $\mu$ M 1NM-PP1 or DMSO. Scale bar, 5  $\mu$ m. Arrows indicate cells for which the profile of fluorescence intensity along the periphery of both cell sides at 0 and 2 min is shown on the right.

(B) FRAP of Pom1-GFP, Pom1<sup>KD</sup>-GFP, and Pom1<sup>6A</sup>-GFP. The bleached region at cell tips is boxed.

(C) Quantification of FRAP experiments as shown in (B). Each curve represents an average of five experiments.

(D) Protein-lipid overlay assay with MBP-Pom1, with or without PP1 treatment. Loading control is shown as anti-MBP western blot on the left. Full-length proteins are labeled with red arrowheads. Lower bands likely correspond to breakdown products. Note the faster migration of most fragments in the PP1-treated sample. Lipids to which dephosphorylated MBP-Pom1 shows significant association are shown in red. Both blots were treated in parallel using identical conditions throughout.

See also Figure S4.

mutations in the Tea4 SH3 domain (Tea4<sup>SH3\*</sup>) abolished this interaction. In contrast, point mutations in the motif shown to mediate binding to Dis2 (Tea4<sup>RvxP</sup>) did not block Tea4-Pom1 interaction (Alvarez-Tabarés et al., 2007). The Tea4-Pom1 interaction was also not dependent on Pom1 activity or phosphorylation status, as Tea4 was coimmunoprecipitated with Pom1<sup>KD</sup>. SH3 domains often bind polyproline motifs. Sequence alignment revealed five such conserved motifs in Pom1 (Figure S2). We

sequentially mutated two prolines to alanines in each of these to create a Pom1<sup>SPxxP\*</sup> mutant. These mutations also impaired Tea4 binding in coimmunoprecipitation experiments (Figure 5B). We conclude that Tea4 and Pom1 bind to each other through SH3-PxxP interactions.

Pom1-GFP localization was dramatically affected by disruption of its interaction with Tea4. In tea4<sup>SH3\*</sup> cells, Pom1-GFP was cytoplasmic, like in tea4 $\Delta$  cells (Figure 5C). Mutation of

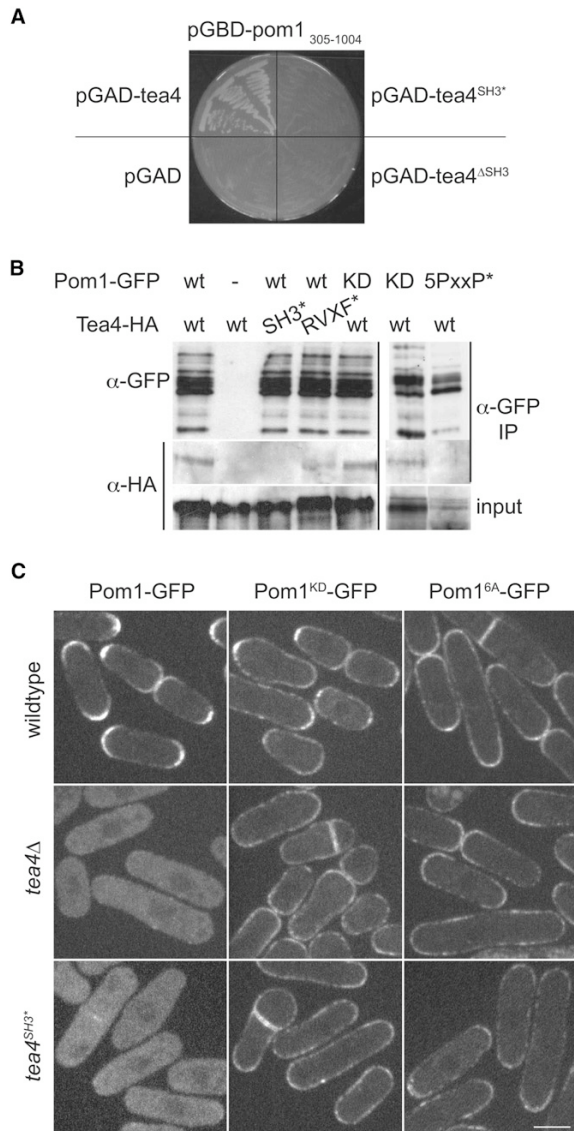


**Figure 5. Tea4 Binds Pom1 and Is Required for the Localization of Wild-Type, but Not Dephosphorylated, Pom1**  
 (A) Two-hybrid interaction between indicated constructs of Tea4 and Pom1. Growth on SD medium lacking histidine is shown.  
 (B) Coimmunoprecipitation of Tea4-HA with Pom1-GFP. Tea4 and Pom1 alleles are indicated at the top. The bottom lane shows Tea4-HA input. The first five and the last two lanes were obtained in distinct experiments. The last two were on the same gel, but not side by side. Note that the patterns of Pom1 breakdown products are similar in strains of distinct genotypes.  
 (C) Localization of Pom1-GFP, Pom1<sup>KD</sup>-GFP, and Pom1<sup>6A</sup>-GFP in wild-type, *tea4Δ*, and *tea4<sup>SH3+</sup>* cells, as indicated. Scale bar, 5 μm.  
 See also Figure S5.

the Pom1 PxxP motifs also increased cytoplasmic Pom1 and reduced Pom1 localization to the cell cortex but did not completely abolish it (Figure S5). Even when Pom1<sup>5PxxP\*</sup>-GFP was expressed at the endogenous genomic locus, residual cortical localization at cell tips was observed, suggesting that the *tea4<sup>SH3+</sup>* and *pom1<sup>5PxxP\*</sup>* mutations are not equivalent (see Figure 6F and below).

### Tea4 Plays a Regulatory, Nonstoichiometric Role in Pom1 Localization

We investigated the localization of inactive Pom1<sup>KD</sup> and unphosphorylatable Pom1<sup>6A</sup> in *tea4* mutant cells. Unexpectedly, both alleles localized efficiently to the cell periphery in *tea4Δ* and *tea4<sup>SH3+</sup>* mutant cells (Figure 5C). In fact, even mutation of one or only a few autophosphorylation sites was sufficient to restore some cortical localization to Pom1 in *tea4Δ* cells (Figure S6). Similarly, inactivating Pom1<sup>5PxxP\*</sup> by constructing a Pom1<sup>KD-5PxxP\*</sup> allele restored efficient cortical localization to this allele (Figure 6A). This indicates that Tea4 binding is not required to localize inactive, unphosphorylated Pom1 to the cell cortex. These results strongly suggest that Tea4 does not act as a physical anchor at the cortex but fulfills a regulatory function.

In agreement with this hypothesis, we observed that amounts of Tea4 below detection levels were sufficient to ensure proper localization of Pom1 (Figure 6B). Here, Tea4-GFP was expressed under repressible promoter in *tea4Δ pom1-tdTomato* cells. Promoter repression reduced Tea4 levels below detection but still allowed correct Pom1 localization. Thus, Tea4 is unlikely to act as a stoichiometric anchor for Pom1 at the cortex.

### Tea4 Promotes Pom1 Dephosphorylation at Cell Tips

Tea4 acts as a PP1 regulatory subunit by recruiting the phosphatase Dis2 to cell tips (Alvarez-Tabarés et al., 2007). We tested the hypothesis that Tea4 mediates the PP1-dependent dephosphorylation of Pom1 at cell tips. In agreement with this idea, we have shown above that recombinant, autophosphorylated Pom1 is dephosphorylated by PP1 (Figure 3F). We first verified the interaction of Tea4 with Dis2. Tea4-HA was readily coimmunoprecipitated with GFP-Dis2 in wild-type cells (Figure 6C). As previously described, this interaction was dependent on the Tea4 RVxF motif (Alvarez-Tabarés et al., 2007). We also found that the integrity of the Tea4 SH3 domain was essential for this interaction. Indeed, both Tea4<sup>RVxF\*</sup> and Tea4<sup>SH3+</sup> failed to coimmunoprecipitate with GFP-Dis2 (Figure 6C). We note that the RVxF\* mutation may not block Dis2 binding completely, as minor amounts of Tea4<sup>RVxF\*</sup> could be detected in the Dis2 immunoprecipitate upon long exposure (data not shown). Accordingly, GFP-Dis2 was delocalized from cell tips (but not from other locations) in *tea4Δ*, *tea4<sup>RVxF\*</sup>*, and *tea4<sup>SH3+</sup>* mutants, but not in *pom1Δ* backgrounds (Figure 6D).

By using the bimolecular fluorescence complementation (BiFC) technique, where two halves of YFP fused to distinct proteins reform an intact fluorescent complex upon interaction (Kerppola, 2006), we determined that Pom1, Tea4, and Dis2 were in close proximity in vivo (Figure 6E). BiFC signal was observed in pairs between Dis2, Pom1, and Pom1<sup>KD</sup> with wild-type Tea4, but not Tea4<sup>SH3+</sup>. However, Tea4<sup>SH3+</sup> was able to form BiFC signals with Tea3, a cell end marker that associates

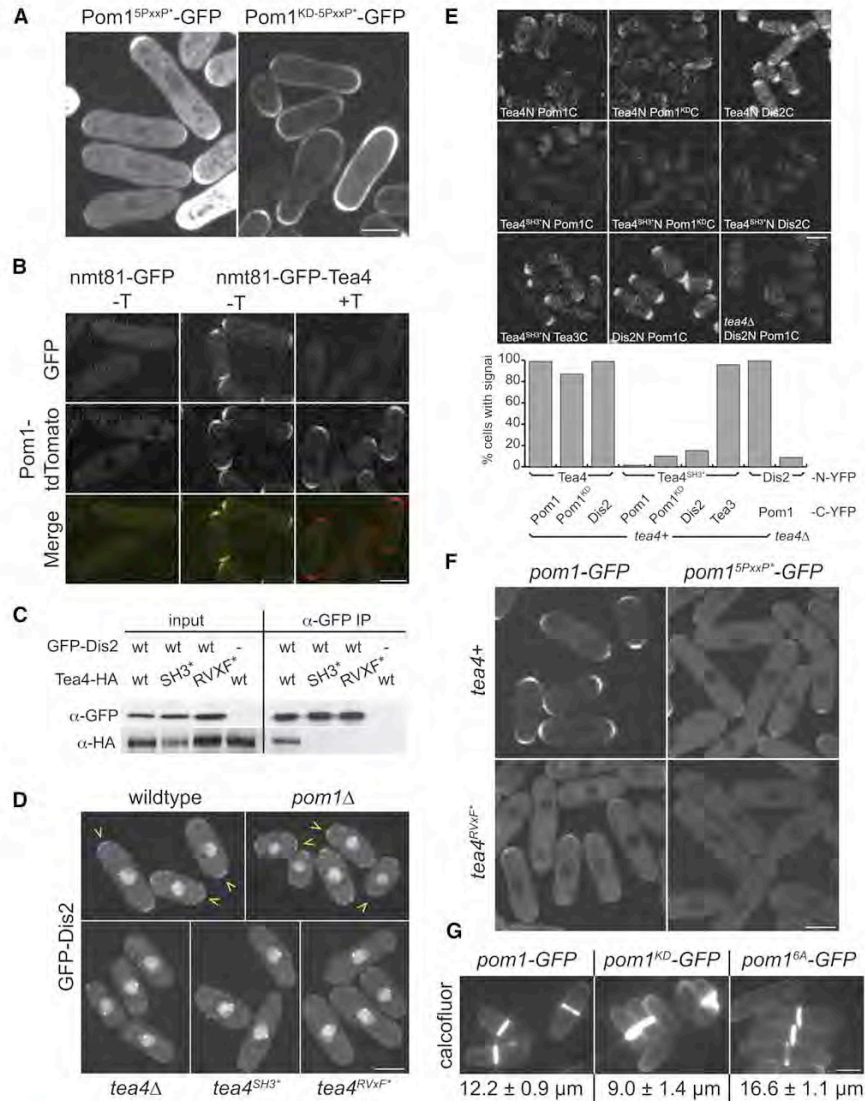


### Figure 6. Tea4 and Dis2 Mediate Pom1 Dephosphorylation

(A) Localization of Pom1<sup>5PxxP</sup>-GFP and Pom1<sup>KD-5PxxP</sup>-GFP expressed from plasmids in *pom1Δ* cells.

(B) Repression of *nmt81-tea4-GFP* by addition of thiamine (T) leads to undetectable Tea4-GFP levels, yet correct Pom1-tdTomato localization. *nmt81-GFP* was expressed as control. GFP, Pom1-tdTomato and merge channels are shown.

(C) Coimmunoprecipitation of Tea4-HA with GFP-Dis2. Tea4 alleles are indicated at the top.

(D) Maximal projection of GFP-Dis2 localization in wild-type, *tea4Δ*, *tea4<sup>SH3+</sup>*, *tea4<sup>RVXF+</sup>*, and *pom1Δ* cells. Yellow arrowheads indicate cell tip localization. Note that other localizations to endocytic vesicles or the nucleus are not affected by *tea4* mutations (Alvarez-Tabares et al., 2007).

(E) BiFC experiment indicating proximity of Tea4, Dis2, and Pom1 in vivo. Top panels show reconstituted fluorescence between indicated full-length proteins expressed under endogenous promoter and tagged with either the N-terminal half (N), or the C-terminal half (C) of YFP. Bottom panel shows quantification of the percentage of cells with cortical signal ( $n > 100$  for each sample).

(F) Localization of Pom1-GFP and Pom1<sup>5PxxP</sup>-GFP expressed under endogenous promoter in wild-type and *tea4<sup>RVXF+</sup>* cells.

(G) Average length and standard deviation of calcofluor-stained septated cells of *pom1-GFP*, *pom1<sup>KD</sup>-GFP*, and *pom1<sup>6A</sup>-GFP* strains. Scale bars, 5 μm.

See also Figure S6.

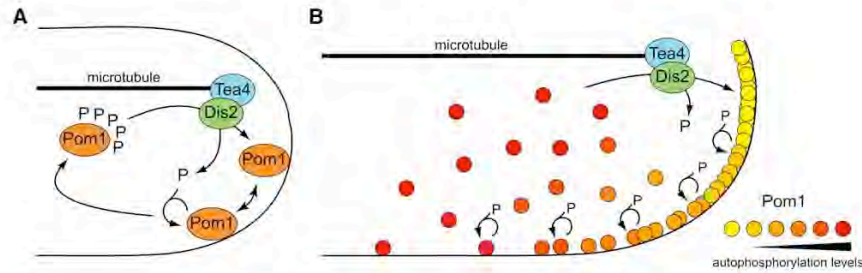


**Figure 7. Model for the Formation of Cortical Pom1 Gradients**

(A) Local dephosphorylation of Pom1, mediated by the Tea4-Dis2 PP1 pair, which is localized to cell tips through microtubule transport, permits association of Pom1 with the plasma membrane at cell tips. Pom1 then diffuses in the plane of the membrane. Autophosphorylation leads to Pom1 detachment from the membrane.

(B) Multiple autophosphorylation events may serve as a timer for shaping Pom1 gradients. After dephosphorylation and plasma membrane association, multiple rounds of autophosphorylation gradually increase the probability of Pom1 detaching from the membrane. Pom1 is shown in various shades of red indicating various degrees of autophosphorylation, from dephosphorylated (yellow) to fully phosphorylated (red).

with Tea1 and Tea4 (Snaith et al., 2005; data not shown). We also detected a BiFC signal between Dis2 and Pom1, which was dependent on *tea4*. These observations are consistent with the idea that Pom1, Tea4, and Dis2 interact at cell tips *in vivo*.

We investigated the effect of blocking the Tea4-Dis2 interaction on the localization of Pom1-GFP (Figure 6F): in *tea4<sup>RVxF<sup>-</sup></sup>* mutant cells, in which Dis2 but not Pom1 fails to bind mutant Tea4, Pom1-GFP was largely diffuse but retained some cell tip localization. In contrast, Pom1<sup>5PxxP<sup>-</sup></sup>-GFP failed to localize to the cell cortex in this background. This combination specifically blocks both the Tea4-Dis2 and Tea4-Pom1 interactions and mimics the *tea4<sup>SH3<sup>-</sup></sup>* mutant situation. Thus, efficient localization of Pom1 to the cell tip cortex requires both binding to Tea4 and interaction between Tea4 and the phosphatase Dis2, indicating that Tea4 bridges Pom1 with Dis2 to promote the dephosphorylation of Pom1 at cell tips.

#### Disruption of Pom1 Gradients Delays the Cell Cycle

We and others previously proposed that Pom1 gradients serve to couple cell length with mitotic entry (Martin and Berthelot-Grosjean, 2009; Moseley et al., 2009). We tested the effect of disturbing Pom1 gradients on cell length by investigating the phenotype of the *pom1<sup>6A</sup>* mutant, which encodes an active kinase that spreads along the lateral cortex (see Figure 3). *pom1<sup>6A</sup>* cells were highly elongated (Figure 6G) but did not show significant morphological defects. This contrasts with the *pom1<sup>KD</sup>* cells, which are short, misshapen, and divide off center. Thus, *pom1<sup>6A</sup>* appears to be a gain-of-function allele and displays a phenotype consistent with previously published data that ectopic localization of active Pom1 to the cell middle inhibits Cdr2 and delays mitotic commitment (Martin and Berthelot-Grosjean, 2009; Moseley et al., 2009). In conclusion, spreading of active Pom1 along the lateral cortex leads to cell cycle delay.

#### DISCUSSION

Concentration gradients pattern cells and organisms. Here, we have dissected with molecular details the mechanism of gradient formation of the DYRK family kinase Pom1. Pom1 gradient initi-

ation relies on the local dephosphorylation of Pom1 at cell tips. This reaction is mediated by microtubule-deposited Tea4, which acts as a PP1 regulatory subunit, bridging the phosphatase Dis2 with its substrate Pom1. Dephosphorylation of Pom1 exposes a positively charged basic region that mediates plasma membrane association. At the membrane, Pom1 moves away from its site of association and autophosphorylates at multiple sites, in particular within its basic region. This autophosphorylation lowers its affinity to the membrane and promotes its detachment, limiting the lateral spreading of Pom1 along the membrane. In the cytoplasm, fast diffusion of Pom1 permits its encounter with Tea4 to initiate a new cycle of membrane association (Figure 7A). In summary we propose that a cycle of local dephosphorylation, lateral movement at the plasma membrane and autophosphorylation shapes Pom1 cortical gradients.

Our data clearly establish Tea4 as a bona fide PP1 regulatory subunit, as it binds both the phosphatase Dis2 and its substrate Pom1 and promotes Pom1 dephosphorylation. This function is likely shared with its homolog in *S. cerevisiae*, Bud14p, which serves as targeting subunit for the PP1 Glc7p (Knaus et al., 2005). However, exactly how a ternary complex forms between Tea4, Dis2, and Pom1 is unclear because both Pom1 and Dis2 require an intact SH3 ligand-binding interface for binding Tea4 and localizing to cell tips. Our data indicate that Tea4 binds Dis2 independently of Pom1 because Pom1 is not required for the localization of Dis2 to cell tips. This interaction requires both the RVxF motif and a nonclassical SH3 interaction (Dis2 does not contain PxxP repeats). Tea4 also binds Pom1 independently of Dis2, as *Tea4<sup>RVxF<sup>-</sup></sup>* still associates with Pom1, but not Dis2. This interaction occurs through classical SH3-PxxP contact. We suggest that the functional phosphatase unit is the Tea4-Dis2 dimer. In the absence of substrate, interaction through the RVxF site may be stabilized through a labile Dis2-Tea4 SH3 contact. However, upon Pom1 encounter this contact may be lost and Pom1 docked, transiently stabilizing the trimeric complex. Alternatively, Tea4 may dimerize, thus providing two independent SH3 domains for binding Pom1 and Dis2.

*In vivo*, Tea4 associates with Tea1, which is transported by microtubules and forms a subcortical network at cell tips (Bicho

et al., 2010; Martin et al., 2005; Tätebe et al., 2005). This may provide a microenvironment favorable to Pom1 dephosphorylation by enhancing the local concentration of Tea4, Pom1, and Dis2. Indeed, in *tea4Δ* cells, in which Tea4 fails to localize to cell tips, Pom1 localizes, albeit poorly, to the cell cortex (Celton-Morizur et al., 2006; Padte et al., 2006), indicating that the Tea4-Dis2 pair also promotes dephosphorylation of Pom1 in these conditions, though inefficiently. Thus, microtubules indirectly define the sites of Pom1 dephosphorylation.

### Shaping the Pom1 Gradients

We and others previously proposed that the gradients of Pom1 serve to measure cell length by inhibiting the medial mitotic inducer Cdr2 (Martin and Berthelot-Grosjean, 2009; Moseley et al., 2009). Consistent with this model, disruption of Pom1 gradients using a nonphosphorylatable but active Pom1 allele (Pom1<sup>6A</sup>) delays cell cycle progression, similar to *cdr2Δ*. One postulate of this model is that the shape of Pom1 gradients should be independent of cell length itself. Our data suggest that, upon plasma membrane association, gradient shape is controlled by two competing activities: lateral movement at the membrane will enhance Pom1 dispersal and promote the formation of a shallow gradient. The lateral movement we show is consistent with diffusion. In contrast, autophosphorylation will favor Pom1 detachment from the membrane and, thus, the formation of a steep gradient. The multiplicity of autophosphorylation sites within the basic region, which likely require sequential autophosphorylation events, may provide a “timer” function affording time for diffusion within the membrane before detachment (Figure 7B). The rate of movement of Pom1 at the plasma membrane appears sufficiently slow to allow the Pom1 concentration gradients to be maintained. Slow lateral mobility of both lipids and proteins has also been observed in the plasma membrane of the budding yeast (Greenberg and Axelrod, 1993; Valdez-Taubas and Pelham, 2003). Thus, the precise shape of the gradients will be defined by the rate of Pom1 lateral movement at the membrane and the time required for autophosphorylation.

Pom1 activity levels may provide a potential regulatory switch for modulating gradient shapes. Interestingly, Bähler and Nurse (2001) described that Pom1 kinase activity is not constant through the cell cycle but appears to increase through G2. This finding is somewhat contradictory with the model that local medial Pom1 activity levels are at their lowest at that time. Our findings can reconcile these two findings: the global increase in Pom1 activity may promote faster detachment of Pom1 from the membrane and formation of steeper gradients in late G2 cells. Thus, paradoxically, higher global Pom1 activity may contribute to reducing its activity at the cell middle by lowering its medial concentration.

If gradient shape is indeed modulated by Pom1 global activity, it will be important to define what controls this variation in activity. Does Pom1 activity increase in response to cell cycle progression itself? If so it may point toward a feedback system, where Pom1 does not provide an absolute measure of cell length but measures this length in a subjective cell cycle context-dependent manner. Quantitative modeling of Pom1 gradients will be necessary to define whether and how variation in Pom1

activity contributes to shaping them. Our molecular dissection of Pom1 gradients now provides the framework for this quantitative analysis.

### Mechanics and Function of Autophosphorylation

Our data show that wild-type Pom1 cannot rescue the localization of inactive Pom1. The simplest interpretation of these results is that Pom1 undergoes intramolecular autophosphorylation events. An alternative possibility is that autophosphorylation events occur *in trans* between distinct Pom1 molecules but that wild-type and inactive Pom1 are blind to each other. Although, to our knowledge, no data exist to distinguish between these two possibilities, evidence suggests that Pom1 associates in large complexes. First, Pom1 forms high molecular weight complexes in biochemical fractionation (Bähler and Nurse, 2001). Second, clusters of Pom1 are detected at the membrane (see Figure 1A). Finally, in backgrounds where Pom1 associates weakly with the plasma membrane, such as the Pom1<sup>1A</sup>-Pom1<sup>3A</sup> alleles, Pom1 forms defined domains of membrane association (Figure S6), suggesting a certain amount of cooperativity between distinct Pom1 molecules to associate at the membrane.

Besides the autophosphorylation sites in the basic region, mass spectrometry identified 39 other sites spread mostly in the noncatalytic regions of Pom1, of which all or only a subset may be phosphorylated on each Pom1 molecule. We note that most of these sites are significantly different from the DYRK consensus previously defined. What is the role of these additional sites? First, autophosphorylation at these sites may further help detach Pom1 from the membrane, similar to the six we characterized. Alternatively, autophosphorylation at these sites may underlie a second function, e.g., modulating Pom1 activity. Current evidence suggests that Pom1 is active at the cell cortex where Cdr2 localizes. Indeed, membrane-associated Pom1<sup>6A</sup> strongly delays mitotic entry. In contrast, cytoplasmic Pom1 in *tea4Δ* cells only causes a modest delay (unpublished data). Although substrate localization and accessibility may underlie this difference, it is also possible that Pom1 is less active in its fully autophosphorylated cytoplasmic state than its membrane-associated state. Finally, these autophosphorylation sites may also influence other Pom1 functions in cell morphogenesis or septum positioning.

### Additional Spatial Cues for Pom1 Localization

The data and model presented above propose that Tea4 is the spatial cue for the formation of membrane-associated Pom1 gradients. (However, we note that Pom1 can localize to the septum independently of Tea4.) Indeed, we show that mislocalization of Tea4 is sufficient to initiate the formation of an ectopic Pom1 gradient. However, it is clear that other factors contribute to Pom1 localization. Although ectopic Tea4 was able to recruit Pom1 to the plasma membrane, it was unable to recruit it to internal membranes: the Ppc89-Tea4 fusion was also localized to the SPB, but Pom1 was not recruited to the nuclear membrane. Similar experiments conducted with a SPB component Sad1-Tea4 fusion confirmed this result (data not shown). Thus, the plasma membrane may be the only permissive membrane for Pom1 binding. In addition we noted that dephosphorylated Pom1 alleles and in particular partly dephosphorylated alleles

(such as Pom1<sup>1A</sup>-Pom1<sup>3A</sup>) show a preferential cortical localization to cell tips even in *tea4*Δ cells. Similarly, Pom1 shows preferential tip cortex localization in *tea1*Δ cells in which Tea4 is homogeneously distributed (Celton-Morizur et al., 2006; Padte et al., 2006). This preference may be conferred by membrane curvature, specific lipid composition of the plasma membrane at cell ends, or as yet uncharacterized membrane proteins.

### Dynamic Maintenance of Cortical Gradients

Intracellular gradients are important for cell patterning. Yet, the mechanisms for gradient formation are generally not well described. Although large-scale gradients that pattern organisms during development, such as the Bicoid or Decapentaplegic gradients, reaching across hundreds of microns, rely on local translation and degradation (Wartlick et al., 2009), these second-order reactions are too slow for the formation of small-scale intracellular gradients. In contrast, intracellular gradients, such as the Ran-GTP gradient around chromatin or the bacterial polar MinCD gradient, are proposed to self-organize through autoregulatory feedbacks (Fuller, 2010; Lutkenhaus, 2007). One general feature is that these gradients are not static systems but are dynamically maintained by a constant flow of proteins cycling through distinct stages of membrane/organelle association and protein modification. Conceptually similar flow models serve for the kinetic polarization of membranes through endocytic recycling in migrating cells or budding yeast (Bretscher, 1996; Valdez-Taubas and Pelham, 2003). Our work now defines a detailed molecular mechanism for one such flow model.

Parallels with the MinCD gradient, where the MinD ATPase forms gradients from the ends of bacterial cells recruiting the division inhibitor MinC (Lutkenhaus, 2007), are particularly intriguing: both MinCD and Pom1 form cortical gradients and function in sensing cell length and regulating cell division. Moreover, these gradients are shaped by first-order reactions through endogenous enzymatic activity, where this activity promotes detachment from the membrane. The strategic similarities used by these unrelated proteins in distinct phyla suggest that the mechanisms we have defined may represent a general blueprint for building gradients along intracellular structures.

### EXPERIMENTAL PROCEDURES

Detailed methods, including strain list (Table S1), are described in the Supplemental Information.

#### Mutants and Construct Information

The mutations introduced in the *tea4*<sup>SH3\*</sup> and *tea4*<sup>RVA\*</sup> alleles are W155A-W156A and V223A-F225A, respectively. All mutations introduced in *pom1* are indicated in Figure S2 and Figure S5, except for *pom1*<sup>KD</sup>, which is K728R (Bähler and Nurse, 2001). The Ppc89-GFP-Tea4 fusion was obtained by fusing in this order and in frame the three ORFs without stop codons in a pRIP81 plasmid. This fusion contains a small AGAGAG linker between GFP and Tea4. After linearization, this plasmid was then integrated at the *ura4* locus. Thus, this construct is present as sole copy in the cell under control of the weak *nmt* promoter.

#### Microscopy and Quantification

Unless stated otherwise, all images are two-dimensional maximum intensity projections of the three medial sections of spinning-disk confocal images, except the BiFC experiments, which are maximum intensity projections of

the entire cell volume of laser-scanning confocal images. Except where stated, all images are of GFP-tagged gene products integrated as sole copy at the endogenous locus and expressed under endogenous promoter. All measurements were performed in ImageJ on images taken in identical conditions. We note that our measurements of fluorescence distribution were only corrected for background values and, thus, serve primarily as illustration of the images shown.

#### Protein-Lipid Binding Assays

Protein-lipid overlay assays were performed using lipid strips purchased from Echelon Inc., essentially according to manufacturer's protocol. We used MBP-Pom1 rather than GST-Pom1 because we found that GST alone bound some lipids with significant affinity. Recombinant Pom1 fragments bearing a functional kinase domain were found to be autophosphorylated in the bacterial cell. For all experiments we used 0.5 μg/ml of recombinant protein and performed control binding reactions in identical conditions in parallel. We reproducibly found that dephosphorylated Pom1 or the Pom1<sub>1-699</sub> fragment bound both lipids and membrane with higher affinity than autophosphorylated forms or MBP alone. The scans of the lipid strips shown have not been modified in any way.

### SUPPLEMENTAL INFORMATION

Supplemental Information includes Extended Experimental Procedures, six figures, and one table and can be found with this article online at doi:10.1016/j.cell.2011.05.014.

### ACKNOWLEDGMENTS

We would like to thank Patrice Waridel and Manfredo Quadroni at the Protein Analysis Facility for the mass spectrometry, Philippe Kircher for technical help, Jürg Bähler, Iain Hagan, and Stuart MacNeill for strains and reagents, Yves Barral, Felipe Bendezú, and Richard Benton for comments on the manuscript, and all members of the lab for advice and discussion. O.H. was supported by a Human Frontiers Science Program (HFSP) long-term fellowship (LT00595/2005-L) and K.K. by a Roche research fellowship (67-2008). Research in S.G.M.'s laboratory is supported by a Swiss National Science Foundation Professorship grant (PP00A-114936), an HFSP Career Development Award (CDA0016/2008), and a European Research Council Starting Grant (260493). We also extend our thanks to the Center for Integrative Genomics at the University of Lausanne, where a large part of this work was conducted, for generous support.

Received: December 22, 2010

Revised: March 23, 2011

Accepted: May 4, 2011

Published: June 23, 2011

### REFERENCES

- Almonacid, M., Moseley, J.B., Janvare, J., Mayeux, A., Fraiser, V., Nurse, P., and Paoletti, A. (2009). Spatial control of cytokinesis by Cdr2 kinase and Mid1/anillin nuclear export. *Curr. Biol.* 19, 961–966.
- Alvarez-Tabarés, I., Grallert, A., Ortiz, J.M., and Hagan, I.M. (2007). *Schizosaccharomyces pombe* protein phosphatase 1 in mitosis, endocytosis and a partnership with Wsh3/Tea4 to control polarised growth. *J. Cell Sci.* 120, 3589–3601.
- Aranda, S., Laguna, A., and de la Luna, S. (2011). DYRK family of protein kinases: evolutionary relationships, biochemical properties, and functional roles. *FASEB J.* 25, 449–462.
- Bähler, J., and Nurse, P. (2001). Fission yeast Pom1p kinase activity is cell cycle regulated and essential for cellular symmetry during growth and division. *EMBO J.* 20, 1064–1073.
- Bähler, J., and Pringle, J.R. (1998). Pom1p, a fission yeast protein kinase that provides positional information for both polarized growth and cytokinesis. *Genes Dev.* 12, 1356–1370.

- Bicho, C.C., Kelly, D.A., Snaith, H.A., Goryachev, A.B., and Sawin, K.E. (2010). A catalytic role for Mod5 in the formation of the Tea1 cell polarity landmark. *Curr. Biol.* *20*, 1752–1757.
- Bretscher, M.S. (1996). Getting membrane flow and the cytoskeleton to cooperate in moving cells. *Cell* *87*, 601–606.
- Campbell, L.E., and Proud, C.G. (2002). Differing substrate specificities of members of the DYRK family of arginine-directed protein kinases. *FEBS Lett.* *510*, 31–36.
- Celton-Morizur, S., Racine, V., Sibarita, J.B., and Paoletti, A. (2006). Pom1 kinase links division plane position to cell polarity by regulating Mid1p cortical distribution. *J. Cell Sci.* *119*, 4710–4718.
- Chang, F., and Martin, S.G. (2009). Shaping fission yeast with microtubules. *Cold Spring Harb. Perspect. Biol.* *1*, a001347.
- Fuller, B.G. (2010). Self-organization of intracellular gradients during mitosis. *Cell Div.* *5*, 5.
- Greenberg, M.L., and Axelrod, D. (1993). Anomalous slow mobility of fluorescent lipid probes in the plasma membrane of the yeast *Saccharomyces cerevisiae*. *J. Membr. Biol.* *137*, 115–127.
- Himpel, S., Tegge, W., Frank, R., Leder, S., Joost, H.G., and Becker, W. (2000). Specificity determinants of substrate recognition by the protein kinase DYRK1A. *J. Biol. Chem.* *275*, 2431–2438.
- Huang, Y., Chew, T.G., Ge, W., and Balasubramanian, M.K. (2007). Polarity determinants Tea1p, Tea4p, and Pom1p inhibit division-septum assembly at cell ends in fission yeast. *Dev. Cell* *12*, 987–996.
- Kerppola, T.K. (2006). Visualization of molecular interactions by fluorescence complementation. *Nat. Rev. Mol. Cell Biol.* *7*, 449–456.
- Knaus, M., Cameroni, E., Pedruzzi, I., Tatchell, K., De Virgilio, C., and Peter, M. (2005). The Bud14p-Glc7p complex functions as a cortical regulator of dynein in budding yeast. *EMBO J.* *24*, 3000–3011.
- Koukou, A.I., Tsoukatos, D., and Drinas, C. (1990). Effect of ethanol on the phospholipid and fatty acid content of *Schizosaccharomyces pombe* membranes. *J. Gen. Microbiol.* *136*, 1271–1277.
- Lochhead, P.A., Sibbet, G., Morrice, N., and Cleghon, V. (2005). Activation-loop autophosphorylation is mediated by a novel transitional intermediate form of DYRKs. *Cell* *121*, 925–936.
- Lutkenhaus, J. (2007). Assembly dynamics of the bacterial MinCDE system and spatial regulation of the Z ring. *Annu. Rev. Biochem.* *76*, 539–562.
- Martin, S.G., and Berthelot-Grosjean, M. (2009). Polar gradients of the DYRK-family kinase Pom1 couple cell length with the cell cycle. *Nature* *459*, 852–856.
- Martin, S.G., McDonald, W.H., Yates, J.R., III, and Chang, F. (2005). Tea4p links microtubule plus ends with the formin for3p in the establishment of cell polarity. *Dev. Cell* *8*, 479–491.
- Mata, J., and Nurse, P. (1997). tea1 and the microtubular cytoskeleton are important for generating global spatial order within the fission yeast cell. *Cell* *89*, 939–949.
- Morrell, J.L., Nichols, C.B., and Gould, K.L. (2004). The GIN4 family kinase, Cdr2p, acts independently of septins in fission yeast. *J. Cell Sci.* *117*, 5293–5302.
- Moseley, J.B., Mayeux, A., Paoletti, A., and Nurse, P. (2009). A spatial gradient coordinates cell size and mitotic entry in fission yeast. *Nature* *459*, 857–860.
- Padte, N.N., Martin, S.G., Howard, M., and Chang, F. (2006). The cell-end factor pom1p inhibits mid1p in specification of the cell division plane in fission yeast. *Curr. Biol.* *16*, 2480–2487.
- Snaith, H.A., Samejima, I., and Sawin, K.E. (2005). Multistep and multimode cortical anchoring of tea1p at cell tips in fission yeast. *EMBO J.* *24*, 3690–3699.
- Tatebe, H., Shimada, K., Uzawa, S., Morigasaki, S., and Shiozaki, K. (2005). Wsh3/Tea4 is a novel cell-end factor essential for bipolar distribution of Tea1 and protects cell polarity under environmental stress in *S. pombe*. *Curr. Biol.* *15*, 1006–1015.
- Tatebe, H., Nakano, K., Maximo, R., and Shiozaki, K. (2008). Pom1 DYRK regulates localization of the Rga4 GAP to ensure bipolar activation of Cdc42 in fission yeast. *Curr. Biol.* *18*, 322–330.
- Valdez-Taubas, J., and Pelham, H.R. (2003). Slow diffusion of proteins in the yeast plasma membrane allows polarity to be maintained by endocytic cycling. *Curr. Biol.* *13*, 1636–1640.
- Wartlick, O., Kicheva, A., and González-Gaitán, M. (2009). Morphogen gradient formation. *Cold Spring Harb. Perspect. Biol.* *1*, a001255.

## EXTENDED EXPERIMENTAL PROCEDURES

### Yeast Strains, Media, and Genetic Methods

Standard methods for *S. pombe* media and genetic manipulations were used throughout. Generally, for imaging, length measurements and biochemistry experiments, cells were grown in synthetic Edinburgh minimal medium (EMM) with appropriate supplements. For induction of *pom1-GFP* expression under *nmt* promoter in the pREP41 plasmid, cells were grown for 21–23h at 25°C in EMM medium lacking thiamine, except for strong overexpression where cells were grown for 24h at 30°C. *GFP*, *tea4-GFP* and *ppc89-GFP-tea4* under the weak *nmt* promoter integrated at the *ura4* locus were induced to steady-state levels for over 24h at 30°C in EMM medium lacking thiamine. Repression of *tea4-GFP* under the weak *nmt* promoter was done by growing cells in presence of 15µM thiamine for > 24h at 30°C.

All strains used in this study are listed in Table S1. Tagged and deletion strains were constructed by using a PCR-based approach (Bähler et al., 1998) and confirmed by PCR. Template for tdTomato and BiFC tagging were used as published (Akman and MacNeill, 2009; Snaith et al., 2005). Integration of mutant alleles at the endogenous genomic locus was performed through a two-step procedure: the wild-type copy was first replaced by a *ura4+* cassette amplified by PCR with 100-mer oligos containing homology to the flanking regions of the fragment to be deleted. This cassette was then further replaced by a mutant gene fragment and selected on 5-FOA medium.

### Molecular Biology and Yeast Two-Hybrid Analysis

All plasmids were constructed using standard molecular biology techniques. In general, genes or gene fragments were cloned after PCR from genomic DNA with primers containing 5' extensions with specific restriction sites. Details of the primers and restriction sites used are available upon request. All Pom1 expression plasmids were generated in the pREP41-GFP backbone (Craven et al., 1998). PCR-based site-directed mutagenesis was performed essentially as described. All plasmids were fully sequenced.

Two-hybrid assays were performed by co-transformation of appropriate pGAD and pGBD plasmids in AH109 host strain (Clontech). Interaction was assessed by growth on SD medium lacking histidine. All pGAD-*tea4* constructs used interacted with pGBD-*tea1* and pGBD-*for3* used as positive controls (Martin et al., 2005).

### Microscopy

Imaging was performed at room temperature on live cells, except where specified, on a PerkinElmer spinning disk microscope, as previously described (Martin and Berthelot-Grosjean, 2009), except for the BiFC experiments. Stacks of z-series confocal sections were acquired at 0.3 µm intervals with the Velocity software and images were rendered by two-dimensional maximum intensity of the 3 medial sections, unless stated otherwise. Figures were prepared with Adobe Photoshop CS5 and Adobe Illustrator CS5. FRAP experiments were performed on the same setup using the PerkinElmer photokinesis module. ROI were bleached with 12 repetitive scans. For Figure 4, post-bleach images were acquired at 5 s intervals for the first 60 s followed by 10 s intervals for the next 140 s and finally 30 s intervals for the last 600 s to minimize bleaching during image acquisition. For Figure 1, post-bleach images were acquired at regular intervals. The BiFC images were acquired on a Zeiss laser-scanning LSM 510 Meta confocal microscope. Except where stated all images are of GFP-tagged gene products integrated as sole copy at the endogenous locus and expressed under endogenous promoter. For imaging Pom1-GFP in *orb* mutants (Figure S1), 5ml exponential cultures were centrifuged at 3000 rpm for 2min, resuspended in -20°C methanol and fixed for 10min at -20°C; cells were then washed 3 times in PBS. Cell length measurements were performed on calcofluor (Sigma)-stained septated cells.

Inhibition of Pom1-as1 was done with 1NM-PP1 (Calbiochem) used at a final concentration of 20 µM from a 10mM stock solution in DMSO and added in YE medium. To follow the same cells before and after inhibitor addition, these experiments were performed in homemade PDMF channels mounted on coverslips. Cycloheximide (Sigma) was used at 0.1mg/ml final concentration.

### Fluorescence Quantification

All measurements and calculations were performed in ImageJ and MS\_Excel, respectively. FRAP quantification was performed as previously described (Martin and Chang, 2006). Time constants were estimated by the intersection of the curve with a line at half-maximal recovery. For whole-cell quantification of the distribution of Pom1-GFP in Figure 1, a sum projection of spinning disk confocal z-stacks of an individual cell was boxed and the ImageJ (10.2) "plot profile" tool was used to compress the fluorescence intensity into a one-dimensional line along the long axis of the cell, as described (Martin and Berthelot-Grosjean, 2009). For measurement of fluorescence intensity along the cell cortex or through the cell middle, a 5 pixel-wide line was drawn by hand at the periphery or along the long axis of the cell in a medial confocal section and fluorescence intensity obtained using the plot profile tool of ImageJ. Background correction was performed by subtracting the background fluorescence intensity measured just outside the cell examined. In Figure 1, data corresponding to 9 µm of the cell perimeter centered around the tip of the cell and 3 µm of the cell perimeter or 1.5 µm perpendicular to the cell periphery centered around Ppc89-GFP-Tea4 was acquired. For each channel, in order to compare fluorescence distribution and not absolute fluorescence levels, the integrated fluorescence intensity over the measured line was normalized to a value of one. We note that our measurements of fluorescence distribution were only corrected for background values and thus serve primarily as illustration of the images shown.

### Coimmunoprecipitations and Electrophoresis

Extracts from yeast grown in EMM medium were prepared in CXS buffer (50 mM HEPES, pH 7.0, 20mM KCl, 1mM MgCl<sub>2</sub>, 2mM EDTA, pH 7.5. and protease inhibitor cocktail) by grinding in liquid nitrogen with a mortar and pestle. After thawing, NaCl and Triton X-100 were added to final concentrations of 150mM and 0.1% respectively. For immunoprecipitations, 150 µl soluble extract was added to 20 µl sheep anti-mouse magnetic Dynabead slurry (Dyna) pre-bound to 2 mg monoclonal anti-GFP antibodies (Roche), and incubated for 2h at 4°C. Magnetic Dynabeads were then washed twice with CXS 150mM NaCl 0.1% Triton X-100 then twice with CXS 75mM NaCl 0.1% Triton X-100 and finally twice with CXS 75mM NaCl. Immunoprecipitated material was then recovered by boiling Dynabeads in 30 µl SDS sample buffer for 5 min at 95°C.

Standard protocols were used for SDS-PAGE and Western blot analysis. Antibodies used on Western blots were: mouse monoclonal anti-HA (HA.11; Covance), anti-GFP (Roche), anti-MBP (Cell Signaling) and anti-GST (Sigma). Silver staining was done using the SilverSNAP Stain Kit II (Pierce).

### Recombinant Protein Expression and In Vitro Assays

MBP-Pom1 and GST-Pom1 fusion proteins were expressed in BL21 cells and purified with amylose resin (NEB) or glutathione sepharose 4B (GE Healthcare) columns according to manufacturers' protocols. 6His-Cdr<sub>2,423-532</sub> was expressed and purified as described (Martin and Berthelot-Grosjean, 2009).

Kinase assays, were performed in 30mM Tris, 100mM NaCl, 10mM MgCl<sub>2</sub>, 1mM EGTA, 10% glycerol, 20 µM ATP and 2 µCi [<sup>32</sup>P] ATP (PerkinElmer #BLU502A250UC) with equivalent amounts of GST-Pom1, GST-Pom1<sup>KD</sup> and GST-pom1<sup>6A</sup> in a 15 µl final volume reaction. After a 30 min incubation at 30°C, the reaction was stopped by boiling in sample buffer and analyzed by SDS-PAGE. <sup>32</sup>P-incorporation was detected in a phosphorimager.

For phosphatase assays, equivalent amounts of GST-Pom1, GST-Pom1<sup>KD</sup> and GST-pom1<sup>6A</sup> were treated with 3,75U of PP1 (NEB #P0754S) in 1X PMP Buffer (NEB) supplemented with 1mM MnCl<sub>2</sub> and incubated at 30°C for 1h.

### Phosphorylation Analysis of Pom1 by LC-MS/MS

Bands corresponding to phosphorylated recombinant GST-Pom1 were excised from SDS-PAGE gel and digested, as described (Shevchenko et al., 1996; Wilm et al., 1996), with sequencing-grade trypsin (Promega), chymotrypsin (Roche), Lys-C (Roche) or Glu-C (Sigma-Aldrich). Extracted peptides were analyzed on a hybrid LTQ Orbitrap Velos mass spectrometer (Thermo Fisher Scientific, Bremen, Germany) interfaced to an Ultimate 3000 RSLC nano HPLC system (Dionex, Olten, Switzerland). In data-dependent acquisition controlled by Xcalibur 2.1 software (Thermo Fisher Scientific), the 15 most intense precursor ions detected in the full MS survey performed in the Orbitrap (range 300-1700 m/z, resolution 30'000 at m/z 400) were selected and fragmented. Only precursors with a charge higher than one were selected for HCD fragmentation and fragment ions were analyzed in the Orbitrap at a resolution of 7'500. From raw files, MS/MS spectra were de-isotoped, deconvoluted and exported as mgf files (Mascot Generic File, text format) using MascotDistiller 2.3.2 (Matrix Science, London, UK). In a parallel experiment, phosphopeptides of Pom1 were enriched on a TiO<sub>2</sub> column (Larsen et al., 2005) after Lys-C digestion and analyzed by LC-MS/MS, in order to clarify some ambiguous phosphosite localization.

MS/MS spectra were analyzed using Mascot 2.2 (Matrix Science, London, UK). Mascot was set up to search the UNIPROT database (SWISSPROT + TrEMBL, [www.expasy.org](http://www.expasy.org)) restricted to *Schizosaccharomyces pombe* taxonomy (database release used was 15.12 of December, 15th 2009, 5'159 sequences after taxonomy filter). Trypsin (semi-specific cleavage at K,R, not before P), chymotrypsin (semi-specific cleavage at F,L;W,Y, not before P), Lys-C (semi-specific cleavage at K, not before P) or Glu-C (semi-specific cleavage at D,E, not before P), was used as the enzyme definition. Mascot was searched with a fragment ion mass tolerance of 0.02 Da, a parent ion tolerance of 10 ppm, allowing four missed cleavages. Iodoacetamide derivative of cysteine was specified in Mascot as a fixed modification. Deamidation of asparagine and glutamine, oxidation of methionine, and phosphorylation of serine, threonine and tyrosine were specified as variable modifications.

Combined analysis of trypsin, chymotrypsin, Lys-C and Glu-C datasets allowed the characterization of 41 phosphosites with 95.9% coverage of Pom1 sequence, using a Mascot ion score threshold of 14. Phosphorylation sites with ambiguous localization were noted as potential, when the difference between the top two Mascot ion scores of two alternative phosphorylation sites in the same peptide sequence was below 5. No peptide covering amino-acids 405 to 429, 436 to 445 and 482 to 487 could be observed in any of the four protease datasets. As these regions are rich in hydrophilic residues (S, T, K, R), the corresponding peptides were probably not retained on the C18 chromatographic column.

### SUPPLEMENTAL REFERENCES

- Akman, G., and MacNeill, S.A. (2009). MCM-GINS and MCM-MCM interactions in vivo visualised by bimolecular fluorescence complementation in fission yeast. *BMC Cell Biol.* 10, 12.
- Alvarez-Tabarés, I., Grallert, A., Ortiz, J.M., and Hagan, I.M. (2007). *Schizosaccharomyces pombe* protein phosphatase 1 in mitosis, endocytosis and a partnership with Wsh3/Tea4 to control polarised growth. *J. Cell Sci.* 120, 3589–3601.
- Bähler, J., and Pringle, J.R. (1998). Pom1p, a fission yeast protein kinase that provides positional information for both polarized growth and cytokinesis. *Genes Dev.* 12, 1356–1370.

- Bähler, J., Wu, J.Q., Longtine, M.S., Shah, N.G., McKenzie, A., III, Steever, A.B., Wach, A., Philippsen, P., and Pringle, J.R. (1998). Heterologous modules for efficient and versatile PCR-based gene targeting in *Schizosaccharomyces pombe*. *Yeast* *14*, 943–951.
- Craven, R.A., Griffiths, D.J., Sheldrick, K.S., Randall, R.E., Hagan, I.M., and Carr, A.M. (1998). Vectors for the expression of tagged proteins in *Schizosaccharomyces pombe*. *Gene* *227*, 59–68.
- Larsen, M.R., Thingholm, T.E., Jensen, O.N., Roepstorff, P., and Jørgensen, T.J. (2005). Highly selective enrichment of phosphorylated peptides from peptide mixtures using titanium dioxide microcolumns. *Mol. Cell. Proteomics* *4*, 873–886.
- Martin, S.G., and Berthelot-Grosjean, M. (2009). Polar gradients of the DYRK-family kinase Pom1 couple cell length with the cell cycle. *Nature* *459*, 852–856.
- Martin, S.G., and Chang, F. (2006). Dynamics of the formin for3p in actin cable assembly. *Curr. Biol.* *16*, 1161–1170.
- Martin, S.G., McDonald, W.H., Yates, J.R., III, and Chang, F. (2005). Tea4p links microtubule plus ends with the formin for3p in the establishment of cell polarity. *Dev. Cell* *8*, 479–491.
- Padte, N.N., Martin, S.G., Howard, M., and Chang, F. (2006). The cell-end factor pom1p inhibits mid1p in specification of the cell division plane in fission yeast. *Curr. Biol.* *16*, 2480–2487.
- Shevchenko, A., Wilm, M., Vorm, O., and Mann, M. (1996). Mass spectrometric sequencing of proteins silver-stained polyacrylamide gels. *Anal. Chem.* *68*, 850–858.
- Snaith, H.A., Samejima, I., and Sawin, K.E. (2005). Multistep and multimode cortical anchoring of tea1p at cell tips in fission yeast. *EMBO J.* *24*, 3690–3699.
- Wilm, M., Shevchenko, A., Houthaeve, T., Breit, S., Schweigerer, L., Fotsis, T., and Mann, M. (1996). Femtomole sequencing of proteins from polyacrylamide gels by nano-electrospray mass spectrometry. *Nature* *379*, 466–469.

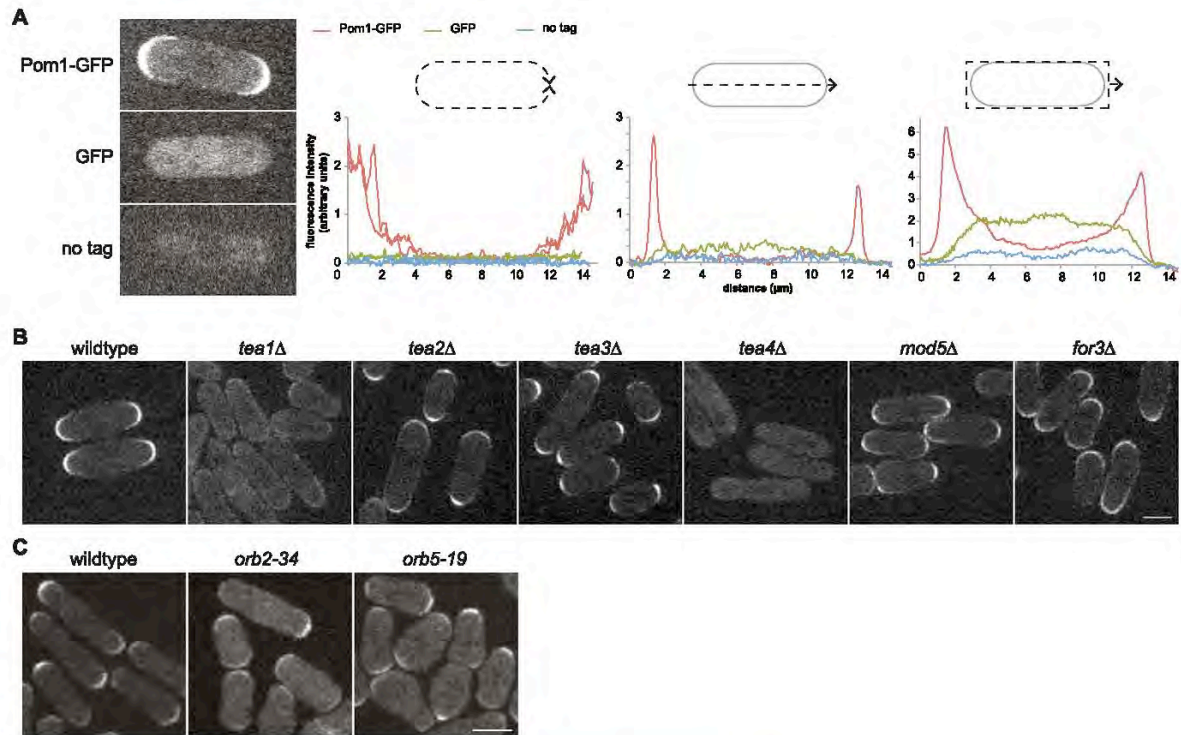


**Figure S1. Pom1 Localization in Wild-Type Cells and in Polarity Mutants, Related to Figure 1**

(A) Localization of Pom1-GFP and GFP, as well as background fluorescence intensity of unlabelled cells. Cells were imaged in identical conditions and a single medial confocal section is shown. The fluorescence intensity was measured along the periphery of each cell half (graph on the left) and across the cell length (middle graph), as in Figure 1A. The sum fluorescence intensity of the entire cell volume along the length of the cell is shown on the graph on the right. While neither GFP nor background signal are distributed in a graded pattern, Pom1-GFP forms cortical concentration gradients.

(B) Localization of Pom1-GFP in indicated genotypes in live cells grown at 30°C.

(C) Localization of Pom1-GFP in cells of indicated genotypes grown at the restrictive temperature of 36°C for 2h30 and fixed. Scale bars are 5 $\mu\text{m}$ .

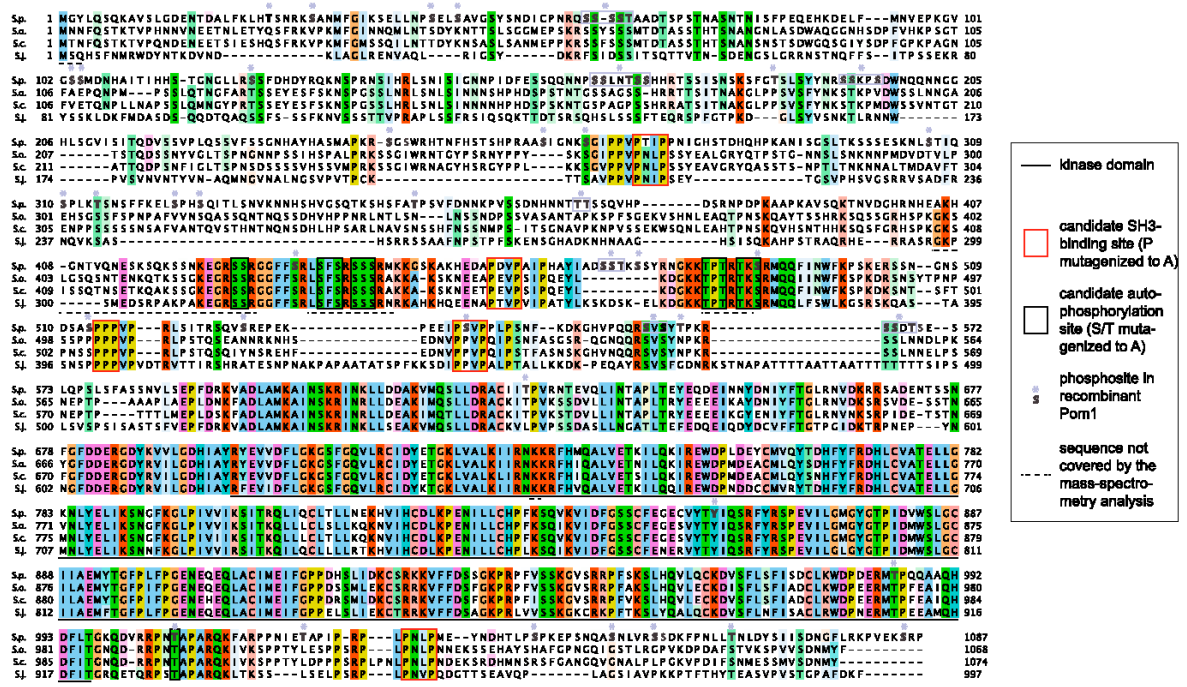
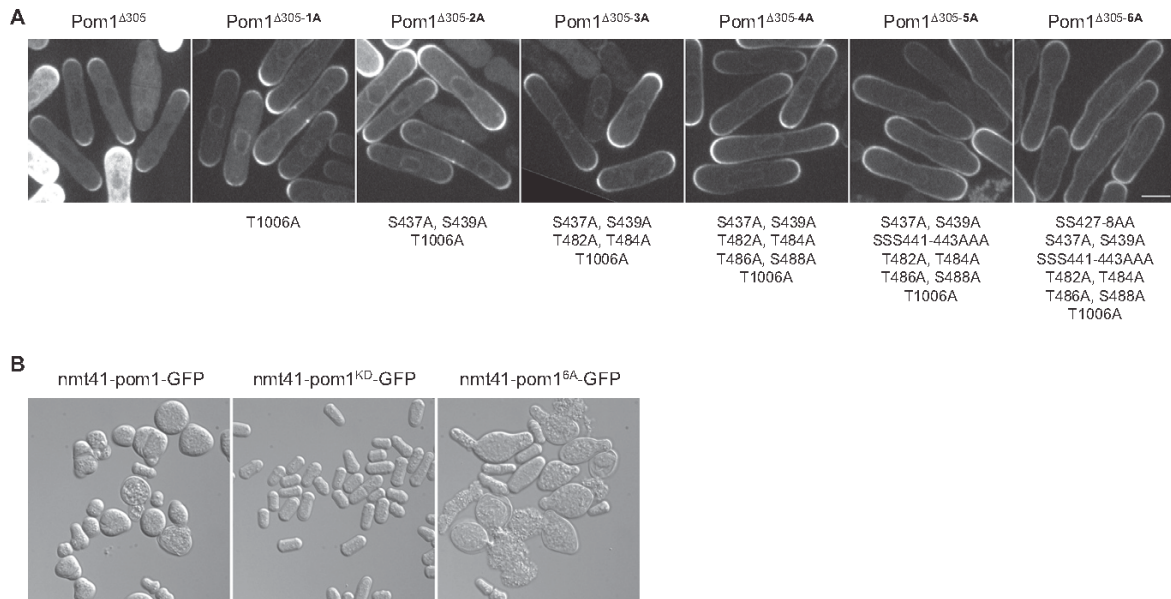
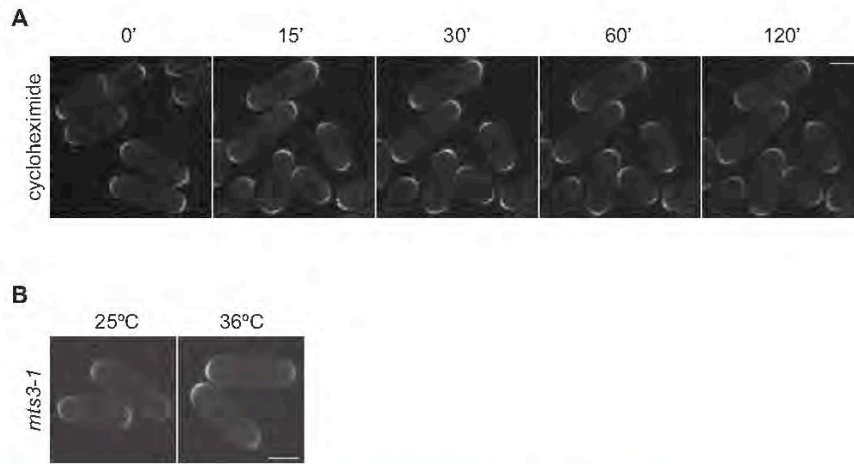


Figure S2. Alignment of Pom1 with Orthologs from Other *Schizosaccharomyces* Species, Related to Figure 2

Alignment of Pom1 orthologs in 4 *Schizosaccharomyces* species (S.p.: *pombe*, S.o.: *octosporus*, S.c.: *cryophobus*, S.j.: *japonicus*). The kinase domain is underlined. Serine/threonine residues mutated to alanine in the Pom1<sup>6A</sup> allele are boxed in black. Proline residues mutated to alanine in the Pom1<sup>5PxxP</sup> allele are boxed in red. All phosphorylated residues identified by mass-spectrometry are in bold and highlighted by a purple asterisk. Purple boxes around some of these indicate that only one of the two or more boxed residues are phosphorylated, but that the exact phosphorylated residue could not be precisely resolved. Regions for which no peptides were recovered in the mass-spectrometry are underlined with a dashed line.



**Figure S3. Mutation of Pom1 Autophosphorylation Sites Causes Progressive Cortical Spreading of Active Pom1, Related to Figure 3**  
 (A) Localization of indicated Pom1-GFP alleles expressed from plasmids in *pom1Δ* cells. The corresponding mutations are indicated at the bottom. Note that all mutations were introduced in the N-terminal truncated Pom1<sup>Δ305</sup> allele, which lacks the first 305 amino acids not essential for localization. Scale bar is 5μm.  
 (B) Strong overexpression of wild-type or Pom1<sup>6A</sup>-GFP, but not Pom1<sup>KD</sup>-GFP leads to morphological defects. The constructs were expressed on plasmid under *nmt41* promoter and induced for 24h at 30°C. The cells were fixed in 70% EtOH.



**Figure S4. Pom1 Localization Is Not Controlled by Translation and Degradation, Related to Figure 4**

(A) Localization of Pom1-GFP after indicated time in cycloheximide.

(B) Localization of Pom1-GFP in the thermosensitive *mts3-1* proteasome mutants grown at 25°C or 36°C for 2h30. Scale bars are 5µm.

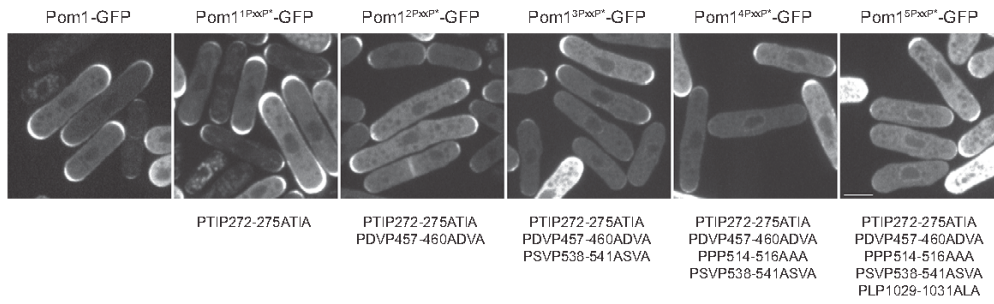


**Figure S5. Mutation of PxxP Motifs Reduces Pom1 Localization to Cell Tips, Related to Figure 5**

Localization of indicated Pom1-GFP alleles expressed from plasmids in *pom1Δ* cells. The corresponding mutations are indicated at the bottom. Scale bar is 5μm.

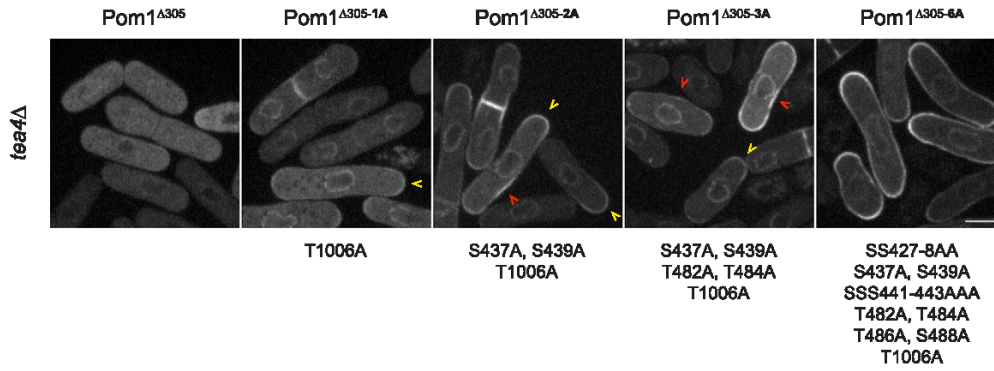


**Figure S6. Mutation of Autophosphorylation Sites Bypasses the Need for Tea4 for Pom1 Localization to the Cell Periphery, Related to Figure 6**

Localization of indicated Pom1-GFP alleles expressed from plasmids in *tea4Δ* cells. The corresponding mutations are indicated at the bottom. As in Figure S3, all mutations were introduced in the N-terminal truncated Pom1<sup>Δ305</sup> allele, which lacks the first 305 amino acids not essential for localization. Note that even mutation of few autophosphorylation sites is sufficient to restore partial localization of Pom1 to the cell periphery in *tea4Δ* cells. While these Pom1 alleles can localize anywhere around the periphery of the cell (red arrowheads), there appears to be a preference for cell tips (yellow arrowheads). Note that Pom1 does not appear to localize uniformly at the cortex, but forms domains of higher intensity. Scale bar is 5μm.

# **Chapter 4**

## **Tea4-mediated ectopic morphogenesis**

### **4.1. Introduction**

As described in Chapter 1, Cdc42 is a small GTPase of the Rho-subfamily that is conserved from yeast to humans and it is highly important for regulating cell growth and polarity (Chang et al., 1994; Miller and Johnson, 1994; Nobes and Hall, 1999; Pruyne et al., 2004b). Cdc42 is functioning as a molecular switch that transits from a GDP-bound inactive state to a GTP-bound active state. Guanine Exchange Factors (GEF) and GTPase Activating Proteins (GAP) are the proteins involved in the activation and inactivation of GTPases, respectively. The importance of Rho GTPases, especially Cdc42, in establishing polarized growth has been mostly investigated in budding yeast. In budding yeast cells, Cdc42 is activated by its sole GEF protein Cdc24 that restricts Cdc42 activity to a single concentrated region at the plasma membrane. Active Cdc42 controls the actin assembly through the formin Bni1, activates the Arp2/3 complex that nucleates actin filaments from pre-existing filaments, and is required for polarized localization of the exocyst (Lechler et al., 2001; Pruyne et al., 2004; Zhang et al., 2001). While only one GEF for Cdc42 has been identified in budding yeast, four GAPs: Rga1, Rga2, Bem2 and Bem3 can stimulate the hydrolysis of Cdc42-GTP (Marquitz et al., 2002; Smith et al., 2002). Rga2, Bem2 and Bem3 may not share identical localization patterns but initially localize at the incipient bud site and then are present mostly at the bud tip and the bud cortex during bud emergence and bud growth (Knaus et al., 2007; Sopko et al., 2007). Rga1 is also present at the site of bud emergence but then concentrates in the mother-bud neck until the end of the cell cycle and is the only GAP that must be present at the division site to prevent subsequent polarization toward that site (Caviston et al., 2003; Tong et al., 2007). In conclusion, GEF and GAPs regulate the proper localization and timing of Cdc42 (in-) activation leading to correct polarized growth.

To initiate polarized growth, symmetry breaking first has to occur. Models for symmetry breaking leading to polarization propose that stochastic fluctuations generate small clusters of polarity factors at random sites. Through autocatalytic amplification mechanisms, a small cluster can grow through positive feedback mechanisms to generate a dominating asymmetry (Turing, 1990) that will eventually initiate polarized growth. As described in Chapter 1, studies in budding yeast have shown that direct interactions between Rsr1 and Bem1, Cdc24, and Cdc42 (Kozminski et al., 2003; Park et al., 1997; Zheng et al., 1995)

combined with the active Cdc42 and actin positive feedback loops and possibly a negative loop ensure polarized growth and correct bud site selection.

In fission yeast, less is known regarding Cdc42 regulation and feedback loops. As mentioned in the general introduction, control of Cdc42 depends on two GEFs called Gef1 and Scd1 and only one known GAP named Rga4 (Chang et al., 1994; Das et al., 2007; Garcia et al., 2006; Tatebe et al., 2008). A protein called Scd2, the homologue of budding yeast protein Bem1, is necessary for the localization of Scd1 and is believed to serve as a scaffold protein mediating the interaction between Scd1 and Cdc42 (Endo et al., 2003; Wheatley and Rittinger, 2005). In this study, I will try to investigate the molecular mechanisms that could link microtubule-associated protein Tea4 with the activation of Cdc42.

## 4.2. Results

### 4.2.1. Ectopically targeted Tea4 induces growth

As described in Chapter 3, Tea4 mediates Pom1 localization. During this study a chimera was generated by Sophie Martin by fusing Cdr2-GFP with Tea4 (Cdr2-GFP-Tea4N) to test whether ectopic Tea4 could recruit Pom1. Ectopic Tea4N recruited successfully Pom1 at the medial cortex where Cdr2 is localized in interphase cells (Morrell et al., 2004). This chimera relied on a truncated fragment of Tea4 (Tea4 1-521, called Tea4N) that abolishes binding to Tea1 (Martin et al., 2005), therefore allowing the study of Tea4 independently of its normal localization at cell tips. Interestingly, ectopically localized Tea4N fused with Cdr2-GFP not only mediated Pom1 recruitment but also initiated growth in *tea4* $\Delta$  background suggesting Tea4 is instructive for growth. The finding of initiating growth by ectopically recruited Tea4 led me to the idea to study polarity away from the cell tips. The Tea4N fragment abolishes Tea1 binding but still includes the Tea4 SH3 domain and RVxF motif. In this chapter, I tried to investigate the mechanisms of how ectopic Tea4 induces growth in *tea4* $\Delta$  cells expressing the Cdr2-GFP-Tea4N chimera.

First, I would like to describe the genetic engineering strategy of Tea4 ectopic recruitment. Tea4N was recruited to the cell sides by fusing it with the cortical protein kinase Cdr2 tagged with GFP (Fig. 4.1A). Cdr2 is normally localized to a broad medial band during interphase regulating the timing of mitotic entry (Morrell et al., 2004) and it has been shown that Pom1 negatively regulates its localization (Martin and Berthelot-Grosjean, 2009; Moseley et al., 2009). Thus Cdr2-Tea4N fusion probably affects its own localization through recruitment of Pom1 and resulting localization of the fusion may not be as tight as that of Cdr2 alone. The Cdr2-Tea4N fusion is expressed under the control of the mild promoter *nmt81* and integrated at the *ura4* locus. In all experiments shown below, cells expressing the Cdr2-Tea4N fusion are having endogenous *tea4* deleted and are growing 20 hours in the presence of the promoter repressor thiamine in EMM medium supplied with the necessary supplements. Then thiamine is washed away allowing the fusion to be expressed to steady state levels for approximately 28-32 hours. The same fusion, but without Tea4N, was used as negative control. 48 $\pm$ 6% of cells (n=100) expressing the Cdr2-GFP-Tea4N fusion exhibit ectopic growth (Fig. 4.1B). This ectopic growth is triggered when ectopic Tea4 localization leads to the formation of a curved shape at the cell middle, which after time grows to a round-shaped bump, which I will refer to as "bulging". To characterize the formation of these ectopic "bulges", I followed their growth over time using microfluidic chambers (CellAsic). As shown in Fig. 4.2B they show a growth of approximately 2 $\mu$ m in width over 4-6 hours. I also

constructed similar fusion protein with distinct fluorescent tags (GFP/CFP/mCherry). These fusions had similar effect, causing ectopic growth in about half of the cells. For instance Cdr2-CFP-Tea4N fusion led to in bulge formation in 55+/-5% of cells (See Fig. 4.7A).

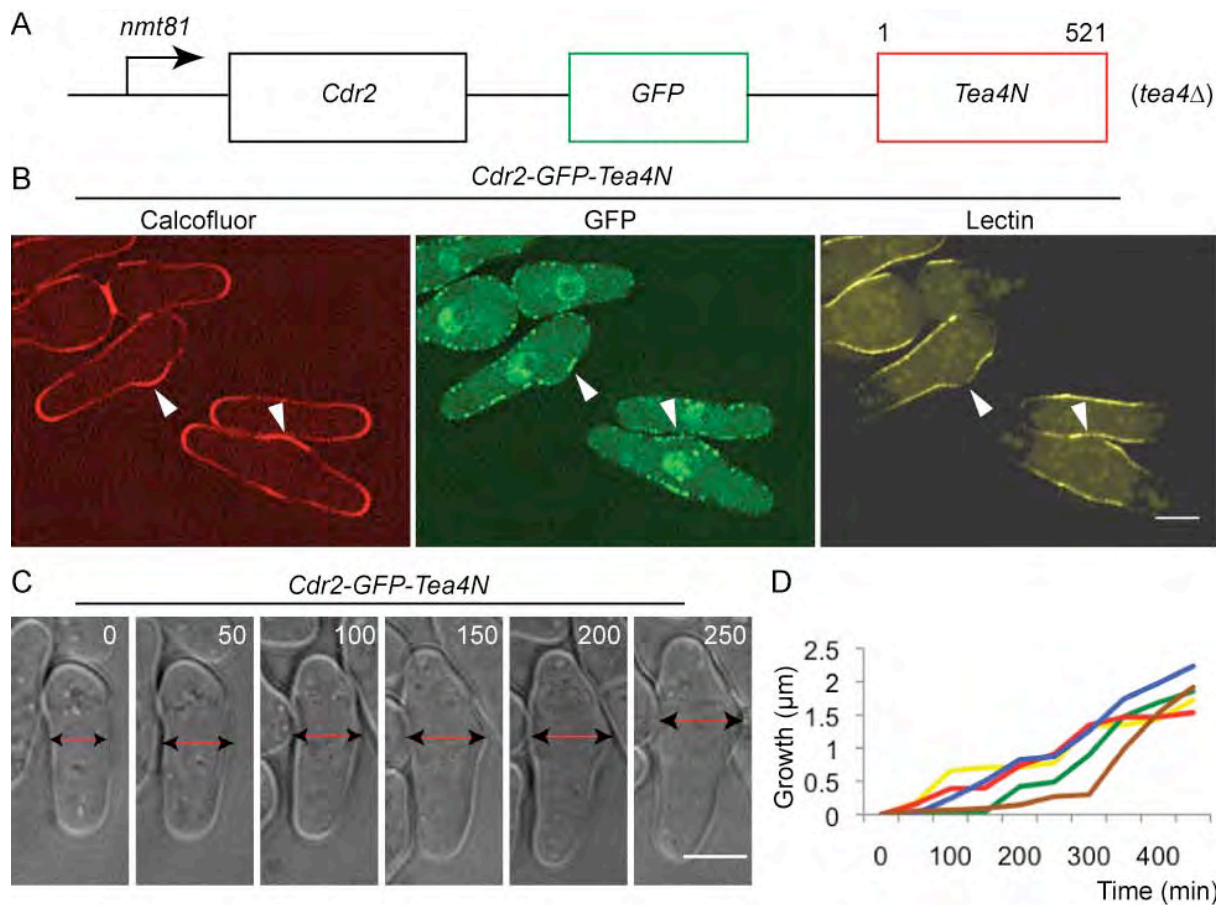


**Figure 4.1. Ectopically targeted Tea4N initiates growth.** (A) Genetic engineering of targeting Tea4 ectopically. Tea4 fragment 1-521 (Tea4N) is fused with cortical protein Cdr2-GFP. This chimera is under control of the mild promoter *nmt81* and is expressed in *tea4Δ* cells. (B) Staining with 10μg/ml calcofluor labels newly formed cell wall indicating growth (left image). Cdr2-GFP-Tea4N fusion is localized at cell sides and at the sites of ectopic growth (middle image). Staining with 10μg/ml lectin, a drug that binds to cell wall, was added for 15 minutes then washed away and cells continued to grow for 1 hour. Lectin binds pre-existing cell wall and abolishment of lectin staining indicates cell regions of new cell wall synthesis (right image). Scale bar 5μm. (C) Formation of a new bulge and measurement of its width over time. Scale bar 5μm. (D) The bulge grows approximately 2μm in width over 4-6 hours as measured in 5 individual cells.

Further investigation of the bulged cells indicated that these cells could continue dividing “happily” and cells could grow for at least 72 hours (approximately 12-16 generations), (Fig. 4.2B). In addition as shown in Fig. 4.2A: 1) Cells (50+/-5%, n=100) could grow from both cell tips suggesting that Tea4N fusion also partly rescues the monopolar growth pattern of *tea4Δ* cells. In *tea4Δ* cells, Cdr2 localizes around the non-growing cell end (Martin and Berthelot-Grosjean, 2009; Moseley et al., 2009) hence the fusion is also localized at the non-growing end resulting in rescuing the monopolar defects of *tea4Δ* cells, 2) It seems that once the bulge is formed, it perdures through generations, and 3) A few cells (9+/-3%, n=100) die immediately after cell division.

I checked the cytoskeletal organization in bulged cells first by staining cells with AlexaFluor 488-phalloidin to visualize actin. Actin patches are present at the bulge and actin filaments seem to emanate from the ectopic growth site (Fig. 4.2C). Interestingly, in cells expressing the Cdr2-Tea4N fusion but not yet exhibiting ectopic growth, it is clear that actin structures localize at the cell tip similar to control cells (Fig. 4.2C). Visualization of microtubules through tagging of tubulin alpha-2 (*atb2*) shows microtubules to be misaligned and oriented towards the bulge site with their plus ends headed towards the tip of the bulge (Fig. 4.2D, time-lapse videos not shown). Interestingly, in cells expressing the Cdr2-Tea4N fusion but not yet exhibiting ectopic growth, it is clear that microtubules exhibit the typical anti-parallel structure along the long axis similar to control cells (Fig. 4.2D) suggesting that MTs re-organization in bulged cells is a consequence of shape. I will further investigate in the following sectors of this chapter how ectopic growth is initiated in cells expressing the Cdr2-Tea4N fusion prior to bulge formation.

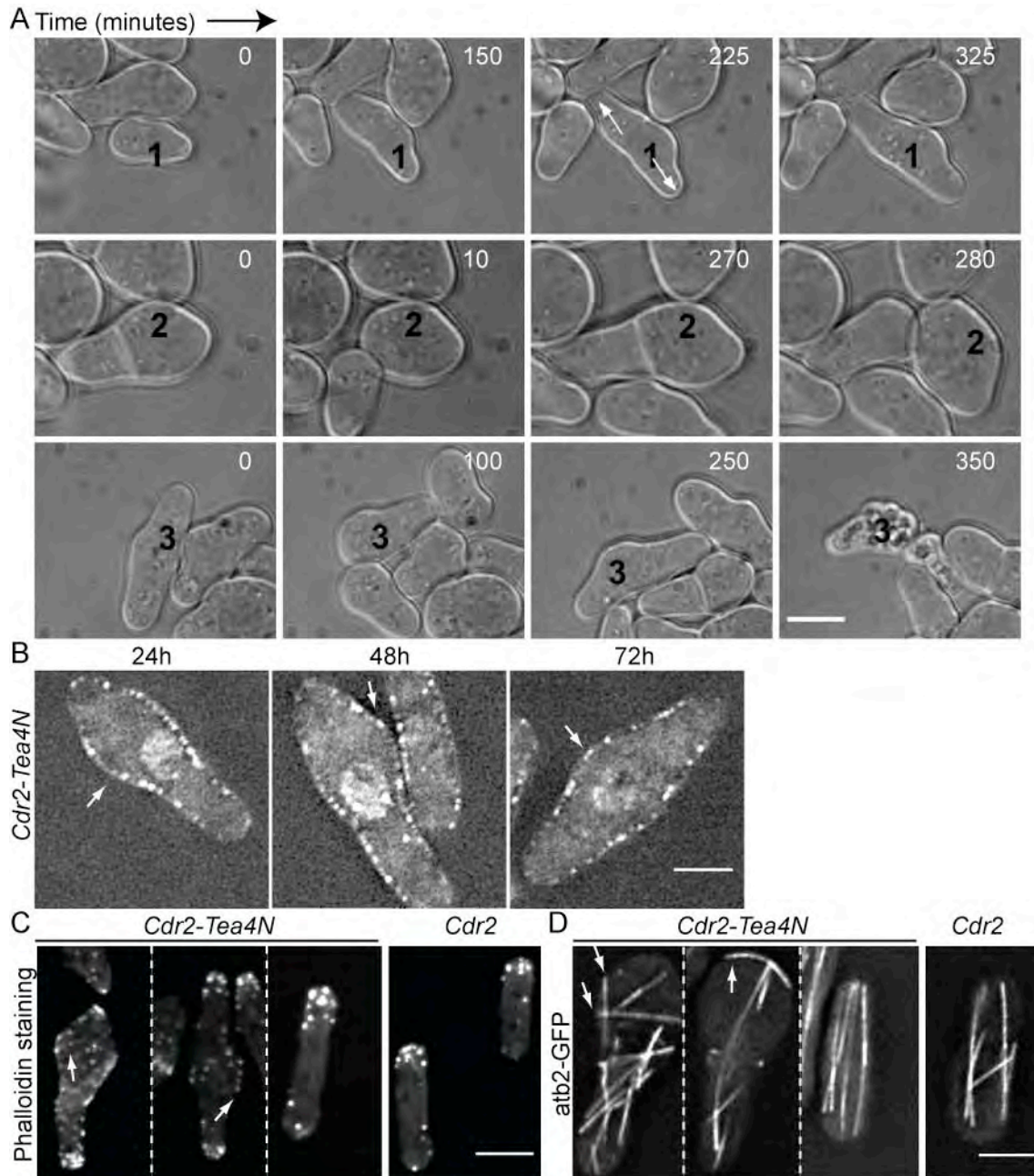


**Figure 4.2. Characteristics of bulged cells.** (A) Arrows indicate tip growth in bulged cells (50 $\pm$ 5%, n=100) can grow from both cell ends (1), once the bulge is formed, it perdures through generations (2) and 9 $\pm$ 3% (n=100) of cells die directly after cell division (3). Scale bar 5 $\mu$ m. (B) Cells continue to express Cdr2-GFP-Tea4N (arrows) even after 72 hours of growth in exponential phase and to exhibit ectopic growth. Scale bar 5 $\mu$ m. (C) AlexaFluor 488-phalloidin staining shows actin patches at the bulge tip and emanating actin filaments at the site of ectopic growth (arrows), in addition to their physiological cell tip localization either in rod-shaped cells expressing the Cd2-Tea4N fusion or in control cells. Scale bar 5 $\mu$ m. (D) Visualization of microtubules through tagging of tubulin alpha-2 (atb2) shows that MTs seem to be more abundant, misaligned and re-directed towards the tip of the bulge (arrows), in contrast to their physiological anti-parallel structure along the long axis of the cell observed either in rod-shaped cells expressing the Cd2-Tea4N fusion or in control cells. Scale bar 5 $\mu$ m. Time is in minutes.

#### 4.2.2. Localization of cell polarity regulators at ectopic growth site

Since cells expressing Cdr2-Tea4N fusion exhibit ectopic growth I investigated which proteins were localized at the bulge. I first checked the localization of the major regulator of polarized growth Cdc42. CRIB-GFP (Cdc42/Rac-interactive binding) that binds to the active GTP-bound form of Cdc42 (Tatebe et al., 2008) localizes at the ectopic growth site (Fig. 4.3). Furthermore, I checked whether GEFs, the activators of Cdc42 also localize ectopically and as observed at Fig. 4.3 that was the case.

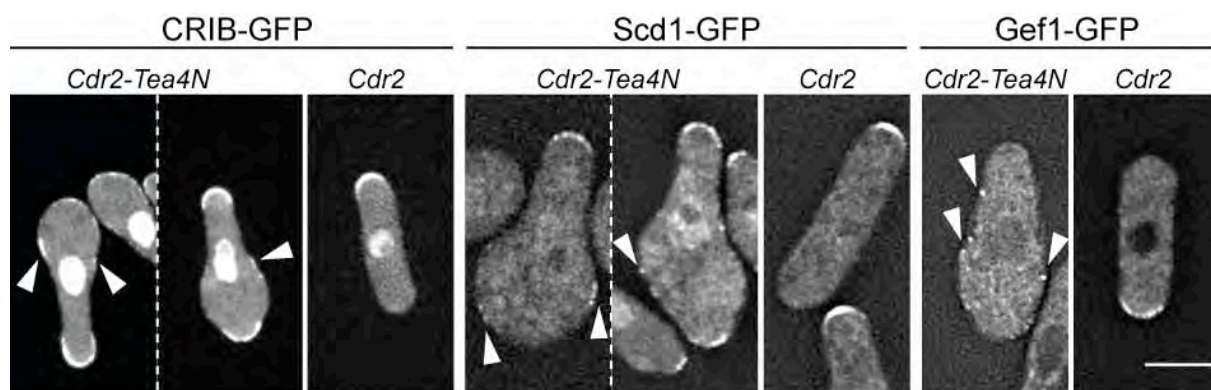


**Figure 4.3. Active Cdc42 and its GEFs localize at sites of ectopic growth.** CRIB, Scd1 and Gef1 are present at sites of ectopic growth (arrowheads) where Cdr2-Tea4N fusion is expressed. Scale bar 5 $\mu$ m.

Tea4 is directly associated with Pom1 and Dis2 (Alvarez-Tabares et al., 2007; Hachet et al., 2011) so I tested whether these proteins are recruited by ectopic Tea4. Both proteins were present at the ectopic growth site (Fig 4.4A). In addition I checked whether other factors of the polarisome would be present at ectopic sites in cells expressing the fusion. Major proteins of the polarisome such as Tea1, For3 and Exo70 were also localized at the ectopic growth site (Fig. 4.4A). Even though only the Tea4N fragment is recruited ectopically, and thus should not directly bind Tea1, one explanation could be that since microtubules are oriented towards the bulge Tea1 could be delivered at the ectopic growth site and then “trapped” there. Positive feedback loop mechanisms could subsequently recruit additional polarity factors at this site (see conclusions and discussion at the end of this chapter).

To this point, I have simplified the growth process by making it entirely Tea4-dependent. The recruitment of a large set of factors exemplifies the robustness of this process. The localization of some of these proteins might be a consequence of ectopic growth as previously mentioned for Tea1. To distinguish which of all these proteins are directly linked with Tea4, I checked their localization in cells expressing the Cdr2-Tea4N fusion prior to bulge formation. Polarity factors such, as For3, Tea1 and Exo70 were absent from the side of cells expressing the Cdr2-Tea4N fusion. In contrast, Pom1 and Dis2 are present at the cell side where the Tea4N is present (Fig. 4.4B) supporting the data showing their direct binding with Tea4 (Alvarez-Tabares et al., 2007; Hachet et al., 2011). Interestingly, CRIB also localizes to the cell sides (Fig. 4.4B) indicating that Tea4 recruits active Cdc42 independently of growth. This suggests a possible direct link between Tea4 and Cdc42.

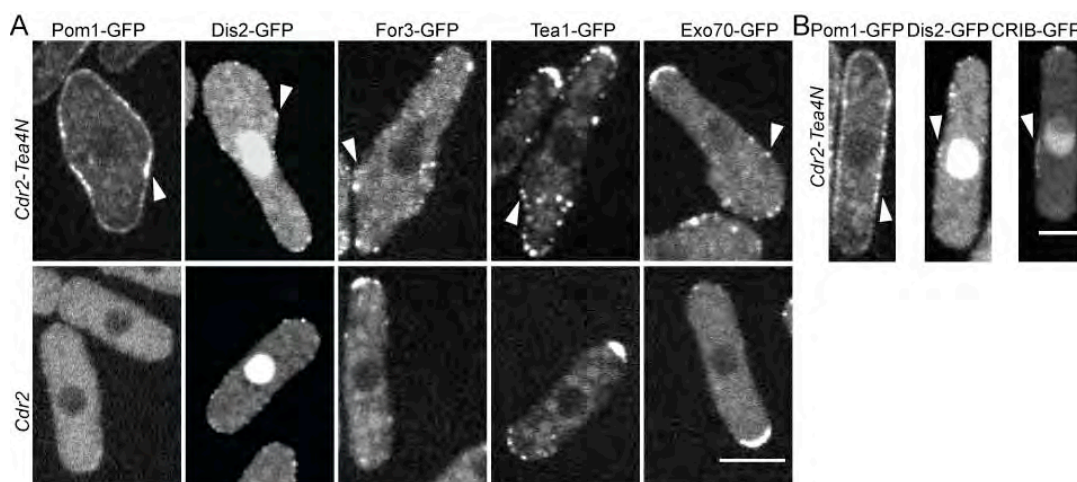


**Figure 4.4. Localization of polarity factors in cell expressing the Cdr2-Tea4N fusion.** (A) Multiple polarity factors (Pom1, Dis2, For3, Tea1 and Exo70) localize at sites of ectopic growth (arrowheads) where Cdr2-Tea4N fusion is expressed. Scale bar 5µm. (B) Only Pom1, Dis2 and CRIB are present at the cell side (arrowheads) in cells expressing the fusion Cdr2-Tea4N that have not formed yet bulges, supporting their association with Tea4N independent of growth process. Scale bar 5µm.

#### 4.2.3. Dis2 essentiality for bulge formation

After investigating the protein localization in the ectopic growth site, a following step was to determine what genes are essential for this growth. I generated strains where the gene of interest was deleted and then I quantified the number of bulged cells. As shown in Fig. 4.5A, *tea1*, *for3*, *exo70*, *dis2* and *sds21* gene deletion did not alter significantly the bulge formation. I would like to remark that *for3* gene deletion in cells expressing the Cdr2-Tea4N fusion results in micro colonies that do not grow efficiently, but clearly exhibit ectopic growth as shown in Fig. 4.5B. An additional clarification is that since Dis2 and Sds21 are redundant proteins, deletion of each gene could not address their importance in the ectopic growth process described. Therefore, in order to study whether *dis2* is essential for bulge formation I mutated the RVxF motif in Cdr2-Tea4N fusion. As shown by Alvarez-Tabares et al. in 2007, Dis2 binds Tea4 directly. In agreement with this, I showed in Chapter 2 (Fig. 2.8B) that Dis2 associated with purified Tea4-TAP. I confirmed this interaction through co-IP and further showed that this interaction depends on both Tea4 RVxF motif and SH3 domain (Hachet et al., 2011), (See Chapter 3, Fig. 6D). Excitingly, Cdr2-Tea4N<sup>RVxF</sup> and Cdr2-Tea4N<sup>SH3</sup> mutant cells severely diminish bulge formation (Fig. 4.5C) suggesting that *dis2* is essential for ectopic growth. To dissect whether *pom1* gene would play an essential role for bulge formation I deleted *pom1* and found that the bulges still occur but in fewer cells (from approximately 55% in Cdr2-Tea4N to 30% in Cdr2-Tea4N *pom1*Δ) (Fig. 4.5A). These data show that Dis2 is a key Tea4 binding partner for polarized growth and Pom1 is likely not the only target of Tea4-Dis2 dephosphorylation.

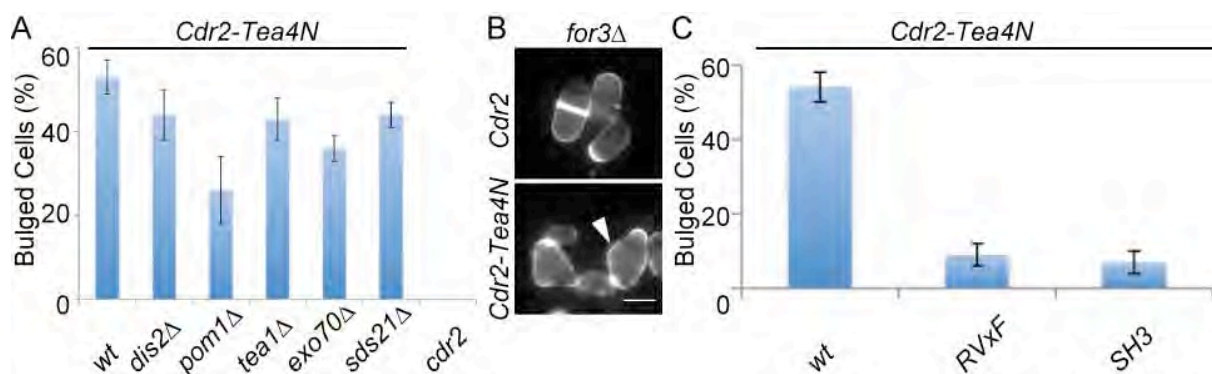


**Figure 4.5. Dis2 essentiality for bulge formation.** (A) Deletion of multiple polarity genes does not inhibit bulge formation. Only when *pom1*Δ is deleted, cells exhibit partial inhibition of ectopic growth. Cdr2-GFP was used as a negative control and it did not exhibit any bulge formation. Graph shows the average of 3 different experiments with standard deviation bars (n=100 cells per experiment). (B) Cells expressing Cdr2Tea4N in *for3*Δ background do not grow efficiently but still exhibit ectopic growth (arrowheads, no quantification data). Scale bar 5μm. (C) Cdr2-Tea4N<sup>RVxF</sup> and Cdr2Tea4N<sup>SH3</sup> do not promote bulge formation. Graph shows the average of 3 different experiments with standard error bars (n=100 cells).

To further support that Pom1 may not be the sole target of Tea4-Dis2 dephosphorylation, I tested whether Pom1 delocalization was the reason of the *tea4<sup>SH3</sup>* mutant phenotypes (see Fig. 2.5A and B in Chapter 2). I used a *pom1* allele that localizes to the cell periphery independently of Tea4, called Pom1-6A mutant (see Fig. 3C in Chapter 3). Pom1 contains multiple predicted autophosphorylation sites and mutating 6 of these sites resulted in the Pom1-6A mutant (Hachet et al., 2011) (see Chapter 3 for details). Pom1-6A mutant localizes at the cortex constitutively (see Fig. 3C in Chapter 3), independently of Tea4 and it remains kinase active (Hachet et al., 2011). I checked the phenotype of the double mutant *pom1-6A-GFP tea4<sup>SH3</sup>*. While cortical active Pom1 (Pom1-6A-GFP) did not cause monopolar growth in wild type cells (Fig. 4.6A and B), it also could not rescue the monopolar growth of *tea4<sup>SH3</sup>* mutant. *pom1-6A-GFP* and *pom1-6A-GFP tea4<sup>SH3</sup>* cells seem to have positioned the septum at the cell middle ( $0.52 \pm 0.01$  and  $0.53 \pm 0.02$ , respectively) compared to *tea4<sup>SH3</sup>* mutant that exhibits septum misplacement equal to  $0.56 \pm 0.02$  (Fig. 4.6A and B). I further tested whether the double mutant *pom1-6A-GFP tea4<sup>SH3</sup>* could rescue the T-shapes observed in *tea4<sup>SH3</sup>* mutant in re-feeding experiments. Interestingly, in *pom1-6A-GFP tea4<sup>SH3</sup>* double mutant, cells still exhibit T-shapes (40% +/- 6) and cells also appear to have more aberrant shapes (52% +/- 6 multi-branched cells) and only 8% +/- 4 of cells are rod-shaped (Fig. 4.6A and C). These data suggest that cortical active Pom1 cannot rescue the T-shaped cells observed in *tea4<sup>SH3</sup>* mutant and Pom1-6A-GFP may have an additive effect with *tea4<sup>SH3</sup>* mutant regarding the aberrant cell shape observed in re-feeding experiments. Both *pom1-6A-GFP* and *pom1-6A-GFP tea4<sup>SH3</sup>* also exhibit a higher number of multi-septated cells compared to *tea4<sup>SH3</sup>* mutant in re-feeding experiments (Fig. 4.6A and C). In conclusion, although Pom1 delocalization seems to be responsible for the off-center septum observed in *tea4<sup>SH3</sup>* mutant, monopolar growth and aberrant cell shape observed in *tea4<sup>SH3</sup>* cells were not rescued by cortical active Pom1 (Fig. 4.6). These results further support that Tea4 is not only important for regulating Pom1 localization but also regulates the function of other targets to establish cell polarization.

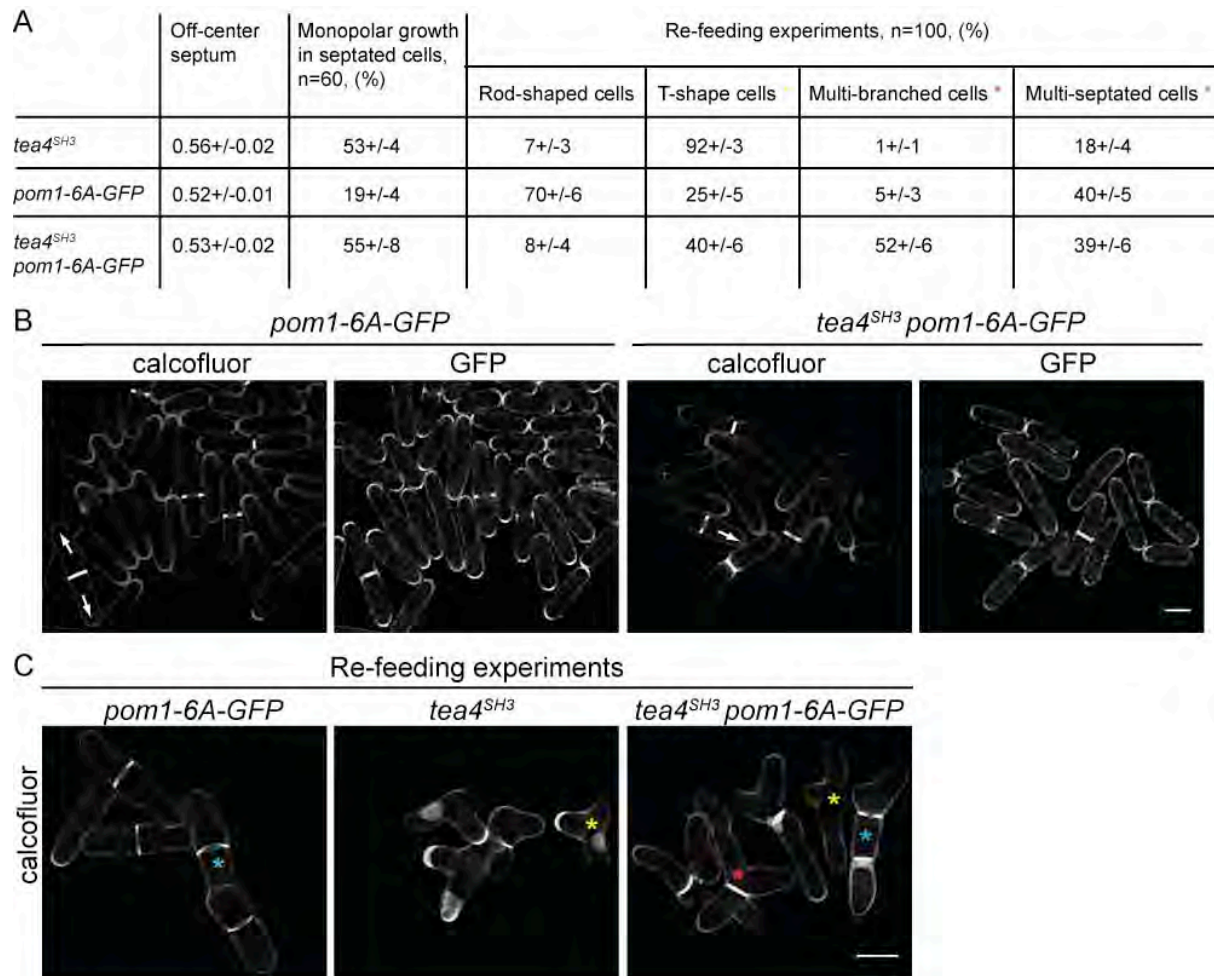


**Figure 4.7. Cortical active Pom1 is not able to rescue the monopolar growth and T-shaped cells observed in *tea4<sup>SH3</sup>*.** (A) Pom1-6A-GFP cannot rescue the monopolar growth and T-shaped cells observed in *tea4<sup>SH3</sup>* cells but it seems to correct the septum misplacement observed in *tea4<sup>SH3</sup>* mutant. In re-feeding experiments, first, double mutant *pom1-6A-GFP tea4<sup>SH3</sup>* still forms T-shapes and also exhibits more aberrant shapes (multi-branches) compared to the T-shapes observed in *tea4<sup>SH3</sup>* mutant, second, *pom1-6A-GFP* and *pom1-6A-GFP tea4<sup>SH3</sup>* show increased number of multi-septated cells compared to *tea4<sup>SH3</sup>* mutant. (B) Even though Pom1-6A-GFP localizes all over the cortex it cannot rescue the monopolar growth of *tea4<sup>SH3</sup>* cells growing in exponential phase. Scale bar 5 $\mu$ m. (C) In re-feeding experiments, both *pom1-6A-GFP* and *pom1-6A-GFP tea4<sup>SH3</sup>* exhibit a higher number of multi-septated cells (blue asterisk) compared to *tea4<sup>SH3</sup>* mutant. Pom1-6A-GFP cells do not exhibit T-shapes compared to *tea4<sup>SH3</sup>* and *pom1-6A-GFP tea4<sup>SH3</sup>* (yellow asterisk). Double mutant *pom1-6A-GFP tea4<sup>SH3</sup>* also forms multi-branched shapes (red asterisk). Scale bar 5 $\mu$ m.

#### 4.2.4. Gef1 and Rga4 essentiality for bulge formation

I investigated how Tea4 and Dis2 may promote the ectopic activation of Cdc42. To this aim, I investigated the possible function of Cdc42 regulators. *scd1* and *scd2* deletion mutants have a rounded shape phenotype (Chang et al., 1994), which is difficult to analyze thus I decided to delete *gef1*, which is one of the two Cdc42 GEFs. Interestingly, there are almost no bulged cells when *gef1* gene is deleted (Fig. 4.7A) suggesting that Gef1 is required to activate Cdc42 in the ectopic growth site. Since I checked the essentiality of Cdc42 activator I was intrigued to investigate whether Rho GAP protein Rga4 would play a role in bulge formation. Strikingly, deletion of *rga4* gene also repressed ectopic growth (Fig. 4.7A). Thus, Cdc42 regulators are critical for ectopic growth, suggesting a possible link with Tea4.

Rga4 is normally localized to the cell sides as a patchy cortical line in wild type cells and excluded from the cell ends but when *tea4* is deleted Rga4 also accumulates at the non-growing end (Tatebe et al., 2008). In *cdr2-tea4N* fusion cells, Rga4 seems to be more spread with small gaps and having lower levels in its cortical localization where Cdr2-tea4N is present, especially at the bulge site (Fig. 4.7B). From now on, I will refer to this Rga4 localization pattern observed in Cdr2-tea4N cells as either dispersion or exclusion. To show local exclusion of Rga4 by Tea4, I measured the cortical levels of both proteins and then I compared them to see whether their localization anti-correlates. For measurement of cortical fluorescence intensity, a 5 pixel-wide line was drawn by hand at the cell side in a medial confocal section and fluorescence intensity obtained using the plot profile tool of ImageJ after subtracting the background. Interestingly, it seems that Cdr2-Tea4N locally excludes Rga4 since their localization exhibit anti-correlation (n=8 cells, one shown) (Fig. 4.7B) in contrast to the correlation pattern observed between Cdr2-mcherry and Rga4-GFP in control cells (n=8 cells, one shown) (Fig. 4.7B).

To explore the genetic relationship between *rga4* and *gef1* I performed the following experiment: I deleted either *rga4* or *gef1* in cells expressing Cdr2-Tea4N fusion and I checked the localization of the other one (Fig. 4.7C). As shown in Fig. 4.7C there is no longer Gef1 at the cell sides in Cdr2-GFP-Tea4N *rga4* $\Delta$  cells but interestingly Rga4 seems to be still dispersed or excluded by the presence of Tea4N in Cdr2-GFP-Tea4N *gef1* $\Delta$  cells. These results indicate that Tea4 controls Rga4 localization. One possibility is that Tea4 may associate with Rga4, as observed in the mass spectrometry results shown in Chapter 2 (Fig. 2.8B). In *rga4* $\Delta$  *gef1* $\Delta$  double mutant, ectopic Tea4 was unable to initiate ectopic growth (Fig. 4.7A) indicating that lack of ectopic growth was not simply due to a global unbalance in Cdc42 activation.

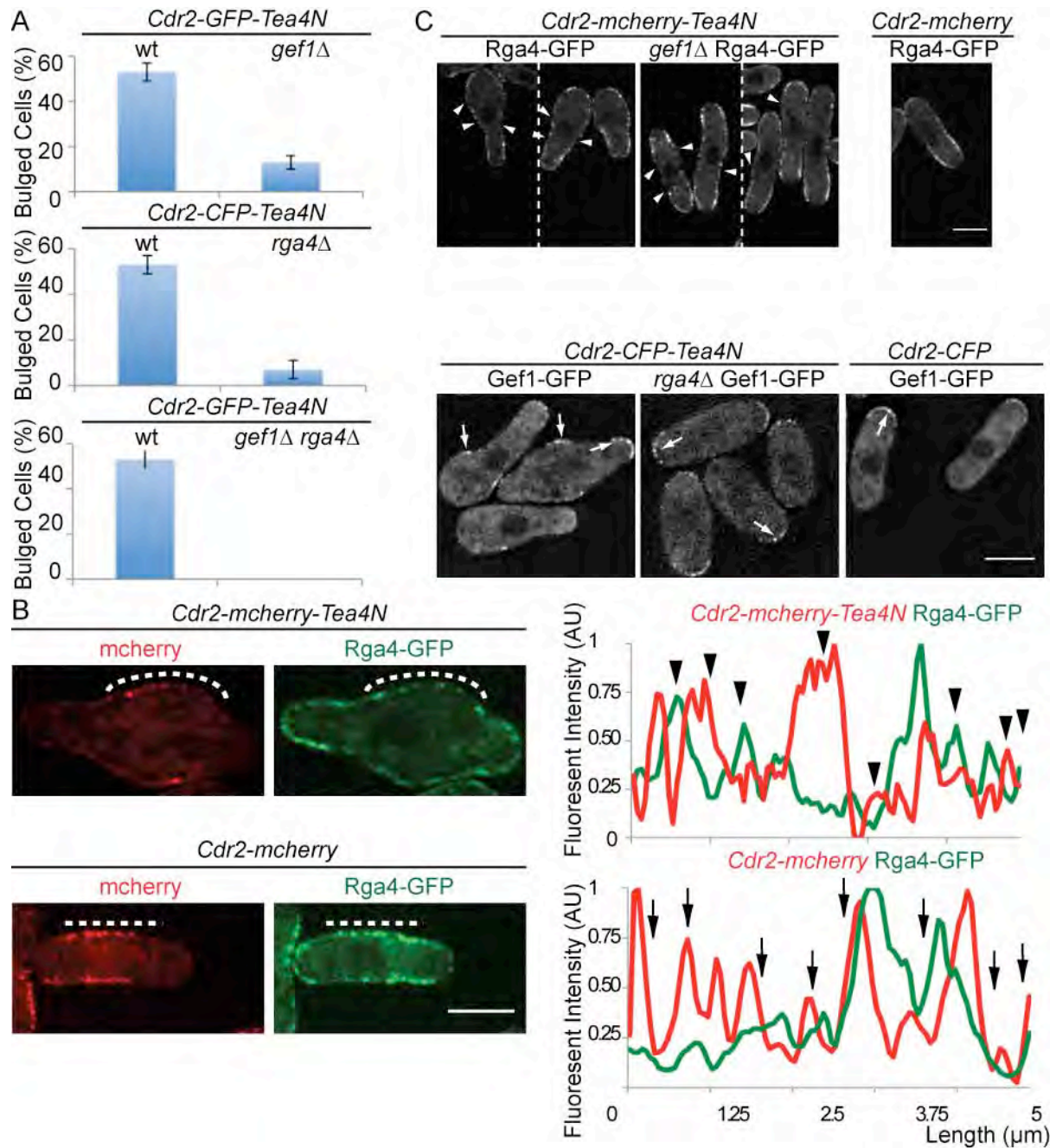


**Figure 4.7. Gef1 and Rga4 are essential for ectopic growth and ectopic Tea4 affects Rga4 localization.** (A) Ectopic growth is inhibited in cells expressing Cdr2-Tea4N in *gef1Δ* and *rga4Δ* background and bulge formation is completely abolished in *gef1Δ rga4Δ* double mutant. (B) According to the graph Rga4-GFP localization seems to anti-correlate with Cdr2-mcherry-Tea4N localization (arrowheads) suggesting that Tea4 may locally exclude Rga4. Rga4 localization seems to correlate with Cdr2-mcherry localization (arrows) in control cells in which Tea4 is no longer ectopically localized (n=8 cells, one shown). White dashed lines show the cortical mcherry and GFP intensities measured in the graphs. Graphs showing anti-correlation were performed for at least 8 individual cells but only one is shown. Scale bar 5μm. (C) Arrowheads and arrows indicate Rga4 and Gef1 localization in cells expressing Cdr2-Tea4N chimera, respectively. While Rga4 is required for Gef1 recruitment, Gef1 is not required for Rga4 exclusion suggesting an association of Tea4 with Rga4. Scale bar 5μm.

#### 4.2.5. Tea4-Dis2-Rga4 interplay

Mass spectrometry results in Chapter 2 (Fig. 2.8B) showed that Rga4 associates with *tea4*<sup>SH3</sup>. These results in combination of the localization patterns observed in Fig. 4.7C suggest that Tea4 and Rga4 may associate. To test this hypothesis I carried on testing whether Tea4 binds *in vivo* Rga4 with co-immunoprecipitation experiments. Co-IP showed that Tea4 binds Rga4 and this binding does not depend on Tea4 SH3 domain (Fig. 4.8). Furthermore the Tea4-Rga4 interaction was not dependent on Pom1 (Fig. 4.8), which has been previously shown to associate with Rga4 (Tatebe et al., 2008). I would like to comment that the TAP purification did not identify Rga4 association with wild type Tea4. The different experimental conditions between co-IP and mass spectrometry analysis could explain why Rga4 was not detected to associate with wild type Tea4 by TAP. All buffers and timing for TAP and co-IP experiments were the same suggesting that the long stay of the purified samples after TAP for several hours at 4°C before proceeding to mass spectrometry analysis could result in loss of Tea4-Rga4 binding, especially if this binding occurs transiently. Direct mass spectrometry analysis after TAP could potentially identify Rga4 to associate with Tea4. In conclusion, co-IP experiments showed that Tea4 associates *in vivo* with Rga4 and in addition Tea4 seems to negatively regulate Rga4. Since Tea4 associates *in vivo* and also recruits ectopically Dis2 we could hypothesize that Tea4 delivers Dis2 at the cell sides and that could result in the negative regulation of Rga4 localization by possible dephosphorylation.

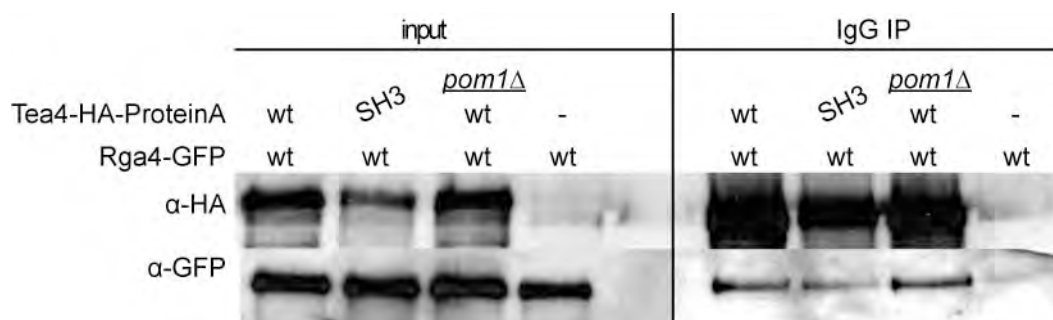


**Figure 4.8. Tea4 associates *in vivo* with Rga4.** Tea4 binds *in vivo* Rga4 and this interaction seems not to be dependent on either Tea4 SH3 domain or Pom1.

#### 4.2.6. Rga4 analysis

I tried to elucidate the significance of different Rga4 regions that could play a role for its localization. First, having a look at the schematic structure of Rga4 (Fig. 4.9A) we observe two adjacent LIM-LIM domains that usually play a role in protein-protein interaction. Downstream of the LIM-LIM domains there are two Coiled-Coil domains. CC domains are also one of the most abundant protein-protein interaction domains. I performed co-immunoprecipitation experiment to test whether Rga4 binds itself, which was the case (Fig. 4.9B). Plasmid containing Rga4-GFP was transformed in wild type cells with endogenous Rga4 tagged with myc and then expressed under control of the promoter *nmt41* to steady state for approximately 28-32 hours in the absence of thiamine. In addition, the Rga4 region containing the CC domains is sufficient for Rga4 binding and when it is deleted this binding is abolished (Fig. 4.9B). Finally at the C-terminus there is the GAP domain responsible for Rga4 activity.

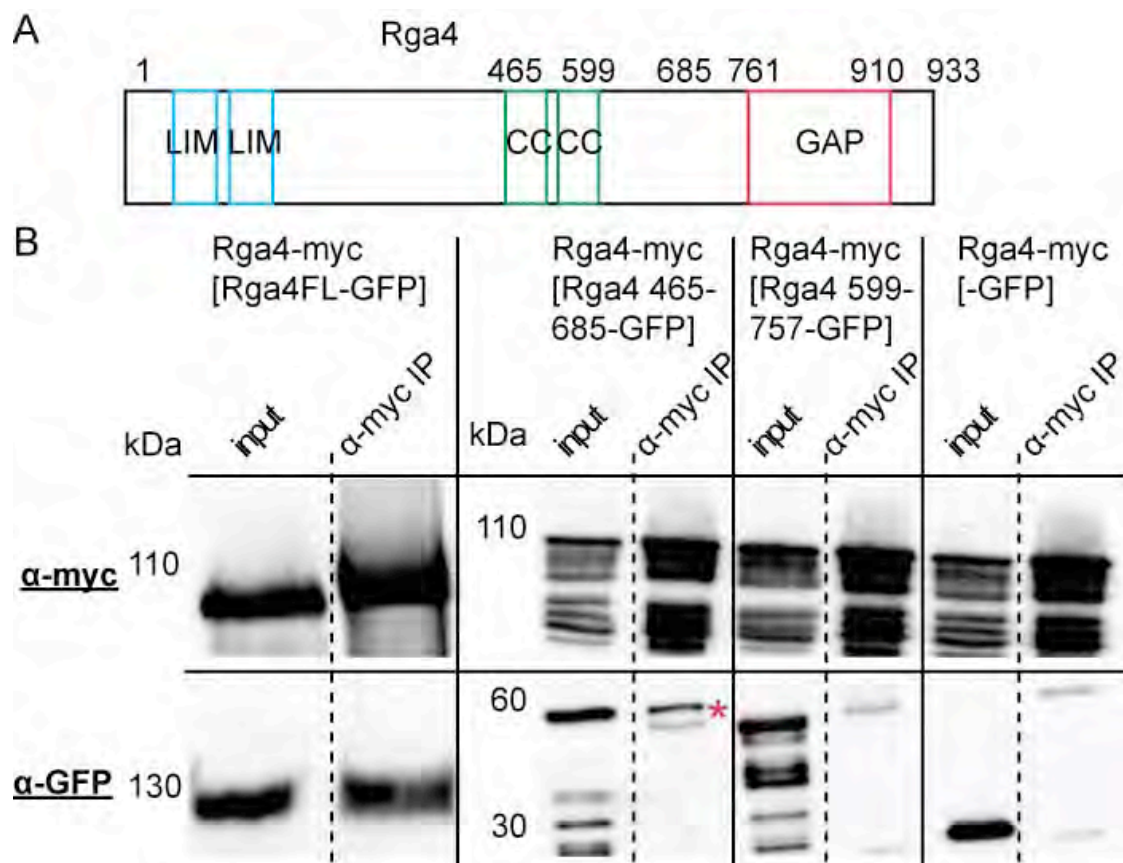


**Figure 4.9. Rga4 analysis.** At the N-terminus, Rga4 has two adjacent LIM-LIM domains and downstream of them there are two Coiled-Coil (CC) domains. At the C-terminus there is the GAP domain. (B) Co-immunoprecipitation of Rga4 with itself (first column) seems to be mediated by the region containing its CC domains. Rga4 465-685-GFP containing Rga4 CC domains expressed from plasmid co-immunoprecipitates with Rga4-myc (red asterisk). This experiment has been performed only one time.

To better understand the functionality of different Rga4 regions, I analyzed different Rga4 fragments. Plasmid containing truncated Rga4 fragments were transformed in wild type and Cdr2-Tea4N *tea4* $\Delta$  cells and then expressed under control of the promoter *nmt41* to steady state for approximately 28-32 hours in the absence of thiamine. It seems that LIM-LIM domains and the GAP domain are not necessary for Rga4 membrane anchoring (Fig. 4.10A). Rga4 1-685 fragment is still localized at the cortex but Rga4 1-623 is no longer localized at the cortex (Fig. 4.10A). Furthermore, Rga4 465-685 and Rga4 599-757 fragments bind to the membrane in contrast to Rga4 599-685 fragment, which becomes cytosolic. Altogether this suggests that the minimal Rga4 fragments for binding to the cortex are 465-685 and 599-757 and the Rga4 623-685 region is required for membrane binding, but is not sufficient (Fig. 4.10A). These fragments expressed in wild type cells localize all around the cortex and they are mostly enhanced at the cell sides. Interestingly when expressed from plasmid in Cdr2-Tea4N *tea4* $\Delta$  cells, the Rga4 465-685 and 599-757 fragments are still cortical but are enhanced at the cell tips indicating that ectopic Tea4 can still affect the localization of these Rga4 fragments (Fig. 4.10B). In addition, expressing these minimal Rga4 fragments in Cdr2-Tea4N cells abolishes bulge formation (Fig. 4.10B) suggesting that these fragments have a dominant-negative phenotype.

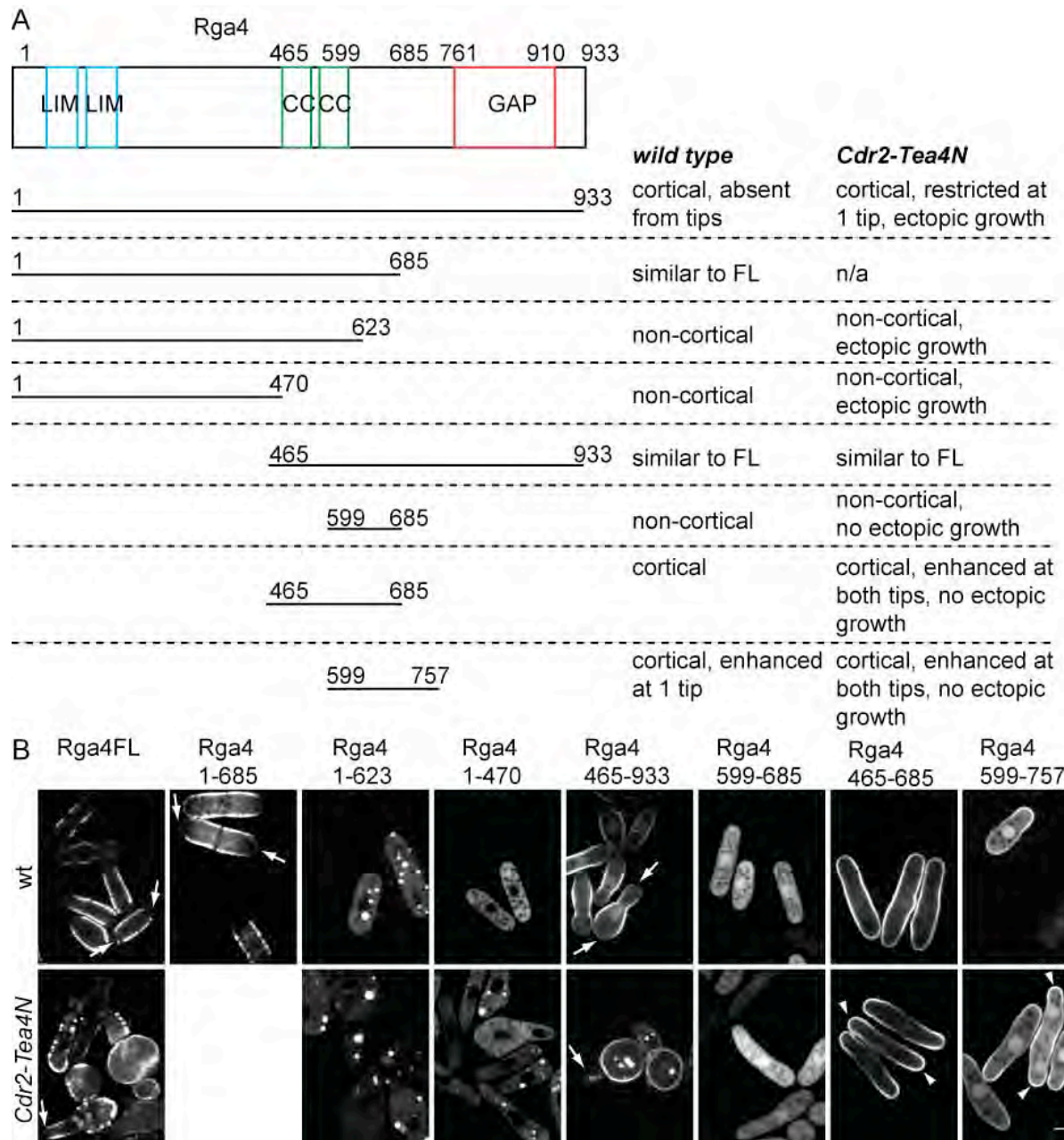


**Figure 4.10. Analysis of different Rga4 regions.** (A) Different Rga4 fragments were expressed from plasmid to steady state for approximately 28-32 hours in wild type and in *Cdr2-Tea4N* fusion cells. The Rga4 623-685 fragment is required for membrane binding, but is not sufficient. (B) Rga4FL and Rga4 465-933 are excluded from both cell tips in wt cells and from the growing end in *Cdr2-Tea4N tea4Δ* background. The Rga4 465-685 and Rga4 599-757 fragments interestingly exhibit Rga4 enhancement at cell tips when expressed in *Cdr2-Tea4N tea4Δ* cells (arrowheads). Expressing from plasmid Rga4 465-685 fragment in *Cdr2-Tea4N* cells inhibits ectopic growth to almost all cells and there is also Rga4 enhancement at cell tips. Scale bar 5μm.

Hachet et al. in 2011 showed that Tea4 SH3 domain binds to Pom1 PxxP motifs to regulate Pom1 cortical localization. This finding suggested that a similar binding between Tea4 and Rga4 could regulate Rga4 localization. After identifying four PxxP sites in Rga4 sequence, I investigated what could happen in *rga4<sup>PxxP</sup>* mutant. To generate the *rga4<sup>PxxP</sup>* mutant an *rga4* fragment containing the mutations was synthesized (Eurofins). This fragment was subsequently cloned in a vector containing full-length genomic *rga4* in order to replace the PxxP motifs by the mutated ones. This modified version of *rga4* was then integrated in *rga4Δ* cells at the endogenous locus, under the *rga4* promoter.

I checked the effect in bulge formation in Cdr2-Tea4N fusion in *rga4<sup>PxxP</sup>* background and interestingly, cells with PxxP mutations inhibit ectopic growth to approximately 50% (Fig. 4.11A). I checked the localization pattern of Rga4-GFP and Rga4<sup>PxxP</sup>-GFP in cells expressing the Cdr2-Tea4N fusion by measuring the cortical levels of Rga4-GFP and Rga4<sup>PxxP</sup>-GFP and then I compared them to Cdr2-mcherry-Tea4N. As described in Fig. 4.6C, the localization of Rga4-GFP exhibits anti-correlation compared to the localization of Cdr2-mcherry-Tea4N (n=6 cells, one shown) (Fig. 4.11A). Rga4<sup>PxxP</sup>-GFP seems to abolish this anti-correlation pattern and Rga4<sup>PxxP</sup>-GFP appears to localize all along the cell side independent of Cdr2-Tea4N localization (Fig. 4.11A) suggesting that Tea4 binding to Rga4 regulates Rga4 localization. Therefore, abolishment of this binding can no longer locally exclude Rga4 thus no ectopic growth can occur.

Since I hypothesize that Tea4 induces ectopic growth by locally excluding or significantly reducing Rga4 level, I tried to measure the cortical distribution of Rga4-GFP in *Rga4<sup>PxxP</sup>* and *tea4Δ* mutants and compared them to wild type cells (Fig. 4.11C). Rga4-GFP levels are higher at the non-growing cell end when either *tea4* is deleted or Tea4 SH3 domain is mutated compared to wild type cells (Fig. 4.11C). Visualizing the localization of Rga4<sup>PxxP</sup> tagged with GFP, it seems that there is a more spread and less patchy cortical distribution compared to wild type Rga4. However, when I measured Rga4<sup>PxxP</sup>-GFP cortical levels, it seems to share similar cortical fluorescent intensity patterns with wild type cells (Fig. 4.11C). To better understand whether Rga4 PxxP motifs might play an important role for binding Tea4, I performed co-immunoprecipitation experiments between Tea4 and *rga4<sup>PxxP</sup>* mutant. Unfortunately, due to limited time, I performed only once the co-immunoprecipitation experiment. This co-IP showed that Tea4 still binds *rga4<sup>PxxP</sup>* mutant (Fig. 4.11A) suggesting that might be other and/or additional Rga4 binding sites. However, in this co-IP, it seems that Rga4<sup>PxxP</sup> levels are lower than wild type Rga4 thus it could be possible that low levels of Rga4<sup>PxxP</sup> behave similar to *rga4* null mutant explaining why ectopic growth is reduced in Cdr2-mcherry-Tea4N *rga4<sup>PxxP</sup>* cells. It still remains unclear the role of the Rga4 PxxP motifs.

Although my current analysis probably suggests that  $Rga4^{PxxP}$  is an *rga4* hypomorph allele, a more detailed quantitative analysis of the cortical  $Rga4^{PxxP}$  levels and repeat of co-IP experiments could clarify the exact role of these motifs. In addition, investigating the localization of  $Rga4^{PxxP}$  in different Tea4 mutant backgrounds such as *tea4<sup>RVxF</sup>* and *tea4<sup>SH3</sup>* could elucidate the Tea4-dependency of Rga4 localization.

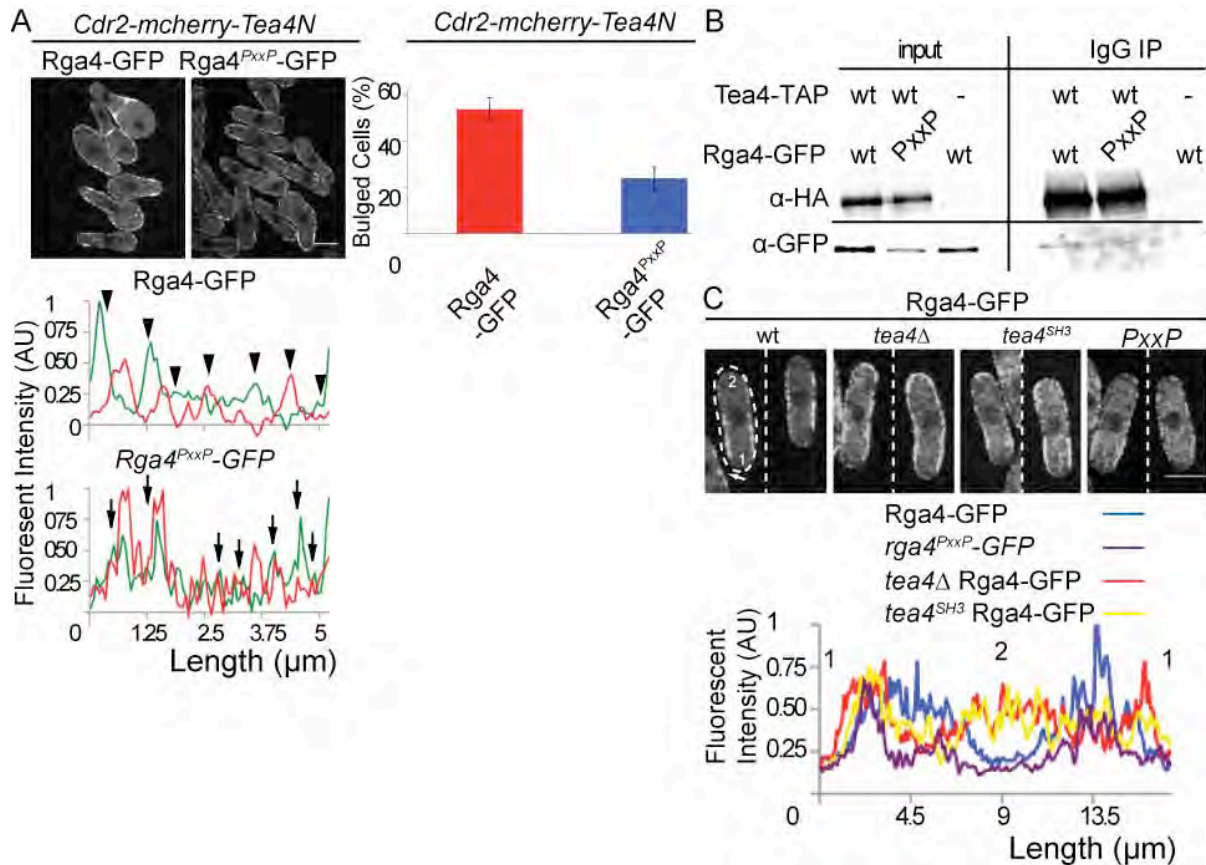


**Figure 4.11. Rga4 cortical distribution.** (A) Significant reduction in bulge formation in *Cdr2-Tea4N* cells in *rga4<sup>PxxP</sup>* background. According to the graph *Rga4<sup>PxxP</sup>-GFP* localization seems to correlate with *Cdr2-mcherry-Tea4N* localization (arrows) suggesting that Tea4 may no longer locally exclude Rga4 when the PxxP domains are mutated (n=6 cells, one shown). In contrary, *Rga4-GFP* localization seems to anti-correlate with *Cdr2-mcherry-Tea4N* localization (arrowheads), as also shown in Fig. 4.6. Graphs were performed for at least 6 individual cells but only one is shown. Scale bar 5μm. (B) Tea4 co-immunoprecipitates with Rga4 even when Rga4 PxxP domains are mutated (co-IP is performed only once). *Rga4<sup>PxxP</sup>* seems to be expressed at lower levels in this particular experiment (C) Graphs represent cortical *Rga4-GFP* intensity in different backgrounds. Measurements started at the cell tip with the less *Rga4-GFP* (arrow, 1-2-1, dashed circular white line). Wild type *Rga4-GFP* (blue line) is normally localized at the cell sides of the cell excluded from the tips (low peak in positions 1 and 2). When *tea4* is deleted *Rga4-GFP* forms a sock-like localization at on one cell tip (high peak in position 2), similar to *tea4<sup>SH3</sup>* (red and yellow line, respectively). *Rga4<sup>PxxP</sup>-GFP* seems not to have a different localization pattern compared to wild type *Rga4-GFP* cells (purple and blue line, respectively). Each graph represents an average of at least five independent measurements. Scale bar 5μm.

#### 4.2.7. Ectopically targeted Dis2 initiates growth in almost all cells and may negatively regulate Rga4 localization

I am currently proposing that Dis2 delocalizes laterally Rga4 and that results in local growth. To support this thought I targeted Dis2 ectopically following the same strategy as mentioned in Fig. 4.1A. I genetically engineered Cdr2-Dis2 fusion in *tea4* $\Delta$  cell background and cells were grown for approximately 20 hours in the presence of thiamine and then thiamine was washed away and the cells continued to grow for 28-32 hours. Excitingly ectopically targeted Dis2 promotes ectopic growth in almost all cells (90+/-4%) (Fig. 4.12A).

I have previously proposed that low Rga4 levels may allow ectopic growth. Thus I checked the localization pattern of Rga4 in the Cdr2-Dis2 fusion. Rga4 seems to be excluded at the cell sides, similar to the Cdr2-Tea4N fusion cells, supporting that Dis2 may directly negatively regulate Rga4 (Fig. 4.12B). After deleting *rga4*, cells did not exhibit bulges anymore (Fig. 4.12A) supporting the previous results of Rga4 importance of restricting and concentrating active Cdc42 for ectopic growth initiation. I will talk in more details about ideas how a GAP protein could be essential for growth in the discussion section. I also tested whether deleting *pom1* could play a role in growth process and Cdr2-GFP-Dis2 *pom1* $\Delta$  cells exhibited a small decrease in the number of cells exhibiting ectopic growth (Fig. 4.12A). In conclusion, it seems that Pom1 plays a minor role for ectopic growth. Rga4 is dispersed or excluded at ectopic growth sites but still is essential for bulge formation.

Pom1 binds the membrane when hypophosphorylated and Tea4 is responsible for localizing Dis2 to cell tips to promote local Pom1 dephosphorylation and therefore membrane binding (Hachet et al., 2011). In this process, Tea4 also binds directly to Pom1 through SH3-PxxP interaction motifs. The Cdr2-Dis2 fusion mimics the Tea4 mediator role by transporting Dis2 to the cell sides. Consequently Pom1 possibly binds to the cortex all around the cell due to Dis2-dependent dephosphorylation (Fig. 4.12C). The Dis2-dependent cortical localization of Pom1 shows that Dis2 remains functional in this fusion, and suggests that Tea4 is not essential for Pom1 dephosphorylation but serves as a Dis2 transporter, since in *tea4* $\Delta$  cells expressing Cdr2-Dis2 fusion Pom1 is successfully recruited at the cortex. Sequence alignment of Dis2 with identified orthologs in other fungal species, combined with the knowledge that histidine residue could be responsible for PP1 phosphatase activity (Kim et al., 1993), predicted that the 247 Histidine (H) residue of Dis2 may play that role. Indeed, Dis2 with mutated 247H to Lysine (K) abolishes its dephosphorylation activity since Pom1 becomes cytosolic in *Cdr2-GFP-dis2H247K* mutant cells (Fig. 4.12C). Although there is still a small amount of Pom1 anchored to the cell membrane. Moreover *Cdr2-GFP-dis2H247K* cells have no longer Dis2-dependent local Rga4 exclusion and bulge formation (Fig. 4.12A and B).

Ectopic Dis2 seems to affect Rga4 localization thus I checked the phenotype of cells expressing from plasmid the Rga4 465-685 fragment. The Rga4 465-685 is still cortical but interestingly is enhanced at the cell tips indicating that ectopic Dis2 can still affect Rga4 localization (Fig. 4.12D), similar to Cdr2-Tea4N cells (Fig. 4.10B). In addition, expressing Rga4 465-685 in Cdr2-Dis2 cells abolishes bulge formation (Fig. 4.12D) suggesting that this fragment has a dominant-negative effect.

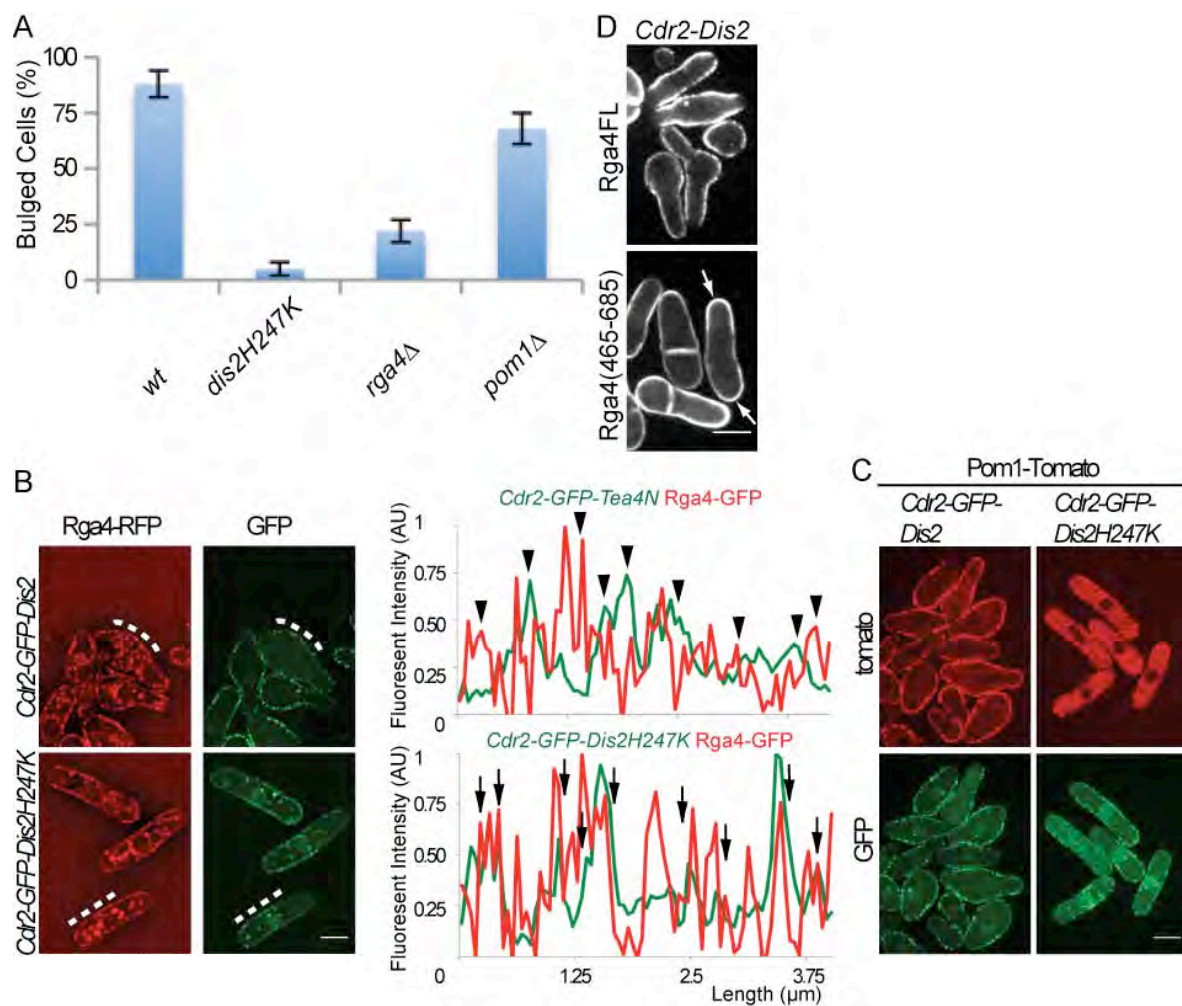


**Figure 4.12. Ectopically targeted Dis2 initiates growth in almost all cells and may negatively regulate Rga4 localization.** (A) 90% cells of cells expressing Cdr2-Dis2 fusion exhibit ectopic growth and this ectopic growth depends on the activity of Dis2, Rga4 and to a small extent on Pom1. (B) According to the graph Rga4-RFP localization seems to anti-correlate with Cdr2-GFP-Dis2 localization (arrowheads) suggesting that Dis2 may locally exclude Rga4. Rga4-RFP localization seems to correlate with Cdr2-GFP-Dis2H247K localization (arrows) in cells in which Dis2 is inactive. White dashed lines show the cortical RFP and GFP intensities measured in the graphs. Graphs showing anti-correlation were performed for at least 6 individual cells but only one is shown. Scale bar 5µm. (C) Ectopically targeted Dis2 results in Pom1 cortical localization. In *cdr2-dis2H247K* cells, Pom1 becomes cytosolic, although there is still a small amount of cortical Pom1. Scale bar 5µm. (C) Expressing from plasmid Rga4 465-685 fragment in Cdr2-Dis2 cells enhances Rga4 at cell tips (arrows) and diminishes ectopic growth to almost all cells. Scale bar 5µm.

#### 4.2.8. Re-targeted cortical Rga4 inhibits ectopic growth

The idea that growth occurs when Rga4 is locally excluded motivated me to check whether re-targeted Rga4 at the medial cortex in Cdr2-Tea4N fusion would inhibit ectopic growth. To achieve this experiment I used a strain generated in the laboratory of Paul Nurse. Cytosolic Rga4 (cytoRga4 622-760aa deleted) is fused with the cortical protein Blt1 to re-target Rga4 to the cell cortex and this chimera successfully anchors Rga4 to the cortex (Kelly and Nurse, 2011a). I would like to point out that Blt1 co-localizes with Cdr2 and its localization is Cdr2-dependent (Moseley et al., 2009). Thus Rga4-Blt1 is likely to localize at the same sites as Cdr2-Tea4N therefore forcing a Tea4-Rga4 co-localization. In agreement with my hypothesis, expressing Blt1-cytoRga4 in Cdr2-Tea4N cells resulted in abolishment of bulges (Fig. 4.13B) since Tea4N cannot any longer locally exclude Rga4 even in presence of endogenous Rga4 (Fig. 4.13A). These data emphasize the fact that continuous Rga4 localization at the cell sides inhibits growth. When *rga4* is deleted, both cytoRga4 and Blt1-cytoRga4 cells also do not exhibit bulges (Fig. 4.13B).

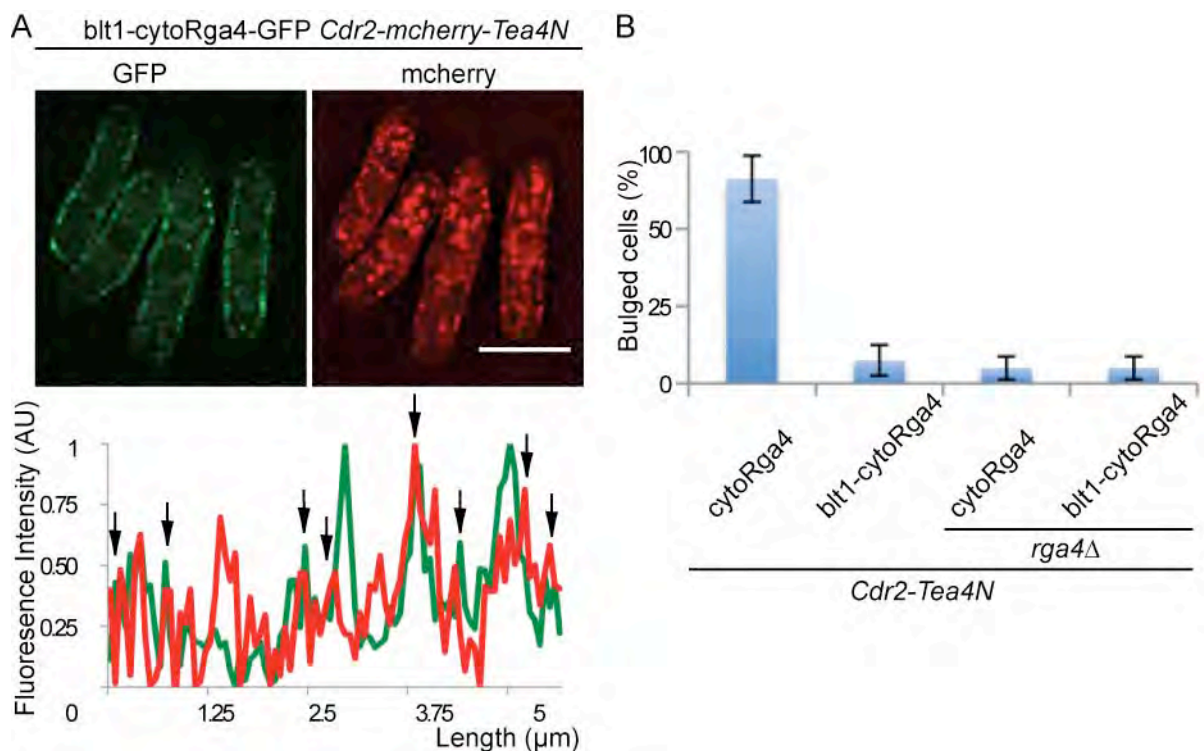


**Figure 4.13. Re-targeted cortical Rga4 inhibits growth.** (A) Cytosolic Rga4 (cytoRga4) fused with cortical protein Blt1 re-targets Rga4 to the cell sides in Cdr2-Tea4N cells and inhibits bulge formation. According to the graph and in agreement with published data (Kelly and Nurse, 2011a), Blt1-cytoRga4-GFP localization seems to correlate with Cdr2-mcherry-Tea4N (arrows). Scale bar 5μm. (B) Almost all cells exhibit no ectopic growth when Blt1-cytoRga4 is expressed. Both cytoRga4 and Blt1-cytoRga4 cells also do not support bulge formation in *rga4*Δ background.

### 4.3. Conclusions and discussion

In this study, I tried to dissect the molecular mechanism by which Tea4 promotes polarized growth. To achieve that I ectopically targeted Tea4 and excitingly ectopic Tea4 initiates growth. Physiologically, Tea4 is transported by microtubules to cell tips and it plays important role for cell shape maintenance and bipolar growth (Martin et al., 2005). I hypothesize that Tea4 mediates the negative regulation of Rga4 localization through Type I Phosphatase Dis2 (Fig. 4.14). Dis2 may cause the local removal, the significant reduction and/or inhibition of Rga4 GAP protein levels, which in turn allows the accumulation of active GTPase Cdc42. Then this active GTPase initiates growth. Rga4 binds to Cdc42 and inactivates it. Activation of Cdc42 is re-established when it binds a GEF protein that catalyzes the release of GDP. GTP cellular levels are higher than GDP suggesting that when Cdc42 is inactive there is enough GTP to bind and go back to its active state (Perez and Rincon, 2010). This constant switch of Cdc42 active and inactive stage plays an important role for cell polarity regulation indicating that specific levels of active Cdc42 may be necessary for growth. Thus, ectopic growth in Cdr2-Tea4N/Dis2 cells could be explained by this mechanism of ectopic active Cdc42 increased levels due to limited amounts of Rga4 to inhibit Cdc42 activation at cell sides.

My results propose that negative regulation of Rga4 by Tea4 is likely mediated by Dis2-dependent dephosphorylation. To show local exclusion of Rga4 by Tea4, I measured the cortical levels of both proteins and then I compared them to see whether their localization anti-correlates. Although these anti-correlation graphs exhibit Rga4 and Tea4 peaks that anti-correlate, unfortunately I did not perform a statistical approach to show whether this anti-correlation is significant. An analytical study of more cells (I tested only 8 cells) could give the evidence that this anti-correlation is indeed significant. An additional difficulty to show local exclusion of Rga4 by Tea4 is the fact that in *tea4Δ* background Cdr2 and Rga4 localize at different regions of the cortex. Rga4 mostly accumulates at the cell sides near the growing end and Cdr2 mostly accumulates at the cell sides near the growing end making an anti-correlation study difficult to achieve. In addition, Pom1 negatively regulates Cdr2 localization, thus Cdr2-Tea4N fusion probably affects its own localization through recruitment of Pom1 and resulting cell side localization of the fusion may not be as tight as that of Cdr2 alone. A new experimental approach where Tea4 localizes at the cell sides independent of Cdr2, where Rga4 is present, could further support the hypothesis that Rga4 is locally excluded by Tea4-Dis2 mediated dephosphorylation. A possible fusion of the spindle pole body component Ppc89 with Tea4 (see Fig.1E in Chapter 3) in *tea4Δ* background could target Tea4 at the cell sides where Rga4 is exactly present. Then, Tea4 could lead to Rga4 local

exclusion. Although my research suggests that Tea4 may link microtubules for the regulation of Cdc42 activity, further analysis is needed to be done to better establish my hypothesis.

An interesting finding is that *rga4* deletion diminishes ectopic growth meaning that Rga4 may be essential for restricting active Cdc42 to generate growth. When *rga4* is deleted the cells are wider showing a more spread distribution of active Cdc42. Cdc42 can still be activated at the cell tip but that activation is not as well focused and as a consequence growth may occur over a wider area, resulting in a wider cell. This hypothesis is also supported by the fact that when *scd1* or *scd2* is deleted Rga4 becomes the major determinant of cell width, as shown by the additive effects of *rga4Δ scd1Δ* and *rga4Δ scd2Δ* cells (Kelly and Nurse, 2011b). Therefore, an additional role of Rga4 seems to be the formation of a boundary preventing the spread of activated Cdc42 away from the cell tip leading to proper polarized growth. In agreement with that, one hypothesis is that Tea4 serves to locally exclude Rga4, but that surrounding Rga4 is necessary to define the boundaries of active Cdc42. In budding yeast, only Rga1 has been shown to locally exclude active Cdc42 resulting in inhibition of polarization by exclusion of polarity factors at this site (Tong et al., 2007). In fission yeast, we could imagine that Rga4 plays a similar role like Rga1. Rga4 is inhibiting Cdc42 to be active but in addition is also necessary to restrict it in a specific site where active Cdc42 could initiate growth through positive feedback loops, similar to budding yeast. Cdc42 could ectopically polarize the formin For3 and in turn actin cables could concentrate more active Cdc42 ectopically triggering growth. In addition, factors of the polarisome and the exocyst could accumulate at this site resulting in proper growth similar to the cell tip. However, just Cdc42 presence is not sufficient to initiate growth since localization of Cdc42 at both tips in *pom1Δ rga4Δ* double mutant cells does not result in bipolar growth (Tatebe et al., 2008). Specifically, actin presence is a key factor for growth per se since the formation of a Tea1-For3 complex at the new cell end is sufficient to initiate bipolar growth in *tea4Δ* monopolar cells (Martin et al., 2005). Under physiological conditions Tea4 is proposed to link Tea1 with For3 at the new cell end for NETO establishment (Martin and Chang, 2005; Martin et al., 2005) supporting the role of actin presence for growth to occur. These data suggest that active Cdc42 at both ends is not sufficient to initiate bipolar growth if there is not also bipolar distribution of actin. All these suggest that first ectopic Tea4 provides the initial cue where growth will occur. Second, a possible Tea4-mediated Rga4 local exclusion allows local activation of Cdc42 and subsequent actin presence. Third, feedback loops between Cdc42 and actin could establish and maintain ectopic growth, similar to budding yeast.

It has been shown that Tea4 and Pom1 are required for the exclusion of the Rga4 from the cell tip and in *tea4Δ* and *pom1Δ* monopolar mutants Rga4 localize at the non-growing end

(Tatebe et al., 2008). However, it is suggested that Rga4 may not be a direct substrate of Pom1 and Rga4 also appears hyperphosphorylated when *pom1* is deleted (Tatebe et al., 2008). Dis2 might be the sole direct regulator of Rga4 cortical anchoring. Since Dis2 is a Type 1 protein phosphatase and PP1 are phosphoproteins, which their regulation depends on the phosphorylation status of their serine and threonine residues (Ingebritsen and Cohen, 1983), Pom1 could phosphorylate Dis2 to activate it. In turn, Dis2 dephosphorylates Pom1 for its membrane association (Hachet et al., 2011). Dis2 and Pom1 could share positive feedback loops to regulate Pom1 localization and Dis2 activity, respectively. In *pom1Δ* cells Dis2 may have decreased activity and can no longer exclude Rga4 from the cell tip. Furthermore, in *tea4Δ* cells, there is no Dis2 at the cell tip for Rga4 exclusion. However, in *pom1Δ* cells ectopic growth still occurs suggesting that Pom1 may not be the sole kinase to phosphorylate and activate Dis2. Interestingly, in *pom1-6A tea4<sup>SH3</sup>* double mutant, active Pom1 is cortical but cells still grow in a monopolar manner suggesting that cortical Pom1 is not able to bypass the Tea4 necessity and Rga4 is present at the cell tip. This hypothesis proposes that Rga4 localization may depend on active Dis2 since in the double mutant *pom1-6A tea4<sup>SH3</sup>*, Dis2 is more likely absent from the cell tips due to mutated Tea4 SH3 domain, thus Dis2 can no longer exclude Rga4. However, in cells expressing Cdr2-Tea4N, ectopic growth is only inhibited to some extent when *pom1* is deleted proposing that not only Pom1 but also other kinases unknown till now could possibly phosphorylate and activate Dis2.

My results imply that Dis2 may exclude or significantly reduce the Rga4 levels suggesting that Rga4 phosphorylation-dephosphorylation levels have to be specifically regulated for tip exclusion. Rga4 is highly phosphorylated and has 21 potential CDK phosphorylation sites (Tatebe et al., 2008) so it can not be excluded the possibility that cyclin-dependent kinases could also play a role for Rga4 phosphorylation status as suggested for Cdc42 GAPs in budding yeast (Knaus et al., 2007; Sopko et al., 2007). A fluctuation of Rga4 phosphorylated levels could alter its localization depending on CDKs, Pom1 and Dis2. These observations indicate that (de)-phosphorylation events likely play a major role for Rga4 localization. Further identification of Rga4 phosphorylated residues seems important for understanding Rga4 localization pattern. In conclusion, I hypothesize that negative regulation of Rga4 by Tea4 is likely mediated by Dis2-dependent dephosphorylation. Hence, Tea4 may link microtubules for the regulation of Cdc42 activity resulting to bipolar growth in fission yeast cells.

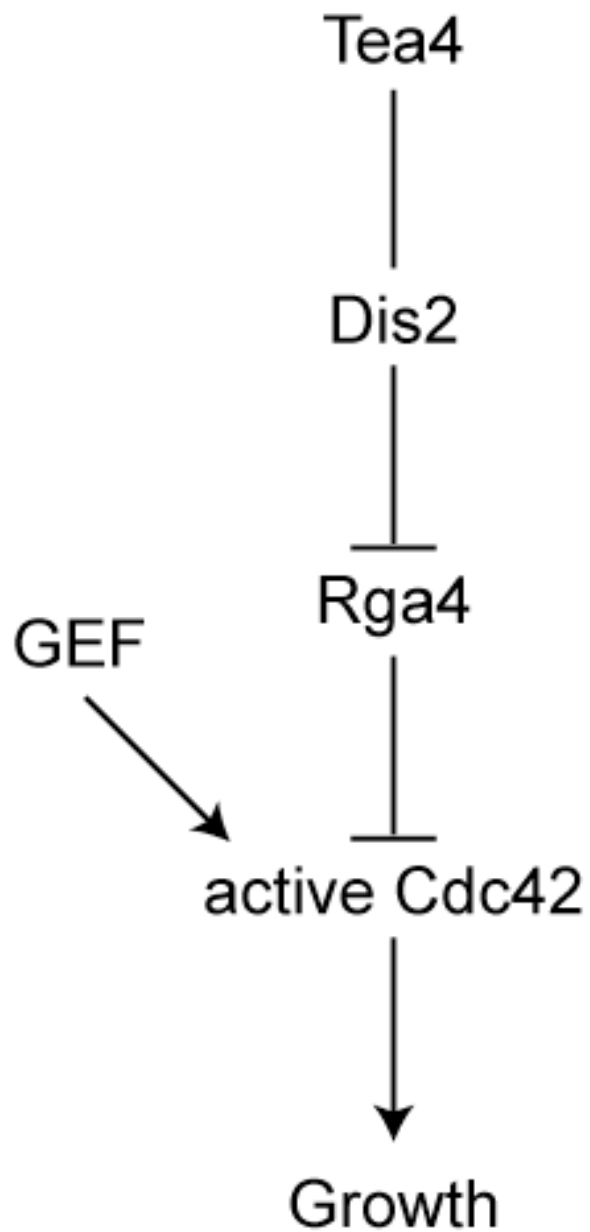


**Figure 4.14. New mechanisms of cell polarity control.** Minimal factors for polarized growth regulation. Tea4 negatively regulates Rga4 through Dis2. Tea4 is the Dis2 transporter and Dis2 may locally exclude Rga4 allowing local Cdc42 activation by GEF and consequently growth.

# General conclusions and discussion

## Tea4 functions

Tea4 has been first suggested to regulate cell polarity by initiating a second zone of growth through reorganization of the actin cytoskeleton (Martin et al, 2005). Tea4 was proposed to bind the formin For3, which is an actin nucleator responsible for the polarized assembly of actin cables. These data showed that Tea4 is a possible direct molecular link between microtubule plus ends and actin assembly. Second, It has been shown that Tea4 bridges Pom1 with Dis2 to promote Pom1 dephosphorylation at cell tips resulting in Pom1 binding to the cell membrane, then followed by Pom1 lateral diffusion and autophosphorylation leading to Pom1 membrane detachment (Hachet et al., 2011). This study showed how Tea4 mediates the Pom1 gradient formation, which regulates cell size homeostasis. During my study I showed that Pom1 might not be the sole target of Tea4-Dis2 dependent dephosphorylation. I demonstrated that in addition of Tea4 role for NETO establishment and regulation of Pom1 localization, Tea4 might also control Cdc42 activation by negatively regulating Rga4 localization through Dis2-dependent dephosphorylation. These evidence emphasize the role of Tea4 to link microtubules with actin by acting on different targets. To sum up, Tea4 seems to have multiple important roles, which altogether results in cell polarity establishment and shape maintenance of fission yeast cells.

## Mass spectrometry results

Mass spectrometry results not only identified Rga4 and Dis2 as Tea4 partners, which I investigated thoroughly during my research showing their importance for polarized growth, but also other proteins that could potentially play an important role for cell polarization. The pseudokinase Ppk2 was found to associate with Tea4 even when the Tea4 SH3 was mutated. I showed that Ppk2 plays an important role for bipolar growth but I did not further test its role in cell polarity regulation. Ppk2 could play a significant role for cell polarity control and it would be intriguing to be further studied. Pseudokinases have most probably evolved from active kinases and they lack conserved residues responsible for kinase activity (Manning et al., 2002). A recent review in pseudokinases suggests that these proteins may act either as scaffold proteins, regulators or partially active kinases and they are involved in fundamental processes such as cell proliferation and differentiation (Zhang et al., 2012). Much remains to be learnt about the function of pseudokinases and It would be important to identify Ppk2 binding partners since it is suggested that a key role of these proteins is their

participation in protein complexes (Zhang et al., 2012). Ppk2 could potentially have a dominant negative role by binding to polarity proteins and prevent their phosphorylation by protein kinases. It would be fascinating to introduce mutations in Ppk2 that restore its catalytic activity and observe this phenotype. It would also be interesting to perform a Ppk2 sequence analysis and to determine whether Ppk2 evolved from any known kinases. In addition to Ppk2 investigation, future studies with Tea4-associated proteins identified in the mass spectrometry (see mass spectrometry results section in materials and methods) such as the molecular chaperone T-complex, the proteasome and the Sjogren syndrome protein could unravel key aspects of cell polarity and morphogenesis.

## Tea4 beyond fission yeast

*S. cerevisiae* and *S. pombe* are the unicellular fungi that are considered to be the ideal organisms to study polarized growth. However, phylogenetic studies have suggested that these two species are separated by about one billion years and in addition, fission yeast has been highly diverged in gene homology not only from budding yeast but also from other ascomycetes and filamentous fungi (Hedges, 2002; Wood et al., 2002). Interestingly, Tea4 is homologous to *S. cerevisiae* Bud14, which is required for polarized bud growth (Ni and Snyder, 2001) and specifically Bud14 seems to regulate microtubule dynamics at the cortex by increasing the dynein activity (Knaus et al., 2005). Tea4 seems to share similar properties with its budding yeast homologue. Bud14 localizes to sites of polarized cell growth and it also has an RVxF motif and an SH3 domain that both contribute to efficient binding with Type-1 protein phosphatase Glc7 (Knaus et al., 2005), similar to Tea4 binding with Dis2. However, Bud14 cortical localization is actin-dependent in contrast to Tea4 microtubule-dependent localization supporting the distinct role of microtubules in polarized growth in fission yeast. Future studies of whether the function of Tea4 and Bud14 has been conserved through evolution could be of major importance. Expressing Bud14 in a *tea4Δ* fission yeast mutant and checking whether the phenotypic defects would be rescued could be of major interest. Complete or partial rescue of the *tea4Δ* phenotype would indicate that the function supported by the SH3 domain has been conserved. In addition, a chimeric molecule could be constructed in which the SH3 domain of Bud14 replaces the Tea4 SH3 domain and assay the properties of this chimera in *S. pombe*. Even though fission yeast and budding yeast are highly divergent organisms, both organisms may share similar mechanisms to control cell polarity. The above comparative analysis of Tea4 with its closest homologue in budding yeast could indicate that Tea4 functions may be conserved in higher eukaryotes contributing to build a conserved model of cell polarity regulation.

## Feedback loops

In fission yeast, it is demonstrated that cytoskeleton controls cell polarity and cell shape and that cell shape also controls the organization of the cytoskeleton in a feedback loop (Minc et al., 2009; Terenna et al., 2008). Rga4 also seems to restrict active Cdc42 at the cell tips where through positive feedback loops similar to budding yeast, it could initiate growth. Cdc42 may polarize actin and in turn actin cables concentrate more active Cdc42 triggering growth. In addition, factors of the polarisome accumulate at this site resulting in proper tip growth. We could think that the landmark component Cdc42 maintains and is maintained inside this loop and when correct localization of the landmark is disturbed then fission yeast admits additional growth patterns such as T-shape cells. My results show that ectopically recruited Tea4 initiates growth in the middle of the cell. My current work supports that *S. pombe* morphogenesis is governed by feedback loops between the cell shape and cytoskeleton. Ectopic Tea4 provides the initial cue where growth will occur by defining where active Cdc42 will be present. This artificial system shows an intracellular association between cytoskeletal elements and morphogenesis and points out the importance of feedback loops to establish and maintain growth.

## Rho GAPs importance

There are Rho GAPs in multicellular eukaryotes that share parallel roles with fission yeast Rga4. In *Caenorhabditis elegans*, the GAP protein CHIN-1 is required for Cdc42 cortical polarization at the one-cell stage (Kumfer et al., 2010). In addition at the eight-cell *C. elegans* embryo, the GAP PAC-1 is necessary to restrict active Cdc42 for polarized growth (Anderson et al., 2008) similar to my hypothesis of Rga4 role to restrict active Cdc42 to initiate ectopic growth in fission yeast. These parallels with metazoan systems show the importance of GAPs to control the localization of active Cdc42 and therefore growth. In fission yeast, there are eight putative Rho GAPs in *S. pombe*, Rga1-Rga8 (Nakano et al., 2001) but only Rga4 has been shown to be a GAP for Cdc42 (Das et al., 2007; Tatebe et al., 2008). The exact function of the other Rho GAPs is not studied extensively. It would be interesting to further investigate the role of the other GAPs and try to identify whether Rga4 associates with one or more of them for Cdc42 negative regulation. In addition, the role of Tea4 for the regulation of these Rho GAPs could build a more solid model explaining how microtubules and Cdc42 “communicate” to establish growth.

## **The role of phospholipids in polarized growth**

My results suggest that there are additional mechanisms such as endocytosis that play a role in transport and anchoring of cell polarity proteins linking growth with polarity factors presence. But it still remains unclear how exactly that happens. In eukaryotic cells, phospholipids are important mediators of many cellular events including polarized growth even in the absence of linear cytoskeletal elements (Bendezu and Martin, 2011; Harkins et al., 2010; Jenkins and Frohman, 2005). In fission yeast little is known regarding the role of phospholipids for cell polarity regulation, Exocyst components Sec6 and Sec8 localize to cell tips in a phospholipid phosphatidylinositol 4,5-bisphosphate (PIP2)-dependent manner (Bendezu and Martin, 2011). It is also proposed that Sec3 and Exo70 tether the exocyst complex and the vesicle by binding PIP2 at the cell poles (Bendezu et al., 2012). Changing fission yeast membrane's electrostatic status or composition could affect its affinity to bind polarity proteins leading to their cell tip dissociation. Non-functional Tea4 could result in change either of phospholipid composition or phospholipid electrostatic charge and kinase Pom1 and phosphatase Dis2 could possibly regulate membrane composition and charge by targeting phospholipid regulators. In agreement with that, the composition of phospholipids seems to directly modulate Cdc42 association with the membrane in budding yeast (Das et al., 2012a). Monopolar pre-NETO cells might require increased amounts of lipids to bind polarity proteins leading to their cell tip association and eventually growth in the non-growing end. Taking into account that the total concentration of lipids within the cell decreases drastically by 50% directly after cell division (Huang et al., 2012) could give an alternative explanation why pre-NETO fission yeast cells are monopolar. Re-establishing the phospholipid amount and composition of the membrane at the non-growing end of pre-NETO cells could lead to localization of the necessary proteins to initiate bipolar growth. However, the exact role of phospholipids for polarized growth is as yet unknown.

## **Linking MTs with Cdc42 activation**

In rod-shaped fission yeast cells, microtubules align along the growth axis with well-defined tip growth. MTs transport Tea4 to cell tips and are necessary for maintaining cell shape and for initiation of a second site of growth during NETO (Martin et al., 2005). Cdc42 positively regulates the formin For3 to form actin cables and the exocyst complex to promote exocytosis at cell tips (Bendezu and Martin, 2011). Although our understanding of polarized growth is expanded, it is not clear yet how microtubule machinery and specifically Tea4 regulates the growth elements and in particular active Cdc42. My data show that growth is based on specific cytoskeletal arrangements and landmark proteins. Actin and microtubules

cooperate to establish growth. Tea4 may regulate Cdc42 activation by negative regulation of Rga4 in a Dis2-dependent manner. Even if there is diversity in different cell types my research indicates that the growth process can be simplified to achieve the same result. In conclusion, my research may reveal robustness for cell polarization and morphogenesis by bridging a molecular pathway between microtubule-associated factor Tea4 and Cdc42.



# Materials and methods

## Yeast strains and genetic manipulations

I used standard methods for fission yeast media and genetic manipulations. Tagged and deletion strains were constructed by using a PCR-based approach (Bahler et al., 1998).

To integrate Tea4<sup>RVxF</sup>, the Tea4<sup>RVxF</sup> fragment was released from pSM832 after digestion with SalI. Transformed into YSM328 and selected on 5FOA plate and then sequenced.

To tag Tea4<sup>SH3</sup> with HA, I amplified with WACH PCR the HA cassette from pSM686 using osm315 and osm316. Transformed into YSM751 and selected on G418 plate. Sequenced.

To tag Ppk2 with GFP, I amplified with WACH PCR the GFP cassette from pSM675 with osm902 and osm903. Transformed into YSM1182 and selected on G418 plate. Sequenced.

To tag Tea4<sup>RVxF</sup> with GFP, I amplified with WACH PCR the GFP cassette from pSM675 with osm315 and osm316. Transformed into YSM1182 and selected on G418 plate. Sequenced.

To tag Tea4<sup>RVxF</sup> with HA, I amplified with WACH PCR the HA cassette from pSM686 with osm315 and osm316. Transformed into YSM1183 and selected on G418 plate. Sequenced.

To generate the strain *ura4-294::nmt81:cdr2-GFP-tea4N<sup>RVxF</sup>-ura4+*, linearized plasmid pSM919 with Stul was transformed into YSM486 and selected in EMM-AL plate. Stable insertion selected by checking growth of single colonies on EMM-ALT after growth on YE plate.

To generate the strain *ura4-294::nmt81:cdr2-GFP-tea4N<sup>SH3</sup>-ura4+*, linearized plasmid pSM920 with Stul was transformed into YSM486 and selected in EMM-AL plate. Stable insertion selected by checking growth of single colonies on EMM-ALT after growth on YE plate.

To generate the strain *ura4-294::nmt81:cdr2-mcherry-Tea4N-ura4+*, linearized plasmid pSM1024 with AvrII was transformed into YSM486 and selected in EMM-AL plate. Stable insertion selected by checking growth of single colonies on EMM-ALT after growth on YE plate.

To generate the strain *ura4-294::nmt81:cdr2-mcherry-ura4+*, linearized plasmid pSM1023 with AvrII was transformed into YSM486 and selected in EMM-AL plate. Stable insertion selected by checking growth of single colonies on EMM-ALT after growth on YE plate.

To generate the strain *ura4-294::nmt81:cdr2-CFP-tea4N-ura4+*, linearized plasmid pSM927 with *StuI* was transformed into YSM486 and selected in EMM-AL plate. Stable insertion selected by checking growth of single colonies on EMM-ALT after growth on YE plate.

To generate the strain *ura4-294::nmt81:cdr2-CFP-ura4+*, linearized plasmid pSM926 with *StuI* was transformed into YSM486 and selected in EMM-AL plate. Stable insertion selected by checking growth of single colonies on EMM-ALT after growth on YE plate.

To generate the strain *ura4-294::nmt81:cdr2-GFP-Dis2-ura4+*, linearized plasmid pSM1025 with *StuI* was transformed into YSM486 and selected in EMM-AL plate. Stable insertion selected by checking growth of single colonies on EMM-ALT after growth on YE plate.

To generate the strain *ura4-294::nmt81:cdr2-mcherry-Dis2-ura4+*, linearized plasmid pSM1093 with *StuI* was transformed into YSM486 and selected in EMM-AL plate. Stable insertion selected by checking growth of single colonies on EMM-ALT after growth on YE plate.

To generate the strain *ura4-294::nmt81:cdr2-mcherry-Dis2<sup>H247K</sup>-ura4+*, linearized plasmid pSM1130 with *StuI* was transformed into YSM486 and selected in EMM-AL plate. Stable insertion selected by checking growth of single colonies on EMM-ALT after growth on YE plate.

To generate the strain *leu1-32::shk1 promoter:ScGIC2 CRIB:GFP3:leu1+*, linearized plasmid pSM1129 with *NruI* was transformed into YSM1180 and selected in EMM-AU plate. Stable insertion selected by checking growth of single colonies on EMM-AUT after growth on YE plate.

The Rga4 different fragments were expressed in pSM621 and transformed into YSM1183, YSM1406, KK214 and KK363 and selected in EMM-AU plate.

To generate the mutations of the predicted phosphorylated residues of Tea4 I used the site-directed mutagenesis kit protocol (Stratagene). pSM361 or pSM758 were used as template and amplified with either *osm880* and *osm881* or *osm882* and *osm883* or *osm884* and *osm885*. Then Tea4 or Tea4<sup>WW155-156AA</sup> with mutated phosphorylated residues (pSM839-pSM844) were digested with *Sall* and *BglII* and transformed into YSM328 and selected on 5FOA plate (*ura4*<sup>-</sup>). Sequenced.

I used the following cloning strategy to get Rga4<sup>PxxP</sup>: PxxP mutated fragment ordered from Eurofins with following sequence (SacII site mutated) pEX-A-rga4-PxxP (pSM1109):

GCATGCgaaGcagtttctcaaggcaaagctcagtagtaataataatagcgtgcagcaacctgttgcttatcacgccttggc  
aatcaccaaccgaaaatggtacgcttGctcaacttGctaaaaatgaaagcgttgtaatcctcctccacttcgccgctcttactat  
gaattacaaatctgtttcgacaacaacatcacctctaaatggaatgtgtctggcagaatagctctatctctatccatttaagg  
gtgctcttctgtgatgtcacaataaatgtaattaaaggttctagaaatcgaaacagtttatctaatcttgacgaatattacgtaacg  
gattgaaagcgacgaaactcctacaaaggctagattGctagatatGctacggtattaataagttagatgacaaacgacttagt  
agcgaaccaaacggctgaagaaaagattgacgaactctcaaatatgaggctccccAcggggccaaaagtttaattgtcgc  
aagttagttgcatcaagcatgtgaacctgaatacaatcgaagtctttggttagagcaagtgatgtgttactcaaacgtattgatg  
ctacagaggaaagcgcaaatgaactcgccattcgtatttcagagcttcaagctgaggttgaacctattgttgaagcgacttcgt  
tgcttctatcatagagcagcagactGccgtgtcccTcgaG

1. Rga4 3'UTR between SacI and SacII (amplified from genomic DNA with osm1607 and osm1608) was cloned in pSM206 (pSM110). 2. In the resulting vector pSM110 it was cloned the fragment: 5'UTR amplified from genomic DNA osm1609 and osm1610 and the start of *rga4* ORF till the first PxxP, Sall-SphI (mutated PxxP sites)- BamHI sites (pSM1112). 3. In parallel to step2 the fragment from the end of *rga4* ORF from the last PxxP, SphI-XhoI (mutated PxxP sites)- BamHI (amplified from genomic DNA with osm1611 and osm1612) was cloned in pSM1109 (pSM1128). 4. Extended synthesized fragment from pSM1128 was cloned into SphI- BamHI sites of pSM1112 (pSM1206). 5. pSM1206 digested with Sall- SacII and transformed into YSM1404 and selected on G418 plate. In parallel, transformants should not grow on EMM-AL plate. Sequenced.

#### Generation of plasmids

*pSM919: pRIP82-cdr2-GFP-tea4N 222-225RVXF-RAXA*. I inserted point mutations with site directed mutagenesis (Stratagene). Primers used osm1045 and osm1046 and plasmid used pSM868. Selected in LB-amp plates. Sequenced.

*pSM920: pRIP82-cdr2-GFP-tea4N W155A-W156A*. I inserted point mutations with site directed mutagenesis (Stratagene). Primers used osm380 and osm381 and plasmid used pSM868. Selected in LB-amp plates. Sequenced.

*pSM926: pRIP82-cdr2-CFP*. CFP amplified from pSM688 with primers osm204 and osm205. Digested with BamHI-XmaI and cloned into pSM744 digested with the same enzymes. This removes the GFP and replaces it with CFP in pSM744. Sequenced with osm204 to check for CFP.

*pSM927: pRIP82-cdr2-CFP-tea4N.* Tea4N fragment from pSM866 excised with Xma1 and cloned into pSM926 also digested with Xma1 followed by CIP. PCR (osm204-osm598) verified the correct orientation of insert. Re-digestion with Xma1 releases the insert.

*pSM1023: pRIP82-cdr2-mCherry.* mCherry amplified from pSM684 with primers osm1363 and osm1364. Digested with BamHI-Xma1 and cloned into pSM926 digested with the same enzymes. This removes the CFP and replaces it with mCherry. Sequenced with osm1363-osm1364 to check for mCherry.

*pSM1024: pRIP82-cdr2-mCherry-Tea4N.* TeaN fragment from pSM868 excised with Xma1 and cloned into pSM1023 also digested with Xma1 followed by CIP. Re-digestion with Xma1 releases the insert.

*pSM1025: pRIP82-cdr2-GFP-Dis2.* Dis2 amplified from cDNA with primers osm1266 and osm1267. Digested with Xma1 and cloned into pSM868 also digested with Xma1 followed by CIP. This removes the Tea4N and replaces it with Dis2 in pSM868. Sequenced with osm1266 and osm1267 to check for Dis2.

*pSM1093: pRIP82-cdr2-mCherry-Dis2.* Dis2 fragment from pSM868 excised with Xma1 and cloned into pSM1023 also digested with Xma1 followed by CIP. Re-digestion with Xma1 releases the insert.

*pSM1129: pBluescript SK+ ScGIC2 CRIB:GFP3NMT1 terminator.* Leu1 Pombe gene amplified from gDNA with primers osm1663 and osm1664, digested with Sal1 and cloned into pSM1100 also digested with Sal1 followed by CIP. Re-digestion with Xma1 releases the insert.

*pSM1130: pRIP82-cdr2-GFP-Dis2H247K.* I inserted point mutations with site directed mutagenesis (Stratagene). Primers used osm1613 and osm1614 and plasmid used pSM1025. Selected in LB-amp plates. Sequenced.

S. pombe strains used in this study

Number	Genotype	Source
KK12	tea4WW155-156AA pom1-GFP-KanMX ade6- leu1- ura4-	This study
KK13	h- tea4WW155-156AA ade6-M216 leu1-32 ura4-D18	This study
KK15	tea4WW155-156AA tip1-GFP-kanMX ade6- leu1- ura4-	This study
KK17	tea4Δ::kanMX tip1-GFP-kanMX ade6- leu1- ura4-	This study
KK18	h+ tea4WW155-156AA HA-TEV-ProteinA ade6-M216 leu1-32 ura4-D18	This study
KK19	h+ tea4-HA-TEV-ProteinA ade6-M216 leu1-32 ura4-D18	This study
KK21	tea4WW155-156AA tea1-GFP kanR ade6- leu1- ura4-	This study
KK24	tea4WW155-156AA dis2-NEGFP-ura4+ ade6-M216 leu1-32 ura4-D18	This study
KK26	tea4WW155-156AA for3-3GFP-ura4+ ade6-M216 leu1-32 ura4-D18	This study
KK27	tea4WW155-156AA bud6-3GFP-kanMX ade6-M216 leu1-32 ura4-D18	This study
KK29	tea4WW155-156AA-GFP-kanMX mod5::kanMX ade6- leu1-32 ura4-D18	This study
KK32	h+ tea4-GFP-kanMX RFP-atb2 ade6- leu1-32 ura4-D18	This study
KK33	tea4WW155-156AA-GFP-kanMX RFP-atb2 ade6- leu1-32 ura4-D18	This study
KK40	h+ tea4WW155-156AA rga4-GFP-KanMx6 ade6-M216 leu1-32 ura4-D18	This study
KK41	ppk2::ura4+ tea4-GFP-kanMX ade6- leu1-32 ura4-D18	This study
KK44	h- tea4Δ::kanMX rga4-GFP-KanMx6 ade6-M216 leu1-32 ura4-	This study
KK48	tea4WW155-156AA ura4-294::shk1 promoter:ScGIC2 CRIB:GFP3:ura4+ ade6-M216 leu1-32	This study
KK50	h+ ppk2-GFP-KanMX ade6-M216 leu1-32 ura4-D18	This study
KK53	tea4WW155-156AA ppk2-GFP-KanMX ade6-M216 leu1-32 ura4-D18	This study
KK54	tea4Δ::kanMX ppk2-GFP-KanMX ade6-M216 leu1-32 ura4-D18	This study
KK55	tea4Δ::kanMX ura4-294::shk1 promoter:ScGIC2 CRIB:GFP3:ura4+ ade6-M216 leu1-32	This study

Number	Genotype	Source
KK57	h+ tea4WW155-156AA SSYS425-428AAAA	This study
KK107	h+ ura4-294::nmt81:cdr2-GFP-tea4N-ura4+ tea4Δ::kanMX ade6-M216 leu1-32	This study
KK109	h- ura4-294::nmt81:cdr2-GFP-tea4N-ura4+ tea4Δ::kanMX tea1::ura4+ ade6-M216 leu1-32	This study
KK114	h+ ura4-294::nmt81:cdr2-GFP-ura4+ tea4Δ::kanMX ade6- M216 leu1-32	This study
KK116	ura4-294::nmt81:cdr2-GFP-tea4N-ura4+ tea4Δ::kanMX exo70::nat ade6- leu1-32	This study
KK118	ura4-294::nmt81:cdr2-GFP-tea4N-ura4+ tea4Δ::kanMX for3::kanMX6 ade6- leu1-32	This study
KK127	ura4-294::nmt81:cdr2-GFP-ura4+ tea4Δ::kanMX for3::kanMX6 ade6- leu1-32	This study
KK133	h- tea4Δ::kanMX ura4-294::nmt81:cdr2-GFP-tea4N222- 225RVXF-RAXA-ura4+ ade6? leu1-32	This study
KK135	tea4Δ::kanMX ura4-294::nmt81:cdr2-GFP-tea4NW155A- W156A-ura4+ ade6? leu1-32	This study
KK177	h+ rga4-GFP-KanMx6 leu1-32 ura4-D18	This study
KK188	ura4-294::nmt81:cdr2-GFP-tea4N-ura4+ tea4Δ::kanMX rga4- RFP-KanMx6 gef1::kanMX ade6- leu1-32	This study
KK189	ura4-294::nmt81:cdr2-GFP-ura4+ tea4Δ::kanMX rga4-RFP- KanMx6 gef1::ura4+ ade6- leu1-32	This study
KK190	ura4-294::nmt81:cdr2-CFP-ura4+ tea4Δ::kanMX rga4Δ::ura4+ gef1-GFP-kanMX ade6- leu1-32	This study
KK191	ura4-294::nmt81:cdr2-CFP-tea4N-ura4+ tea4Δ::kanMX rga4Δ::ura4+ gef1-GFP-kanMX ade6- leu1-32	This study
KK196	tea4WW155-156AA-HA-TEV-ProteinA rga4-GFP-KanMx6 ade6- leu1-32 ura4-D18	This study
KK197	tea4-HA-TEV-ProteinA rga4-GFP-KanMx6 ade6- leu1-32 ura4-D18	This study
KK205	h+ ura4-294::nmt81:cdr2-GFP-Dis2-ura4+ tea4Δ::kanMX ade6- leu1-32	This study
KK212	h- ura4-294::nmt81:cdr2-mCherry-Tea4N-ura4+ tea4Δ::kanMX rga4-GFP-KanMx6 ade6- leu1-32	This study

Number	Genotype	Source
KK214	h+ ura4-294::nmt81:cdr2-mCherry-Tea4N-ura4+ tea4Δ::kanMX ade6- leu1-32	This study
KK215	ura4-294::nmt81:cdr2-mCherry-Tea4N-ura4+ tea4Δ::kanMX dis2-NEGFP-ura4+ ade6- leu1-32	This study
KK216	ura4-294::nmt81:cdr2-mCherry-Tea4N-ura4+ tea4Δ::kanMX pom1-GFP-kanMX ade6- leu1-32	This study
KK217	h+ ura4-294::nmt81:cdr2-mCherry-ura4+ tea4Δ::kanMX ade6- leu1-32	This study
KK219	ura4-294::nmt81:cdr2-mCherry-Tea4N-ura4+ tea4Δ::kanMX for3-3GFP-ura4+ ade6- leu1-32	This study
KK220	ura4-294::nmt81:cdr2-mCherry-ura4+ tea4Δ::kanMX tea1- GFP::kanMX ade6- leu1-	This study
KK228	tea4-HA-TEV-ProteinA pom1Δ::ura4+ rga4-GFP-KanMx6 ade6-	This study
KK232	ura4-294::nmt81:cdr2-mCherry-Tea4N-ura4+ tea4Δ::kanMX tea1-GFP::kanMX ade6- leu1-32	This study
KK234	ura4-294::nmt81:cdr2-mCherry-Tea4N-ura4+ tea4Δ::kanMX scd1-3GFP-ura4+ ade6- leu1-32	This study
KK236	ura4-294::nmt81:cdr2-mCherry-ura4+ tea4Δ::kanMX pom1- GFP-kanMX ade6- leu1-32	This study
KK239	ura4-294::nmt81:cdr2-GFP-Dis2-ura4+ tea4Δ::kanMX rga4Δ::ura4+ ade6- leu1-32	This study
KK240	h- [pREP41-Rga4-GFP (leu2+)] ade6-M216 ura4-D18 ade6- M216 ura4-D18	This study
KK242	[pREP41-Rga4(1-685)-GFP (leu2+)] ade6-M216 ura4-D18	This study
KK244	[pREP41-Rga4(1-470)-GFP (leu2+)] ade6-M216 ura4-D18	This study
KK248	[pREP41-Rga4(599-685)-GFP (leu2+)] ade6-M216 ura4-D18	This study
KK249	[pREP41-Rga4(465-685)-GFP (leu2+)] ade6-M216 ura4-D18	This study
KK252	[pREP41-Rga4(599-757)-GFP (leu2+)] ade6-M216 ura4-D18	This study
KK266	[pREP41-Rga4-GFP (leu2+)] ura4-294::nmt81:cdr2-mCherry- Tea4N-ura4+ tea4Δ::kanMX ade6-	This study
KK267	[pREP41-Rga4(1-623)-GFP (leu2+)] ura4-294::nmt81:cdr2- mCherry-Tea4N-ura4+ tea4Δ::kanMX ade6-	This study
KK268	[pREP41-Rga4(1-470)-GFP (leu2+)] ura4-294::nmt81:cdr2- mCherry-Tea4N-ura4+ tea4Δ::kanMX ade6-	This study

Number	Genotype	Source
KK270	[pREP41-Rga4(599-685)-GFP (leu2+)] ura4-294::nmt81:cdr2-mCherry-Tea4N-ura4+ tea4Δ::kanMX ade6-	This study
KK271	[pREP41-Rga4(465-685)-GFP (leu2+)] ura4-294::nmt81:cdr2-mCherry-Tea4N-ura4+ tea4Δ::kanMX ade6-	This study
KK272	[pREP41-Rga4(599-757)-GFP (leu2+)] ura4-294::nmt81:cdr2-mCherry-Tea4N-ura4+ tea4Δ::kanMX ade6-	This study
KK283	ura4-294::nmt81:cdr2-mCherry-ura4+ tea4Δ::kanMX scd1-3GFP-ura4+ ade6- leu1-32	This study
KK290	h- ura4-294::nmt81:cdr2-mCherry-ura4+ tea4Δ::kanMX gef1-3GFP-kanMX ade6- leu1-32	This study
KK291	h+ ura4-294::nmt81:cdr2-mCherry-tea4N-ura4+ tea4Δ::kanMX gef1-3GFP-kanMX ade6- leu1-32	This study
KK293	ura4-294::nmt81:cdr2-GFP-Dis2-ura4+ tea4Δ::kanMX pom1-Tomato-NatMX ade6- leu1-32	This study
KK294	ura4-294::nmt81:cdr2-mCherry-tea4N-ura4+ tea4Δ::kanMX exo70-GFP-ura4+ ade6- leu1-32	This study
KK295	ura4-294::nmt81:cdr2-mCherry-ura4+ tea4Δ::kanMX exo70-GFP-ura4+ ade6- leu1-32	This study
KK299	ura4-294::nmt81:cdr2-mCherry-Tea4N-ura4+ tea4Δ::kanMX pSV40-atb2GFP-leu+ ade6-	This study
KK302	ura4-294::nmt81:cdr2-GFP-tea4N-ura4+ tea4Δ::kanMX sds21::leu2 ade6- leu1-32	This study
KK330	ura4-294::nmt81:cdr2-GFP-Dis2-ura4+ tea4Δ::kanMX pom1Δ::ura4+ ade6- leu1+	This study
KK346	ura4-294::nmt81:cdr2-mCherry-Tea4N-ura4+ leu1-32::nmt41:cytoRga4-GFP-leu1+ tea4Δ::kanMX ade6?	This study
KK347	ura4-294::nmt81:cdr2-mCherry-ura4+ leu1-32::nmt41:cytoRga4-GFP-leu1+ tea4Δ::kanMX ade6?	This study
KK348	h- ura4-294::nmt81:cdr2-mCherry-ura4+ leu1-32::nmt41:blt1-cytoRga4-GFP-leu1+ tea4Δ::kanMX ade6?	This study
KK349	h- ura4-294::nmt81:cdr2-mCherry-Tea4N-ura4+ leu1-32::nmt41:blt1-cytoRga4-GFP-leu1+ tea4Δ::kanMX ade6?	This study
KK350	tea4Δ::kanMX pom1Psites to A (1,2,3,4,5,8)-GFP-KanMx6 ade6-M216 leu1-32 ura4-D18	This study

Number	Genotype	Source
KK358	tea4WW155-156AA pom1Psites to A (1,2,3,4,5,8)-GFP-KanMx6 ade6-M216 leu1-32 ura4-D18	This study
KK370	ura4-294::nmt81:cdr2-mCherry-Dis2 tea4Δ::kanMX ade6? [pREP41-Rga4(465-685)-GFP (leu2+)]	This study
KK371	ura4-294::nmt81:cdr2-mCherry-Dis2 tea4Δ::kanMX ade6? [pREP41-Rga4-GFP (leu2+)]	This study
KK377	tea4 222-225RVXF-RAXA rga4-GFP-KanMx6 leu1-32 ura4-D18 ade6? leu1-32 ura4-D18	This study
KK381	ura4-294::nmt81:cdr2-GFP-tea4N-ura4+ tea4Δ::kanMX dis2::hphMX ade6-M216 leu1-32	This study
KK390	ura4-294::nmt81:cdr2-GFP-Dis2H247K tea4Δ::kanMX rga4-RFP-KanMx6 ade6? leu1-32	This study
KK391	ura4-294::nmt81:cdr2-GFP-Dis2-ura4+ tea4Δ::kanMX rga4-RFP-KanMx6 ade6? leu1-32	This study
KK395	h- ura4-294::nmt81:cdr2-mCherry-ura4+ tea4Δ::kanMX leu1-32::shk1 promoter:ScGIC2 CRIB:GFP3:leu1+ ade6-	This study
KK396	h- ura4-294::nmt81:cdr2-mCherry-Tea4N-ura4+ tea4Δ::kanMX leu1-32::shk1 promoter:ScGIC2 CRIB:GFP3:leu1+ ade6-	This study
KK399	h- Rga4-PxxP-GFP ade6? leu1-32 ura4-D18	This study
KK400	ura4-294::nmt81:cdr2-GFP-Dis2H247K tea4Δ::kanMX pom1-Tomato-NatMX ade6? leu1-32	This study
KK403	h- ura4-294::nmt81:cdr2-mCherry-Tea4N-ura4+ tea4Δ::kanMX Rga4-PxxP-GFP ade6? leu1-32	This study
MBG194	h+ pom1Psites to A (1,2,3,4,5,8)-GFP ade6-M216 leu1-32 ura4-D18	Lab stock
YSM119	h- pom1-GFP-kanMX ade6+ leu1+ ura4+	(Bahler and Pringle, 1998)
YSM120	h+ tea4-GFP-kanMX ade6- leu1-32 ura4-D18	Lab stock
YSM138	tea4-GFP::kanMX tea2::HIS3	Lab stock
YSM144	h+ tea4Δ::kanMX ade6-M216 leu1-32 ura4-D18	Lab stock
YSM163	h- tea4Δ::kanMX tea1-GFP::kanMX ade6- leu1- ura4-	Lab stock
YSM165	h- tea4Δ::kanMX pom1-GFP-kanMX ura4-	Lab stock
YSM200	h- tea4Δ::kanMX bud6-GFP::kanMX leu1- ura4-	Lab stock

<b>Number</b>	<b>Genotype</b>	<b>Source</b>
YSM239	h+ tea4 $\Delta$ ::kanMX kanMX::nmt81 GFP-mod5 ade6- leu1-32 ura4-D18	Lab stock
YSM243	mod5::kanMX tea4-GFP::kanMX ade6- leu1-32 ura4-D18	Lab stock
YSM423	h- for3-3GFP-ura4+ ade6-M216 leu1-32 ura4-D18	Lab stock
YSM441	h- for3-3GFP-ura4+ tea4 $\Delta$ ::kanMX ade6-M216 leu1-32 ura4-D18	Lab stock
YSM733	h+ bud6-3GFP-kanMX ade6-M216 leu1-32 ura4-D18	Lab stock
YSM1035	h- tea1-GFP kanR ade6- leu1- ura4-	Lab stock
YSM1078	h- tip1-GFP-kanMX ade6- leu1- ura4-	(Browning et al., 2003)
YSM1182	h+ ade6-M216 leu1-32 ura4-D18	Lab stock
YSM1183	h- ade6-M216 leu1-32 ura4-D18	Lab stock
YSM1184	h- dis2-NEGFP-ura4+ leu1-32 ura4-D18	(Alvarez-Tabares et al., 2007)
YSM1408	h- rga4-GFP-KanMx6 leu1-32 ura4-D18	(Tatebe et al., 2008)
YSM1798	h- ura4-294::nmt81:cdr2-GFP-tea4N-ura4+ pom1 $\Delta$ ::ura4+ tea4 $\Delta$ ::kanMX leu1-32	Lab stock

## Microscopy and FRAP Analysis

Microscopy was performed at room temperature on live cells by using either an inverted spinning disk microscope consisting of a Leica DMI4000B inverted microscope equipped with an HCX PL APO 100×/1.46 NA oil objective and a PerkinElmer Ultraview confocal system (including a Yokagawa CSU22 real-time confocal scanning head, an argon/krypton laser, and a cooled 14-bit frame transfer EMCCD C9100-50 camera) or a wide-field Leica AF6000 system consisting of a DM6000B upright microscope fitted with a 40× or 63×/0.75 NA objective, a Leica DFC350x CCD camera, a Leica EL6000 light source and Chrome filter sets. Images were also acquired on DeltaVision system composed of a customized Olympus IX-71 inverted microscope stand fitted with a Plan Apo 60× or 100×/1.42 NA oil objective, a CoolSNAP HQ2 camera, and an Insight SSI 7 color combined unit illuminator. Images were acquired with softWoRx software.

Tea4-GFP movements were analyzed with kymographs, which were constructed with the "Make Montage" tool of the ImageJ software. Tea4-GFP movies were a single medial section taken with inverted spinning disk microscope. Measurements of Tea4 dynamics were performed by recording the x and y positions of moving Tea4 over at least four consecutive time points. The rate of movement was calculated as the sum of the distances between the points divided by time.

For analysis of the FRAP experiments, the mean fluorescence intensities were measured over time in the photo-bleached region, the background near to the photobleached region and another nonbleached cell. For each time point, the intensities of the bleached region and of the unrelated cell were adjusted by subtracting background signal. To correct for loss of signal due to imaging, the adjusted bleached region intensity was then divided by the adjusted intensity of the other cell. Time constants were estimated by the intersection of the curve with a line at half maximal recovery. All measurements and calculations were performed in ImageJ and MS\_Excel, respectively. All images are two-dimensional maximum intensity projections of a single medial section. Figures were prepared with ImageJ and Adobe Illustrator CS3.

In all experiments expressing either the Cdr2-Tea4N or Cdr2-Dis2 fusion cells were growing 20 hours in the presence of the promoter repressor thiamine in EMM medium supplied with the necessary supplements. Then thiamine was washed away allowing the fusion to be expressed to steady state levels for approximately 28-32 hours. For time-lapse videos after the fusion was expressed to steady state levels for approximately 20-24 hours in EMM

medium, then I followed cell growth over time using microfluidic chambers supplying the chambers with the same medium overnight (Classic).

For measurement of fluorescence intensity along the cell cortex, a 5 pixel-wide line was drawn by hand at the cell periphery in a medial co focal section and fluorescence intensity obtained using the plot profile tool of ImageJ. The fluorescence intensity of a field without any cells was measured using the same line, preferably next to the cell of interest, to subtract the background signal. All measurements and calculations were performed in ImageJ and MS\_Excel respectively. All images are two-dimensional maximum intensity projections of a single medial section. Figures were prepared with ImageJ and Adobe Illustrator CS3.

Methyl benzimidazole carbonate (MBC, Sigma) was used at a final concentration of 25 µg/ml from a stock of 2.5 mg/ml in DMSO to disrupt microtubules. Latrunculin A (LatA; Phillip Crews, University of California, Santa Cruz) was used from a stock of 20mM in DMSO at a final concentration of 200µM to disassemble all actin structures. Both MBC and LatA treatment were performed at 30°C for 15 minutes unless otherwise indicated.

Actin staining was performed as described (Pelham and Chang, 2001) using AlexaFluor 488-phalloidin (Invitrogen, Carlsbad, CA) with a fixation time of 60 minutes.

All length measurements were performed on Calcofluor-stained satiated cells with the "Measure" tool in ImageJ 1.41 and then analyzed with Microsoft Excel.

## **TAP purification and immunoprecipitation**

For TAP purification of Tea4-TAP and Tea4<sup>SH3</sup>-TAP, extracts from yeast grown in YE5S in 1<sup>st</sup> TAP and in EMM medium containing the required supplements in 2<sup>nd</sup> TAP were prepared in CXS buffer (50mM Hepes pH7.0, 150mM KCl, 1mM MgCl<sub>2</sub>, 2mM EDTA and protease inhibitor cocktail) by grinding in liquid nitrogen with mortar and pestle as described (Feierbach et al., 2004). During thawing PMSF and protease inhibitor cocktail were added to a final concentration of 1% and 0.1% respectively. After thawing samples were spinned in a table centrifuge at 13krpm for 5 minutes at 4<sup>0</sup>C. The supernatant was collected and Tris pH8.0, NaCl and NP-40 were added to a final concentration of 10mM, 150mM and 0.1% respectively and high-speed soluble extracts were prepared by centrifugation at 45krpm for 30min in the S100-3 rotor (Beckman). In parallel, 600µl of dynabeads Protein G (Invitrogen) were incubated with 200µg rabbit IgG (Sigma) for 1hour at room temperature with rotation. To remove non-covalently-coupled IgG, the beads were washed once with 1ml cold 1x PBS and twice with 1ml cold IPP150 (10mM Tris pH8.0, 150mM NaCl, 0.5mM EDTA, 0.1% NP-40). Soluble extracts (corresponding to about 3l of log-phase culture) were added to the

beads and incubated for 2h at 4°C. Beads were washed 7x with 1ml cold IPP150 buffer, 1x in 1ml cold TEV buffer (10mM Tris pH8.0, 150mM NaCl, 0.5mM EDTA, 0.01% NP-40) and incubated for 1.5h at room temperature in 500µl TEV buffer + 1mM DTT and 20µl TEV protease (Invitrogen). 20µl of the supernatant was set apart for analysis by SDS-PAGE and silver staining with a SilverSNAP Stain Kit II (Pierce) and the rest was precipitated with TCA and dried. Then, the samples were sent to the Protein Analysis Facility (PAF) of University of Lausanne.

For Rga4-myc co-immunoprecipitation with Rga4-GFP different fragments, 200µl soluble extract (corresponding to about 75ml of log-phase culture) was added to 30µl dynabeads Protein G (Invitrogen) pre-bound to 2µg myc antibody and incubated for 2h at 4°C. After incubation, the beads were washed 7x with 1ml cold IPP150 buffer, resuspended in 50µl sample buffer, boiled and analyzed by SDS-PAGE and Western blotting. Antibodies used on Western blots were: mouse monoclonal anti-myc (1:3000) and anti-GFP (1:2000) (Roche).

For Rga4-GFP co-immunoprecipitation with Tea4-HA-ProteinA different fragments, 400µl soluble extract (corresponding to about 150ml of log-phase culture) was added to 50µl dynabeads Protein G (Invitrogen) pre-bound to 3µg rabbit IgG (Sigma) and incubated for 2h at 4°C. After incubation, the beads were washed 7x with 1ml cold IPP150 buffer, 1x in 1ml cold TEV buffer (10mM Tris pH8.0, 150mM NaCl, 0.5mM EDTA, 0.01% NP-40, 0.01% Tween20) and incubated for 45 minutes at room temperature with regular mixing (every 10 minutes) in 28µl TEV buffer + 1mM DTT and 1.7µl TEV protease (Invitrogen). Supernatant (30µl) was removed and 28µl TEV buffer + 1mM DTT and 1.7µl TEV protease was further added and incubated for 45 minutes at room temperature with regular mixing (every 10 minutes). Then 30µl of 3 times sample buffer was added to the 60µl (30ml + 30µl) of the supernatant, boiled and analyzed by SDS-PAGE and Western blotting. Antibodies used on Western blots were: mouse monoclonal anti-GFP (1:2000) (Roche) and anti-HA.11 (1:1000) (Covance).

## Mass spectrometry results

	Tea4- TAP YE5S	Tea4- TAP EMM	Tea4SH3 -TAP YE5S	Tea4SH3 -TAP EMM	Tea4 YE5S	Tea4 EMM
Accession numbers						
TEA1_SCHPO	179	809	536	607	0	0
TEA4_SCHPO	82	210	213	179	0	0
HSP72_SCHPO	84	163	175	98	25	18
TEA3_SCHPO	19	210	50	252	0	0
G3P1_SCHPO	53	126	131	77	39	13
MU131_SCHPO	0	0	0	0	0	36
EF1A2_SCHPO	38	111	82	60	28	30
K6PF_SCHPO	26	92	57	68	15	1
ACT_SCHPO	17	70	67	32	18	11
HSP75_SCHPO	10	31	28	22	15	5
O74819_SCHPO/ Q9HDZ4_SCHPO,UBIQ_SCHPO	0	24	0	24	0	0
HSP7M_SCHPO	14	14	19	11	12	11
EF2_SCHPO	5	16	27	8	12	0
ILVB_SCHPO	10	18	27	9	3	0
ADH_SCHPO	11	5	28	4	12	0
PYR1_SCHPO	0	24	8	11	1	1
RAD24_SCHPO	6	10	18	11	4	4
ILV5_SCHPO	8	14	12	9	12	3
PGK_SCHPO	0	23	3	9	4	11
HSP60_SCHPO	4	5	12	4	9	7
PPK2_SCHPO	0	25	0	35	0	0

Accession numbers	Tea4-TAP YE5S	Tea4-TAP EMM	Tea4SH3-TAP YE5S	Tea4SH3-TAP EMM	Tea4 YE5S	Tea4 EMM
RAD25_SCHPO	6	22	11	14	3	0
ENO11_SCHPO	0	26	11	11	4	2
METK_SCHPO	0	22	1	14	3	7
ALF_SCHPO	3	22	7	7	10	6
DED1_SCHPO	1	15	2	19	1	0
PRS10_SCHPO	9	7	11	7	3	0
PRS8_SCHPO	2	8	13	7	0	1
GRP78_SCHPO	7	9	9	6	2	0
PRS6B_SCHPO	0	8	9	10	0	0
TCPQ_SCHPO	4	8	8	5	0	0
RPN1_SCHPO	1	12	13	5	0	0
SEC7C_SCHPO	0	0	0	0	0	3
LEU3_SCHPO	3	7	13	6	3	0
CSK2A_SCHPO	4	13	4	3	3	0
RPN2_SCHPO	2	6	10	1	4	0
KPYK_SCHPO	0	12	4	2	4	4
MAS5_SCHPO	0	7	12	3	0	0
ATPB_SCHPO	0	22	3	6	0	0
TCPZ_SCHPO	0	8	12	0	0	0
CDC48_SCHPO	0	3	3	1	3	1
IDH1_SCHPO	1	9	2	6	0	0
FBRL_SCHPO	3	0	1	0	9	0
ODPB_SCHPO	2	12	3	4	0	3

Accession numbers	Tea4-TAP YE5S	Tea4-TAP EMM	Tea4SH3-TAP YE5S	Tea4SH3-TAP EMM	Tea4 YE5S	Tea4 EMM
ADH4_SCHPO	0	18	0	3	0	1
HMT2_SCHPO	0	8	0	12	0	0
RS3_SCHPO	3	5	5	4	3	0
P78913_SCHPO,PDC2_SCHPO	0	9	5	2	3	2
TCPA_SCHPO	0	5	3	1	0	0
PP12_SCHPO	7	9	0	0	0	0
GLYD_SCHPO	0	11	0	4	1	2
RL4A_SCHPO	0	7	6	4	2	0
THI3_SCHPO	0	13	0	2	0	4
HSP90_SCHPO	3	3	5	2	3	0
O59716_SCHPO	0	8	0	6	0	0
PP11_SCHPO	6	12	0	0	0	0
PRS4_SCHPO	1	4	7	0	0	0
RGA4_SCHPO	0	0	0	11	0	0
RLA0_SCHPO	4	5	3	3	5	0
RUVB1_SCHPO	0	3	3	0	2	0
THI2_SCHPO	0	12	0	5	0	0
METE_SCHPO	0	10	0	2	0	0
YC35_SCHPO	0	0	0	0	0	4
PMA1_SCHPO	3	0	2	0	5	0
MPG1_SCHPO	0	2	2	5	3	0
GBLP_SCHPO	4	5	0	0	2	0
PRS6A_SCHPO	0	5	6	0	0	0

Accession numbers	Tea4-TAP YE5S	Tea4-TAP EMM	Tea4SH3-TAP YE5S	Tea4SH3-TAP EMM	Tea4 YE5S	Tea4 EMM
PRS7_SCHPO	0	5	2	2	0	0
O43060_SCHPO	1	0	1	0	3	0
HOSM_SCHPO	0	6	1	4	0	0
RPA2_SCHPO	0	0	0	0	0	1
RPN8_SCHPO	0	4	3	0	0	0
CARA_SCHPO	0	0	5	3	0	0
TBB_SCHPO	0	4	2	0	0	0
PDX1_SCHPO	0	2	0	0	3	0
CASP_SCHPO	0	0	0	0	0	2
ARGD_SCHPO	0	0	0	0	0	1
TCPG_SCHPO	0	3	3	0	0	0
TBA1_SCHPO	0	6	0	3	0	0
EF3_SCHPO	0	0	5	0	4	0
COPA_SCHPO	0	1	0	0	0	0
GLT1_SCHPO	0	3	0	0	0	0
TIM44_SCHPO	0	0	4	0	0	0
SYMC_SCHPO	0	5	2	0	0	0
Q96WV0_SCHPO	3	0	5	0	0	0
Q6LA55_SCHPO	0	0	0	0	0	2
IF2A_SCHPO	0	2	0	0	2	0
RUVB2_SCHPO	0	3	4	0	0	0
ADT_SCHPO,P78754_SCHPO	0	0	3	0	0	0
EIF3I_SCHPO	0	2	0	0	4	0

Accession numbers	Tea4-TAP YE5S	Tea4-TAP EMM	Tea4SH3-TAP YE5S	Tea4SH3-TAP EMM	Tea4 YE5S	Tea4 EMM
YDR1_SCHPO	0	0	0	0	0	2
UBLH2_SCHPO	1	0	0	0	0	0
IPYR_SCHPO	0	4	0	0	1	0
LYS12_SCHPO	3	0	3	0	0	0
TCPD_SCHPO	0	2	3	0	0	0
SYG_SCHPO	1	0	0	0	3	0
RS0A_SCHPO	0	3	0	0	1	0
ARP2_SCHPO	0	0	2	0	0	0
ARG56_SCHPO	0	0	3	0	0	0
RPN9_SCHPO	0	3	0	0	0	0
TAL1_SCHPO	0	2	0	0	1	0
EIF3G_SCHPO	0	0	0	0	1	0
YI7E_SCHPO	2	0	0	0	0	0
G3P2_SCHPO	0	4	0	0	0	0
RPN5_SCHPO	1	0	1	0	0	0
COPB_SCHPO	0	2	0	0	0	0
THI4_SCHPO	0	3	0	0	0	0
MDJ1_SCHPO	0	0	1	0	0	0
Q1L854_SCHPO,YBI8_SCHPO	0	0	0	0	2	0
SAHH_SCHPO	0	4	0	0	0	0
YF19_SCHPO	0	2	0	0	0	0
RS3B_SCHPO	0	0	2	0	0	0
O74919_SCHPO	0	0	1	0	2	0

	Tea4- TAP YE5S	Tea4- TAP EMM	Tea4SH3 -TAP YE5S	Tea4SH3 -TAP EMM	Tea4 YE5S	Tea4 EMM
Accession numbers						
EIF3H_SCHPO	0	0	0	2	0	0
MDHM_SCHPO	0	0	1	0	0	0
PYRG_SCHPO	0	0	2	0	0	0
SLBR2_SCHPO	0	1	0	0	0	0
RS2_SCHPO	0	0	2	0	0	0
RL3A_SCHPO,RL3B_SCHPO	0	0	2	0	0	0
Q9Y7Y6_SCHPO	0	2	0	0	0	0
ACAC_SCHPO	0	2	0	0	0	0
ATPA_SCHPO	0	2	0	0	0	0
EFTU_SCHPO	0	1	0	0	0	0
RPN11_SCHPO	0	1	0	0	0	0
COPE_SCHPO	0	3	0	0	0	0
RPB2_SCHPO	0	0	0	0	2	0
BCA1_SCHPO	0	0	0	0	2	0
RL13_SCHPO	0	0	2	0	0	0
GPD2_SCHPO	0	0	0	0	2	0
LSB5_SCHPO	0	0	0	2	0	0
RL4B_SCHPO	0	0	2	0	0	0
SLT1_SCHPO	0	2	0	0	0	0
PEX7_SCHPO	0	2	0	0	0	0
ARPC2_SCHPO	0	0	2	0	0	0
AROG_SCHPO	0	0	0	0	1	0
Q9USL6_SCHPO	0	1	0	0	0	0

Predicted phosphorylated sites

**S residue with top score**

S residue possibly also phosphorylated

**In green: only detected in Tea4<sup>SH3</sup> mutant**

Sample: Tea4-TAP phosphopeptides detected

Tea4

Matched peptides shown in **Bold Red**

1 MEIMESHFDPTQQNDSTIIE SR**Y****S****P****E****E****Y****L****E** **Q****S****F****E****I****Q****R****I****I****S**  
GENSEPQTVA  
51 SQEISDSQEE DTTLTSSQFE DCGTEYNEVV EDDEFRSEDE  
DDFMDEEEY  
101 ALYEAELSSS PSIHVEVIDC NRVHAIKGFV ATVEGQVDAT  
KGDMMILLDD  
151 SNSYWLVKMK**C****N****L****A****I****G****Y****L****P** **A****E****Y****I****E****T****P****S****E****R** LARLNKYK**N****S**  
**E****T****S****N****S****Q****Q****S****V****T**  
201 **L****P****P****L****D****I****V****E****K****T** **L****E****A****P****S****P****N****F****R****I** KRVTFTCSSN SSDDEMSEN  
DYEAMVNRTV  
251 AENGLIEFSDSSDSSLSAE YRSESEDHVT DSPAYVDLTE  
LEGGFNQFNS  
301 TSFQSTSPLEIVETEING SSTTADSKNS HSPYSK**F****S****S****A**  
**Y****P****D****A****E****N****S****N****I****S**  
351 **K****I****N****I****S****I****A****G****N****K** **E****L****Y****G****N****A****T****Q****S****D** **P****S****L****Y****S****T****W****I****A****N** **K****H****K****T****A****S****S****A****T****V**  
**D****S****P****L****R****R****S****L****S****V**  
401 **D****A****M****Q****S****N****A****S****F****S** **S****Y****S****T****S****N****T****D****K** **S****L****R****P****S****S****Y****S****A****V** **S****E****S****S****N****F****T****H****D****V**  
**S****R****D****N****K****E****I****S****L****N**  
451 **A****P****K****S****I****I****V****S****Q****S** D<sup>S</sup>FDTSNVTQ DAPNDVEKEP ISGQMPNNLS  
VQSLK**Q****L****E****V****Y**  
501 **P****I****R****H****S****V****S****I****E****M** **P****S****E****K****L****L****S****P****R****L** **Y****S****S****S****T****P****S****S****P****T** **K****G****F****Q****K****D****D****E****E****D**  
SEN**R****K****Q****A****D****K****V**  
551 **E****L****S****P****S****S****L****L****R****Q** **M****S****L****P****V****D****S****S****S****Q** **S****D****A****Q****C****T****T****S****S****V** **Y****I****T****A****E****R****K****A****F****S**  
**Q****S****S****I****D****L****S****T****L****S**  
601 **N****H****H****V****N****N****E****I****N****R** **R****S****F****A****G****G****F****T****S****L** **A****D****E****L****S****E****M****R****E****L** **L****H****E****S****P****A****P****L****E****C**  
**N****E****E****M****V****I****P****T****P****E**  
651 **L****D****A****S****S****A****I****P****S****S** **S****I****S****H****D****E****D****L****L****P** **R****K****N****T****E****E****S****T****S****S** **S****S****F****S****S****L****I****T****S****P**  
**A****S****L****Q****Y****D****E****N****P****F**  
701 **K****Q****S****V****V****A****E****L****N****N** **N****S****S****S****V****P****F****V****D****S** **A****H****A****S****D****I****H****A****Y****D** **N****D****H****V****S****T****K****N****K****E**  
FN**R****R****L****R****E****F****I****L**  
751 **D****P****D****S****L****S****G****L****Y****W** **S****V****K****S****A****G****V****R****A****S** **R****R****V****S****R****N****I****E****G****E** **S****V****S****S****D****L****D****D****I****F**  
**A****N****V****L****K****G****L****S****D****E**  
801 **M****A****S****L****L****N****T****N****R**

Sample: Tea4-TAP phosphopeptides detected

Tea4

```

23 - 37      999.4304  1996.8462  1996.8455  0      0  R.YSPEEYLEQSFEIQR.I
Phospho (ST) (Ions score 62)
210 - 219   606.2766  1210.5387  1210.5383  0      0  K.TLEAPSPNFR.I
Phospho (ST) (Ions score 25)
520 - 531   667.7983  1333.5820  1333.5803  1      0  R.LYSSSTPSSPTK.G
Phospho (ST) (Ions score 25)
520 - 531   667.7983  1333.5820  1333.5803  1      0  R.LYSSSTPSSPTK.G
Phospho (ST) (Ions score 28)
520 - 531   667.7986  1333.5827  1333.5803  2      0  R.LYSSSTPSSPTK.G
Phospho (ST) (Ions score 22)
546 - 559   811.9110  1621.8074  1621.8076 -0      1  K.QADKVELSPSSLLR.Q
Phospho (ST) (Ions score 21)
546 - 559   811.9121  1621.8096  1621.8076  1      1  K.QADKVELSPSSLLR.Q
Phospho (ST) (Ions score 29)
629 - 671   1202.0611  4804.2153  4804.2136  0      0
R.ELLHESAPAPLECNEEMVIPTPELDASSAIPSSSISHDEDLLPR.K Phospho (ST) (score 36)
629 - 671   1202.0611  4804.2153  4804.2136  0      0
R.ELLHESAPAPLECNEEMVIPTPELDASSAIPSSSISHDEDLLPR.K Phospho (ST) (score 22)

```

Sample: Tea4<sup>SH3</sup>-TAP phosphopeptides detected

Tea4

```

TEA4_SCHPO
421 - 442   831.7061  2492.0963  2492.0969  -0     0
K.SLRPSSYSAVSESSNFTHDVS.R.D Phospho (ST) (Ions score 105)
421 - 442   831.7069  2492.0989  2492.0969  1     0
K.SLRPSSYSAVSESSNFTHDVS.R.D Phospho (ST) (Ions score 83)
421 - 442   832.0403  2493.0992  2493.0809  7     0
K.SLRPSSYSAVSESSNFTHDVS.R.D Deamidated (NQ); Phospho (ST) (Ions 48)
520 - 531   667.7965  1333.5785  1333.5803  -1    0  R.LYSSSTPSSPTK.G
Phospho (ST) (Ions score 27)
520 - 531   667.7984  1333.5823  1333.5803  2     0  R.LYSSSTPSSPTK.G
Phospho (ST) (Ions score 19)
520 - 531   667.7987  1333.5828  1333.5803  2     0  R.LYSSSTPSSPTK.G
Phospho (ST) (Ions score 17)
546 - 559   811.9119  1621.8092  1621.8076  1     1  K.QADKVELSPSSLLR.Q
Phospho (ST) (Ions score 15)
546 - 559   811.9125  1621.8104  1621.8076  2     1  K.QADKVELSPSSLLR.Q
Phospho (ST) (Ions score 24)
629 - 671   1202.0614  4804.2165  4804.2136  1     0
R.ELLHESAPAPLECNEEMVIPTPELDASSAIPSSSISHDEDLLPR.K Phospho (ST) (Ions 14)
629 - 671   1202.0614  4804.2165  4804.2136  1     0
R.ELLHESAPAPLECNEEMVIPTPELDASSAIPSSSISHDEDLLPR.K Phospho (ST) (Ions 28)
629 - 671   1202.0622  4804.2197  4804.2136  1     0
R.ELLHESAPAPLECNEEMVIPTPELDASSAIPSSSISHDEDLLPR.K Phospho (ST) (Ions 42)

```

## Sample: Tea4-TAP phosphopeptides detected

### Tea1

461 - 473	716.8454	1431.6762	1431.6759	0	0	R.ASN <del>D</del> L <del>P</del> S <del>P</del> V <del>V</del> P <del>T</del> R.S	Phospho
(ST) (Ions score 39)							
461 - 473	716.8455	1431.6765	1431.6759	0	0	R.ASN <del>D</del> L <del>P</del> S <del>P</del> V <del>V</del> P <del>T</del> R.S	Phospho
(ST) (Ions score 40)							
495 - 514	1143.9752	2285.9358	2285.9397	-2	0	R.NTND <del>D</del> D <del>D</del> Q <del>S</del> S <del>L</del> NS <del>Q</del> QL <del>S</del> N <del>Q</del> AK.A	Phospho
(ST) (Ions score 70)							
495 - 514	1143.9772	2285.9398	2285.9397	0	0	R.NTND <del>D</del> D <del>D</del> Q <del>S</del> S <del>L</del> NS <del>Q</del> QL <del>S</del> N <del>Q</del> AK.A	Phospho
(ST) (Ions score 87)							
495 - 514	1143.9778	2285.9410	2285.9397	1	0	R.NTND <del>D</del> D <del>D</del> Q <del>S</del> S <del>L</del> NS <del>Q</del> QL <del>S</del> N <del>Q</del> AK.A	Phospho
(ST) (Ions score 108)							
495 - 514	762.9878	2285.9415	2285.9397	1	0	R.NTND <del>D</del> D <del>D</del> Q <del>S</del> S <del>L</del> NS <del>Q</del> QL <del>S</del> N <del>Q</del> AK.A	Phospho
(ST) (Ions score 50)							
495 - 514	762.9878	2285.9416	2285.9397	1	0	R.NTND <del>D</del> D <del>D</del> Q <del>S</del> S <del>L</del> NS <del>Q</del> QL <del>S</del> N <del>Q</del> AK.A	Phospho
(ST) (Ions score 44)							
495 - 514	1143.9785	2285.9424	2285.9397	1	0	R.NTND <del>D</del> D <del>D</del> Q <del>S</del> S <del>L</del> NS <del>Q</del> QL <del>S</del> N <del>Q</del> AK.A	Phospho
(ST) (Ions score 110)							
495 - 514	1143.9789	2285.9432	2285.9397	2	0	R.NTND <del>D</del> D <del>D</del> Q <del>S</del> S <del>L</del> NS <del>Q</del> QL <del>S</del> N <del>Q</del> AK.A	Phospho
(ST) (Ions score 72)							
495 - 514	1143.9790	2285.9434	2285.9397	2	0	R.NTND <del>D</del> D <del>D</del> Q <del>S</del> S <del>L</del> NS <del>Q</del> QL <del>S</del> N <del>Q</del> AK.A	Phospho
(ST) (Ions score 86)							
515 - 552	971.6843	3882.7081	3882.7116	-1	0	K.AQGEV <del>S</del> P <del>T</del> L <del>S</del> FV <del>P</del> SS <del>H</del> S <del>M</del> E <del>Q</del> G <del>N</del> G <del>S</del> V <del>S</del> A <del>N</del> N <del>A</del> Q <del>S</del> E <del>A</del> A <del>T</del> R.S	Phospho (ST) (score 56)
515 - 552	971.6845	3882.7090	3882.7116	-1	0	K.AQGEV <del>S</del> P <del>T</del> L <del>S</del> FV <del>P</del> SS <del>H</del> S <del>M</del> E <del>Q</del> G <del>N</del> G <del>S</del> V <del>S</del> A <del>N</del> N <del>A</del> Q <del>S</del> E <del>A</del> A <del>T</del> R.S	Phospho (ST) (score 64)
515 - 552	1295.2438	3882.7096	3882.7116	-1	0	K.AQGEV <del>S</del> P <del>T</del> L <del>S</del> FV <del>P</del> SS <del>H</del> S <del>M</del> E <del>Q</del> G <del>N</del> G <del>S</del> V <del>S</del> A <del>N</del> N <del>A</del> Q <del>S</del> E <del>A</del> A <del>T</del> R.S	Phospho (ST) (score 98)
515 - 552	1295.2440	3882.7102	3882.7116	-0	0	K.AQGEV <del>S</del> P <del>T</del> L <del>S</del> FV <del>P</del> SS <del>H</del> S <del>M</del> E <del>Q</del> G <del>N</del> G <del>S</del> V <del>S</del> A <del>N</del> N <del>A</del> Q <del>S</del> E <del>A</del> A <del>T</del> R.S	Phospho (ST) (score 105)
515 - 552	1295.2444	3882.7114	3882.7116	-0	0	K.AQGEV <del>S</del> P <del>T</del> L <del>S</del> FV <del>P</del> SS <del>H</del> S <del>M</del> E <del>Q</del> G <del>N</del> G <del>S</del> V <del>S</del> A <del>N</del> N <del>A</del> Q <del>S</del> E <del>A</del> A <del>T</del> R.S	Phospho (ST) (score 131)
515 - 552	1300.9045	3899.6917	3899.6905	0	0	K.AQGEV <del>S</del> P <del>T</del> L <del>S</del> FV <del>P</del> SS <del>H</del> S <del>M</del> E <del>Q</del> G <del>N</del> G <del>S</del> V <del>S</del> A <del>N</del> N <del>A</del> Q <del>S</del> E <del>A</del> A <del>T</del> R.S	Deamidated (NQ); Oxidation (M); Phospho (ST)
(score 79)							
515 - 552	1321.8992	3962.6758	3962.6779	-1	0	K.AQGEV <del>S</del> P <del>T</del> L <del>S</del> FV <del>P</del> SS <del>H</del> S <del>M</del> E <del>Q</del> G <del>N</del> G <del>S</del> V <del>S</del> A <del>N</del> N <del>A</del> Q <del>S</del> E <del>A</del> A <del>T</del> R.S	2 Phospho (ST) (Ions score 56)
553 - 564	700.3273	1398.6401	1398.6392	1	0	R.SIN <del>S</del> I <del>S</del> E <del>V</del> SE <del>V</del> R.F	Phospho
(ST) (Ions score 71)							
553 - 564	700.3278	1398.6411	1398.6392	1	0	R.SIN <del>S</del> I <del>S</del> E <del>V</del> SE <del>V</del> R.F	Phospho
(ST) (Ions score 65)							
553 - 564	700.3279	1398.6411	1398.6392	1	0	R.SIN <del>S</del> I <del>S</del> E <del>V</del> SE <del>V</del> R.F	Phospho
(ST) (Ions score 49)							
553 - 572	1151.5524	2301.0902	2301.0889	1	1	R.SIN <del>S</del> I <del>S</del> E <del>V</del> SE <del>V</del> RF <del>P</del> E <del>Q</del> SS <del>V</del> K.T	Phospho (ST) (Ions score 97)
553 - 572	1151.5528	2301.0910	2301.0889	1	1	R.SIN <del>S</del> I <del>S</del> E <del>V</del> SE <del>V</del> RF <del>P</del> E <del>Q</del> SS <del>V</del> K.T	Phospho (ST) (Ions score 124)
553 - 572	768.0379	2301.0920	2301.0889	1	1	R.SIN <del>S</del> I <del>S</del> E <del>V</del> SE <del>V</del> RF <del>P</del> E <del>Q</del> SS <del>V</del> K.T	Phospho (ST) (Ions score 38)
553 - 572	1151.5534	2301.0922	2301.0889	1	1	R.SIN <del>S</del> I <del>S</del> E <del>V</del> SE <del>V</del> RF <del>P</del> E <del>Q</del> SS <del>V</del> K.T	Phospho (ST) (Ions score 87)
553 - 572	768.0384	2301.0933	2301.0889	2	1	R.SIN <del>S</del> I <del>S</del> E <del>V</del> SE <del>V</del> RF <del>P</del> E <del>Q</del> SS <del>V</del> K.T	Phospho (ST) (Ions score 43)
1051 - 1075	983.7956	2948.3650	2948.3652	-0	1	K.LKSE <del>E</del> D <del>T</del> S <del>L</del> E <del>T</del> P <del>I</del> H <del>E</del> N <del>Q</del> S <del>I</del> Q <del>S</del> D <del>Q</del> IK.E	Phospho (ST) (Ions score 49)
1051 - 1075	983.7957	2948.3654	2948.3652	0	1	K.LKSE <del>E</del> D <del>T</del> S <del>L</del> E <del>T</del> P <del>I</del> H <del>E</del> N <del>Q</del> S <del>I</del> Q <del>S</del> D <del>Q</del> IK.E	Phospho (ST) (Ions score 51)
1053 - 1075	903.4027	2707.1864	2707.1861	0	0	K.S <del>E</del> E <del>D</del> T <del>S</del> L <del>E</del> T <del>P</del> I <del>H</del> E <del>N</del> Q <del>S</del> I <del>Q</del> S <del>D</del> Q <del>IK</del> .E	Phospho (ST) (Ions score 38)

Sample: Tea4<sup>SH3</sup>-TAP phosphopeptides detected

Tea1

Matched peptides shown in **Bold Red**

1 MSFLFKRNKG SAHKPTKPNF SKTSTTPSTS QLKHSHESNV **KMSTSTVTEH**

51 **RKKPTGSGSH** ITASPWSKLT VRGSSNVLPR **YSHASHLYAE** GGQEIIYIFGG  
101 **VASDSQPKND** LWVLNLATSQ FTSLRSLGET **PSPRLGHASI** LIGNAFIVFG  
151 **GLTNHDVADR** QDNSLYLLNT **SSLVWQKANA** SGARPSGRYG HTISCLGSKI  
201 **CLFGGRLLDY** YFNDLVCFDL **NNLNTSDSRW** ELASVNDPP PARAGHVAFT  
251 **FSDKLYIFGG** TDGANFFNDL **WCYHPKQSAW** SKVETFGVAP NPRAGHAASV  
301 **VEGILYVFGG** RASDGTFLND **LYAFRLSSKH** WYKLSDLPFT **PSPRSSHTLS**  
351 **CSSLTLLVIG** GKQKGASDS **NVYMLDTSRF** RLGSVPTSG **RQRNTSFFSN**  
401 **STGNTNPSAF** NGLLTSSRIP SYNGSKVRST **SHPSRQQYIG** SSNSRFNTRH  
451 **QTISTPVSGR** ASNDLPS**VPV** PTRSNSSSIL **QPSYNLNSHS** SDRRNTNDDD  
501 **QSSLNSQQLS** NQAKAQGEV**S** **PTLS**FVPSSH **SMEQNGSVA** SANNAQSEAA  
551 **TRSINSiSeV** SEVRFPQSS **VKTVDERKSL** DGRITSVTLE **TLVEKYSELS**  
601 **KQIVVEWFKS** KLYEILRDSA SKIDSLTEKL **KVANAENAA** LCEAALEKVP  
651 **LAKHNKLSDG** TFSTPKENV **QSTNDAHIMQ** ENFSLHKALE VMRETSSDL  
701 **KQLKDATASQ** KELIVQTSF **QKELVEERER** HNAISKRLQE **IESLYRDREL**  
751 **LVTNLEDQLV** DQVTINKFA FERDQFRERS **MGFENTIKDL** TRKMEATDML  
801 **NVSLHESLRS** VQTENSELVT **EMALLKAELV** KKQAIIDANA **NIYDKLTADH**  
851 **TNYETVSADI** NQNLKETLDK **LLNGSSDFKN** NEIELLHDQI **RITNAKLEKR**  
901 **EKLINASKYI** EDTLRSEIQE **AAEKVSNLEF** SNFNLKEENS **NMQLQLMKAL**  
951 **EQRNTGAKQL** VNLRMQLSTA **TSELDMLKLK** LRTTALALEE **SPDDYSDILS**  
1001 **ILRADMSPFH** DLHKQCGVLI **DTLNGVKRGF** GIFEK<sup>K</sup>FTDY **HKFLENISDK**  
1051 **LKSEEDTSLE** TPIHENQ**SIQ** **SDQIKEVGEV** LSAIKSLSDS **VMLLKNQIDD**  
1101 **LAKEKLPLSS** SDDEKVN**IK**E **KTDFMKLLVK** **SGLSNPPAKE** PVHDNEN

Sample: Tea4<sup>SH3</sup>-TAP phosphopeptides detected

Tea1

```

KK2
TEA1_SCHPO
 461 - 473      716.8448  1431.6750  1431.6759      -1      0  R.ASNLPSVPVPT.R.S
Phospho (ST) (Ions score 34)
 461 - 473      716.8452  1431.6759  1431.6759       0      0  R.ASNLPSVPVPT.R.S
Phospho (ST) (Ions score 31)
 495 - 514      762.9867  2285.9382  2285.9397      -1      0
R.NTNDQSSLSNQAK.A Phospho (ST) (Ions score 57)
 495 - 514      1143.9771  2285.9396  2285.9397      -0      0
R.NTNDQSSLSNQAK.A Phospho (ST) (Ions score 98)
 495 - 514      762.9873  2285.9402  2285.9397       0      0
R.NTNDQSSLSNQAK.A Phospho (ST) (Ions score 40)
 495 - 514      1143.9780  2285.9414  2285.9397       1      0
R.NTNDQSSLSNQAK.A Phospho (ST) (Ions score 87)
 495 - 514      1143.9787  2285.9428  2285.9397       1      0
R.NTNDQSSLSNQAK.A Phospho (ST) (Ions score 95)
 495 - 514      1143.9787  2285.9428  2285.9397       1      0
R.NTNDQSSLSNQAK.A Phospho (ST) (Ions score 81)
 515 - 552      971.6829  3882.7026  3882.7116      -2      0
K.AQGEVPTLSFVPSHSMQNGSVASANNAQSEATR.S Phospho (ST) (Ions score 44)
 515 - 552      1295.2440  3882.7102  3882.7116      -0      0
K.AQGEVPTLSFVPSHSMQNGSVASANNAQSEATR.S Phospho (ST) (Ions score 108)
 515 - 552      1295.2442  3882.7108  3882.7116      -0      0
K.AQGEVPTLSFVPSHSMQNGSVASANNAQSEATR.S Phospho (ST) (Ions score 104)
 553 - 564      700.3265  1398.6384  1398.6392      -1      0  R.SINSISEVSEVR.F
Phospho (ST) (Ions score 48)
 553 - 564      700.3268  1398.6391  1398.6392      -0      0  R.SINSISEVSEVR.F
Phospho (ST) (Ions score 73)
 553 - 564      700.3271  1398.6396  1398.6392       0      0  R.SINSISEVSEVR.F
Phospho (ST) (Ions score 58)
 553 - 564      700.3271  1398.6397  1398.6392       0      0  R.SINSISEVSEVR.F
Phospho (ST) (Ions score 87)
 553 - 572      768.0369  2301.0888  2301.0889      -0      1
R.SINSISEVSEVRFPEQSSVK.T Phospho (ST) (Ions score 51)
 553 - 572      1151.5518  2301.0890  2301.0889       0      1
R.SINSISEVSEVRFPEQSSVK.T Phospho (ST) (Ions score 76)
 553 - 572      1151.5518  2301.0890  2301.0889       0      1
R.SINSISEVSEVRFPEQSSVK.T Phospho (ST) (Ions score 80)
 553 - 572      768.0370  2301.0893  2301.0889       0      1
R.SINSISEVSEVRFPEQSSVK.T Phospho (ST) (Ions score 50)
 1051 - 1075    983.7954  2948.3645  2948.3652      -0      1
K.LKSEEDTSLETPIHENQSIQSDQIK.E Phospho (ST) (Ions score 37)
 1053 - 1075    903.4026  2707.1859  2707.1861      -0      0
K.SEEDTSLETPIHENQSIQSDQIK.E Phospho (ST) (Ions score 42)
 1053 - 1075    903.7364  2708.1874  2708.1702       6      0
K.SEEDTSLETPIHENQSIQSDQIK.E Deamidated (NQ); Phospho (ST) (Ions score 24)

```

Sample: Tea4-TAP phosphopeptides detected

Tea3

Matched peptides shown in **Bold Red**

1 MVQKVL**SRQS** **DNSQDVSAEQ** **LDVVESGSID** **QQNIRAWVVR** KVKENDKRTS  
51 TNQSF**KWEAV** **KPASCLDAAN** **EK**FMYLHGGR **EK**SGISNSLF **KLDLDSCTVY**  
101 **SHNR**GEDNDS PARVGHSIVC SADTIYLFGG CDSETDSTFE VGDNSLYAYN  
151 **FK****SNQWN**LVS **TQSPLSPRT** **GHSMLLVDSK** **LWIFGGECQG** **KYLNDIHLFD**  
201 **TK**GVD**RR**TQS ELKQKANANN VE**KANMEFDE** **TDWSWETPFL** **HSSSPPPRSN**  
251 H**SV**TLVQ**GKI** F**VHGG**HNDTG PLSDLWLFDL ETL**SWTE**VRS IGRFP**GP**REG  
301 **HQATTID**DTV **YIYGGR**DNKG **LILNELWAFN** **YSQQRW**SLVS **NPIPILL**SDS  
351 **SSYK**IVSK**NN** **HILLLYL**NAL **DAPKQL**LCYE **ADPKN**LYWDK DKFSDIPVLQ  
401 HISM**KPS**NAS NHTVSLG**YLN** DRPNH**SK**KNS **VTSTSS**SQFN **NFLEQ**NQKAV  
451 RSARHR**HYAS** **LDEQGL**HSLR NLSKTSGMNH SAD**FS**LHEFG QADPFAYEIE  
501 KPIASLPLPN GNDTISR**SSE** SSSPINESES NSLLKLQSD**F** KFSNSDDRVA  
551 WLEEQ**LL**YCM Q**Q**GYTLKPPN LFQHVDEKLR LE**K**KEQLSYL **EILK**VIEQML  
601 **ESNEQ**KFKKQ **IVSLAS**ENAK LAAQRDAVE NANYSRSLIQ **KTT**DET**VGS**  
651 **LIEK**VLG**KLEY** **EVQGT**LEEAT **SYQK**NTELQ **QLLKQ**NESAS **ELLK**SRNEKL  
701 **CVDYD**KLRSV FEEDSSKILS LQ**KENEN**LQS **QILQ**ISEELV **DYRSR**CEALE  
751 **YGN**YELETKL IEMH**DR**VEMQ **TNVIE**ASASA LDVSN**T**AILS **FED**SLRRERD  
801 EKSTLQ**Q**CKL **NLQY**EYENVR **I**ELENLQ**SRA** **LELES**ALEQS **VSDAK**YSKAI  
851 **RQ**SGLSK**LLS** **SINENK**DNLK EF**SK**SKQ**KIS** **Y**LESQLEGLH **ELL**RESQRLC  
901 EGRTK**ELL**NS Q**Q**KLYDLK**HS** **YSSV**MTEKSK **LSDQ**VNDL**TE** **QAK**ITQRKLS  
951 **EVQ**IALADSK MN**Q**QLSGKDS **TDVHL**PTDFS **A**SS**S**PLRSYF **NEED**SFNNAS  
1001 **AAHSS**KE**S**DI **PSG**GVFTKYR **NHFG**NLMTSE **ETK**APDNNDL **HKRL**S**D**VINS  
1051 **Q**Q**K**FLSL**SPQ** **VSK**DYD**VRS** **KLN**D**TAG**S**F**S **G**EMRAIDN **Y**YASRIK**Q**LE  
1101 **DDY**Q**K**AITYA NCSDES**F**QQL SHSFM

Sample: Tea4-TAP phosphopeptides detected

Tea3

969 - 987	1056.4679	2110.9212	2110.9209	0	0
K.DSTDVHLPTDFSA <b>SSS</b> PLR.S	Phospho (ST)	(Ions score 77)			
969 - 987	704.6478	2110.9216	2110.9209	0	0
K.DSTDVHLPTDFSA <b>SSS</b> PLR.S	Phospho (ST)	(Ions score 34)			
969 - 987	1056.4683	2110.9220	2110.9209	1	0
K.DSTDVHLPTDFSA <b>SSS</b> PLR.S	Phospho (ST)	(Ions score 54)			
969 - 987	1056.4687	2110.9228	2110.9209	1	0
K.DSTDVHLPTDFSA <b>SSS</b> PLR.S	Phospho (ST)	(Ions score 76)			
1043 - 1053	684.3371	1366.6597	1366.6606	-1	1
K.RL <b>S</b> DVINSQ <b>K</b> .F	Phospho (ST)	(Ions score 32)			
1072 - 1085	797.3166	1592.6185	1592.6178	0	0
K.LND <b>TAG</b> S <b>F</b> S <b>G</b> EMR.A	Phospho (ST)	(Ions score 78)			
1072 - 1085	797.3166	1592.6187	1592.6178	1	0
K.LND <b>TAG</b> S <b>F</b> S <b>G</b> EMR.A	Phospho (ST)	(Ions score 72)			

Sample: Tea4<sup>SH3</sup>-TAP phosphopeptides detected

Tea3

KK2						
TEA3_SCHPO						
969 - 987	1056.4672	2110.9198	2110.9209		-0	0
K.DSTDVHLPTDFSASSSPLR.S	Phospho (ST)	(Ions score 68)				
969 - 987	1056.4673	2110.9200	2110.9209		-0	0
K.DSTDVHLPTDFSASSSPLR.S	Phospho (ST)	(Ions score 56)				
969 - 987	1056.4675	2110.9204	2110.9209		-0	0
K.DSTDVHLPTDFSASSSPLR.S	Phospho (ST)	(Ions score 48)				
969 - 987	704.6480	2110.9221	2110.9209		1	0
K.DSTDVHLPTDFSASSSPLR.S	Phospho (ST)	(Ions score 34)				
969 - 987	1056.4685	2110.9224	2110.9209		1	0
K.DSTDVHLPTDFSASSSPLR.S	Phospho (ST)	(Ions score 35)				
1043 - 1053	684.3397	1366.6648	1366.6606		3	1
K.RLSDVINSQQK.F	Phospho (ST)	(Ions score 28)				
1072 - 1085	797.3155	1592.6164	1592.6178		-1	0
K.LNDTAGSFSGEEMR.A	Phospho (ST)	(Ions score 96)				
1072 - 1085	797.3163	1592.6180	1592.6178		0	0
K.LNDTAGSFSGEEMR.A	Phospho (ST)	(Ions score 92)				

# References

- Adams, A.E., Johnson, D.I., Longnecker, R.M., Sloat, B.F., and Pringle, J.R. (1990). CDC42 and CDC43, two additional genes involved in budding and the establishment of cell polarity in the yeast *Saccharomyces cerevisiae*. *J Cell Biol* *111*, 131-142.
- Alvarez-Tabares, I., Grallert, A., Ortiz, J.M., and Hagan, I.M. (2007). Schizosaccharomyces pombe protein phosphatase 1 in mitosis, endocytosis and a partnership with Wsh3/Tea4 to control polarised growth. *J Cell Sci* *120*, 3589-3601.
- Anderson, D.C., Gill, J.S., Cinalli, R.M., and Nance, J. (2008). Polarization of the *C. elegans* embryo by RhoGAP-mediated exclusion of PAR-6 from cell contacts. *Science* *320*, 1771-1774.
- Arai, R., and Mabuchi, I. (2002). F-actin ring formation and the role of F-actin cables in the fission yeast *Schizosaccharomyces pombe*. *J Cell Sci* *115*, 887-898.
- Arellano, M., Duran, A., and Perez, P. (1997). Localisation of the *Schizosaccharomyces pombe* rho1p GTPase and its involvement in the organisation of the actin cytoskeleton. *J Cell Sci* *110* ( Pt 20), 2547-2555.
- Arellano, M., Niccoli, T., and Nurse, P. (2002). Tea3p is a cell end marker activating polarized growth in *Schizosaccharomyces pombe*. *Curr Biol* *12*, 751-756.
- Arimura, N., and Kaibuchi, K. (2007). Neuronal polarity: from extracellular signals to intracellular mechanisms. *Nat Rev Neurosci* *8*, 194-205.
- Aznar, S., and Lacal, J.C. (2001). Rho signals to cell growth and apoptosis. *Cancer Lett* *165*, 1-10.
- Bahler, J., and Nurse, P. (2001). Fission yeast Pom1p kinase activity is cell cycle regulated and essential for cellular symmetry during growth and division. *EMBO J* *20*, 1064-1073.
- Bahler, J., and Pringle, J.R. (1998). Pom1p, a fission yeast protein kinase that provides positional information for both polarized growth and cytokinesis. *Genes Dev* *12*, 1356-1370.
- Bahler, J., Wu, J.Q., Longtine, M.S., Shah, N.G., McKenzie, A., 3rd, Steever, A.B., Wach, A., Philippsen, P., and Pringle, J.R. (1998). Heterologous modules for efficient and versatile PCR-based gene targeting in *Schizosaccharomyces pombe*. *Yeast* *14*, 943-951.
- Becker, W., Weber, Y., Wetzel, K., Eirnbter, K., Tejedor, F.J., and Joost, H.G. (1998). Sequence characteristics, subcellular localization, and substrate specificity of DYRK-related kinases, a novel family of dual specificity protein kinases. *J Biol Chem* *273*, 25893-25902.
- Behrens, R., and Nurse, P. (2002). Roles of fission yeast tea1p in the localization of polarity factors and in organizing the microtubular cytoskeleton. *J Cell Biol* *157*, 783-793.
- Bendezu, F.O., and Martin, S.G. (2011). Actin cables and the exocyst form two independent morphogenesis pathways in the fission yeast. *Mol Biol Cell* *22*, 44-53.
- Bendezu, F.O., Vincenzetti, V., and Martin, S.G. (2012). Fission yeast sec3 and exo70 are transported on actin cables and localize the exocyst complex to cell poles. *PLoS One* *7*, e40248.
- Bicho, C.C., Kelly, D.A., Snaith, H.A., Goryachev, A.B., and Sawin, K.E. (2010). A catalytic role for Mod5 in the formation of the Tea1 cell polarity landmark. *Curr Biol* *20*, 1752-1757.
- Bieling, P., Laan, L., Schek, H., Munteanu, E.L., Sandblad, L., Dogterom, M., Brunner, D., and Surrey, T. (2007). Reconstitution of a microtubule plus-end tracking system in vitro. *Nature* *450*, 1100-1105.

- Boudaoud, A. (2003). Growth of walled cells: from shells to vesicles. *Phys Rev Lett* *91*, 018104.
- Browning, H., Hackney, D.D., and Nurse, P. (2003). Targeted movement of cell end factors in fission yeast. *Nat Cell Biol* *5*, 812-818.
- Browning, H., Hayles, J., Mata, J., Aveline, L., Nurse, P., and McIntosh, J.R. (2000). Tea2p is a kinesin-like protein required to generate polarized growth in fission yeast. *J Cell Biol* *151*, 15-28.
- Brunner, D., and Nurse, P. (2000). CLIP170-like tip1p spatially organizes microtubular dynamics in fission yeast. *Cell* *102*, 695-704.
- Bryant, D.M., and Mostov, K.E. (2008). From cells to organs: building polarized tissue. *Nat Rev Mol Cell Biol* *9*, 887-901.
- Butty, A.C., Perrinjaquet, N., Petit, A., Jaquenoud, M., Segall, J.E., Hofmann, K., Zwahlen, C., and Peter, M. (2002). A positive feedback loop stabilizes the guanine-nucleotide exchange factor Cdc24 at sites of polarization. *EMBO J* *21*, 1565-1576.
- Caviston, J.P., Longtine, M., Pringle, J.R., and Bi, E. (2003). The role of Cdc42p GTPase-activating proteins in assembly of the septin ring in yeast. *Mol Biol Cell* *14*, 4051-4066.
- Cerione, R.A. (2004). Cdc42: new roads to travel. *Trends Cell Biol* *14*, 127-132.
- Chang, E.C., Barr, M., Wang, Y., Jung, V., Xu, H.P., and Wigler, M.H. (1994). Cooperative interaction of *S. pombe* proteins required for mating and morphogenesis. *Cell* *79*, 131-141.
- Chang, F., Drubin, D., and Nurse, P. (1997). cdc12p, a protein required for cytokinesis in fission yeast, is a component of the cell division ring and interacts with profilin. *J Cell Biol* *137*, 169-182.
- Chant, J., and Herskowitz, I. (1991). Genetic control of bud site selection in yeast by a set of gene products that constitute a morphogenetic pathway. *Cell* *65*, 1203-1212.
- Chen, L., Liao, G., Yang, L., Campbell, K., Nakafuku, M., Kuan, C.Y., and Zheng, Y. (2006). Cdc42 deficiency causes Sonic hedgehog-independent holoprosencephaly. *Proc Natl Acad Sci U S A* *103*, 16520-16525.
- Cortes, J.C., Carnero, E., Ishiguro, J., Sanchez, Y., Duran, A., and Ribas, J.C. (2005). The novel fission yeast (1,3)beta-D-glucan synthase catalytic subunit Bgs4p is essential during both cytokinesis and polarized growth. *J Cell Sci* *118*, 157-174.
- Das, A., Slaughter, B.D., Unruh, J.R., Bradford, W.D., Alexander, R., Rubinstein, B., and Li, R. (2012a). Flippase-mediated phospholipid asymmetry promotes fast Cdc42 recycling in dynamic maintenance of cell polarity. *Nat Cell Biol* *14*, 304-310.
- Das, M., Drake, T., Wiley, D.J., Buchwald, P., Vavylonis, D., and Verde, F. (2012b). Oscillatory dynamics of Cdc42 GTPase in the control of polarized growth. *Science* *337*, 239-243.
- Das, M., Wiley, D.J., Chen, X., Shah, K., and Verde, F. (2009). The conserved NDR kinase Orb6 controls polarized cell growth by spatial regulation of the small GTPase Cdc42. *Curr Biol* *19*, 1314-1319.
- Das, M., Wiley, D.J., Medina, S., Vincent, H.A., Larrea, M., Oriolo, A., and Verde, F. (2007). Regulation of cell diameter, For3p localization, and cell symmetry by fission yeast Rho-GAP Rga4p. *Mol Biol Cell* *18*, 2090-2101.
- Dhonukshe, P. (2009). Cell polarity in plants: Linking PIN polarity generation mechanisms to morphogenic auxin gradients. *Commun Integr Biol* *2*, 184-190.

- Drummond, D.R., and Cross, R.A. (2000). Dynamics of interphase microtubules in *Schizosaccharomyces pombe*. *Curr Biol* 10, 766-775.
- Dumais, J., Shaw, S.L., Steele, C.R., Long, S.R., and Ray, P.M. (2006). An anisotropic-viscoplastic model of plant cell morphogenesis by tip growth. *Int J Dev Biol* 50, 209-222.
- Eaton, S., Wepf, R., and Simons, K. (1996). Roles for Rac1 and Cdc42 in planar polarization and hair outgrowth in the wing of *Drosophila*. *J Cell Biol* 135, 1277-1289.
- Endo, M., Shirouzu, M., and Yokoyama, S. (2003). The Cdc42 binding and scaffolding activities of the fission yeast adaptor protein Scd2. *J Biol Chem* 278, 843-852.
- Feierbach, B., and Chang, F. (2001). Roles of the fission yeast formin for3p in cell polarity, actin cable formation and symmetric cell division. *Curr Biol* 11, 1656-1665.
- Feierbach, B., Verde, F., and Chang, F. (2004). Regulation of a formin complex by the microtubule plus end protein tea1p. *J Cell Biol* 165, 697-707.
- Fritz, G., Brachetti, C., Bahlmann, F., Schmidt, M., and Kaina, B. (2002). Rho GTPases in human breast tumours: expression and mutation analyses and correlation with clinical parameters. *Br J Cancer* 87, 635-644.
- Fritz, G., Just, I., and Kaina, B. (1999). Rho GTPases are over-expressed in human tumors. *Int J Cancer* 81, 682-687.
- Gachet, Y., and Hyams, J.S. (2005). Endocytosis in fission yeast is spatially associated with the actin cytoskeleton during polarised cell growth and cytokinesis. *J Cell Sci* 118, 4231-4242.
- Garcia, P., Tajadura, V., Garcia, I., and Sanchez, Y. (2006). Role of Rho GTPases and Rho-GEFs in the regulation of cell shape and integrity in fission yeast. *Yeast* 23, 1031-1043.
- Gomez Del Pulgar, T., Valdes-Mora, F., Bandres, E., Perez-Palacios, R., Espina, C., Cejas, P., Garcia-Cabezas, M.A., Nistal, M., Casado, E., Gonzalez-Baron, M., *et al.* (2008). Cdc42 is highly expressed in colorectal adenocarcinoma and downregulates ID4 through an epigenetic mechanism. *Int J Oncol* 33, 185-193.
- Goode, B.L., and Eck, M.J. (2007). Mechanism and function of formins in the control of actin assembly. *Annu Rev Biochem* 76, 593-627.
- Goryachev, A.B., and Pokhilko, A.V. (2008). Dynamics of Cdc42 network embodies a Turing-type mechanism of yeast cell polarity. *FEBS Lett* 582, 1437-1443.
- Gould, K.L., Ren, L., Feoktistova, A.S., Jennings, J.L., and Link, A.J. (2004). Tandem affinity purification and identification of protein complex components. *Methods* 33, 239-244.
- Hachet, O., Berthelot-Grosjean, M., Kokkoris, K., Vincenzetti, V., Moosbrugger, J., and Martin, S.G. (2011). A phosphorylation cycle shapes gradients of the DYRK family kinase Pom1 at the plasma membrane. *Cell* 145, 1116-1128.
- Harkins, A.L., Yuan, G., London, S.D., and Dolan, J.W. (2010). An oleate-stimulated, phosphatidylinositol 4,5-bisphosphate-independent phospholipase D in *Schizosaccharomyces pombe*. *FEMS Yeast Res* 10, 717-726.
- He, B., and Guo, W. (2009). The exocyst complex in polarized exocytosis. *Curr Opin Cell Biol* 21, 537-542.
- Hedges, S.B. (2002). The origin and evolution of model organisms. *Nat Rev Genet* 3, 838-849.
- Heider, M.R., and Munson, M. (2012). Exorcising the exocyst complex. *Traffic* 13, 898-907.

- Hoog, J.L., Schwartz, C., Noon, A.T., O'Toole, E.T., Mastronarde, D.N., McIntosh, J.R., and Antony, C. (2007). Organization of interphase microtubules in fission yeast analyzed by electron tomography. *Dev Cell* 12, 349-361.
- Howell, A.S., Jin, M., Wu, C.F., Zyla, T.R., Elston, T.C., and Lew, D.J. (2012). Negative feedback enhances robustness in the yeast polarity establishment circuit. *Cell* 149, 322-333.
- Huang, C.K., Ando, M., Hamaguchi, H.O., and Shigeto, S. (2012). Disentangling Dynamic Changes of Multiple Cellular Components during the Yeast Cell Cycle by in Vivo Multivariate Raman Imaging. *Anal Chem* 84, 5661-5668.
- Huang, Y., Chew, T.G., Ge, W., and Balasubramanian, M.K. (2007). Polarity determinants Tea1p, Tea4p, and Pom1p inhibit division-septum assembly at cell ends in fission yeast. *Dev Cell* 12, 987-996.
- Huffaker, T.C., Thomas, J.H., and Botstein, D. (1988). Diverse effects of beta-tubulin mutations on microtubule formation and function. *J Cell Biol* 106, 1997-2010.
- Ingebritsen, T.S., and Cohen, P. (1983). Protein phosphatases: properties and role in cellular regulation. *Science* 221, 331-338.
- Irazoqui, J.E., Gladfelter, A.S., and Lew, D.J. (2003). Scaffold-mediated symmetry breaking by Cdc42p. *Nat Cell Biol* 5, 1062-1070.
- Jacobs, C.W., Adams, A.E., Szaniszlo, P.J., and Pringle, J.R. (1988). Functions of microtubules in the *Saccharomyces cerevisiae* cell cycle. *J Cell Biol* 107, 1409-1426.
- Jaffe, A.B., and Hall, A. (2005). Rho GTPases: biochemistry and biology. *Annu Rev Cell Dev Biol* 21, 247-269.
- Jenkins, G.M., and Frohman, M.A. (2005). Phospholipase D: a lipid centric review. *Cell Mol Life Sci* 62, 2305-2316.
- Johnson, D.I. (1999). Cdc42: An essential Rho-type GTPase controlling eukaryotic cell polarity. *Microbiol Mol Biol Rev* 63, 54-105.
- Johnson, D.I., and Pringle, J.R. (1990). Molecular characterization of CDC42, a *Saccharomyces cerevisiae* gene involved in the development of cell polarity. *J Cell Biol* 111, 143-152.
- Johnson, J.M., Jin, M., and Lew, D.J. (2011). Symmetry breaking and the establishment of cell polarity in budding yeast. *Curr Opin Genet Dev* 21, 740-746.
- Kamai, T., Yamanishi, T., Shirataki, H., Takagi, K., Asami, H., Ito, Y., and Yoshida, K. (2004). Overexpression of RhoA, Rac1, and Cdc42 GTPases is associated with progression in testicular cancer. *Clin Cancer Res* 10, 4799-4805.
- Kelly, F.D., and Nurse, P. (2011a). De novo growth zone formation from fission yeast spheroplasts. *PLoS One* 6, e27977.
- Kelly, F.D., and Nurse, P. (2011b). Spatial control of Cdc42 activation determines cell width in fission yeast. *Mol Biol Cell* 22, 3801-3811.
- Kerber, R.A., O'Brien, E., and Cawthon, R.M. (2009). Gene expression profiles associated with aging and mortality in humans. *Aging Cell* 8, 239-250.
- Kim, Y., Huang, J., Cohen, P., and Matthews, H.R. (1993). Protein phosphatases 1, 2A, and 2C are protein histidine phosphatases. *J Biol Chem* 268, 18513-18518.
- Knaus, M., Camerini, E., Pedruzzi, I., Tatchell, K., De Virgilio, C., and Peter, M. (2005). The Bud14p-Glc7p complex functions as a cortical regulator of dynein in budding yeast. *Embo J* 24, 3000-3011.

- Knaus, M., Pelli-Gulli, M.P., van Drogen, F., Springer, S., Jaquenoud, M., and Peter, M. (2007). Phosphorylation of Bem2p and Bem3p may contribute to local activation of Cdc42p at bud emergence. *EMBO J* 26, 4501-4513.
- Knoblich, J.A. (2008). Mechanisms of asymmetric stem cell division. *Cell* 132, 583-597.
- Kovar, D.R., Sirotkin, V., and Lord, M. (2011). Three's company: the fission yeast actin cytoskeleton. *Trends Cell Biol* 21, 177-187.
- Kozminski, K.G., Beven, L., Angerman, E., Tong, A.H., Boone, C., and Park, H.O. (2003). Interaction between a Ras and a Rho GTPase couples selection of a growth site to the development of cell polarity in yeast. *Mol Biol Cell* 14, 4958-4970.
- Kozubowski, L., Saito, K., Johnson, J.M., Howell, A.S., Zyla, T.R., and Lew, D.J. (2008). Symmetry-breaking polarization driven by a Cdc42p GEF-PAK complex. *Curr Biol* 18, 1719-1726.
- Kumfer, K.T., Cook, S.J., Squirrell, J.M., Eliceiri, K.W., Peel, N., O'Connell, K.F., and White, J.G. (2010). CGEF-1 and CHIN-1 regulate CDC-42 activity during asymmetric division in the *Caenorhabditis elegans* embryo. *Mol Biol Cell* 21, 266-277.
- Lechler, T., Jonsdottir, G.A., Klee, S.K., Pellman, D., and Li, R. (2001). A two-tiered mechanism by which Cdc42 controls the localization and activation of an Arp2/3-activating motor complex in yeast. *J Cell Biol* 155, 261-270.
- Lee, I.J., Coffman, V.C., and Wu, J.Q. (2012). Contractile-ring assembly in fission yeast cytokinesis: Recent advances and new perspectives. *Cytoskeleton* (Hoboken).
- Liu, Y., Wang, Y., Zhang, Y., Miao, Y., Zhao, Y., Zhang, P.X., Jiang, G.Y., Zhang, J.Y., Han, Y., Lin, X.Y., *et al.* (2009). Abnormal expression of p120-catenin, E-cadherin, and small GTPases is significantly associated with malignant phenotype of human lung cancer. *Lung Cancer* 63, 375-382.
- Lo Presti, L., and Martin, S.G. (2011). Shaping fission yeast cells by rerouting actin-based transport on microtubules. *Curr Biol* 21, 2064-2069.
- Luo, L., Liao, Y.J., Jan, L.Y., and Jan, Y.N. (1994). Distinct morphogenetic functions of similar small GTPases: *Drosophila* Drac1 is involved in axonal outgrowth and myoblast fusion. *Genes Dev* 8, 1787-1802.
- Manning, G., Whyte, D.B., Martinez, R., Hunter, T., and Sudarsanam, S. (2002). The protein kinase complement of the human genome. *Science* 298, 1912-1934.
- Marquitz, A.R., Harrison, J.C., Bose, I., Zyla, T.R., McMillan, J.N., and Lew, D.J. (2002). The Rho-GAP Bem2p plays a GAP-independent role in the morphogenesis checkpoint. *EMBO J* 21, 4012-4025.
- Martin, S.G. (2009). Microtubule-dependent cell morphogenesis in the fission yeast. *Trends Cell Biol* 19, 447-454.
- Martin, S.G., and Berthelot-Grosjean, M. (2009). Polar gradients of the DYRK-family kinase Pom1 couple cell length with the cell cycle. *Nature* 459, 852-856.
- Martin, S.G., and Chang, F. (2005). New end take off: regulating cell polarity during the fission yeast cell cycle. *Cell Cycle* 4, 1046-1049.
- Martin, S.G., McDonald, W.H., Yates, J.R., 3rd, and Chang, F. (2005). Tea4p links microtubule plus ends with the formin for3p in the establishment of cell polarity. *Dev Cell* 8, 479-491.
- Martin, S.G., Rincon, S.A., Basu, R., Perez, P., and Chang, F. (2007). Regulation of the formin for3p by cdc42p and bud6p. *Mol Biol Cell* 18, 4155-4167.

- Mata, J., and Nurse, P. (1997). *tea1* and the microtubular cytoskeleton are important for generating global spatial order within the fission yeast cell. *Cell* 89, 939-949.
- Mayer, B.J. (2001). SH3 domains: complexity in moderation. *J Cell Sci* 114, 1253-1263.
- Mayer, B.J., and Baltimore, D. (1993). Signalling through SH2 and SH3 domains. *Trends Cell Biol* 3, 8-13.
- Miller, P.J., and Johnson, D.I. (1994). Cdc42p GTPase is involved in controlling polarized cell growth in *Schizosaccharomyces pombe*. *Mol Cell Biol* 14, 1075-1083.
- Minc, N., Bratman, S.V., Basu, R., and Chang, F. (2009). Establishing new sites of polarization by microtubules. *Curr Biol* 19, 83-94.
- Mitchison, J.M., and Nurse, P. (1985). Growth in cell length in the fission yeast *Schizosaccharomyces pombe*. *J Cell Sci* 75, 357-376.
- Mogilner, A., Allard, J., and Wollman, R. (2012). Cell polarity: quantitative modeling as a tool in cell biology. *Science* 336, 175-179.
- Morrell, J.L., Morphew, M., and Gould, K.L. (1999). A mutant of Arp2p causes partial disassembly of the Arp2/3 complex and loss of cortical actin function in fission yeast. *Mol Biol Cell* 10, 4201-4215.
- Morrell, J.L., Nichols, C.B., and Gould, K.L. (2004). The GIN4 family kinase, Cdr2p, acts independently of septins in fission yeast. *J Cell Sci* 117, 5293-5302.
- Moseley, J.B., Mayeux, A., Paoletti, A., and Nurse, P. (2009). A spatial gradient coordinates cell size and mitotic entry in fission yeast. *Nature* 459, 857-860.
- Motegi, F., Arai, R., and Mabuchi, I. (2001). Identification of two type V myosins in fission yeast, one of which functions in polarized cell growth and moves rapidly in the cell. *Mol Biol Cell* 12, 1367-1380.
- Musacchio, A., Gibson, T., Lehto, V.P., and Saraste, M. (1992). SH3--an abundant protein domain in search of a function. *FEBS Lett* 307, 55-61.
- Nakano, K., Imai, J., Arai, R., Toh, E.A., Matsui, Y., and Mabuchi, I. (2002). The small GTPase Rho3 and the diaphanous/formin For3 function in polarized cell growth in fission yeast. *J Cell Sci* 115, 4629-4639.
- Nakano, K., Mutoh, T., and Mabuchi, I. (2001). Characterization of GTPase-activating proteins for the function of the Rho-family small GTPases in the fission yeast *Schizosaccharomyces pombe*. *Genes Cells* 6, 1031-1042.
- Nakano, K., Toya, M., Yoneda, A., Asami, Y., Yamashita, A., Kamasawa, N., Osumi, M. and Yamamoto, M. (2011), Pob1 Ensures Cylindrical Cell Shape by Coupling Two Distinct Rho Signaling Events During Secretory Vesicle Targeting. *Traffic*, 12: 726–739.
- Ni, L., and Snyder, M. (2001). A genomic study of the bipolar bud site selection pattern in *Saccharomyces cerevisiae*. *Mol Biol Cell* 12, 2147-2170.
- Nobes, C.D., and Hall, A. (1999). Rho GTPases control polarity, protrusion, and adhesion during cell movement. *J Cell Biol* 144, 1235-1244.
- Ohkura, H., Kinoshita, N., Miyatani, S., Toda, T., and Yanagida, M. (1989). The fission yeast *dis2+* gene required for chromosome disjoining encodes one of two putative type 1 protein phosphatases. *Cell* 57, 997-1007.
- Orlando, K., and Guo, W. (2009). Membrane organization and dynamics in cell polarity. *Cold Spring Harb Perspect Biol* 1, a001321.
- Park, H.O., and Bi, E. (2007). Central roles of small GTPases in the development of cell polarity in yeast and beyond. *Microbiol Mol Biol Rev* 71, 48-96.

- Park, H.O., Bi, E., Pringle, J.R., and Herskowitz, I. (1997). Two active states of the Ras-related Bud1/Rsr1 protein bind to different effectors to determine yeast cell polarity. *Proc Natl Acad Sci U S A* 94, 4463-4468.
- Pawson, T., and Schlessingert, J. (1993). SH2 and SH3 domains. *Curr Biol* 3, 434-442.
- Pawson, T., and Scott, J.D. (1997). Signaling through scaffold, anchoring, and adaptor proteins. *Science* 278, 2075-2080.
- Pelham, R.J., Jr., and Chang, F. (2001). Role of actin polymerization and actin cables in actin-patch movement in *Schizosaccharomyces pombe*. *Nat Cell Biol* 3, 235-244.
- Perez, P., and Rincon, S.A. (2010). Rho GTPases: regulation of cell polarity and growth in yeasts. *Biochem J* 426, 243-253.
- Petersen, J., Weilguny, D., Egel, R., and Nielsen, O. (1995). Characterization of fus1 of *Schizosaccharomyces pombe*: a developmentally controlled function needed for conjugation. *Mol Cell Biol* 15, 3697-3707.
- Proctor, S.A., Minc, N., Boudaoud, A., and Chang, F. (2012). Contributions of Turgor Pressure, the Contractile Ring, and Septum Assembly to Forces in Cytokinesis in Fission Yeast. *Curr Biol*.
- Pruyne, D., Evangelista, M., Yang, C., Bi, E., Zigmund, S., Bretscher, A., and Boone, C. (2002). Role of formins in actin assembly: nucleation and barbed-end association. *Science* 297, 612-615.
- Pruyne, D., Gao, L., Bi, E., and Bretscher, A. (2004a). Stable and dynamic axes of polarity use distinct formin isoforms in budding yeast. *Mol Biol Cell* 15, 4971-4989.
- Pruyne, D., Legesse-Miller, A., Gao, L., Dong, Y., and Bretscher, A. (2004b). Mechanisms of polarized growth and organelle segregation in yeast. *Annu Rev Cell Dev Biol* 20, 559-591.
- Rincon, S.A., Ye, Y., Villar-Tajadura, M.A., Santos, B., Martin, S.G., and Perez, P. (2009). Pob1 participates in the Cdc42 regulation of fission yeast actin cytoskeleton. *Mol Biol Cell* 20, 4390-4399.
- Rodriguez, O.C., Schaefer, A.W., Mandato, C.A., Forscher, P., Bement, W.M., and Waterman-Storer, C.M. (2003). Conserved microtubule-actin interactions in cell movement and morphogenesis. *Nat Cell Biol* 5, 599-609.
- Sagolla, M.J., Uzawa, S., and Cande, W.Z. (2003). Individual microtubule dynamics contribute to the function of mitotic and cytoplasmic arrays in fission yeast. *J Cell Sci* 116, 4891-4903.
- Sagot, I., Rodal, A.A., Moseley, J., Goode, B.L., and Pellman, D. (2002). An actin nucleation mechanism mediated by Bni1 and profilin. *Nat Cell Biol* 4, 626-631.
- Sawin, K.E., and Tran, P.T. (2006). Cytoplasmic microtubule organization in fission yeast. *Yeast* 23, 1001-1014.
- Scott, E.K., Reuter, J.E., and Luo, L. (2003). Small GTPase Cdc42 is required for multiple aspects of dendritic morphogenesis. *J Neurosci* 23, 3118-3123.
- Shin, K., Fogg, V.C., and Margolis, B. (2006). Tight junctions and cell polarity. *Annu Rev Cell Dev Biol* 22, 207-235.
- Slaughter, B.D., Smith, S.E., and Li, R. (2009). Symmetry breaking in the life cycle of the budding yeast. *Cold Spring Harb Perspect Biol* 1, a003384.
- Smith, G.R., Givan, S.A., Cullen, P., and Sprague, G.F., Jr. (2002). GTPase-activating proteins for Cdc42. *Eukaryot Cell* 1, 469-480.

- Snaith, H.A., Samejima, I., and Sawin, K.E. (2005). Multistep and multimode cortical anchoring of tea1p at cell tips in fission yeast. *EMBO J* 24, 3690-3699.
- Snaith, H.A., and Sawin, K.E. (2003). Fission yeast mod5p regulates polarized growth through anchoring of tea1p at cell tips. *Nature* 423, 647-651.
- Snaith, H.A., Thompson, J., Yates, J.R., 3rd, and Sawin, K.E. (2011). Characterization of Mug33 reveals complementary roles for actin cable-dependent transport and exocyst regulators in fission yeast exocytosis. *Journal of cell science* 124, 2187-2199.
- Snell, V., and Nurse, P. (1994). Genetic analysis of cell morphogenesis in fission yeast--a role for casein kinase II in the establishment of polarized growth. *EMBO J* 13, 2066-2074.
- Snyder, M. (1994). The spindle pole body of yeast. *Chromosoma* 103, 369-380.
- Sopko, R., Huang, D., Smith, J.C., Figeys, D., and Andrews, B.J. (2007). Activation of the Cdc42p GTPase by cyclin-dependent protein kinases in budding yeast. *EMBO J* 26, 4487-4500.
- Stengel, K., and Zheng, Y. (2011). Cdc42 in oncogenic transformation, invasion, and tumorigenesis. *Cell Signal* 23, 1415-1423.
- Tatebe, H., Goshima, G., Takeda, K., Nakagawa, T., Kinoshita, K., and Yanagida, M. (2001). Fission yeast living mitosis visualized by GFP-tagged gene products. *Micron* 32, 67-74.
- Tatebe, H., Nakano, K., Maximo, R., and Shiozaki, K. (2008). Pom1 DYRK regulates localization of the Rga4 GAP to ensure bipolar activation of Cdc42 in fission yeast. *Curr Biol* 18, 322-330.
- Tatebe, H., Shimada, K., Uzawa, S., Morigasaki, S., and Shiozaki, K. (2005). Wsh3/Tea4 is a novel cell-end factor essential for bipolar distribution of Tea1 and protects cell polarity under environmental stress in *S. pombe*. *Curr Biol* 15, 1006-1015.
- TerBush, D.R., Maurice, T., Roth, D., and Novick, P. (1996). The Exocyst is a multiprotein complex required for exocytosis in *Saccharomyces cerevisiae*. *EMBO J* 15, 6483-6494.
- Terenna, C.R., Makushok, T., Velve-Casquillas, G., Baigl, D., Chen, Y., Bornens, M., Paoletti, A., Piel, M., and Tran, P.T. (2008). Physical mechanisms redirecting cell polarity and cell shape in fission yeast. *Curr Biol* 18, 1748-1753.
- Toda, T., Umesono, K., Hirata, A., and Yanagida, M. (1983). Cold-sensitive nuclear division arrest mutants of the fission yeast *Schizosaccharomyces pombe*. *J Mol Biol* 168, 251-270.
- Tong, Z., Gao, X.D., Howell, A.S., Bose, I., Lew, D.J., and Bi, E. (2007). Adjacent positioning of cellular structures enabled by a Cdc42 GTPase-activating protein-mediated zone of inhibition. *J Cell Biol* 179, 1375-1384.
- Tran, P.T., Marsh, L., Doye, V., Inoue, S., and Chang, F. (2001). A mechanism for nuclear positioning in fission yeast based on microtubule pushing. *J Cell Biol* 153, 397-411.
- Tucci, M.G., Lucarini, G., Brancorsini, D., Zizzi, A., Pugnali, A., Giacchetti, A., Ricotti, G., and Biagini, G. (2007). Involvement of E-cadherin, beta-catenin, Cdc42 and CXCR4 in the progression and prognosis of cutaneous melanoma. *Br J Dermatol* 157, 1212-1216.
- Turing, A.M. (1990). The chemical basis of morphogenesis. 1953. *Bull Math Biol* 52, 153-197; discussion 119-152.
- Umesono, K., Toda, T., Hayashi, S., and Yanagida, M. (1983). Cell division cycle genes *nda2* and *nda3* of the fission yeast *Schizosaccharomyces pombe* control microtubular organization and sensitivity to anti-mitotic benzimidazole compounds. *J Mol Biol* 168, 271-284.

- van Hengel, J., D'Hooge, P., Hooghe, B., Wu, X., Libbrecht, L., De Vos, R., Quondamatteo, F., Klempt, M., Brakebusch, C., and van Roy, F. (2008). Continuous cell injury promotes hepatic tumorigenesis in *cdc42*-deficient mouse liver. *Gastroenterology* *134*, 781-792.
- Vavylonis, D., Wu, J.Q., Hao, S., O'Shaughnessy, B., and Pollard, T.D. (2008). Assembly mechanism of the contractile ring for cytokinesis by fission yeast. *Science* *319*, 97-100.
- Verde, F., Mata, J., and Nurse, P. (1995). Fission yeast cell morphogenesis: identification of new genes and analysis of their role during the cell cycle. *J Cell Biol* *131*, 1529-1538.
- Wedlich-Soldner, R., Altschuler, S., Wu, L., and Li, R. (2003). Spontaneous cell polarization through actomyosin-based delivery of the Cdc42 GTPase. *Science* *299*, 1231-1235.
- Wedlich-Soldner, R., Wai, S.C., Schmidt, T., and Li, R. (2004). Robust cell polarity is a dynamic state established by coupling transport and GTPase signaling. *J Cell Biol* *166*, 889-900.
- Wheatley, E., and Rittinger, K. (2005). Interactions between Cdc42 and the scaffold protein Scd2: requirement of SH3 domains for GTPase binding. *Biochem J* *388*, 177-184.
- Wilhelm, B.T., Marguerat, S., Watt, S., Schubert, F., Wood, V., Goodhead, I., Penkett, C.J., Rogers, J., and Bahler, J. (2008). Dynamic repertoire of a eukaryotic transcriptome surveyed at single-nucleotide resolution. *Nature* *453*, 1239-1243.
- Win, T.Z., Gachet, Y., Mulvihill, D.P., May, K.M., and Hyams, J.S. (2001). Two type V myosins with non-overlapping functions in the fission yeast *Schizosaccharomyces pombe*: Myo52 is concerned with growth polarity and cytokinesis, Myo51 is a component of the cytokinetic actin ring. *J Cell Sci* *114*, 69-79.
- Wixon, J. (2002). Featured organism: *Schizosaccharomyces pombe*, the fission yeast. *Comp Funct Genomics* *3*, 194-204.
- Wood, V., Gwilliam, R., Rajandream, M.A., Lyne, M., Lyne, R., Stewart, A., Sgouros, J., Peat, N., Hayles, J., Baker, S., *et al.* (2002). The genome sequence of *Schizosaccharomyces pombe*. *Nature* *415*, 871-880.
- Wu, X., Xiang, X., and Hammer, J.A., 3rd (2006). Motor proteins at the microtubule plus-end. *Trends Cell Biol* *16*, 135-143.
- Yu, I.M., and Hughson, F.M. (2010). Tethering factors as organizers of intracellular vesicular traffic. *Annu Rev Cell Dev Biol* *26*, 137-156.
- Zhang, X., Bi, E., Novick, P., Du, L., Kozminski, K.G., Lipschutz, J.H., and Guo, W. (2001). Cdc42 interacts with the exocyst and regulates polarized secretion. *J Biol Chem* *276*, 46745-46750.
- Zhang, H., Photiou, A., Grothey, A., Stebbing, J., and Giamas, G. (2012). The role of pseudokinases in cancer. *Cell Signal* *24*, 1173-1184.
- Zheng, Y., Bender, A., and Cerione, R.A. (1995). Interactions among proteins involved in bud-site selection and bud-site assembly in *Saccharomyces cerevisiae*. *J Biol Chem* *270*, 626-630.



# Acknowledgments

I thank Sophie Martin for invaluable help and advice. I am also grateful to the committee of my PhD defense, colleagues, friends and professors from the CIG and Biophore building of University of Lausanne. I also acknowledge Manfredo Quadroni and Patrice Waridel at the Protein Analysis Facility for performing the mass spectrometry analysis. This thesis would not have been possible without the continuous help of my friends and family that supported me in every possible way. I will not list name by name all these persons since they are so many and I would not like to forget anyone. Nevertheless, I acknowledge every single person that helped me to accomplish this research in scientific, social and personal level. The Roche Research Foundation and Swiss National Science Foundation financially supported this work.



# Kyriakos KOKKORIS Resume

LinkedIn: <http://www.linkedin.com/pub/kyriakos-kokkoris/23/453/6b9>

E-mail: kyriakos.kokkoris@gmail.com, Cell: +41 78 640 8223

Strong assets: management and coordination of scientific projects, hypothesis driven mind, expertise in cell biology, microscopy and biochemical techniques, international team player, organizational and communication skills, creative, ambitious

---

## Professional Experience

2007- 2012, **Research Assistant**, Faculty of Biology and Medicine, University of Lausanne

- Project management related to cancer initiation
- Establishment of new research unit (lab management and administration)
- Teaching and supervision of undergraduate students
- Design of posters and PowerPoint presentations presented in scientific meetings
- Analysis and conduct of critical discussion on research articles in a limited given time (5')

2006- 2007, **Junior Researcher**, Department of Molecular Cell Biology, University of Uppsala, Sweden

- Project management related to RNA degradation

2004, **Infantry Sergeant**, Military Services, Greece

- Training and supervision of 20 inductees
- Management of a restaurant for high-ranking military officers

2003, **Desk Officer**, Institute for Social Insurance, Greece

- Client complaints management / Appointment arrangement between doctors and patients

## Academic Education

2007- 2012, **Ph.D in Fundamental Microbiology**, University of Lausanne

- Thesis under supervision of Professor Sophie Martin: Linking Microtubules to Activation of Cdc42 in fission yeast

2005- 2006, **Master of Science in Molecular Cell Biology**, University of Uppsala, Sweden

- Thesis under supervision of Professor Anders Virtanen: RNA binding properties of poly(A) specific ribonuclease

1998- 2003, **Bachelor in Medical Laboratories**, Technological Educational Institute of Athens, Greece

## Extracurricular Activities and Awards

2009- 2011, Organization and participation in 3 days event "Les mystères de l'UNIL" for introducing science to general public

2008- 2009, Awarded Roche Research Foundation Grant

2003, Exchange student at University of Helsinki, Finland through the Leonardo Da Vinci Program

2001, Exchange student at University of Uppsala, Sweden through the Erasmus/Socrates Program

## Computer Skills

MS Office (Excel/Word/PowerPoint), Adobe Photoshop/Illustrator, ImageJ, EndNote

## Languages

Greek: Native language, English: Very good, French: Intermediate, actively improving

## Hobbies and Interests

Fly Fishing and Cooking, Chess: Participated in Greek local championships,

Sailing: Having a diploma for open-sea sailing, Traveling: Long stays in foreign countries experiencing different cultures (Switzerland, Sweden, Finland, Australia)

**References available upon request**



# List of Publications

A phosphorylation cycle shapes gradients of the DYRK family kinase Pom1 at the plasma membrane. Hachet O, Berthelot-Grosjean M, **Kokkoris K**, Vincenzetti V, Moosbrugger J, Martin SG. *Cell*. 2011 Jun 24;145(7):1116-28.

Structural basis of m(7)GpppG binding to poly(A)-specific ribonuclease. Wu M, Nilsson P, Henriksson N, Niedzwiecka A, Lim MK, Cheng Z, **Kokkoris K**, Virtanen A, Song H. *Structure*. 2009 Feb 13;17(2):276-86.

A multifunctional RNA recognition motif in poly(A)-specific ribonuclease with cap and poly(A) binding properties. Nilsson P, Henriksson N, Niedzwiecka A, Balatsos NA, **Kokkoris K**, Eriksson J, Virtanen A. *J Biol Chem*. 2007 Nov 9;282(45):32902-11. Epub 2007 Sep 4.



VINI VIDI VICI

*The End*